

575  
6-21-84 JS (2)

DR# 0139-2

Energy

S  
O  
L  
A  
R

DOE/JPL-1012-92  
(DE84008524)

PROCEEDINGS OF THE FLAT-PLATE SOLAR ARRAY  
PROJECT RESEARCH FORUM ON PHOTOVOLTAIC  
METALLIZATION SYSTEMS

November 15, 1983

Work Performed Under Contract No. AI01-76ET20356

Jet Propulsion Laboratory  
California Institute of Technology  
Pasadena, California

Technical Information Center  
Office of Scientific and Technical Information  
United States Department of Energy



## **DISCLAIMER**

**This report was prepared as an account of work sponsored by an agency of the United States Government. Neither the United States Government nor any agency Thereof, nor any of their employees, makes any warranty, express or implied, or assumes any legal liability or responsibility for the accuracy, completeness, or usefulness of any information, apparatus, product, or process disclosed, or represents that its use would not infringe privately owned rights. Reference herein to any specific commercial product, process, or service by trade name, trademark, manufacturer, or otherwise does not necessarily constitute or imply its endorsement, recommendation, or favoring by the United States Government or any agency thereof. The views and opinions of authors expressed herein do not necessarily state or reflect those of the United States Government or any agency thereof.**



## **DISCLAIMER**

**Portions of this document may be illegible in electronic image products. Images are produced from the best available original document.**

## DISCLAIMER

This report was prepared as an account of work sponsored by an agency of the United States Government. Neither the United States Government nor any agency thereof, nor any of their employees, makes any warranty, express or implied, or assumes any legal liability or responsibility for the accuracy, completeness, or usefulness of any information, apparatus, product, or process disclosed, or represents that its use would not infringe privately owned rights. Reference herein to any specific commercial product, process, or service by trade name, trademark, manufacturer, or otherwise does not necessarily constitute or imply its endorsement, recommendation, or favoring by the United States Government or any agency thereof. The views and opinions of authors expressed herein do not necessarily state or reflect those of the United States Government or any agency thereof.

This report has been reproduced directly from the best available copy.

Available from the National Technical Information Service, U. S. Department of Commerce, Springfield, Virginia 22161.

Price: Printed Copy A19  
Microfiche A01

Codes are used for pricing all publications. The code is determined by the number of pages in the publication. Information pertaining to the pricing codes can be found in the current issues of the following publications, which are generally available in most libraries: *Energy Research Abstracts (ERA)*; *Government Reports Announcements and Index (GRA and I)*; *Scientific and Technical Abstract Reports (STAR)*; and publication NTIS-PR-360 available from NTIS at the above address.

5101-239  
Flat-Plate  
Solar Array Project

DOE/JPL-1012-92  
(CONF-8303143)  
(DE84008524)  
Distribution Category UC-63b

# Proceedings of the Flat-Plate Solar Array Project Research Forum on Photovoltaic Metallization Systems

(March 16, 17, 18, 1983, at Pine Mountain, Georgia)

November 15, 1983

Prepared for  
U.S. Department of Energy  
Through an Agreement with  
National Aeronautics and Space Administration

by  
Jet Propulsion Laboratory  
California Institute of Technology  
Pasadena, California

JPL Publication 83-93

THIS PAGE  
WAS INTENTIONALLY  
LEFT BLANK



## ABSTRACT

A Photovoltaic Metallization Research Forum, under the sponsorship of the Jet Propulsion Laboratory's Flat-Plate Solar Array Project and the U. S. Department of Energy, was held March 16-18, 1983 at Pine Mountain, Georgia. The Forum consisted of five sessions, covering (1) the current status of metallization systems, (2) system design, (3) thick-film metallization, (4) advanced techniques and (5) future metallization challenges. Twenty-three papers were presented.

THIS PAGE  
WAS INTENTIONALLY  
LEFT BLANK

## FOREWORD

The objectives of the Research Forum on Photovoltaic Metallization Systems were to clarify and define the state of the art of current metallization systems for solar cells; to report on performance experience with these systems, including advances made and problems encountered; to describe advanced processing techniques under development, and to discuss expectations for future improvements.

The approach was to present invited and submitted papers on various aspects of photovoltaic metallization systems; to invite acknowledged experts in the field, who would lend perspective as well as technical expertise, to attend; and to provide an atmosphere and a setting that would provide ample opportunity for discussion.

More than 64 specialists came to Pine Hill, Georgia, March 16-18, 1983, to participate in this PV Metallization Forum. These scientists and engineers came from industrial laboratories, government laboratories and universities engaged in research and development in metal-semiconductor systems.

These Proceedings contain the texts of the presentations made at the Forum as submitted by their authors to the Committee at the beginning of the Forum. Thus, they may vary from the actual presentations in the technical sessions. The discussions following each presentation were tape-recorded at the conference and have been edited for clarity and continuity.

THIS PAGE  
WAS INTENTIONALLY  
LEFT BLANK



**PARTICIPANT LIST**

**PHOTOVOLTAIC METALLIZATION SYSTEMS  
RESEARCH FORUM**

**March 16-18, 1983**

**AMICK, James A.**  
Exxon Research and Engineering Co.  
P. O. Box 45  
Linden, NJ 07036  
(201) 474-2594

**ASHOK, S.**  
Department of Engineering Sciences  
Hammond Building  
Pennsylvania State University  
University Park, PA 16802  
(814) 865-4931

**BACHNER, Robert**  
Silicon Sensors, Inc.  
Highway 18 East  
Dodgeville, WI 53533  
(608) 935-2707

**BEAVIS, Len C.**  
Sandia National Laboratories  
Division 9724  
Albuquerque, NJ 87185  
(505) 844-2231

**BICKLER, Donald B.**  
Jet Propulsion Laboratory  
4800 Oak Grove Dr., M/S 512-103  
Pasadena, CA 91109  
(213) 577-9219

**BLAKE, Julian G., Jr.**  
Solar Power Corp.  
20 Cabot Rd.  
Woburn, MA 01801  
(617) 935-4600 X185

**BOLLINGER, David**  
VEECO, Industrial Equipment Division  
Terminal Drive  
Plainview, NY 11803  
(516) 349-8300

**BURGER, Dale R.**  
Jet Propulsion Laboratory  
4800 Oak Grove Dr., M/S 512-103  
Pasadena, CA 91109  
(213) 577-9219

**CALAHAN, Don**  
NASA Headquarters  
600 Independence Ave. SW, RJE  
Washington DC 20546  
(202) 755-2403

**CAMPBELL, Robert B.**  
Westinghouse Advanced Energy Systems Div.  
P. O. Box 10864  
Pittsburgh, PA 15202  
(412) 892-5600

**CHAMBERLAIN, Merrill B.**  
Sandia National Laboratories  
Div. 1823  
Albuquerque, NM 87185  
(505) 844-8749

**COLE, Lee**  
Solar Energy Research Institute  
1617 Cole Blvd.  
Golden, CO 80401  
(303) 231-1841

**CULIK, Jerry**  
Solarex  
1335 Piccard Dr.  
Rockville, MD 20850  
(301) 948-0202

**CULL, Ronald C.**  
Standard Oil Company of Ohio  
3092 Broadway Ave.  
Cleveland, OH 44115  
(216) 271-8952

DANIEL, Ronald E.  
Jet Propulsion Laboratory  
4800 Oak Grove Dr., M.S. 506-316  
Pasadena, CA 91109  
(213) 577-9189

DUTTA, Subhadra  
Westinghouse R&D Center  
1310 Beulah Rd.  
Pittsburgh, PA 15235  
(412) 256-7281

FIRESTER, Arthur  
RCA Corp.  
David Sarnoff Research Center  
Princeton, NJ 08540  
(609) 734-2516

GALLAGHER, Brian D.  
Jet Propulsion Laboratory  
4800 Oak Grove Dr., M/S 512-103  
Pasadena, CA 91109  
(213) 577-9115

GARCIA, Alec  
Spectrolab, Inc.  
12500 Gladstone Ave.  
Sylmar, CA 91342  
(213) 365-4611

HARTMAN, Robert A.  
Standard Oil Company of Ohio  
3092 Broadway  
Cleveland, OH 44115  
(216) 271-8144

HAWKINS, Dexter  
Clemson University  
Department of Electrical Engineering  
Clemson, SC 28631  
(803) 656-3190

HOGAN, Steve J.  
Solar Energy Research Institute  
1617 Cole Blvd.  
Golden, CO 80401  
(303) 231-1778

HORNE, Edward  
Boeing Aerospace  
P. O. Box 3999  
Seattle, WN 98124  
(206) 655-4045

HUANG, Cornelius Y.D.  
Electro-Science Laboratories, Inc.  
2211 Sherman Ave.  
Pennsauken, NJ 08110  
(609) 603-7777

ILES, Peter A.  
Applied Solar Energy Corp.  
15251 Don Julian Rd.  
City of Industry, CA 91749  
(213) 968-6581 X 306

KIRKPATRICK, Allen  
Eaton Corporation  
16 Tozer Rd.  
Beverly, MA 01915  
(617) 927-9100

KRAUSE, Fred  
Georgia Power Company, Solar Ops. Dept.  
7 Solar Circle  
Shenandoah, GA 30625  
(404) 526-4745

LANDEL, Robert F.  
Jet Propulsion Laboratory  
4800 Oak Grove Dr., M/S 67-201  
Pasadena, CA 91109  
(213) 354-4402

LAVENDEL, Henry W.  
Lockheed Palo Alto Research Laboratory  
3251 Hanover Street, Bldg. 204/Org. 52-31  
Palo Alto, CA 94304 (415)  
493-4411 X45678

LINHOLM, Loren  
National Bureau of Standards  
Building 225, Room B310  
Washington, DC 20234  
(202) 921-3541

LITTLE, Roger  
Spire Corp.  
Patriots Park  
Bedford, MA 01730  
(617) 275-6000

LIVESAY, Billy R.  
Georgia Institute of Technology  
Engineering Experimental Station  
Atlanta, GA 30332  
(404) 894-3489

MISIAKOS, Konstantinos  
Clemson University  
Department of Electrical Engineering  
Clemson, SC 29631  
(803) 656-3190

MON, Gordon R.  
Jet Propulsion Laboratory  
4800 Oak Grove Dr., M.S. 506-328  
Pasadena, CA 91109  
(213) 577-9242

MRIG, Laxmi  
Solar Energy Research Institute  
1617 Cole Blvd.  
Golden, CO 80401  
(303) 231-7178

NATH, Prem  
Energy Conversion Devices  
32400 Edwards Street  
Madison Heights, MI 48071  
(313) 585-7880

NAZARENKO, Nicholas  
E. I. du Pont de Nemours & Company  
Experimental Station E334  
Wilmington, DE 19898  
(302) 772-2827

NICOLET, Marc  
California Institute of Technology  
321 Steele  
273 S. Catalina  
Pasadena, CA 91106  
(213) 795-4803

PARKER, Joseph  
Electrink, Inc.  
7554 A Trade St.  
San Diego, CA 92131  
(619) 566-7707

PATEL, Kirit B.  
Mobil Solar Energy Corp.  
16 Hickory Dr.  
Waltham, MA 02154  
(617) 667-5900

PHILLIPS, Mary  
Jet Propulsion Laboratory  
4800 Oak Grove Dr., M/S 502-422  
Pasadena, CA 91109  
(213) 577-9096

PROVANCE, Jason D.  
Ferro Corporation  
Thick Film Systems Division  
324 Palm Ave.  
Santa Barbara, CA 93101  
(805) 963-7757

PRYOR, Robert A.  
Solavolt International  
P. O. Box 2934  
Phoenix, AZ 85062  
(602) 231-6454

RAI-CHOUDHURY, Prosejitt  
Westinghouse Electric Corp. R&D Center  
1310 Beulah Rd.  
Pittsburgh, PA 15235  
(412) 256-3682

RIEL, Robert K.  
Westinghouse Electric Corp. R&D Center  
1310 Beulah Rd.  
Pittsburgh, PA 15235  
(412) 256-3614

ROBINSON, John C.  
Lockheed Missiles and Space  
3251 Hanover Street  
Palo Alto, CA 94304  
(415) 424-2378

ROYAL, Ed L.  
Jet Propulsion Laboratory  
4800 Oak Grove Dr., M.S. 506-328  
Pasadena, CA 91109  
(213) 577-9580

SCHRODER, D.  
Arizona State University  
Electrical Engineering Department  
Tempe, AZ 85287  
(602) 965-6621

SCHWUTKE, Guenter H.  
GHS Research and Development  
8162 E. Del Pico Dr.  
Scottsdale, AZ 85258  
(602) 951-0422

SHAFRANEK, Robert J.  
Ametek  
627 Blake Street  
Kent, OH 44240  
(216) 673-3451

SOMBERG, Howard  
Global Photovoltaic Specialists, Inc.  
22432 De Grasse Dr.  
Woodland Hills, CA 91364  
(213) 999-4399

STEIN, Sidney J.  
Electro-Science Laboratories, Inc.  
2211 Sherman Ave.  
Pennsauken, NJ 08110  
(609) 663-7777

TAYLOR, William E.  
Photowatt International, Inc.  
2414 W. 14th St.  
Tempe, AZ 85282  
(602) 894-9564

TUSTIN, David  
Jet Propulsion Laboratory  
4800 Oak Grove Dr., M/S 502-422  
Pasadena, CA 91109  
(213) 577-9597

van der LEEDEN, Gerard  
Helionetics, Inc.  
3878 Ruffin Rd., Bldg. 10A  
San Diego, CA 92123  
(619) 560-6273

VEST, Geraldine  
Purdue University  
Potter Building - 322  
West Lafayette, IN 47907  
(317) 494-7009

VEST, Robert  
Purdue University  
CMET Bldg.  
West Lafayette, IN 47907  
(317) 494-4110

WEAVER, Robert W.  
Jet Propulsion Laboratory  
4800 Oak Grove Dr., M/S 248-101  
Pasadena, CA 91109  
(213) 354-4984

WOLF, Martin  
University of Pennsylvania  
308 Moore D2  
Philadelphia, PA 19104  
(215) 243-4822

WONG, Boon  
ARCO Solar, Inc.  
21011 Warner Center Lane  
Woodland Hills, CA 91367  
(213) 700-7040

YOO, Henry  
ARCO Solar Inc.  
P. O. Box 4400  
Woodland Hills, CA 91365  
(805) 484-7981 X351

ZWERDLING, Solomon  
Jet Propulsion Laboratory  
4800 Oak Grove Dr. M/S 507-228  
Pasadena, CA 91109  
(213) 577-9193



CONTENTS

OPENING REMARKS (Brian D. Gallagher, Jet Propulsion Laboratory,  
Forum Chairman) . . . . . 1

SESSION I: STATUS OF PHOTOVOLTAIC METALLIZATION SYSTEMS  
(M. Wolf, University of Pennsylvania, Chairman) . . . . . 3

Solar Cell Metallization: Historical Perspective  
(William E. Taylor, Photowatt International, Inc.) . . . . . 9

Discussion . . . . . 17

Economic Implications of Current Systems  
(R.E. Daniel and R.W. Aster, Jet Propulsion Laboratory) . . . . . 19

Discussion . . . . . 31

Accelerated Degradation of Silicon Metallization Systems  
(Jay W. Lathrop, Clemson University) . . . . . 35

Discussion . . . . . 54

Field Test Experience  
(R.W. Weaver, Jet Propulsion Laboratory) . . . . . 59

Discussion . . . . . 67

Fundamentals of Metal-Semiconductor Contacts  
(Dieter K. Schroder, Arizona State University) . . . . . 69

Discussion . . . . . 91

SESSION II: METALLIZATION SYSTEM DESIGN  
(Dale R. Burger, Jet Propulsion Laboratory, Chairman) . . . . . 93

Getting the Current Out  
(Dale R. Burger, Jet Propulsion Laboratory) . . . . . 95

A Direct Measurement of Interfacial Contact Resistance  
(S.J. Proctor and L.W. Linholm, National Bureau  
of Standards) . . . . . 99

A Microelectronic Test Structure for Interfacial  
Contact Resistance Measurement  
(L.W. Linholm, J.A. Mazer and S.J. Proctor, National  
Bureau of Standards) . . . . . 103

Discussion . . . . . 111

Diffusion Barriers  
(Marc-A. Nicolet, California Institute of Technology) . . . . . 113

Discussion . . . . . 135

Observations of Solar-Cell Metallization Corrosion (G.R. Mon, Jet Propulsion Laboratory) . . . . .	137
Module Degradation Catalyzed by Metal-Encapsulation Reactions (B.D. Gallagher, Jet Propulsion Laboratory) . . . . .	147
Discussion . . . . .	153
Metallization Problems With Concentrator Cells (P.A. Iles, Applied Solar Energy Corp.) . . . . .	159
Discussion . . . . .	165
SESSIONS I AND II GENERAL DISCUSSION . . . . .	167
SESSION III: THICK-FILM METALLIZATION SYSTEMS (J. Parker, Electrink, Inc., Chairman). . . . .	171
Effects of Particle Size Distribution in Thick Film Conductors (Robert W. Vest, Purdue University) . . . . .	173
Discussion . . . . .	190
Particle Size Effects on Viscosity of Silver Pastes -- a Manufacturer's View (Jason Provance and Kevin Allison, Ferro Corp.) . . . . .	195
Discussion . . . . .	208
Non-Noble Metal Based Metallization Systems (Alexander Garcia III, Spectrolab, Inc.) . . . . .	215
Discussion . . . . .	236
Polymer Thick Film Conductors and Dielectrics for Membrane Switches and Flexible Circuitry (N. Nazarenko, E.I. Du Pont de Nemours & Co., Inc.) . . . . .	241
Discussion . . . . .	256
ADDITIONAL DISCUSSION OF SESSION III . . . . .	259
SESSION IV: ADVANCED TECHNIQUES (R. Landel, Jet Propulsion Laboratory, Chairman). . . . .	263
Ionized Cluster Beam Deposition (Allen R. Kirkpatrick, Eaton Ion Materials Systems) . . . . .	265
Discussion . . . . .	272
Metallization With Generic Metallo-Organic Inks (Geraldine M. Vest, Purdue University). . . . .	277
Discussion . . . . .	297

Dry Etching of Metallizations (David Bollinger, Veeco Instruments) . . . . .	301
Discussion . . . . .	314
Laser Assisted Deposition (Subhadra Dutta, Westinghouse R&D Center) . . . . .	317
Discussion . . . . .	327
SESSION V: FUTURE METALLIZATION CHALLENGES (G. Schwuttke, Consultant, Chairman) . . . . .	333
Transparent Conductive Coatings (S. Ashok, Pennsylvania State University) . . . . .	335
Discussion . . . . .	361
A Metallization System for Thin-Film Photovoltaic Modules (A.H. Firester, RCA Laboratories) . . . . .	365
Discussion . . . . .	371
Iron-Copper Metallization for Flexible Solar Cell Arrays (Henry W. Lavendel, Lockheed Palo Alto Research Laboratory) . . . . .	375
Discussion . . . . .	392
SUMMARY AND CLOSING REMARKS (Brian D. Gallagher, Forum Chairman) . . . . .	397
APPENDIX A. CALCULATING SOLAR-CELL POWER LOSSES BY CELCAL (Dale R. Burger, Jet Propulsion Laboratory) . . . . .	A-1
APPENDIX B. OPTIMIZATION PROGRAM AND METHODOLOGY FOR DESIGNING SOLAR-CELL GRID PATTERNS (R. Daniel, D. Burger and H. Stone, Jet Propulsion Laboratory) . . . . .	B-1

## OPENING REMARKS

Brian D. Gallagher  
Jet Propulsion Laboratory  
Forum Chairman

GALLAGHER: Ladies and gentlemen, I would like to welcome you to this Research Forum on Photovoltaic Metallization Systems, which is sponsored jointly by the Jet Propulsion Laboratory and the U. S. Department of Energy. As in all projects, this one has some very specific concerns.

### Project Constraints

- Economic
  - Module \$0.70/watt
  - Metallization Variable
- Reliability
  - Module 30 years
  - Metallization Compatible
- Efficiency, NOC >11%

These are 1984 constraints, which are relatively new. The metallization systems we are talking about are very definitely an important portion of it. It is still one of our major cost drivers. The future constraints are going to get worse, not better. With that in mind, I would like to cover a few things that are on the viewgraph. We do have economic constraints on finished modules sitting in a box, packaged and ready to ship out. It is still \$0.70/watt and that \$0.70/watt is in 1980 dollars. The metallization portion of that is variable, because we have a number of systems, most of them synergistic.

There are many metal systems you will hear of in the second talk, with more information on how some of these systems interact and what the effect really is on a finished module.

To give you a feeling for the amount of money that we have allocated to us from the FSA Project Analysis and Integration Area, the total cell fabrication cost of an 11% cell is something like 21.7¢. With that allocation, we don't pay for the silicon and start with a piece of raw sheet to produce a cell. It is a very tough economic load.

Reliability is a very definite project constraint. We are very used to seeing 20 years in that slot. It has recently been changed to 30 years. Again, putting the economic constraint on the metallization system means it has to be an inexpensive metal system, it has to be compatible with that goal, and it has to have a 30-year lifetime. It is a very difficult goal.



The efficiency goals are changing on us. Remember, it used to be 10%. When I made this viewgraph the efficiency goal was 11%. Last Friday, I received a missive in the mail that said that the 1984 goal is 12%. Now that sounds like a comfortable number, because it is only 2% more than we started with in 1975 and we have had eight years to play with it. But a little thing called NOC makes a lot of difference. That NOC stands for normal operating conditions and that means that the ambient is at 20°C, the module itself is at its NOCT (which is normal operating cell temperature) and, depending on the design of the module, that is nominally 55°C. The wind is one meter per second and the module is measured at an insolation of 100 milliwatts per square centimeter. That is exceedingly tough, because the difference between the standard temperature conditions where it is measured in the lab, extrapolated to NOC, has a degradation factor of 0.91. If you take a look at a cell that we produce in a normal manner and encapsulate, we have another degradation factor that is approximately 0.92. If we look at the packing factor problems we have with round cells, we are lucky to get about a 0.76 degradation factor, and if it is a square cell it is about 0.925. When you multiply all of these nice things together in order to get a square cell into a finished module that has an 11% efficiency, the cell itself has to be 14%. That's tough. If we increase that module efficiency to 12%, that particular cell has to be 15.4%. So when they start talking about those rather mundane numbers and NOCs, we do have problems. So much for the constraints.

## Agenda

- SESSION I: STATUS OF PHOTOVOLTAIC METALLIZATION SYSTEMS
- SESSION II: METALLIZATION SYSTEM DESIGN
- SESSION III: THICK-FILM METALLIZATION SYSTEMS
- SESSION IV: ADVANCED TECHNIQUES
- SESSION V: FUTURE METALLIZATION CHALLENGES

Now I would like to talk a little bit about what you are going to see in the agenda. The first session is involved with the status of photovoltaic metallization systems.

## Session I: Status of Photovoltaic Metallization Systems

M. Wolf (University of Pennsylvania), Chairman

- **Solar-Cell Metallization: Historical Perspective**  
W. Taylor (Photowatt International)
- **Economic Implication of Current Systems**  
R. Daniel (JPL)
- **Accelerated Degradation of Silicon Metallization Systems**  
J. Lathrop (Clemson University)
- **Field-Test Experience**  
R. Weaver (JPL)
- **Fundamentals of Semiconductor Metal Contacts**  
D. Schroder (Arizona State University)

What we are trying to do in this forum is to take a snapshot of where we are now, what sort of problems we have, what we can do about them; take a look at some of the ways of solving the problems by getting interaction between people who perhaps have not interacted before.

Let's find out where we should spend our research dollars. Our research dollars are rapidly diminishing. We need the best bang for a buck we can get. We have to know where to put it and we are not omniscient; we need all the help we can get. So the first session is really going to say, how did we get here? What are some of the economies of scale, and economic factors? There is a lot of theory involved in this thing. A lot of theory that we sometimes forget, that we don't look at. When we start looking at higher efficiencies, and perhaps emerging thin-film technologies, we have to know more about what really makes that contact work.

## Session II: Metallization System Design

D. Burger (JPL), Chairman

HANDOUT: "Getting the Current Out," D. Burger (JPL)

- A Microelectronic Test Structure for Interfacial Contact Resistance Measurement  
L. Linholm (National Bureau of Standards)
- Diffusion Barriers  
M. Nicolet (California Institute of Technology)
- Observation of Solar-Cell Metallization Corrosion  
G. Mon (JPL)
- Module Degradation Catalyzed by Metal Encapsulant Reactions  
B. Gallagher (JPL)
- Metallization Problems with Concentrator Cells  
P. Iles (Applied Solar Energy Corp.)
- Additional Discussion of Sessions I and II

The second session is on metallization system design. We are going to give you some rules, some of the things we have found; we are going to show you that with the best laid plans of mice and men we still have problems; we are going to show you what some of those problems are. Some of them we understand, some of them we don't; but we would like to get all of them out in the open and intensively discussed.

## Session III: Thick-Film Metallization Systems

J. Parker (Electrink, Inc.), Chairman

- Effects of Particle Size Distribution in Thick Film Conductor  
R. Vest (Purdue University)
- Particle Size Effects on Viscosity of Silver Pastes--A Manufacturer's View  
J. Provance (Thick Film Systems, Div. of Ferro Corp.)
- Non-Noble Metal-Based Metallization Systems  
A. Garcia (Spectrolab, Inc.)
- Polymer Thick Film Conductor and Dielectrics for Membrane Switches and Flexible Circuitry  
N. Nazarenko (du Pont)

The third session is on thick-film metallization. Again, a snapshot perhaps of where we are in some systems. A little bit of theory on what some of the things are that we don't know -- areas that we haven't paid enough attention to.

## Session IV: Advanced Techniques

R. Landel (JPL), Chairman

- Ionized Cluster Beam Deposition  
A. Kirkpatrick (Eaton Ion Implantation Systems)
- Metallization with Generic Metallo-Organic Inks  
G. Vest (Purdue University)
- Dry Etching of Metallizations  
D. Bollinger (VEECO)
- Laser Assisted Deposition  
S. Dutta (Westinghouse R&D)

In advanced techniques, we are going to go into something that hasn't really been used within our system. When we took our last snapshot, those things weren't there. What can we do with some of these advanced techniques? Some of them look pretty good.

## Session V: Future Metallization Challenges

G. Schwuttke (Consultant), Chairman

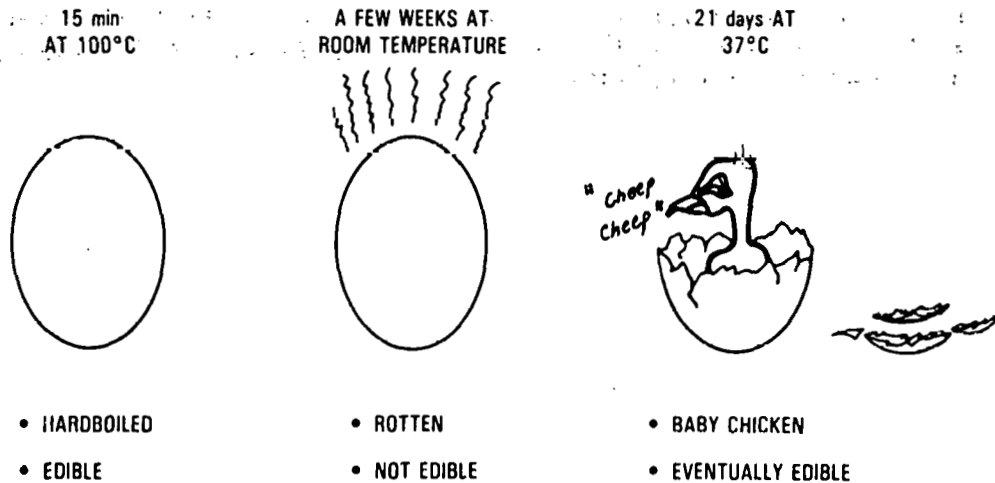
- Transparent Conductive Coatings  
S. Ashok (Pennsylvania State University)
- A Metallization System for Thin Film Photovoltaic Modules  
A. Firester (RCA Laboratories)
- Ion-Copper Metallization for Flexible Arrays  
H. Lavendel (Lockheed Palo Alto Research Laboratory)

Future metallization challenges: in the last session we are going to find out what is good, bad, or indifferent for the future.

Remember, we are looking for discussion and participation. I have one more viewgraph to show you. I will be perfectly honest: I stole this viewgraph.

# Thermal Aging of a Chicken Egg

## (A Problem of Prediction)



I saw it first at a discussion given by a gentleman from Kodak, and it impressed me. Ed Cuddihy of JPL stole it from him, and I made a direct steal from Cuddihy. I will put it up now, for it says a lot about what we are trying to do as well as what he is trying to do. That's why I didn't change it. I don't know if you have seen it before but it really does say a lot. First of all, this forum is being sponsored within the Jet Propulsion Laboratory's Flat-Plate Solar Array Project by the Process Research Task, and we believe that there is a lot to be said for process research. This viewgraph shows you two things we are always concerned with: simple things like temperature and time. Remember: with all these advanced process techniques we hear about, with all these process methods of forming a cell or an interconnect, a lot of things can happen with those two variables.

I turn this over to our first chairman, for the first session: Professor Martin Wolf from the University of Pennsylvania.

SESSION I: STATUS OF PHOTOVOLTAIC METALLIZATION SYSTEMS

Martin Wolf (University of Pennsylvania), Chairman

WOLF: As Brian mentioned, this first session is primarily looking backward. I guess the objective is primarily to get us all on a common denominator, so that from this point on we can start to look forward and have a look at requirements and future developments on an equal basis. The first speaker, therefore, is Bill Taylor, an old hand in the semiconductor device development and in solar cells particularly, from Photowatt International, Inc. He will give us a historical perspective on solar-cell metallization.

THIS PAGE  
WAS INTENTIONALLY  
LEFT BLANK

## SOLAR CELL METALLIZATION: HISTORICAL PERSPECTIVE

WILLIAM E. TAYLOR

Technical Director

Photowatt International, Inc.  
Tempe, AZ 85281

Collector grid design involves a compromise of the dimensions of junction depth, grid spacing and grid width (all of which should be small), and cost, which depends on the technology used and which determines the minimum grid width (Figure 1). As the grid width resolution becomes smaller, the other dimensions can be made smaller and cell performance will improve, but costs tend to be higher for technologies with fine line resolution capability.

1.  $X_j$  should be small:
  - a. increases blue response which increases efficiency,
  - BUT b. increases sheet rho, which increases  $R_s$  and decreases efficiency.
2. For given sheet rho, reducing  $s_g$  will:
  - a. reduce  $R_s$  (increase efficiency)
  - BUT b. increase shaded area, decreasing efficiency.
3. For given  $s_g$ , reducing  $W_g$  will:
  - a. decrease shaded area (increase efficiency)
  - BUT b. this is limited by technology and cost.

For space applications, metallization design is driven by the cost of lifting weight into orbit. Hence space cell technology uses shallow junctions with narrow gridlines at premium prices for high efficiency and high reliability. Metallization technology is evaporation or sputtering with shadow mask or photolithography for pattern definition.

For terrestrial applications, design is driven by cost. Hence terrestrial design compromises performance by using deeper junctions and wider grid lines spaced farther apart in order to achieve lower costs on a per peak watt basis. Current technology favors conductive screen printed inks or electroless nickel plating with pattern definition by screen printed resist.

Typical values of pertinent parameters for current commercial practice are shown in Figure 2.

Contact metallization must satisfy a number of functional criteria (Figure 3). The need to avoid junction degradation during processing and subsequent service life and to attain and maintain good adhesion are critical, and are strong determinants of the metallization system design and materials selection.



## SPACE CELL METALLIZATION TECHNOLOGY

The first solar cells had no front surface metallization. The diffused junction wrapped around the edge of the cell to the back, where contacts were made. This situation was improved on by deploying a grid of metallic conductors across the illuminated surface to collect the current near its origin. Metallization progressed in an evolutionary fashion (Figure 4) from electroless nickel through evaporated titanium-silver contacts, which were invented and patented by Marinaccio and Lepselet at Bell Laboratories, to passivated contacts having a thin layer of palladium under the silver to electrochemically passivate the titanium. Evaporated or printed aluminum is sometimes used to promote ohmicity of the back contact and reduce the titanium sinter temperature. The aluminum may be sintered to establish doping of the silicon surface layers (P plus back surface field).

The Ti-Pd-Ag contact system has become the standard qualified space cell metallization system against which alternatives are compared. Other transition metals are technically acceptable but have not been adopted for commercial practice. The preferred method of fabrication, evaporation through metal shadow masks, limits pattern and hence cell size. Need for large size cells in large space arrays is forcing the use of photolithographic technology for pattern definition.

### TERRESTRIAL SOLAR CELL METALLIZATION: PLATED CONTACTS

Electroless nickel plated contacts offer several advantages (Figure 5). The erratic and unreliable adhesion of electroless nickel can be overcome by sintering the contact, whereby a nickel silicide compound is caused to be formed. The nickel-silicon system is complicated by the formation of several different silicides (Figure 6). Nickel atoms diffusing into the junction depletion region can act as recombination centers and degrade cell performance. Anderson and Peterson observed that with 30 minutes sinter time, junction shunting becomes evident at 350 degrees and catastrophic at 450.

Electroless nickel plated contacts have been modified to improve adhesion and ohmicity by introducing thin layers of gold or palladium deposited by displacement or autocatalytic methods (Figures 8 and 9). The thin palladium deposit is sintered at 600 degrees to form the disilicide. The subsequent electroless nickel deposit is further sintered at 300 degrees to ensure a stable reliable contact.

Nickel plated contacts have a high sheet resistance, commonly overcome by solder coating. Copper plating over the electroless nickel is a cost attractive alternative which has been investigated, but is not yet in commercial use. Grenon and co-workers predict that such systems will have greater than 20 year life for exposure of 6 hours per day at 135 degrees.

### TERRESTRIAL SOLAR CELL METALLIZATION: PRINTED CONTACTS

The use of screen printing for solar cell contact metallization, first described by Ralph in 1972, has been extensively developed and is now widely used for terrestrial solar cells. The original screen printed metallization used commercial fritted silver conductive inks, and this has continued to be the practice.

The use of a brief dip in dilute hydrofluoric acid, frequently resorted to as a means of improving cell performance, results in such undesirable effects as unstable cell performance and erratic adhesion, both of which degrade in humid environments. Good, stable curve shapes can be obtained by the use of short (spike) firing techniques. This is typically achieved by sintering temperatures of 600 to 700 degrees for 30 to 120 seconds in infrared furnace equipment.

Sintering is carried out in an oxidizing atmosphere which generates an oxide layer on the silicon to which the frit can bond. However, the frit, acting as a flux for the oxide can allow the oxidation process to continue and to penetrate the junction. This possibly explains the necessity for the spike firing and the effects of HF treatment. Silver can also migrate to the junction by diffusion, resulting in degradation of cell performance. Junction depths of 0.35 to 0.5 microns are necessary to ensure long service life.

In the area of new developments, procedures to overprint and fire through TiO<sub>2</sub> AR coating have been described by Frisson. In the search for base metal systems, promising developments with molybdenum-tin have been reported by SOLOS and Spectrolab and with fritless copper inks by Ross.

#### TERRESTRIAL SOLAR CELL METALLIZATION: BACK CONTACTS

Back contacts are more difficult to establish because of the tendency to form Schottky barriers. The formation of a more heavily doped layer by boron diffusion or aluminum alloying is advantageous. Both evaporated and printed aluminum have been used to form the P<sup>+</sup> doped layer on the back surface. The aluminum must be sintered above the silicon-aluminum eutectic (577 deg. C) in order to provide the desired aluminum doped regrowth layer (Figure 11) which should be of the order of 1 micron thick. In the case of printed aluminum backs the use of a very short (spike) firing cycle at about 900 degrees has been effective. Overcoating with evaporated Ti-Pd-Ag, by electroless nickel plating or tin-zinc eutectic alloy applied by ultrasonic soldering iron technique have been used to form solderable pads on printed aluminum backs. Alternatively, the printed aluminum may be stripped and replaced with a printed silver contact in a gridded configuration.

Figure 1. Solar-Cell Collector Grid Metallization

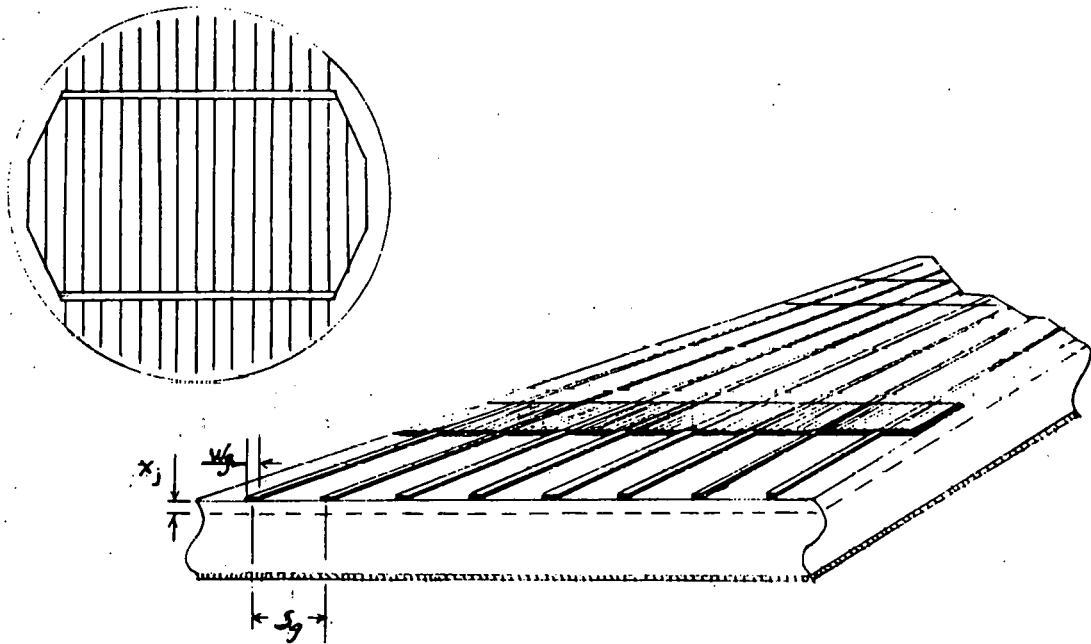


Figure 2. Typical Values

APPLICATION	$x_j$ MICRON	$w_g$ MICRON	$s_g$ MM.	EFF. %
SPACE	0.1	<50	1	14
TERRESTRIAL	0.35	>150	3	12

### Figure 3: Metallization Requirements

1. LOW RESISTANCE OHMIC CONTACT
2. AVOID PERFORMANCE DEGRADATION
  - JUNCTION SHUNTING
  - MINORITY CARRIER LIFETIME
3. GOOD ADHESION
4. LONG TERM STABILITY

### Figure 4. Evolution of Space-Cell Metallization

1. NO ILLUMINATED SURFACE METALLIZATION
2. ELECTROLESS NICKEL FRONT SURFACE GRIDS
3. EVAPORATED TITANIUM - SILVER, SOLDER COATED
4. TI-PD-AG (PASSIVATED)

### Figure 5. Attributes of Plated Contacts

1. SMALL CAPITAL INVESTMENT
2. AMENABLE TO LOW COST, HIGH VOLUME BATCH PROCESS MANUFACTURING
3. ADDITIVE PROCESS LIMITING MATERIAL COSTS
4. INSENSITIVE TO SURFACE IRREGULARITIES

Figure 6. Ni-Si Alloy System

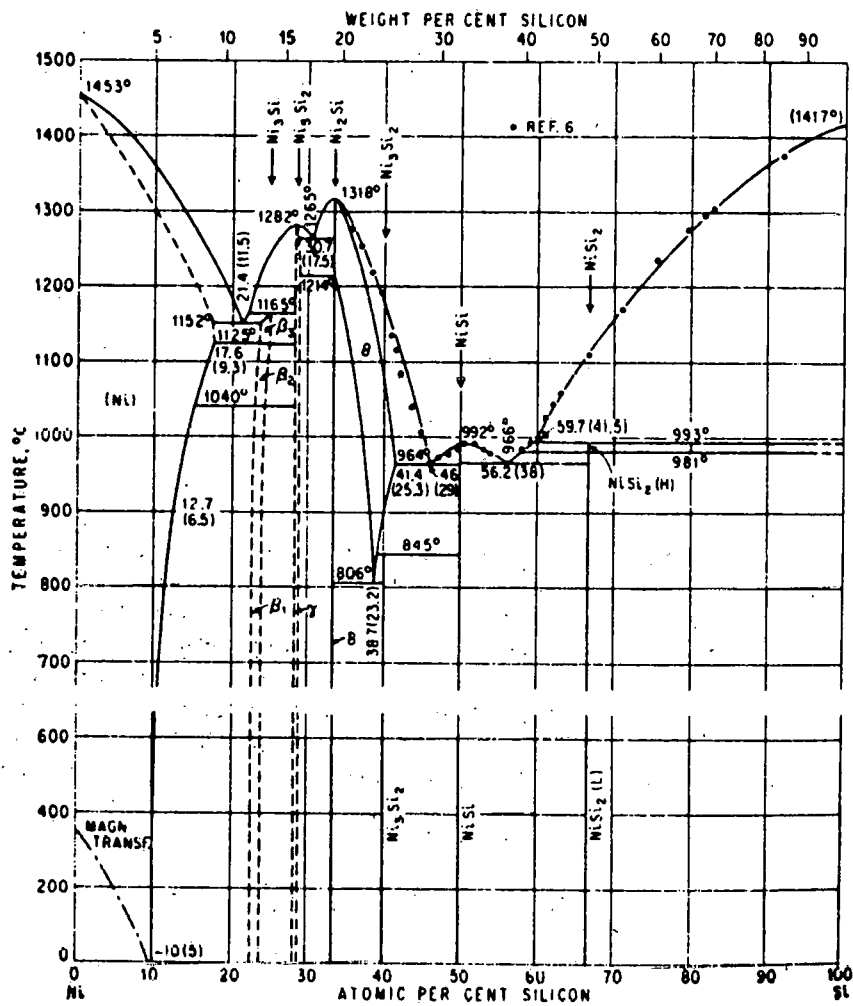


Figure 7. Effect of Sintering on Adhesion of Electroless Nickel Contacts

SINTER TEMPERATURE*	PEEL STRENGTH
No SINTER	90 GRAMS
200°C	332
250	391
275	510
300	618

\*20 SECONDS SINTERING TIME

Figure 8. Pd-Si Alloy System

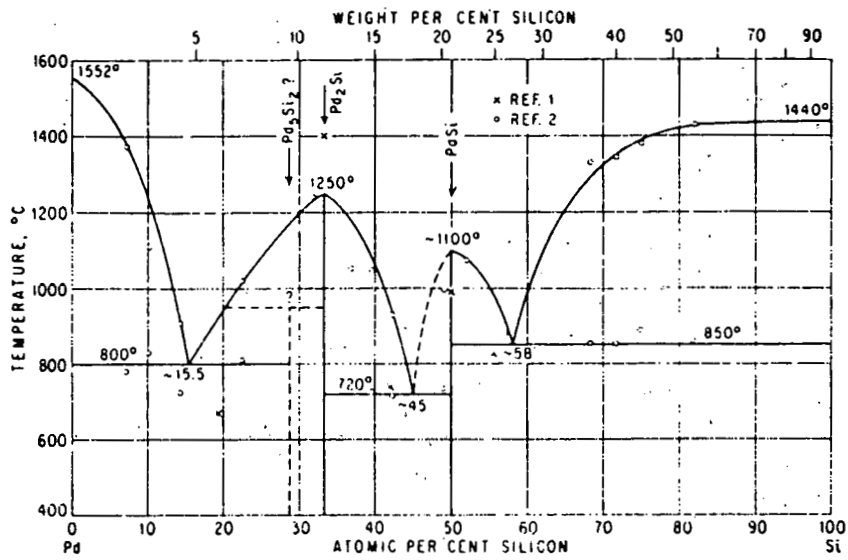
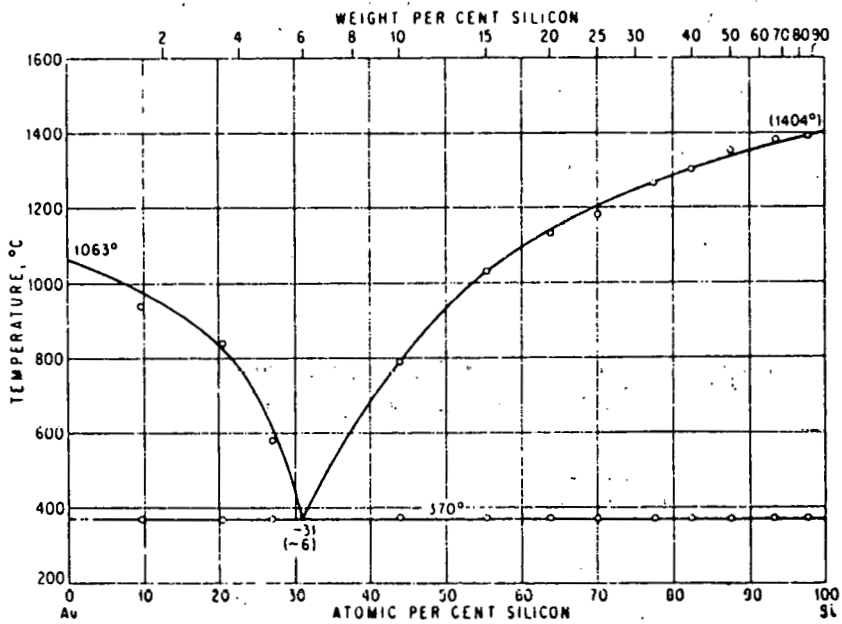


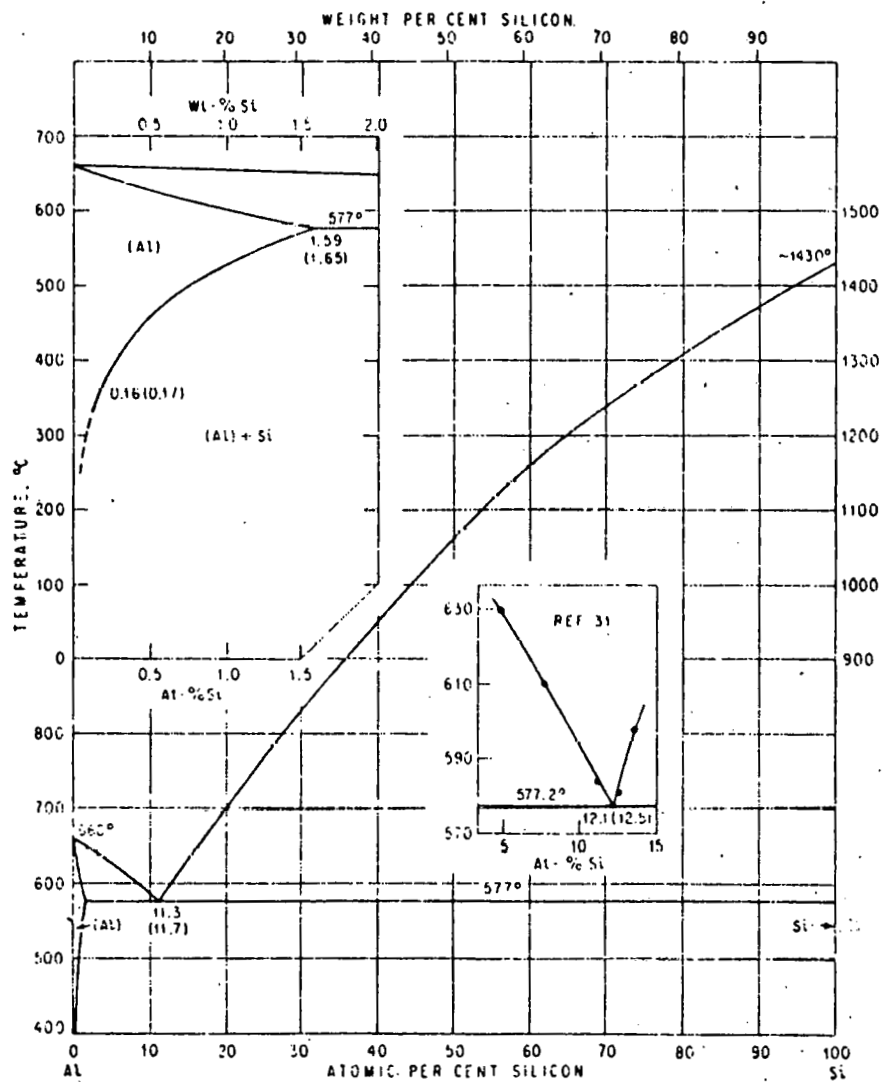
Figure 9. Au-Si Alloy System



## Figure 10. Evolution of Plated Contact Technology

1. SIMPLE ELECTROLESS NICKEL PLATING WITH SOLDER COAT
2. USE OF AR COATING AS PLATING RESIST
3. USE OF AU OR Pd TO PROMOTE ADHESION AND OHMICITY
4. COPPER PLATING TO REPLACE SOLDER COAT

## Figure 11. Aluminum-Silicon Alloy System



## DISCUSSION

WOLF: Thank you very much. At least we have advanced tremendously with our metallization problems at a time when most of the problems were not well understood, particularly these questions of residual chemicals being interfaces -- interacting with environments -- which led in early times to customers concluding that you might as well ship the contacts in one box and the cells in another.

NICOLET: I would like to make a couple of comments. The first one has to do with the nickel-copper system. Nickel and copper form a solid solution, so I think it is evident that by combining these two elements you don't have a stable system. By stability I mean if you wait long enough it will change. The second comment is perhaps worthy of note here. We did investigate the matter, and we found to our surprise that the palladium-silicon phase diagram that you projected, from Hanson, is wrong. The nickel-and-platinum-based systems with silicon are also wrong. If you are interested I can give you a later reference. It surprised me these things are so old and yet not fully understood. PdSi is peritectically dissociating at 70°C.

TAYLOR: I agree with your first comment about the copper-nickel system. If you wait long enough or if you expose the system to high enough temperature, copper is going to migrate. Pryor and coworkers at Motorola have looked at that problem and have shown that for 20-year life, the copper-nickel system is a viable system. With respect to the phase diagram, I find this to be a very interesting question, I have looked at those phase diagrams and there is something about those diagrams that has to be wrong. I think that what we are seeing there is that the early phase-diagram work looked at reactions going on at fairly high temperatures and then they just dropped everything down to lower temperature. We are now dealing with systems in which we are using the low temperatures, and those same reactions are going on, and I think that a reevaluation of those types of systems is a thing we need.

WONG: Bill, I have a question. When you showed the gold silicon phase diagram I saw no significant solubility between those two constituents; I wonder whether you couldn't have adhesion problems at the gold and silicon interface, because thermodynamically it is hard to form the interface.

TAYLOR: Well, one certainly has a certain amount of solid solubility. The diagram I use there was taken from a fairly accurate reference. The solubility is so limited by the chart, there is no way one can get good adhesion.

LAVENDEL: I would like to complement your information on the use of welding to titanium-palladium-silver systems in this country. Lockheed has a very extensive program with respect to solar arrays where the welding of copper interconnect to silver metallization is used. At this present moment extensive tests equivalent to the low earth orbit for five years -- -80° to +80°C cycles -- have been performed and very little damage to the welds were found. We found some traces of some problems



that might not be connected to fatigue but might be connected to entrapment of these pottants in some of the silver compound.

TAYLOR: Yes, I was aware of the Lockheed program and I think you people are perhaps farther along than anybody else that I know. This is still a program that is being proven out.

LAVENDEL: It could be applied to one of the coming shuttle flights.

TAYLOR: I don't think it has as yet been applied. There is in this country a program that was initiated by NASA to reopen the whole subject of welding technology. I have not heard what has been happening this past year. I am sure there is a lot of interest on the part of space people in welding technology.

STEIN: We have done a lot of work on ultrasonic aluminum wire and ribbon bonding to silver-bearing conductive coatings, such as the silver that might be used on a silicon solar cell. We haven't done this on silicon itself as a substrate. However, with some systems we see age stability and thermal cycling stability comparable, certainly, in an accelerated way, to 20 years of life. It is a bit different from welding.

TAYLOR: Thank you for your comment. I don't really have anything to add there. I know that is a technology that is being worked on.

WOLF: We will proceed to the second speaker of the session.

## ECONOMIC IMPLICATIONS OF CURRENT SYSTEMS

R.E. Daniel and R.W. Aster  
Jet Propulsion Laboratory  
California Institute of Technology  
Pasadena, California 91109

### Introduction

The primary goals of this study are to estimate the value of R&D to photovoltaic (PV) metallization systems cost, and to provide a method for selecting an optimal metallization method for any given PV system. The value-added cost and relative electrical performance of 25 state-of-the-art (SOA) and advanced metallization system techniques are compared.

The data for the cost estimates comes from Flat-Plate Solar Array Project (FSA) contractors and other sources. The Improved Price Estimation Guidelines methodology (IPEG2) (Reference 1) was used to make the cost estimates.

Most of the data for the cell-performance calculations comes from a report by Martin Wolf (Reference 2). These data are used in conjunction with a grid optimization model (Reference 3) developed at JPL.

This report introduces two new concepts for evaluating metallization systems: the efficient frontier and the tradeoff slope.

Some study limitations are presented in the viewgraphs. Most notably, advanced metallization costs are usually extrapolated from laboratory-scale experiments, and back-metallization cost and performance data are not included.

### Costing Methodology

The front-metallization process steps, evaluated by the IPEG2 methodology, include masking, metal deposition sintering, mask removal and plate-up. The inclusion of a copper ribbon as a strap, to increase the conductivity of the cell bus bars, increases the material costs and slightly increases the operating cost of the cell-stringing process step.

The IPEG equation is shown in the viewgraphs, as are the data sources for the process costs and the final cost breakdown for both strapped and non-strapped cells. The effects of a price swing for silver from \$10/oz to \$50/oz and for molybdenum-tin from 4.2¢/gm to 8¢/gm are shown in the cost tables.

### Electrical Performance Calculation

In this context, the electrical performance of the solar cells studied is the ratio of the expected output power to the output power of a lossless (no resistive losses or shadow losses) cell. This calculation is made using the JPL grid optimization program (Reference 3). The program takes into

account the resistive losses from the photoconductor sheet, metallization material and contact of the metal with the silicon sheet as well as the loss due to the shadowing of the grid structure. The program also uses the solar-cell operating characteristics as input values. For this study, the solar cell is assumed to be a 10 x 10-cm silicon cell with a sheet resistance of  $40\Omega/\square$ , maximum power voltage of 0.45 V and a maximum power current density of  $30\text{ mA/cm}^2$  at an insolation of  $100\text{ mW/cm}^2$ . Each cell is designed with two bus bars and the fine grid lines evenly spaced and perpendicular to them. It is assumed that the grid lines are rectangular in cross section, of uniform thickness and homogeneous in material content.

For each process studied a maximum metallization thickness and a minimum fine-grid-line width was chosen to be consistent with that process's technology. The program then calculates the optimal bus-bar width and fine-grid-line spacing that minimizes the power loss due to the grid design.

The above optimization procedure was performed twice for every process technology. The cell performance was calculated for cells with only the metallization bus bars for current collection and again for cells having a fine copper ribbon fastened over the metallized bus-bar pattern. The one exception is for state-of-the-art (SOA) screen-printed aluminum, where bonding copper to aluminum is very difficult.

### Efficient Frontier

In the viewgraphs are plots, for the SOA and advanced systems, of the process cost versus the process performance ratio. (Two connected points represent the processes using silver.) A point is said to be on the efficient frontier if there is no other point that has both a higher performance ratio and a lower cost.

A plot of only the points on the efficient frontier for both SOA and advanced systems is shown for comparison in the viewgraphs.

### Tradeoff Slope

The tradeoff slope developed for this study comes from the following consideration: the total area-related system cost [total system cost minus the non-area-related power conditioning system (PCS) cost] times a change in electrical performance yields an allowable change in metallization costs. The ratio of these changes yields the tradeoff slope. (See expression in the viewgraphs.) The reference cost allocations used to make the tradeoff slope calculations come from Sacramento Municipal Utility District (SMUD) data and U.S. Department of Energy (DOE) advanced-system-level cost-goal allocations (to be published).

### Metallization System Optimization

Assuming that the efficient frontier curves represent the best-known systems, then the optimal system, on each curve, is the one that is first

intersected by the tradeoff slope as the tradeoff slope is moved from the highest-performance, lowest-cost position to the lowest-performance, highest-cost position on the graph.

Any system improvements or new system developments that fall on the tradeoff slope line (that is, intersecting the above-described optimal system point) are now equally optimal. Any system that pushes the tradeoff slope line back to the higher-performance, lower-cost corner is an improvement in terms of the total system costs.

### Process Yield Impact

Present understanding of the system process yields suggest a fairly stable yield ( $0.98 \pm 0.01$ ) for all systems investigated.

Two notable exceptions are: SOA evaporation, so far, has a 0.89 mechanical yield because of handling, and the Midfilm process has an 0.80 electrical yield due to sheet-resistance variations.

### Conclusion

The efficient frontier and the tradeoff slope can be used to identify those metallization systems that are either already optimal systems or close enough to warrant additional R&D. Likewise, those systems that are far away from the frontier or the tradeoff slope line should be given careful consideration before receiving more R&D attention.

### References

1. Aster, R.W., and Chamberlain, R.G., Interim Price Estimation Guidelines, JPL Internal Document No. 5101-33, September 1977.
2. Wolf, M., and Goldman, H., Assessment of Metal Deposition Processes, Quarterly Report, July to October 1980, DOE/JPL-954996-81/12, Jet Propulsion Laboratory, Pasadena, California, January 1981.
3. Daniel, R., Burger, D., and Stone, H., "Optimization Program/Methodology for Designing Solar Cell Grid Patterns," Proceedings of the Electrochemical Society, May 1982.

## Introduction

### **Purpose of this analysis:**

- **Compare costs and effectiveness of SOA metallization and projected metallization approaches**
- **Estimate the potential impact of R&D in this area**

### **Approach:**

- **Use data from FSA contractors and other sources with IPEG2 to establish costs**
- **Use Grid Optimization Model to establish electrical performance ratios**

## Study Limitations

- **There are many metallization processes; only 25 have been analyzed so far**
- **SOA metallization costs are typically based on commercial experience of industry**
- **Advanced metallization costs are typically based on laboratory-scale experiments and extrapolations**
- **There are two basic reliability issues:**
  - **Immediate mechanical and subsequent electrical test yields. (This has been addressed by this study)**
  - **Lifetime (e.g., 20-year) performance. (This has not yet been addressed)**
- **Compatibility with other process steps and with unusual sheet specifications will not be addressed**
- **Back metallization cost and performance data not included in the evaluation**

## Candidate Processes and Systems

PROCESS/SYSTEM	DATA SOURCE
<b>Evaporation</b>	
• SOA (Ti/Pd/Ag)	ASEC
• Advanced (Ti/Ni + Cu plating*)	Westinghouse
<b>Screen print</b>	
• SOA (Ag paste)	2.80/W, Block IV
• 1990 (Ag paste*)	JPL BPU
• SOA (Al Paste)	2.80/W, Block IV
• 1990 (Al paste*)	JPL BPU
• 1990 (Mo/Sn*)	JPL BPU, Dr. Macha
<b>Electroless plating</b>	
• SOA (Print resist, Ni-plate, Sinter, Wave solder)	Solarex, Motorola
• SOA (Print resist, Ni-plate, Sinter, Cu plate)	Solarex, Motorola
• Advanced (PR, Ni plate, Sinter, Cu plating*)	Motorola
Midfilm* (Ag)	Spectrolab
Midfilm* (Mo/Sn)	Spectrolab, Dr. Macha
Ion plating* (Ti/Ni/Cu)	Illinois Tool Works

\*Advancement of PV SOA

## Electrical Performance Methodology

- Optimum spacing and dimensions (within process constraints) are calculated using the Grid Optimization Model
- Cell efficiency is strongly influenced by sheet characteristics, junction quality, AR coating, and test conditions as well as by metallization process/system
- Therefore, *relative* electrical performance is derived in this study
- Input data that influence relative electrical performance are:
  - Metallization material resistivity,  $\rho_M$  ( $\Omega$ -cm)
  - Metal-to-silicon contact resistivity,  $\rho_C$  ( $\Omega$ -cm<sup>2</sup>)
  - Metallization thickness, T (cm)
  - Fine grid line width, B (cm)
  - Resistivity of busbar strapping material,  $\rho_{MB}$  ( $\Omega$ -cm)
  - Strapping material thickness, T<sub>B</sub> (cm)
  - Sheet resistance, R<sub>S</sub> ( $\Omega/\square$ )
  - Voltage at max. power, V<sub>m</sub> (volts) and current density, at max. power, J<sub>m</sub>(A/cm<sup>2</sup>)

## Electrical Performance Optimization Model Inputs

PROCESS/SYSTEM	$\rho_M$ ( $\Omega\text{-cm}$ )	$\rho_C$ ( $\Omega\text{-cm}^2$ )	$T_1$ ( $\mu\text{m}$ )	$T_2$ ( $\mu\text{m}$ )	$B$ ( $\mu\text{m}$ )	RATIO	
						STRAP	NO STRAP
Lossless*	0	0	—	—	0	1.000	1.000
EVAP SOA	$1.6 \times 10^{-6}$	$1 \times 10^{-4}$	4	8	38	0.919	0.875
EVAP Advanced	$2.03 \times 10^{-6}$	$1 \times 10^{-4}$	4	8	38	0.914	0.863
Print Ag SOA	$4.77 \times 10^{-6}$	$1 \times 10^{-3}$	8	8	127	0.892	0.790
Print Ag Advanced	$4.77 \times 10^{-6}$	$1 \times 10^{-3}$	12.7	12.7	127	0.898	0.820
Print Al SOA	$2.00 \times 10^{-5}$	$1 \times 10^{-6}$	—	8	127	—	0.652
Print Al Advanced	$2.00 \times 10^{-5}$	$1 \times 10^{-6}$	12.7	12.7	127	0.871	0.705
Print Mo/Sn	$2.95 \times 10^{-5}$	$1 \times 10^{-3}$	12.7	12.7	127	0.856	0.660
Electroless Ni/Solder SOA	$2.00 \times 10^{-5}$	$1 \times 10^{-3}$	50.8	50.8	457.2	0.833	0.760
Electroless Ni/Cu SOA	$2.00 \times 10^{-6}$	$1 \times 10^{-3}$	8	8	457.2	0.835	0.782
Electroless Ni/Cu Advanced	$2.03 \times 10^{-6}$	$1 \times 10^{-4}$	4	8	38	0.914	0.863
Midfilm Ag	$4.77 \times 10^{-6}$	$1 \times 10^{-3}$	10	10	45.7	0.913	0.821
Midfilm Mo/Sn	$2.95 \times 10^{-5}$	$1 \times 10^{-3}$	15	15	45.7	0.871	0.696
Ion Plating, Ti/Ni/Cu	$1.76 \times 10^{-6}$	$1 \times 10^{-4}$	4	8	38	0.917	0.871

\*Baseline values are  $40 \Omega/\square$  sheet resistance, 0.45V max power voltage,  $30 \text{ mA/cm}^2$  max power current density  
 Copper Ribbon Strap —  $\rho_{MB}$  ( $\Omega\text{-cm}$ ) =  $1.76 \times 10^{-6}$ ,  $T_B$  ( $\mu\text{m}$ ) = 63.5

$T_1$  = metallization thickness with strapping,  $T_2$  = metallization thickness without strapping



## Cost Methodology

This study focuses on front metallization, which can include the following process steps:

- Masking
- Metal deposition
- Sintering
- Mask removal
- Plateup

It also includes the cost of strapping with a copper ribbon in some cases; this involves an increase in material costs and a small increase in operating costs at the cell-stringing process step

COST DATA came from sources given on the next viewgraph; actual amounts of metal used came from the electrical performance model and from utilization rates reported by M. Wolf

IPEG2 processed this data to provide total costs of front metallization in terms of \$/m<sup>2</sup>

The expression used was:

$$\frac{C(1)*EQPT + 109*SQFT + 2.1*DLAB + 1.2*(MATS + UTIL)}{QUAN}$$

where C(1) comes from the following table:

EQPT Lifetime	3	5	7	8	10	15	20
C(1)	0.83	0.65	0.57	0.55	0.52	0.48	0.46

## Optimization

- The optimal metallization process/system will be on the efficient frontier
- The optimal point depends on the *total* area-related system cost. Take the total system cost and subtract FCS costs (these are not area-related). The total area-related system cost times a change in electrical performance yields an allowable change in metallization costs. The ratio of these changes yields a tradeoff slope from the expression:

$$1/[1,000 \text{ W/m}^2 * \text{Module Efficiency} * \text{Area-related System Costs}]$$

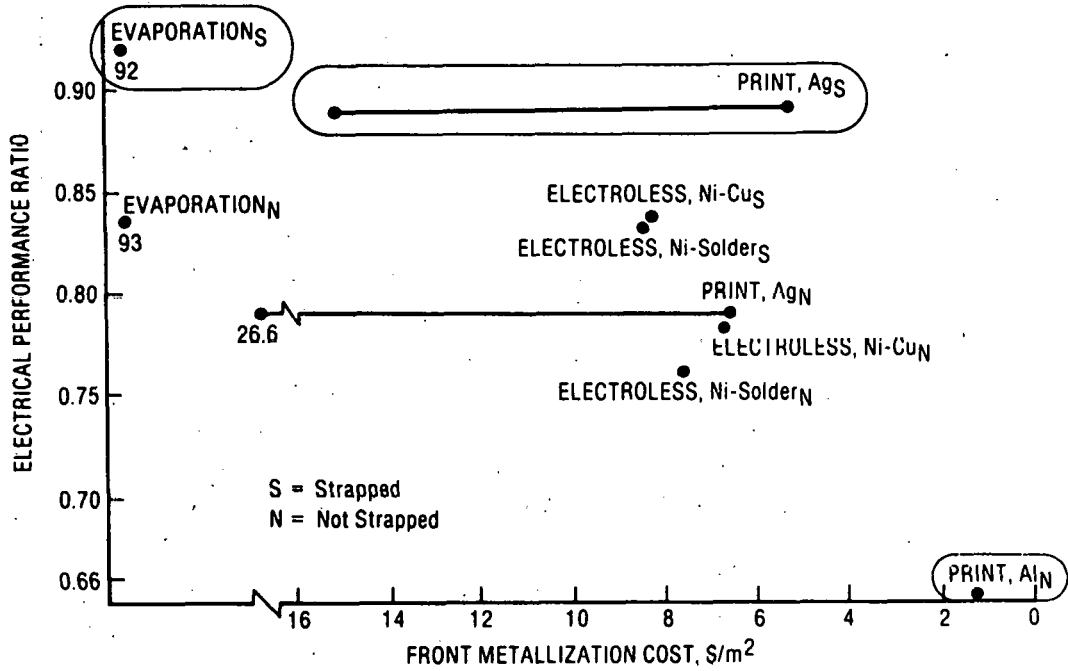
- We have used SMUD data for a SOA slope and 1986 Program goals for an advanced slope in the following table

	Baseline Efficiency	Area-related System Costs	Slope
SMUD SOA	0.11	\$11/W	$8.26 * 10^{-4}$
Advanced	0.14	\$1.2/W	$5.95 * 10^{-3}$

## Process Yields

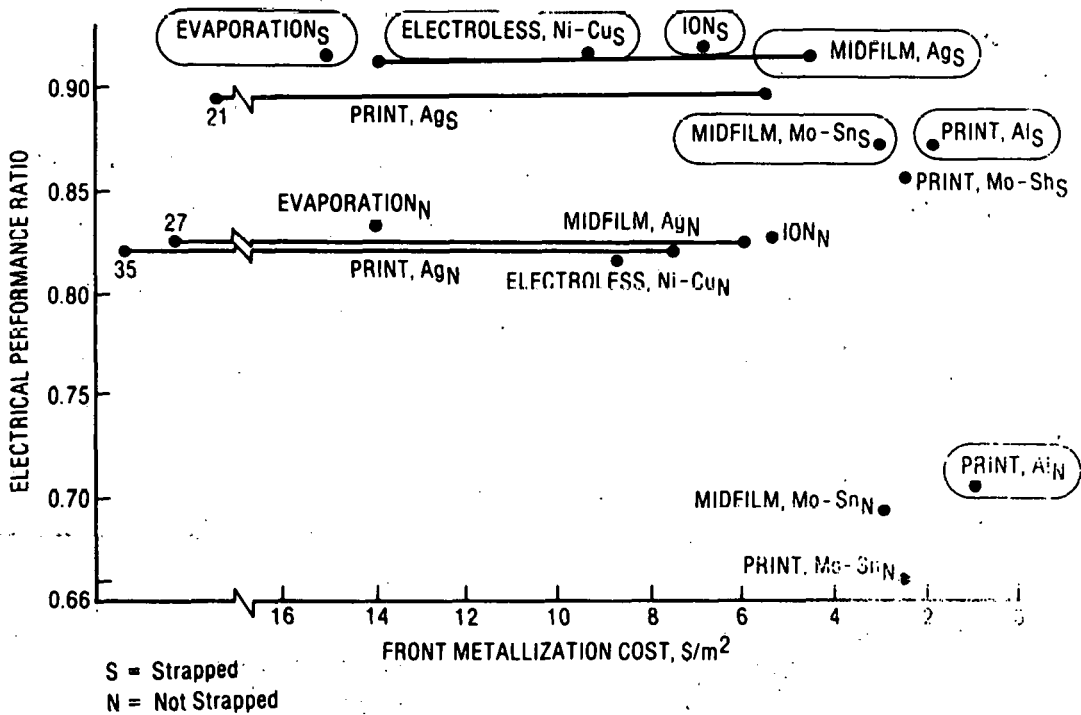
- Nearly all metallization processes appear to have essentially the same yield ( $0.98 \pm 0.01$ ). In these cases there is no significant relative advantage
- There are two exceptions:
  - SOA evaporation includes substantial manual handling of wafers, which results in a 0.89 mechanical yield (ASEC Block IV report)
  - Midfilm has demonstrated a 0.98 mechanical but only a 0.80 electrical yield due to sheet resistance variations. This problem may or may not be resolved through R&D
- A SOA diffused wafer will cost at least \$200/m<sup>2</sup> and a 10% loss adds at least \$20/m<sup>2</sup> to the total cost of the process
- An advanced diffused ribbon could cost from \$10/m<sup>2</sup> to \$40/m<sup>2</sup>

### Efficient Frontier: State of the Art

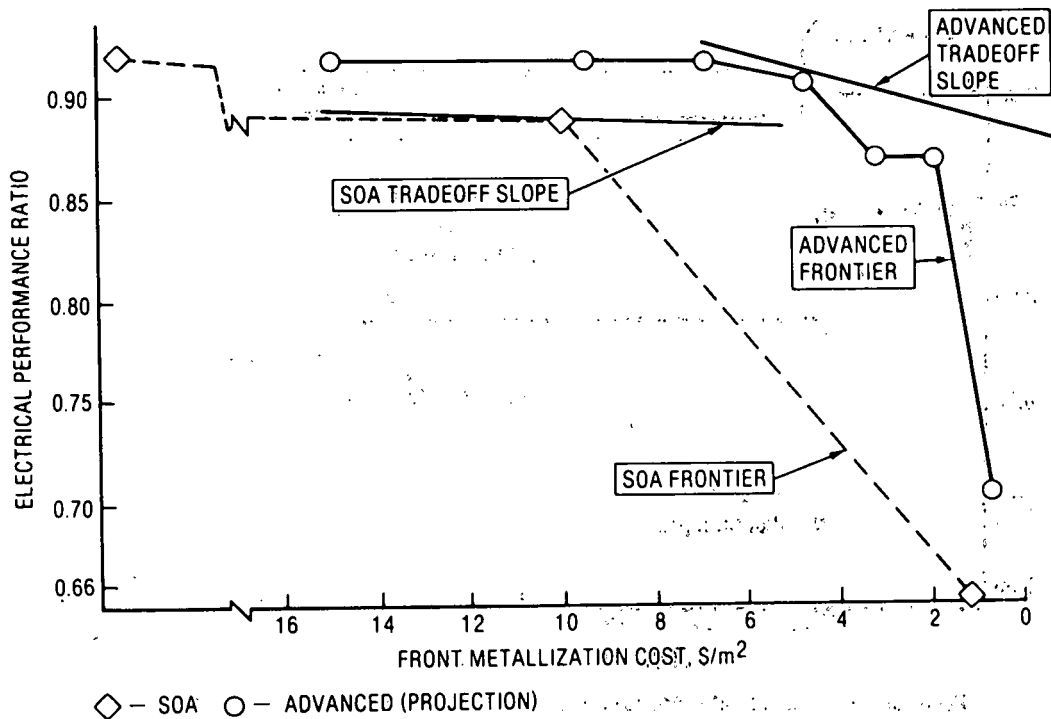


Points on the efficient frontier are as good as any other point in terms of either cost or performance; these are circled

### Efficient Frontier: Advanced Systems



### Combined Efficient Frontiers



### Cost Breakdown, No Strapping (\$/m<sup>2</sup>)

Process/System	C(1)•EQPT	109•SQ FT	2.1•DLAB	1.2•MATS +1.2•UTIL	TOTAL
Evaporation, SOA	7.35	2.42	32.40	50.50	92.7
Evaporation, Advanced	5.26	0.98	4.25	3.61	14.1
Print, Ag, SOA*	0.71	0.30	0.52	5.09-25.07	6.6-26.6
Print, Ag, Advanced*	0.35	0.15	0.26	6.82-33.91	7.6-34.7
Print, Al, SOA	0.71	0.30	0.52	0.21	1.7
Print, Al, Advanced	0.35	0.15	0.26	0.20	1.0
Print, Mo-Sn**	0.35	0.15	0.26	1.20- 2.20	2.0- 3.0
Electroless, Ni-Solder, SOA	1.43	1.89	2.45	1.93	7.7
Electroless, Ni-Cu, SOA	1.61	1.69	2.02	1.34	6.7
Electroless, Ni-Cu, Advanced	1.35	1.75	3.35	2.15	8.6
Midfilm, Ag*	0.20	0.29	0.38	5.55-25.84	6.4-26.7
Midfilm, Mo-Sn**	0.20	0.29	0.38	1.53-2.52	2.4- 3.4
Ion Plating, Ti-Ni-Cu	NA	NA	NA	NA	6.0

\*Ag price range of \$10/oz to \$50/oz

\*\*Mo-Sn price range of 4.2c/g to 8c/g

## Change in Cost Due to Strapping (\$/m<sup>2</sup>)

Process/System	New 1.2•(MATS+UTIL)	Plus Strapping	New Total
Evaporation, SOA	48.68	1.0	91.8
Evaporation, Advanced	3.60	1.0	15.1
Print, Ag, SOA*	2.65-12.88	1.0	5.2-15.4
Print, Ag, Advanced*	3.94-19.52	1.0	5.7-21.3
Print, Al, SOA	0.14	1.0	2.7
Print, Al, Advanced	0.11	1.0	1.9
Print, Mo-Sn**	0.47- 0.85	1.0	2.2- 2.0
Electroless, Ni-Solder, SOA	1.63	1.0	3.4
Electroless, Ni-Cu, SOA	1.33	1.0	7.0
Electroless, Ni-Cu, Advanced	2.14	1.0	9.6
Midfilm, Ag*	2.85-12.37	1.0	4.7-14.2
Midfilm, Mo-Sn**	0.87- 1.23	1.0	2.7- 3.1
Ion Plating, Ti-Ni-Cu	NA	1.0	7.0

\*Ag price range of \$10/oz to \$50/oz

\*\*Mo-Sn price range of 4.2¢/g to 8¢/g

### Summary

- **Cost and effectiveness of metallization systems have been compared**
- **Twenty-Five processes have been examined so far**
- **This study shows that metallization R&D could lead to significant advances in low-cost, high-performance processing**

## DISCUSSION

HOGAN: How viable are the non-noble metal thick-film ink systems?

GALLAGHER: The data you hear will be relatively new, and I doubt that the cost information is available yet, but certainly the electrical performance and some of the physical characteristics of that structure will be.

HOGAN: What was the advanced evaporation system used?

DANIEL: That would be the nickel plus copper plating, and the information for that came from Westinghouse.

CAMPBELL: On one slide you showed the SMUD and the advanced evaporation process area-related cost. I believe SMUD was \$11 and the advanced was \$1.20. Can you tell me how those were derived? And specifically the \$11? Does that include any module cost?

DANIEL: Yes. Those were the total cost less power-conditioning costs that are not area-related. All processing costs are in there. How the \$11 came up, I'm not sure, because they came out of the details of the SMUD work.

CAMPBELL: What about the \$1.20?

DANIEL: The \$1.20 was one of the Project goals.

CAMPBELL: That \$1.20 did not include modules, I believe. My question is: the \$11 per watt you said included the price of the module, which I believe was around \$4.50 or \$5.00. Is that correct?

DANIEL: I don't know the individual breakdown.

CAMPBELL: OK, but it is a total cost. Is it then true that the advanced, the total cost, of getting this thing situated is \$1.20?

DANIEL: Are you talking about installation in the field, or --

CAMPBELL: I am talking about something that is sitting out there, the area-related cost.

DANIEL: No. That is not true then.

WEAVER: Ron, I think he's asking are they both exactly on the same basis.

DANIEL: To my knowledge, they should be. Again, I didn't do this end of the analysis. All I was doing was giving you this information, and I would have to believe it was done on the same basis.

CAMPBELL: The only reason I am asking is, there is a tremendous difference in the area-related costs for only a 3% efficiency.

BICKLER: I think, to be on a comparable basis, the total SMUD cost was something like 15 or 16 bucks. I think it is mistaken to say that the module cost was \$11. I think the \$11 is simply the area-related costs.

GALLAGHER: I think so too, but can we find out before the meeting ends. We have two days and a telephone. We will get you the answer.

(EDITOR'S NOTE: The dollars quoted were for a mounted and installed facility without power-conditioning addition.)

ILES: I was a little disturbed about the yield numbers, 0.98, because for nearly all the processes it makes the Research Forum not worth doing, in many of these cases, because 98% is about as much as you would want. I suspect that because the efficiency is rattling around in there -- I think the needle just moved, and you say it is a live cell, but I think you have to look a little closer at what you mean by electrical efficiency, not in the model but in real life, because some of the newer metallization systems have a lot of problems in many respects. But the question is, whether the lifetime before it peels off is longer than the lifetime in the bulk of the silicon. I really wasn't meaning to be facetious, but I think that 98% gives everybody a very complacent feeling if you don't look at the details. I realize your problem, because not everybody will talk to you and tell you what their yields were. I am sure that most people doing screen printing have some breakage until they get completely mechanized.

DANIEL: Yes. The mechanical yields that we talked about in this discussion were from information that was provided to us through the contractors, and we are using the SAMICS-type analysis, and from what information we have this is what everybody was saying -- either the 0.97 or 0.99 mechanical yield.

WOLF: At that process step.

DANIEL: Yes. At the particular process step under discussion.

AMICK: It's a mechanical yield, not an electrical yield.

DANIEL: Yes. It is a mechanical yield, not electrical, and that of course is another entity analysis. After you have done all that, how well does the cell perform? That particular information generally is left out of the process step analysis, in terms of costing, and we try to put it back in by looking at the metallization characteristics. If we were to do the best job we could with the grid design, what kind of an electrical performance could be expected if everything was working very well? Again, there is no overlapping of the mechanical yield, and in this case, the electrical performance and the lifetime of the whole monitoring system.

RIEL: Back to the same question as Bob Campbell's. The SMUD area-related system cost of \$11 -- does that include the power-conditioning cost?

DANIEL: No, in that case it does not include the power-conditioning costs.

TAYLOR: I would like to come back to Peter's (Iles) discussion of the yield question. He pointed out that there is another aspect to the yield. You have to be careful of that. And that is, yes, these processes are running along at 98% yield and then you have a yield bust. For a week or so your yield is like 40% or 50%. When you ask people what their yields are, they give you the 98% and they don't tell you about the yield bust.

WEAVER: It's the 30-year yield, that's what you really want to know.

DANIEL: Well, certainly, if the lifetime of the whole system were not all integrated into this analysis, and that point is well taken. If you are talking about an instantaneous yield, certainly, if you have this yield bust going on. Until that is solved, not only does it impact that particular cost effort, it impacts all of the upstream processes also, because you have an expected output of production and you are continuing to lose cells at that later point. You have to increase everything upstream so it increases not only the direct cost at the process step -- which, in terms of the yield, is linear if it is only a small yield (over factors of 2 it's probably not linear any more) -- but certainly the impact goes all the way up the chain, so the value-added cost incurred at the metallization process step then becomes misleading because of its impact on certain other process steps preceding it.

WOLF: This seems to exhaust the questions about this paper.



THIS PAGE  
WAS INTENTIONALLY  
LEFT BLANK

## ACCELERATED DEGRADATION OF SILICON METALLIZATION SYSTEMS

Jay W. Lathrop  
Department of Electrical and Computer Engineering  
Clemson University, Clemson, SC 29631

### INTRODUCTION

Clemson University has been engaged for the past five years in a program to determine the reliability attributes of solar cells by means of accelerated test procedures (1). The approach, as shown in Figure 1, is to electrically measure and visually inspect the cells, then subject them for a period of time to stress in excess of that normally encountered in use, and then to remeasure and reinspect the cells. Changes are noted and the process repeated. This testing has thus far involved 23 different unencapsulated cell types from 12 different manufacturers, and 10 different encapsulated cell types from 9 different manufacturers. Unencapsulated cells were subjected to a variety of tests: bias-temperature testing at 75, 135, and 150 °C, bias-temperature-humidity testing at 85% relative humidity and 85 °C, pressure cooker testing at 121 °C and 15 psig steam, and thermal shock and thermal cycle testing from +150 to -65 °C. Encapsulated cells because of the limitations of organic pottants have been subjected mainly to 85/85 testing and to thermal cycle from +95 to -65 °C.

The basic structure of a solar cell is shown schematically in Figure 2. In an effort to simplify the manufacturing process the metallization on both sides of the cell is usually the same. The purpose of the metallization is twofold: to make electrical connection to the silicon and to transport the current to the leads. Solar cell metallization systems in general consist of a thick current carrying layer plus one or more thin barrier/strike layers which interface the conductive layer to the silicon. There are essentially four different generic metallization systems in use today, as shown in Figure 3 -- vacuum deposited silver (titanium/palladium/silver), electroplated copper, screen printed silver frit, and solder coated nickel. In this figure the thick conductive layers are shown approximately to scale and the effect of different electrical conductivities can be easily seen. The thick high conductivity layer primarily influences the cost of the system, while the barrier/strike layers primarily influence the reliability of the system. In a comprehensive study of metallization costs, which considered both materials and processing, Wolf and Goldman (2) showed the thick layer to be the cost driver and they concluded that the only system which could be considered truly low cost was the copper plated structure.

Reliability attributes of metallization systems can be classified as major or minor, depending on the severity of the effects observed. As a result of the accelerated testing conducted under the Clemson program, major effects have been observed related to contact resistance and to mechanical adherence and solderability. Increasing the contact resistance as a result of stress will cause a degradation of the cell's electrical output, while

adherence and solderability problems can result in catastrophic failure through open circuits. Minor effects observed include diffusion of metallization into the bulk semiconductor resulting in decreased minority carrier lifetime and a consequent reduction of  $I_{sc}$  and possibly increased series resistance. Dissolution of metallization through corrosion resulting in increased series resistance is also possible, but has not been identified as a significant problem in cells tested thus far.

As summarized in Figure 4, the thick layer has essentially only two functions -- to transport current and to provide a solder interface to the external lead -- whereas the thin layers have a number of functions. These include making an ohmic, low resistance connection to the silicon, serving as a non-penetrating diffusion barrier, providing a uniform and easily platable surface, serving as the glue for good adherence of the thick layer, and providing a transition layer for any thermal mismatch.

The cells tested in the Clemson program had a wide variety of barrier/strike layers. Conductive layers could easily be identified as belonging to one of the four categories shown in Figure 3, but more often than not the composition and thickness of the barrier/strike layers was unknown. Furthermore, manufacturers are naturally reluctant to release proprietary information on film composition and deposition techniques, which represents one of the key trade secrets of solar cell processing. Therefore, despite the numerous accelerated tests which have been run, it is difficult to interpret the data obtained on specific cell types as relating to generalized metallization systems. In addition to the uncertainty of the metals and the deposition methods involved, it is often difficult to attribute the degradation observed as a result of testing to the metallization, rather than to some other aspect of the solar cell. The loss of mechanical adhesion, for example, would appear to be a straightforward problem of metallization, but an increase in series resistance could be either a contact problem or a change in the bulk resistivity. This paper, therefore, does not attempt a generalized survey of accelerated test results, but rather concentrates on one particular attribute of metallization that has been observed to cause electrical degradation -- increased contact resistance due to Schottky barrier formation. In this example basic semiconductor theory was able to provide an understanding of the electrical effects observed during accelerated stress testing.

#### EXPERIMENTAL OBSERVATIONS

Most cell types when subjected to bias temperature testing in the unencapsulated mode show only a slight increase in series resistance. A few cell types, on the other hand, show a large increase in resistance accompanied by a pronounced non-linearity as shown in Figure 5. Construction of these cell types involved a flash of gold to provide a good plating surface, followed by electroless nickel plating, followed by a solder dip to provide the thick conductive layer. The cell itself was p+ on n. The non-linear shape of the IV characteristic implied the formation of a rectifying contact, and because the back was lightly doped, this would be the most likely location for its formation. To simulate this a discrete Schottky barrier diode was connected to the back of an unstressed cell with the result shown in Figure 6. When the diode by itself was connected into the circuit (using leads having 0.1 ohm resistance) curve B was obtained. In the power quadrant it can be seen that the effect of the forward diode drop was to push the IV characteristic to

lower voltages with a consequent reduction in power output. In the far forward region only the diode leakage current flowed. This gave rise to a pronounced non-linearity. If a 0.5 ohm resistor was placed across the diode, curve C was obtained which showed a less pronounced non-linearity, more nearly approximating the shape of Figure 5. Of course, any rectifying contact which would be formed as a result of accelerated stress would not be expected to be of ideal shape, but only to exhibit greater resistance in one direction than in the other. The presence of such a "poor" rectifying contact was further confirmed by fitting the IV characteristics of stress tested cells using the SPICE computer model. In this simple lumped constant model the solar cell was represented by a current source in parallel with a diode. The rectifying Schottky barrier contact was represented by a diode having a 0.69 eV band gap (vs 1.11 for Si) in series with the cell in exactly the same way as was physically performed for Figure 6. The contact diode's resistance in the reverse direction could then be adjusted to give the best fit to the characteristic. Additional resistance was introduced in series with the cell to simulate the cell's series resistance. Other more complicated models are also possible, but this one gave reasonable results as can be seen from the degree of fit achieved in Figure 7. Also shown is the contact diode characteristic which was required for this fit, illustrating its poor rectification shape. This same shape was also directly confirmed by probing small isolated areas of the back contact relative to the main area.

Having shown that non-linear degradation is diode related, a very simple model of a metal to semiconductor contact will now be developed in order to examine conditions under which a rectifying contact could be formed at the back surface of the cell.

#### METAL TO SEMICONDUCTOR CONTACT THEORY

Figure 8 shows idealized energy band diagrams for an n-type semiconductor and a metal, both when separated and when joined. The work function of a metal is the amount of energy required to remove an electron from the Fermi level of the metal to infinity, whereas the electron affinity of a semiconductor is the energy required to remove an electron at the conduction band edge to infinity. When the metal is far removed from the semiconductor, as in Figure 8(a), both the work function and the electron affinity are referenced to infinity and, in the absence of surface effects, the bands will be flat as shown. When they are brought together in thermal equilibrium, however, the Fermi levels must line up and the difference between the metal's work function and the semiconductor's electron affinity causes the bands to bend as shown in Figure 8(b). Such band bending requires an electric field which comes from negative charge accumulating on the metal and positive charge on the semiconductor. The positive charge in the semiconductor is the result of "uncovered" donor atoms in the space charge region. As a consequence a potential barrier ( $\phi_B$ ) exists between the metal and the semiconductor much as occurs at a semiconductor p-n junction. This is a Schottky barrier and the junction will exhibit rectification properties. In this simple theory the barrier height is the difference between the work function and the electron affinity.

At actual metal-semiconductor contacts the situation is more complicated as shown in Figure 9. As shown in this diagram, a thin insulating layer (oxide) may exist between the metal and the semiconductor. This layer can be so thin as to be transparent to electron conduction, but at the same time

contain charged surface states. Thus, in addition to the charge on the metal ( $Q_m$ ) and the semiconductor ( $Q_{sc}$ ), charge will exist in surface states ( $Q_{ss}$ ) at the semiconductor-oxide interface. The presence of these surface states clamps the barrier height and makes it essentially independent of both the metal work function and the bulk doping of the semiconductor (for light to moderate doping). The barrier height in a practical case thus depends on such factors as the surface preparation (cleanliness) performed prior to deposition of the metal, the presence of a thin layer of native oxide, and the deposition technique used.

When a forward bias is applied across the barrier, conduction may occur by either or both of two mechanisms, as illustrated in Figure 10. Electrons may have sufficient energy to surmount the barrier (which is now slightly rounded as a result of image force effects), or if the barrier is sufficiently thin, they may tunnel through it quantum mechanically. In either case the thin oxide is considered to be essentially transparent to electrons. Thus a metal semiconductor contact may be either ohmic or rectifying depending on the barrier's height and thickness. This is illustrated in Figure 11, where the oxide layer has been omitted for simplicity. If the barrier is low enough electrons are able to pass freely over it and an ohmic contact results. If the barrier is thin enough, as will occur when the substrate is highly doped, as by the  $n^+$  layer of Figure 11a, electrons will tunnel through the barrier and the contact will also be ohmic. Thus either a low barrier, a thin barrier, or a combination of the two results in an ohmic contact. On the other hand, if the barrier is high and thick, as will occur with a lightly to moderately doped substrate having the proper surface state conditions, a rectifying contact can occur as shown in Figure 11b.

The final pieces of information needed to analyze solar cell contacts concern the polarity of the surface states that can be expected on silicon and their effect on the barrier height. As was mentioned, a number of variables can contribute to the magnitude and polarity of the surface states, but recent work (3) using low-energy, ion-scattering spectrometry on thin oxides, such as would be expected to form naturally at room temperature, has determined that the silicon atoms in the oxide adjacent to the interface are deficient in oxygen. A silicon atom with an unsatisfied (dangling) bond represents a positive charge. Hence the effect of this non-stoichiometric layer is to place a positive charge on the oxide side of the semiconductor-oxide interface as was illustrated in Figure 9. It has been demonstrated experimentally (4) that it is possible to control Schottky barrier height over a wide range by using very shallow, highly doped ion implanted layers. The effect of such artificially produced layers will be similar to the naturally occurring surface charge layers we are postulating. It was found in this work that positive charge on n-type silicon reduced the barrier height while positive charge on p-type silicon increased the barrier height. We are now in a position to analyze the non-linear degradation observed after stress on some types of cells.

#### ANALYSIS OF TEST RESULTS

Since the cells in question have a moderately doped n-type substrate the theory presented above would indicate that the contact formed initially to the back should be ohmic because the positive surface state charge at the interface will result in a low barrier height. This agrees with our

experimental observations. In order for the contact to become rectifying under stress testing neutralization of the positive charge at the surface is postulated. The most probable method of neutralization would be for oxygen atoms to complete the dangling silicon bonds (achieve stoichiometry) at the interface. In order for this to occur oxygen must diffuse to the interface from elsewhere in the structure. It would appear difficult for oxygen to diffuse through the thick metal contact from the ambient, and it is more likely that it would come from oxygen dissolved in the metal or in the silicon. The ability of oxygen to diffuse in a metal is related to the free energy of formation of its most stable oxide. If the free energy ( $\Delta F^\circ$ ) is low (small negative value or positive) then oxygen does not react easily with the metal and it can diffuse with ease. As can be seen from the data of Table 1, this would be true for such metals as Au, Cu, Pb, Ni, and Ag. On the other hand, when the free energy is high (large negative values) a strong reaction between the metal and oxygen occurs and diffusion is difficult. Examples are Al, Cr, Mg, Mo, Si, Ta, and Ti. Thus the Si/Au/Ni/Solder structure being considered would allow oxygen dissolved in the metals to freely diffuse to the interface, but not oxygen dissolved in the silicon. Oxygen diffusing to the interface will neutralize the dangling silicon bonds causing the barrier height to increase and the contact to become rectifying. This agrees with the experimental observations shown in Figures 12 and 13. A comparison of the curvature of the far forward characteristics of the two figures indicates that 2300 hours at 135 °C is equivalent to roughly 100 hours at 150 °C. This would correspond to an activation energy of approximately 3 ev., a reasonable value for a diffusion process.

## CONCLUSIONS

Two routes are thus open for the fabrication of ohmic contact to the back surface of a solar cell -- a safe route using a heavily doped substrate (e.g. back surface field) which permits electrons to tunnel through the potential barrier, or a more dangerous route which utilizes a moderately doped substrate plus a low barrier height. The reason the latter route is considered dangerous is that conditions for achieving a low barrier height depend on the density of surface states, which can change under stress. For the particular cells described in this paper it is hypothesized that the surface states were originally positive charges, occurring as a result of dangling silicon bonds, and were later neutralized under high temperature stress by diffusion to the interface of oxygen dissolved in the metal. Modification of surface states in this fashion will tend to make a contact which was originally ohmic become rectifying, and one which was originally rectifying become ohmic.

The effect depends on the existence of a thin oxide layer and will only occur when the metals used do not react with oxygen, i.e. have a low free energy. If a metal is used having a high free energy, and is heat treated, it will react with the oxide and either change the surface states or dope the semiconductor so that a Schottky barrier may no longer exist. A good example is aluminum which has been used for more than two decades in the fabrication of integrated circuits. Aluminum can make a rectifying Schottky barrier contact to either n- and p-type silicon (moderately doped) when originally deposited. Heating to 400 °C, as is normally done during integrated circuit fabrication, allows the aluminum to reduce the native oxide. The solid solubility of silicon in aluminum is sufficiently high that a thin p-type epitaxial layer is produced upon cooling down even though the eutectic.

temperature was not reached. On moderately doped n-type silicon this will result in a rectifying Schottky barrier, while on moderately doped p-type silicon an ohmic contact will result (5). It should be pointed out, however, that random fluctuations in the thickness and doping of the precipitated silicon layer can cause fluctuations in the barrier height, which in turn translate into fluctuations in diode characteristics, so that aluminum is not considered a suitable metal for Schottky barriers in integrated circuits. Platinum silicide which forms a high barrier height (0.84 eV) on n-type silicon and which, by virtue of being an in situ formed compound, is insensitive to interface conditions is now used instead.

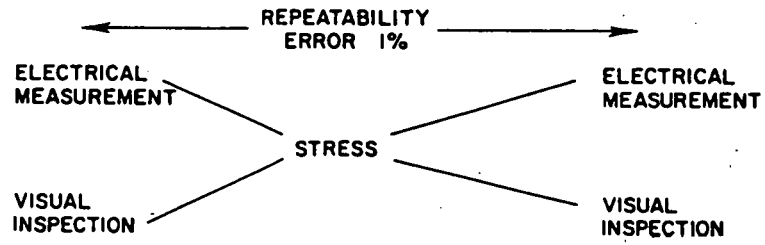
The cells described in this report which exhibited non-linear behavior, and consequent loss of power output, after B-T testing, appeared to have been made in exactly the wrong manner. A moderately doped substrate was used which resulted in a wide barrier not favoring tunneling. The substrate was n-type so that neutralization of the interface charge as a result of stress testing raised the barrier height and made the contact become rectifying. The metals chosen had low values of free energy favoring rapid diffusion of neutralizing oxygen atoms. Finally, although not directly related to Schottky barrier formation, the gold flash used to insure uniform plating was able to diffuse to the junction from the top under some conditions of stress, reducing the minority carrier lifetime and resulting in lower  $I_{sc}$  as seen in Figure 13.

It should be noted that the analysis presented in this paper is based on circumstantial, but self-consistent evidence. The ideas were based on concepts developed over years of single crystal silicon device investigations, but in order to prove (or disprove) the model, micro analytical techniques utilizing methods such as scanning Auger analysis and secondary ion mass spectrometry will need to be used. While many of the ideas presented here should be applicable to other constructions, such as amorphous cells, interpretation will undoubtedly be more difficult since the materials are less well understood than those in silicon cells.

#### REFERENCES

1. Lathrop, J.W. et al, "Accelerated Stress Testing of Terrestrial Solar Cells," IEEE Transactions on Reliability, vol. R-31, p.258 (1982)
2. Wolf, M. and Goldman, H., "Assesment of Metal Deposition Processes," DOE/JPL Report 954976-81/12, January 1981.
3. Harrington, W.L. et al, "Low-energy Ion-scattering Spectrometry (ISS) of the SiO<sub>2</sub>/Si Interface," Applied Physics Letters, vol. 27, p.644 (1975).
4. Shannon, J.M., "Control of Schottky Barrier Height Using Highly Doped Surface Layers," Solid State Electronics, vol. 19, p. 537 (1976).
5. Card, H.C., "Aluminum-Silicon Schottky Barriers and Ohmic Contacts in Integrated Circuits," IEEE Trans. Electron Devices, vol. ED-23, p.538 (1976)

Figure 1.



ELECTRICAL PARAMETERS

$V_{oc}$   $I_{sc}$   $R_s$   $V_m$   $I_m$   $P_m$

INSPECTION

LOW POWER MAGNIFICATION  
PHOTOGRAPHY

Figure 2. Basic Solar Cell Structure

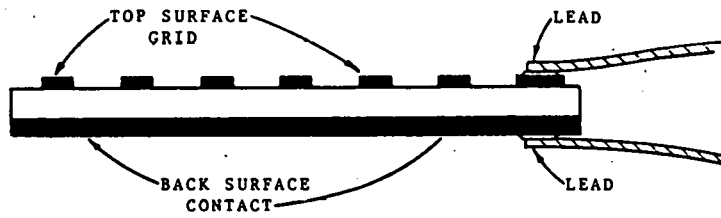
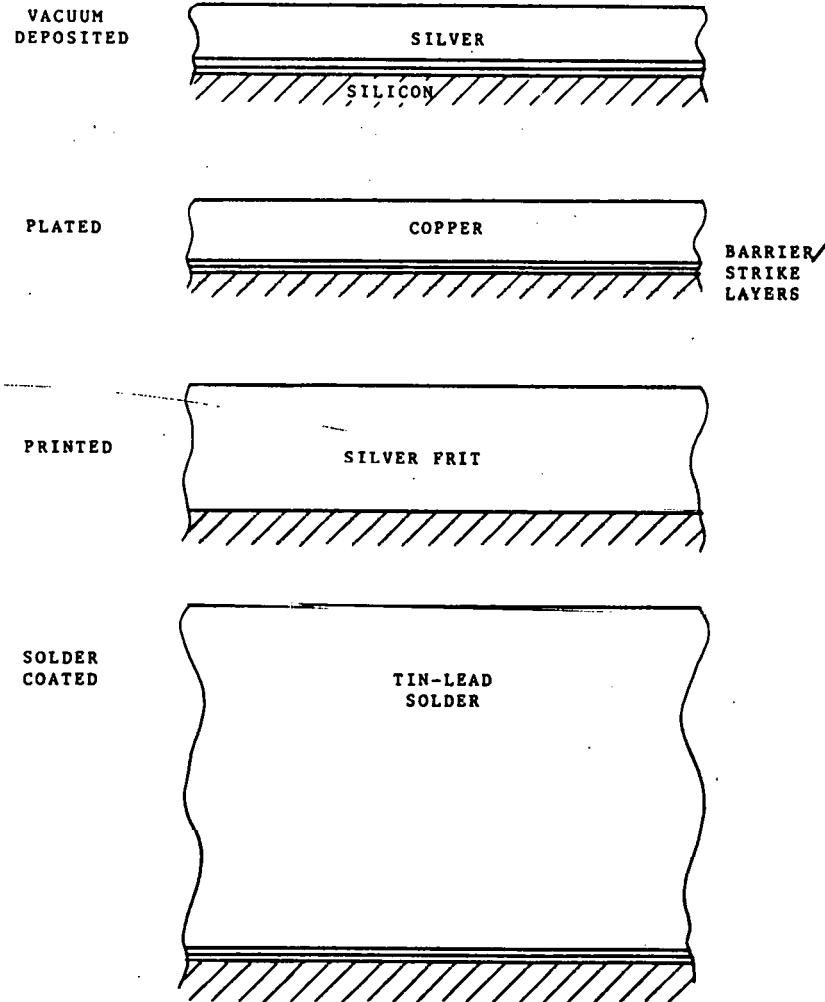


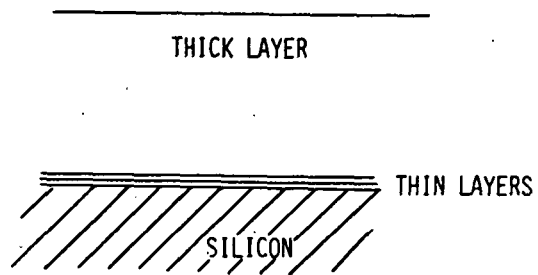


Figure 3. Common Solar-Cell Metallization Systems



(THICK CONDUCTIVE LAYERS APPROXIMATELY TO SCALE)

Figure 4. Metallization Layer Functions



THICK LAYER

- TRANSPORT CURRENT
- SOLDER INTERFACE TO LEAD

THIN LAYERS:

- OHMIC LOW  $R_c$  CONNECTION TO SILICON
- NON PENETRATING DIFFUSION BARRIER
- UNIFORM PLATING SURFACE
- ADHESION (GLUE)
- THERMAL EXPANSION MATCH

Figure 5. Nonlinear I-V Characteristics After Stress

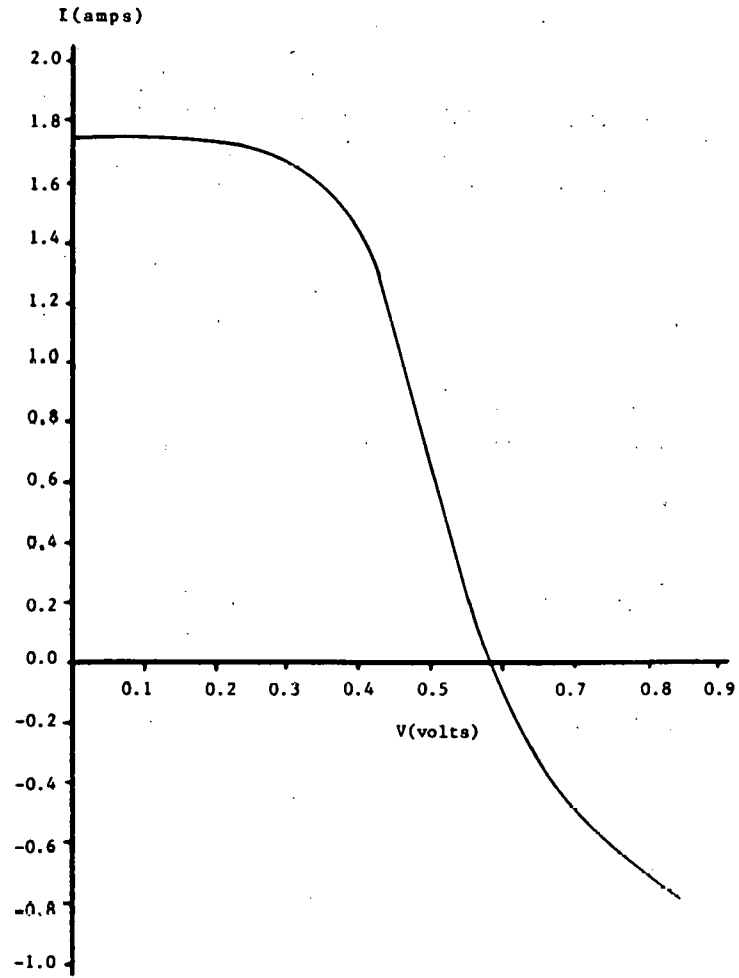


Figure 6: Contact Degradation Simulated by Lumped Constant Method

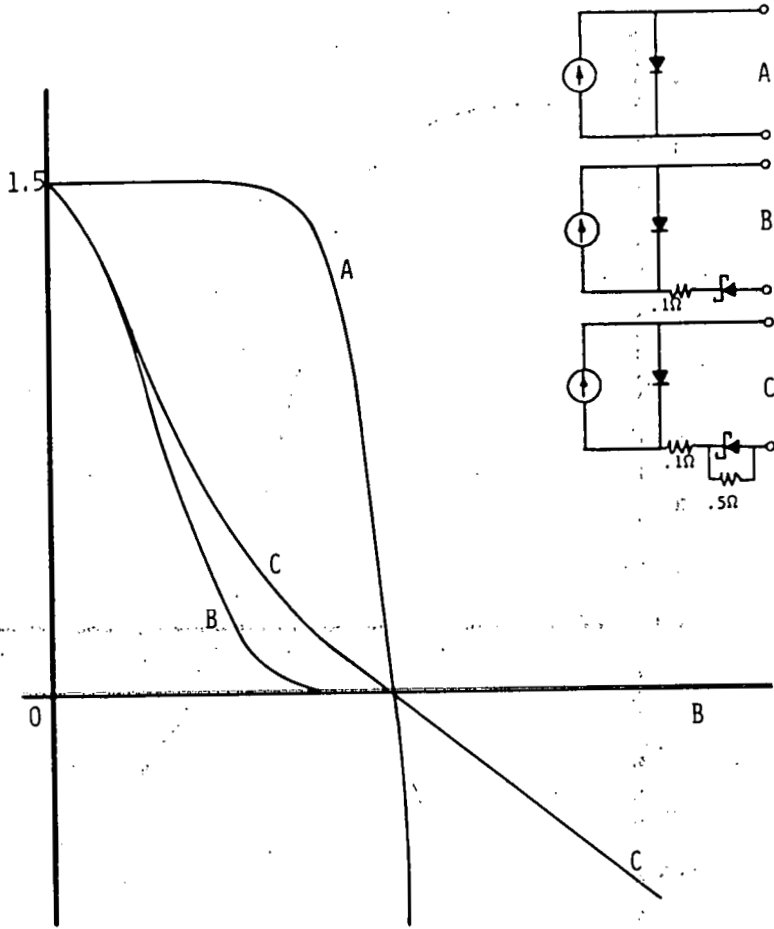


Figure 7. Characteristics of PV Cell After 600 Hours at 150°C as Fitted by Spice Model Incorporating Rectifying Contact

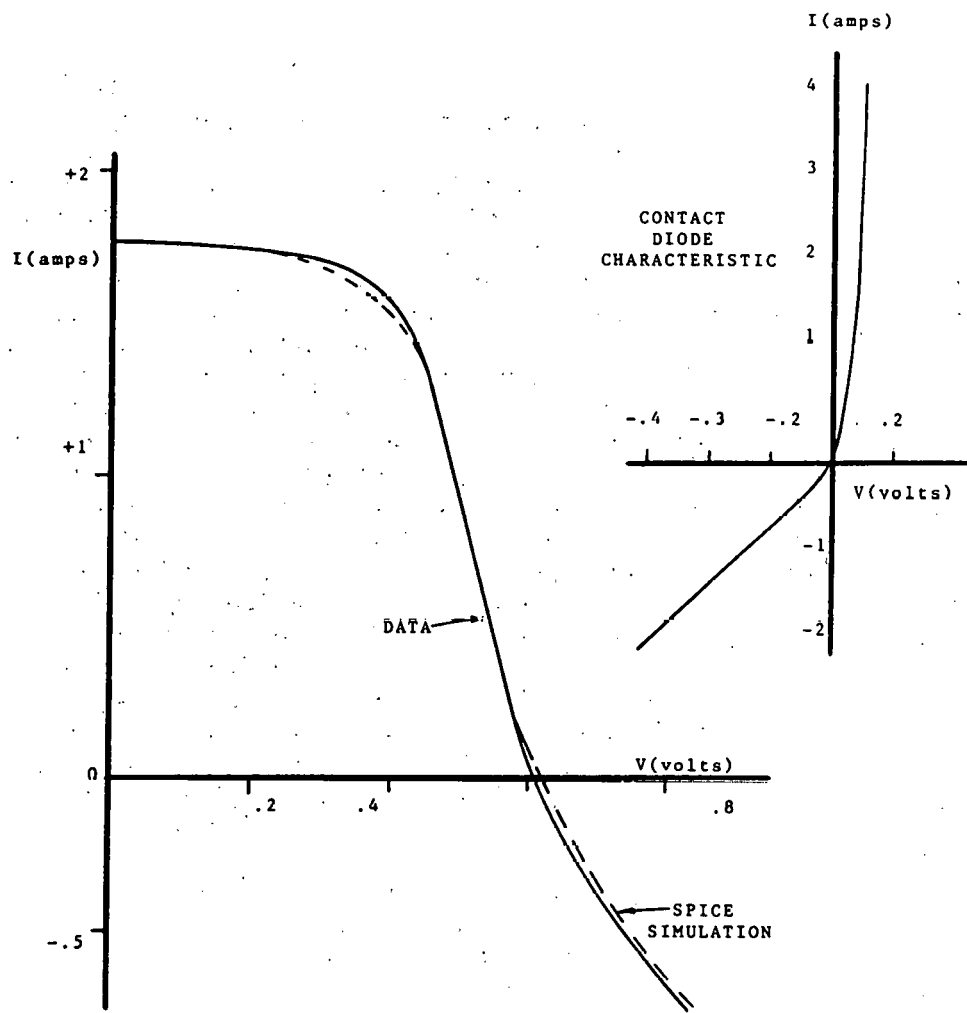
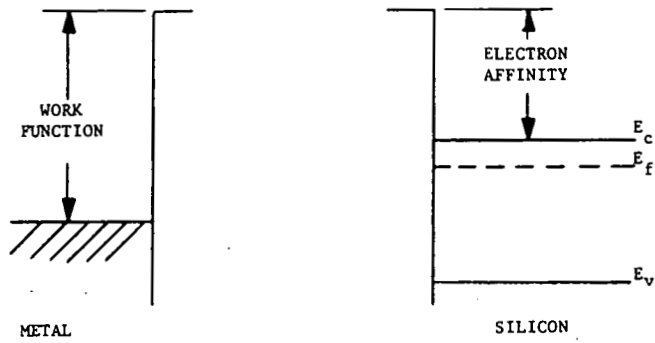
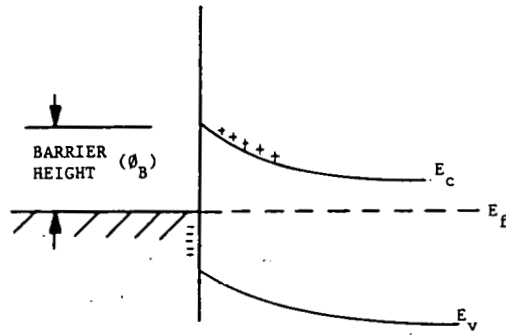


Figure 8. Idealized Energy Band Diagram Without Surface States



a) SEPARATED



METAL  
SILICON  
b) JOINED

Figure 9. Energy Band Diagram With Thin Interfacial Layer Containing Positive Charge

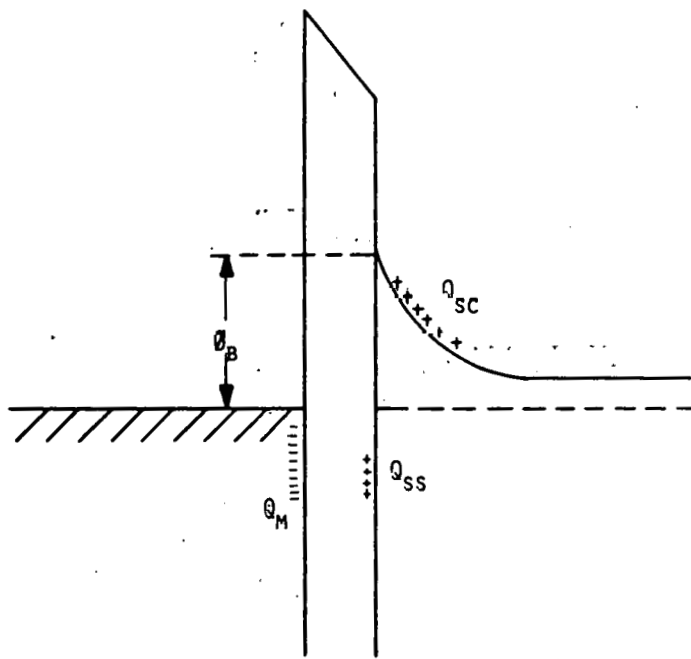
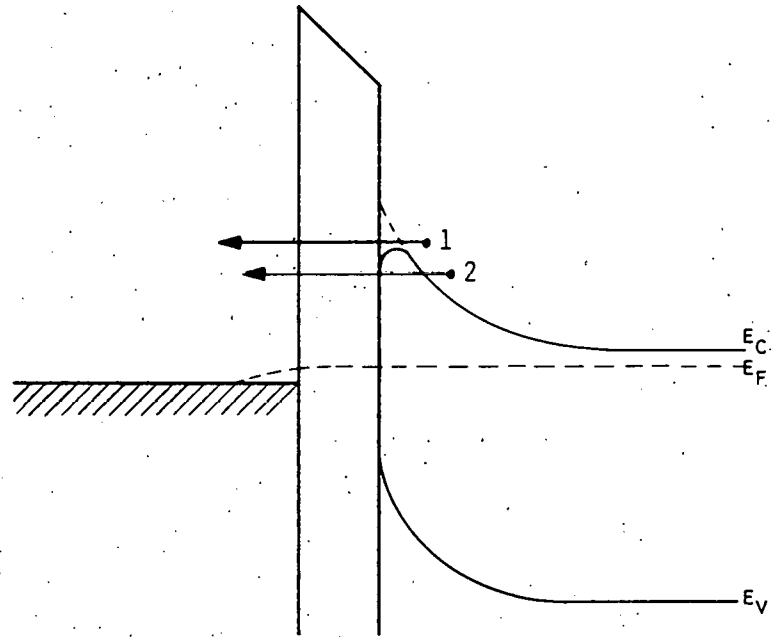


Figure 10. Nonrecombination Transport Mechanisms



- 1) OVER BARRIER TRANSPORT
- 2) QUANTUM-MECHANICAL TUNNELING



Figure 11. Rectifying (Schottky) Contact Ohmic and Rectifying Barrier Configurations

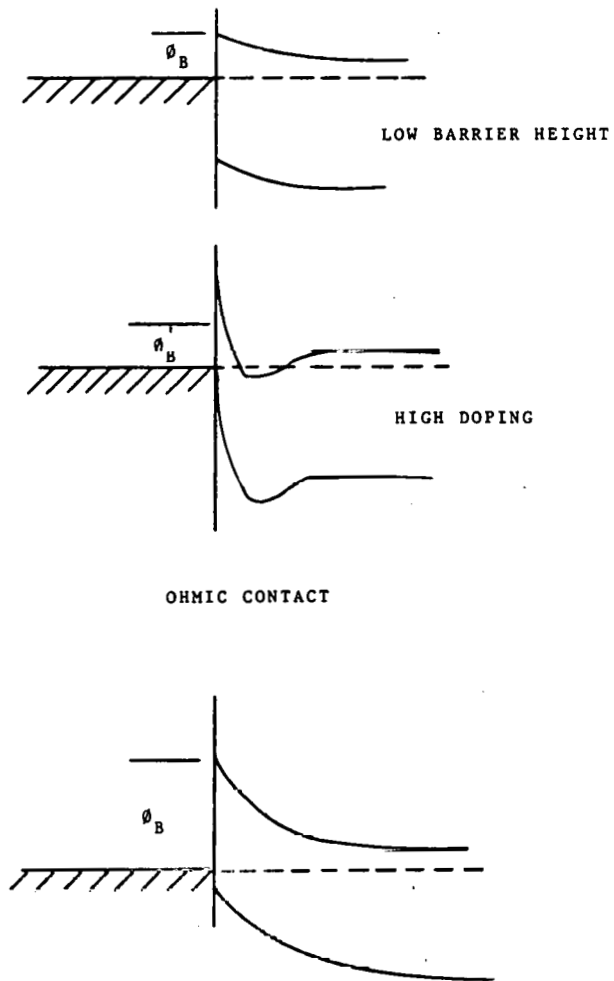


Figure 12. I-V Characteristics for Typical p<sup>+</sup>n Solar Cell Having Au-Ni-Solder Contacts Subjected to 135°C Bias-Temperature Stress

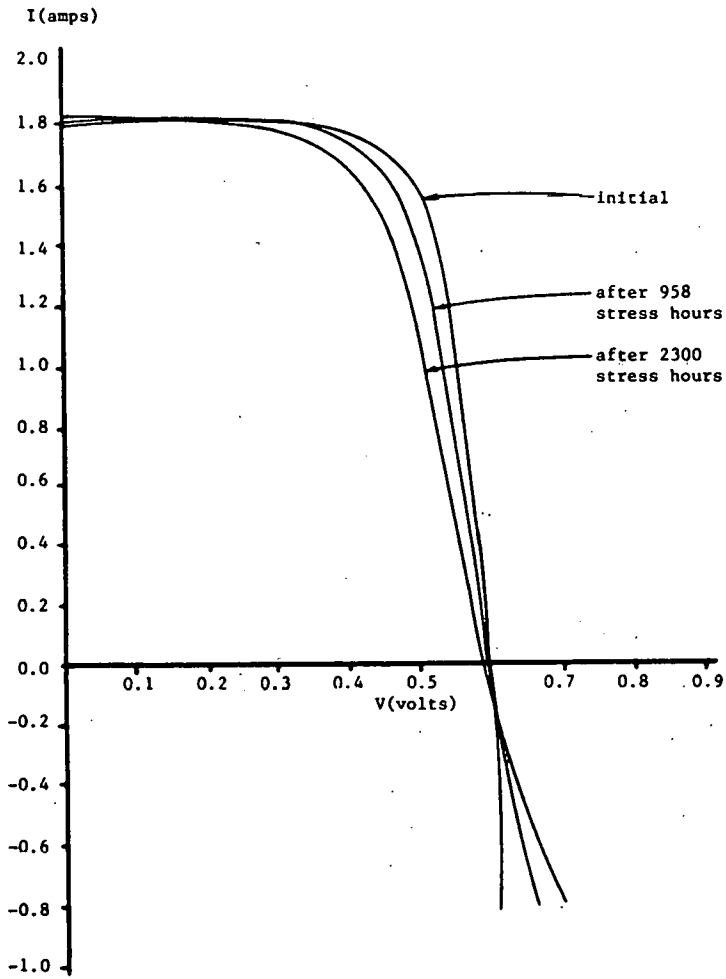


Figure 13. I-V Characteristics for Typical p<sup>+</sup>n Solar Cell Having Au-Ni-Solder Contacts Subjected to 150°C Bias-Temperature Stress

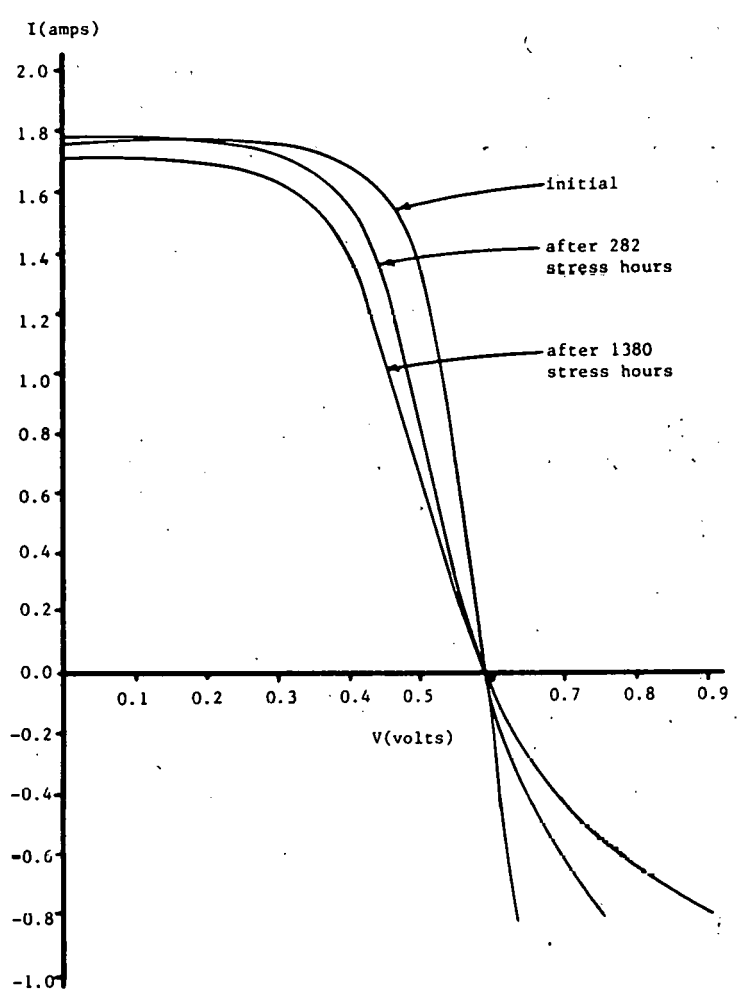


Table 1. Measured Ionization Energy of Various Impurities in Silicon and the Free Energy of Formation of Their Most Stable Oxides

	P-TYPE $E - E_v$ (eV)	N-TYPE $E_c - E$ (eV)	$\Delta F^\circ$ (KCAL)		P-TYPE $E - E_v$ (eV)	N-TYPE $E_c - E$ (eV)	$\Delta F^\circ$ (KCAL)
Al	.067		-376.7	Hg	.76, .81	.79, .87	
Sb		.039		Mo	.33, .78, .82		-161.95
As		.054		Ni	.23, .77		-51.7
Ba	.5	.32		O	.41, .74	.16, .51	
Be	.17, .42			Pd	.34		-52.2
Bi		.069		P		.045	
B	.045			Pt	.36, .87	.82	
Cd	.3, .55, .67, .92		-53.79	K		.26, .77	
C		.25		Se		.25, .4	
Cs	.5	.3		Si	.87	.63, .93	-192.4
Cr		.41	-250	Ag	.76	.79	-2.59
Co	.35, .49, .59		-51.0	Na		.77	
Cu	.24, .4, .53			Sr		.28, .62	
Ga	.072			S	.48	.26	
Ge		.27, .62		Ta		.14, .43	-471
Au	.58	.83	+39.0	Te		.14	
In	.16			Tl	.3		
Fe		.14, .51, .72	-177	Sn	.25	.85	-124.2
Pb	.37	.17	-45.25	Ti		.21	-204
Li		.033		W		.22, .3, .37, .78, .81	-182.47
Mg	.87, 1.01		-136.13	V	.4	.49	-271
Mn	.45	.43, .59		Zn	.26, .57		-76.0

## DISCUSSION

RIEL: Were all the cells fabricated with single-crystal material?

LATHROP: Yes, as far as I know. It's single-crystal, and that is the only way of growing crystals this size.

REIL: I guess the next question is, what was the size of the cell you were using.

LATHROP: There were a couple of sizes, three-inch and four-inch. It was not one cell that showed this, there was --

REIL: Do you know anything about the oxygen concentration that they had in the original materials?

LATHROP: No, I don't, but I don't believe that oxygen will diffuse through silicon very rapidly, because it has high free energy of formation so I don't believe that is the phenomenon that is occurring.

GARCIA: Would it be possible to make a rectifying contact and watch it get better with time to sort of prove this?

LATHROP: In my theory it should be. You have a good point there. This is all based on self-consistent but rather circumstantial evidence. In order to prove it, one would have to go to Auger analysis or low-energy ion mass spectrometry or something like that. It would be very interesting also to look for oxygen, to look for neutralization, to look for diffusion.

GARCIA: I think I can give you a lot of rectifying contacts I have made.

WONG: In your abstract you mentioned the role of encapsulants in encapsulated and unencapsulated cells. Do you have any data?

LATHROP: Yes. We have a lot of data on both. But I did not want to present that in this talk because I really had no way of making a general conclusion, so I thought it would be more interesting to go to a specific thing we saw. I would be happy to talk with you about what we have found in our general testing procedures afterwards.

WONG: Are they all terrestrial cells?

LATHROP: Yes. They are all commercial state-of-the-art terrestrial cells. Not experimental.

WOLF: You mentioned primarily the gold-nickel system as the one that shows the formation of the Schottky barriers. You must have tested other cells and other methods.

LATHROP: That is right.

WOLF: Is that always a predominant failure mechanism that the Schottky barrier develops during various heat treatments --

LATHROP: Not at all. The only one with lightly doped substrate we looked at had gold-nickel, so I can't draw any conclusions about anything else that would happen. All I can say is that had the manufacturer gone to heat treatment of one sort, that probably would have changed things. It might have changed things for the worse. In other words, heat treating with nickel silicide, to form a nickel silicide, I don't know what that is going to do. Bill Taylor could probably tell you but I'm not sure in my own mind whether that is going to make things better or worse than just a plain low-high Schottky barrier. But anyway, the only things that we saw it on were moderately doped substrates. The other cells, in general, had a  $p^+$  substrate,  $p^+$  on  $p$  back-surface field. In these we don't see this rectification. We have never seen rectification on  $p^+$  and so my advice is always use a back-surface field, not for better efficiency but for better reliability.

WOLF: Then the other trends have always given you different material for blackmail other than formation of Schottky barriers.

LATHROP: That's right. I have something on them too. Next meeting, we will talk about that. No. I have something on everybody.

SOMBERG: You mentioned at the beginning of your talk that a lot of your tests were at fairly high or low temperature extremes. It seems, in the FSA program, that most of the thermal cycling is from  $-40^\circ$  to  $+90^\circ\text{C}$  and in real-life situations out in the field modules were sitting typically at relatively moderate temperatures. Would you care to comment about the temperature extremes and any extrapolation you have done in terms of this new 30-year lifetime?

LATHROP: It is very difficult to try to relate accelerated testing to real life unless you have some way to get there. You know you have to have field data and you have to have some way of extrapolating the field data. For example, in bias-temperature testing you can go through a bunch of different temperatures and you can attempt to get some sort of activation energy, which you extrapolate back to room temperature. This is more difficult than something like thermal cycling. I don't know how to do it. The only thing that I can say is that if cell A goes through the thermal cycling with no problems, and then cell B has all kind of problems, cell B is worse than cell A. But both cell A and cell B may last for 30 years. I just don't know. But it behooves the manufacturer of cell B to take a look at it and try to improve it. That's all I can say. All I can talk about at the moment with regard to this is the relative aspects with regard to other cell types, but not with regard to an absolute "will it last 30 years?"

SCHWUTTKE: I have one question. I am interested in your model based on the oxygen. What you say very simply is that the property of the contact depends very much on whether you have an oxygen-rich or an oxygen-poor surface, is this correct?

LATHROP: That's my thinking, yes. Except that --

SCHWUTTKE: Now I would like to bring to your attention that this may not be generally known and I would like to know your thinking how this would tie in. You have very little control on what the oxygen concentration is in a wafer after processing. This depends on, and ties in readily with, the original oxygen content in your wafer. After one heat treatment, depending on the atmosphere -- be it oxygen, be it nitrogen, or whatever -- you may have a surface which is oxygen rich or oxygen poor. Now this would lead to great variety in your contact formation.

LATHROP: Except that in my simple-minded theory I feel that the oxygen is coming from the metal, not from the silicon.

SCHWUTTKE: Yes, but you must have some kind of equilibrium, whether it is coming through the metal, through the interface, and depending on what the oxygen content is in the silicon at the interface. Don't you think so?

LATHROP: Yes. I would think so. Whether we have reached that equilibrium or not, I am not sure.

SCHWUTTKE: This may vary considerably from wafer to wafer. All that I am saying is that you have basically no control at the present time, for the oxygen concentration is in the surface of the wafer before you start putting down your metallization.

LATHROP: That is correct, yes.

SCHWUTTKE: What would be now the interaction? Nevertheless, I find your model very interesting.

LATHROP: I have a feeling that it is not the oxygen in the silicon that is the problem, it's the oxygen--

SCHWUTTKE: If it is the interface, then both sides contribute.

LATHROP: Well, except that the oxygen has got to get into the silicon dioxide, the thin silicon dioxide layer, there and if you have a lot of oxygen on the metal side, which is capable--

SCHWUTTKE: Yes, but the silicon dioxide layer formation will depend on the presence of oxygen in the wafer.

LATHROP: That oxide has already been grown.

SCHWUTTKE: Yes, but --

BICKLER: Would you imagine more than  $10^{16}$  oxygen in the silicon?

SCHWUTTKE: Oh, definitely.

BICKLER: The chemical reaction to give you free bonds at the interface that Jay (Lathrop) is describing is going to be up in the chemical range, up to the  $10^{20}$ 's, so I submit that the background oxygen in the silicon crystal is so slight an influence that . . . .

SCHWUTTKE: That is an order of magnitude difference, so--

BICKLER: More than one magnitude.

WOLF: Yes, there will always be on the free silicon surface something like 20 or more Angstroms of oxide. It depends on the chemical treatment that is being used in getting the metal there. How much of the oxide may or may not be removed, and what is the state exactly of the surfaces, are probably really more important than the  $10^{18}$  oxygen atoms in the bulk below.

COMMENT: I think that is a good point.



THIS PAGE  
WAS INTENTIONALLY  
LEFT BLANK

## FIELD TEST EXPERIENCE

R.W. Weaver  
Jet Propulsion Laboratory  
California Institute of Technology  
Pasadena, California 91109

### INTRODUCTION

As a part of the Flat-Plate Solar Array Project (FSA), a field-test program was developed to obtain solar photovoltaic (PV) module performance and endurance data. These data are used to identify the specific characteristics of module designs under various environmental conditions. The information obtained from field testing is useful to all participants in the National Photovoltaics Program, from the research planner to the life-cycle cost analyst.

### TEST SITES AND DATA PROCESSING

The Field Test Program plan identified four Southern California test sites with characteristics ranging from oceanside to desert environments, including one with high urban pollution. Test facilities at these sites were constructed and modules were deployed in 1977. All of the modules deployed were first tested and inspected at the Jet Propulsion Laboratory (JPL). The testing was done using the Large-Area Pulsed Solar Simulator (LAPSS) to obtain I-V (current-voltage) data, at a reference irradiance level and module temperature, the results of which were used as baseline data whenever the module was returned to JPL for special testing. The pre-deployment inspection was a detailed visual examination of the modules, from which an original-condition report was generated. Subsequent inspection reports were compared with this report to discover and identify physical changes in the module.

In 1978 the FSA Field Test Activity assumed responsibility for 12 more test sites, which had been established originally by the National Aeronautics and Space Administration (NASA) Lewis Research Center as part of the NASA energy program. These sites were situated as far north as Alaska and as far south as the Canal Zone, and covered virtually all climatic conditions. The characteristics of these sites and those of the four JPL sites are shown in Figure 2. Lewis Research Center also furnished JPL with all of the data that had been acquired for the modules at the 12 sites. The resulting site network consisted of 15 remote (unattended) sites and one at JPL.

Two data acquisition systems were developed, one for the remote sites and one for the JPL site. The data system for the remote sites was a portable battery-operated unit that sampled I-V data and displayed the key parameters (e.g., short-circuit current, open-circuit voltage, peak power). After acquiring the data the unit stored it on an erasable storage medium,

which is readable on the JPL site data system. Data were acquired periodically from the remote sites using this unit.

The JPL site data system was designed to sample module performance daily. The system also takes weather and irradiance data every five minutes. All of the data were stored on magnetic disks for processing by scheduled programs or by special programs on demand. This system could also process data from the remote sites.

The endurance data were obtained periodically from all of the sites by means of physical inspections by a JPL quality-assurance team. The results of these inspections were written up as detailed descriptions of the physical states of the modules. These descriptions were then compared with previous inspection reports to identify changes in the modules occurring during the test period.

#### FAILURE PROCESSING

The performance and endurance data were used to determine if a failure analysis of a module were warranted; if so, the module was removed from the field and returned to JPL for further analysis. The criterion for performance failure was failure to produce 75% or more power than it did when it was originally tested. If the module's physical state had deteriorated to the point that it had become hazardous, or when performance failure was imminent, the module was to be considered to have failed. Failed modules were returned to the JPL failure analysis team for detailed analysis to determine the type and cause of the failure. The results were published as Problem/Failure Reports and were distributed to all concerned in the PV program, including the module manufacturer.

#### RESULTS

In the nearly five years of field testing Blocks I, II and III modules, almost 10% failed the performance test. Many more experienced physical degradation that did, or would eventually, result in an unserviceable module. The plot in Figure 5 depicts performance failures as a function of time in the field. The curves show that for the Blocks I and II modules the failure rate increased over the last 18 to 24 months. This means that more modules (per module deployed) were failing after the first three years than before that time. This leads to the conclusion that there is definitely a time-versus-design correlation for field failures.

The results of the physical inspections are shown in the chart in Figure 6 for the Blocks I and II modules (type refers to manufacturer). The defects are ranked by severity for each site and type. No site stands out as being more severe than any other in the chart. However, when the performance data are also considered, the sites with hot-humid climates clearly have more severe environments.

Some results from non-JPL sites are described in Figure 7. The causes of failure are basically the same as for the JPL tests; only the rate of

failures is different. The notable exception is the number of burst cells observed at the Mount Laguna site. The ultimate effects of the three most prevalent defects are shown in Figure 8. All of these defects would eventually require that the module be replaced. Figures 9 and 10 describe several of the prime reasons for cell failure.

During the test period, changes in the cell grid and collector materials were observed. The most common was the discoloring, usually a brown- ing, of the grid and collector material. Several of the modules were disas- sembled and the discolored area was analyzed. The probable cause was a reaction with some residual material from the manufacturing process. The "blossoming" effect found at the ends of some grid lines is attributed to the migration of the silver used in the grid material. This effect was seen only in modules that used silver in the grid material and that were configured so that the end of a grid line was near another part of the electrical circuit that was at much different electrical potential.

The test results also indicated other reasons for loss of power or module degradation. Some of these are presented in Figure 12. The most severe, relative to the loss of power, is the amount of dirt that is deposited on the module surface. Power losses of as much as 12% were observed within a three-month period. The best design for preventing power loss from soiling was that with a glass superstrate on the module.

#### SUMMARY

JPL field test results were compared with test and operational results from other centers in the PV program to determine if similar failures were occurring elsewhere. The consensus as to the principal causes of electrical failure was: (1) cracked cells, (2) broken interconnects, (3) various types of shorts. The principal types of physical degradation were: (1) delamina- tion of encapsulants, (2) discoloration of encapsulants, (3) internal cor- rosion of interconnects and grid connectors, (4) external connector corrosion. There appears to be no correlation between the physical appearance of the module, dirt deposits excepted, and performance. The most severe environment is the hot-humid type.

A representative sample of the modules that were used in this test pro- gram have been relocated at the JPL Goldstone site. Data will be sampled annually to determine what effect further time in the field may have on the modules.

## Figure 1. Objectives of Field-Test Activity

- To obtain in-field performance data for life-cycle endurance evaluation
- To determine degradation characteristics and failure modes as they relate to module design characteristics
- Provide verification data to qualification testing
- Develop improved in-situ diagnostic testing methods and analytical techniques

## Figure 2. Field-Testing History

- 1977
  - Establish four sites in Southern California
  - Automatic data acquisition system installed at the JPL site (Block I and II modules)
- 1978
  - Acquired 12 more test sites from Lewis Research Center (Block I and II modules)
  - Developed a portable Module I-V data acquisition system
  - Initiated semiannual inspections of remote sites
  - Block III modules deployed to sites
- 1979
  - Data analysis techniques developed and applied to all data available
- 1981
  - Remote sites decommissioned
  - Final data analysis for Blocks I, II, and III performed
- 1982
  - Started Block IV deployment and testing

Figure 3. JPL Test Sites

CATEGORY	LOCATION	LATITUDE (degrees)	ALTITUDE (feet)	KEY FEATURES
EXTREME WEATHER	CANAL ZONE (FT. CLAYTON)	9	-0	TYPICAL TROPIC; HOT AND HUMID; 100 INCH-PER-YEAR RAINFALL
	ALASKA (FT. GREELY)	64	1,270	SEMI-ARCTIC; DRY, COLD AND WINDY; -30°F WINTERS
MARINE	POINT VICENTE, CA	34	-0	COOL, DAMP MORNINGS AND CLEAR AFTERNOONS; CORROSIVE SALT SPRAY
	KEY WEST, FLA.	25	-0	HOT AND HUMID; CORROSIVE SALT SPRAY
	SAN NICHOLAS ISLAND, CA	34	-0	SOMEWHAT Milder THAN KEY WEST
MOUNTAIN	TABLE MOUNTAIN, CA	34	7,500	TYPICAL ALPINE ENVIRONMENT; HEAVY WINTER SNOWS AND MILD SUMMERS; HIGH-VELOCITY WINDS
	MINES PEAK, CO	40	13,000	CLEAR AND COLD; HIGH-VELOCITY WINDS, MAX. UV
HIGH DESERT	GOLDSTONE, CA	35	3,400	VERY HOT AND DRY SUMMERS; CLEAR SKIES
	ALBUQUERQUE, NM	35	5,200	DRY WITH CLEAR SKIES; AN ABUNDANCE OF UV
	DUGWAY, UTAH	40	4,300	COLD WINTERS, HOT SUMMERS; ALKALINE SOIL
MIDWEST	CRANE, INDIANA	39	-0	TYPICAL MIDWEST; HOT HUMID SUMMERS, COLD SNOWY WINTERS
NORTHWEST	SEATTLE (FT. LEVIS)	47	-0	TYPICAL NORTHWEST; MILD TEMPERATURES AND AN ABUNDANCE OF RAIN
UPPER GREAT LAKES	HOUGHTON, MICHIGAN	47	750	MILD SUMMERS, SEVERE WINTERS
URBAN SOUTHERN CALIFORNIA	JPL/PASADENA	34	1,250	PRIMARY TEST SITE - HOT SUMMERS AND MILD WINTERS; VERY HIGH POLLUTION ENVIRONMENT
URBAN COASTAL	NEW LONDON, CONNECTICUT	41	-0	TYPICAL NEW ENGLAND COASTAL
	NEW ORLEANS, LOUISIANA	30	-0	HOT AND VERY HUMID; HIGH POLLUTION ENVIRONMENT

Figure 4. Test and Inspection Procedures

**Testing**

- Modules were "stressed" via fixed resistors
- Baseline I-V data acquired during installation
- Periodic I-V data taken
- Performance evaluated

**Inspection**

- Visual inspection prior to shipping to site
- Visual inspection during installation
- Periodic inspections
- Physical change description reports

Figure 5. Blocks I, II and III Results

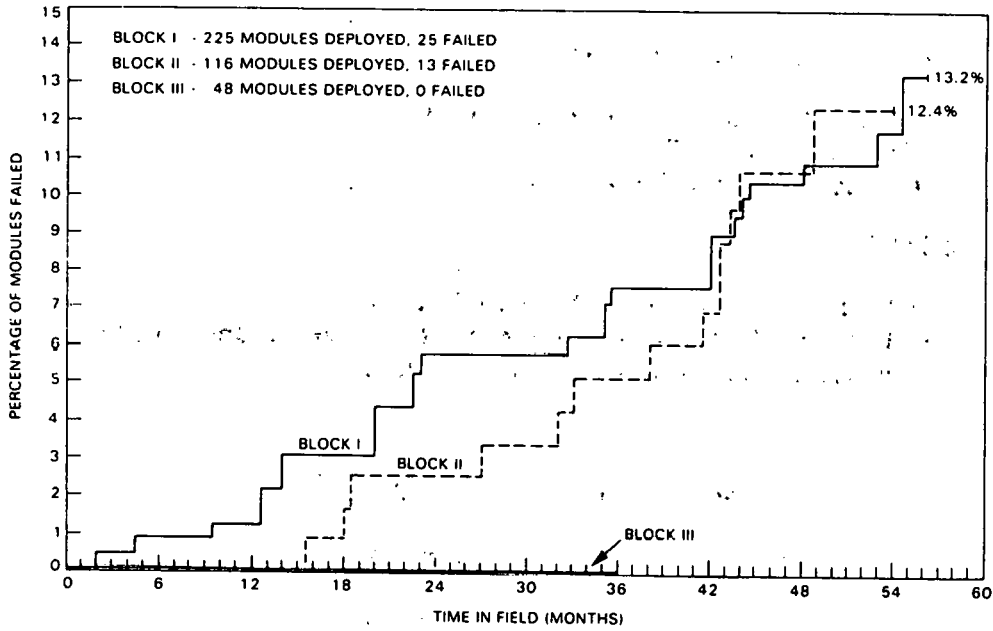


Figure 6. Physical Inspection Summary of Remote-Site Modules

PREVALENT PHYSICAL DEFECTS		SITE										
		CAMA, EDIE	KEY WEST	MIP, DUBUINS	CRANE	HOUGHTON	NEW LONDON	ALBUQUERQUE	DUGWAY	ALASKA	SEATTLE	SAN VICENTUS
TYPE A	CRACKED CELLS											
	GROUND TERMINAL CORROSION	○	●	○	●		○	○			○	●
	PROTECTIVE TERMINAL BOOT DETERIORATION											
	OUTPUT TERMINAL HARDWARE CORROSION											
	EMBEDDED DIRT	○	○	○	○	○	○	○	○	○	○	○
TYPE B	CRACKED CELLS											
	CELL GRID AND COLLECTOR DISCOLORATION	○	○	○	○	○	○	○	○	○	○	○
	MODULE FRAME CORROSION	○	○	○	○	○	○	○	○	○	○	○
	J-BOX AND OUTPUT CONNECTOR CORROSION	○	●	○								○
	EMBEDDED DIRT	○	○	○	○	○	○	○	○	○	○	○
TYPE C	CRACKED CELLS											
	FRAME SEAL/SUBSTRATE DELAMINATION	○	○	○	○	○	○	○	○	○	○	○
	INTERCONNECT/CELL SURFACE CORROSION	○	○	○	○	○	○	○	○	○	○	○
	OUTPUT INTERCONNECT/SOLDER JOINT CORROSION	○	○	○	○	○	○	○	○	○	○	○
	HARD-COAT CRAZING											
	INTERCONNECT BREAKTHROUGH											
	SUBSTRATE DETERIORATION	○	○	○	○	○	○	○	○	○	○	○
EMBEDDED DIRT	○	○	○	○	○	○	○	○	○	○	○	
TYPE D	TERMINAL STRIP/SOLDER JOINT DISCOLORATION	○	○	○	○	○	○	○	○	○	○	○
	RUBBER OUTPUT CONNECTOR DETERIORATION											
	FRAME SCREW FASTENER CORROSION	○	○	○	○	○	○	○	○	○	○	○
	MODULE FRAME CORROSION	○	○	○	○	○	○	○	○	○	○	○

**SEVERITY SCALE**

- NONE
- SOME
- MODERATE AMOUNT
- SIGNIFICANT AMOUNT
- EXTREME CONDITION

## Figure 7. Results From Non-JPL Sites

### Mount Laguna, CA (July 1979 - July 1981)

- Cracked cells: 1500 (950 "burst")
- Output: Down 55%
- Encapsulant: Delamination

### MIT/LL

- In-field, over 30 months: 6.5% failed
- Causes: Cracked cells, broken interconnects and shorts
- Physical: Delamination, cracked glass

## Figure 8. Failure Effects

<u>TYPE</u>	<u>EFFECTS</u>
Cracked cell	<ul style="list-style-type: none"><li>• Loss of power</li><li>• Hot-spot heating</li><li>• Loss of module</li></ul>
Broken interconnect	<ul style="list-style-type: none"><li>• Loss of power</li><li>• Loss of module</li></ul>
Short circuit	<ul style="list-style-type: none"><li>• Loss of power</li><li>• Loss of module</li><li>• Hazardous condition</li></ul>

## Figure 9. Causes of Cracked Cells

### Impact type

- Hail storms
- Rocks
- Other

### "Burst type"

- Outgassing of material between cell and substrate
- Moisture entrapment and subsequent heating

### Other causes

- Manufacturing defects
- Hot spotting
- Module twisting



## Figure 10. Observed Changes in Grids and Collectors

### Discoloring

- Brown coloring - probably due to reaction with contaminants
- White streaking (GE) ??

### Separating from cell

- Manufacturing problem

### "Blossoming"

- Silver migrating to ends of grid that are at a high potential relative to nearby cell or circuit component

## Figure 11. Other Reasons for Loss of Module Output

### Dirt

- 2 to 12% loss
- Partially correctable via cleaning
- Glass is best self cleaner

### Discoloring of encapsulant

- Select proper material-glass

### Thermal related

- Cycling effects
- Expansion stress
- Match materials or compensate

### NSMD

- San Nicolas Island, Mines Peak, Pt. Vicente

### Hazards of field testing

## Figure 12. Conclusions

- Electrical degradation or failure is not necessarily a function of physical appearance
- Three primary known causes of failures were cracked cells, broken interconnects, and electrical shorts
- Most severe environment is hot and humid

## DISCUSSION

CAMPBELL: What percentage of Block I, II and III modules were glass superstrate?

WEAVER: I can't give you a percentage but I think there were only two manufacturers that we tested during that period that used glass.

LAVENDEL: You, in your failure analysis, mentioned discoloration several times. Is this really a hazard or is it mostly cosmetic?

WEAVER: I think it is mostly cosmetic. Like I said, we very seldom, if ever, could find an electrical performance degradation related to a discoloring of the system.

LAVENDEL: Have you ever tried to define the composition of this discolored film?

WEAVER: Yes, we did send it to our Failure Analysis group and I think they have found what other people have found, if they peel the encapsulant away. Brian (Gallagher), do you want to field that?

GALLAGHER: I am going to give a short presentation this afternoon on metal degradation of a very specific encapsulant, and to answer your first question, you will see this afternoon that the first property that degrades that is visible is transmission at 400 nanometers: it starts to turn yellow. To your question about whether it really degrades the modules or not -- if the yellow transmission at 400 nanometers degrades down to 10% of its original value, which looks like a lot, you only have from 5% to 10% degradation in the electrical properties of the module of the total integrated area from 400 nanometers to 1.1 micron. You would still only have 5% to 10% degradation. We will cover it a little more detail this afternoon.

AMICK: You showed that Block III modules are much better from the standpoint of reliability than I or II. Do you understand the reasons why the Block III modules have improved so dramatically? I and II look pretty much the same.

WEAVER: Well, we would like to think it because we told them what was wrong with I and II. Redundant interconnects came on very strongly in Block III, there were some in II, but basically in Block III. The redundant interconnects; a better understanding of stress relief in interconnects. Better encapsulation procedures, we think, came into effect there. Glass, more glass. There was a Block II contractor that used glass that I don't think is still in the business of terrestrial PV; I think they are still in the space business, and some of their Block II modules are actually putting out more now than when we originally put them in the field. That was a small cell. But they were so expensive there was no point in going on.

SCHWUTTKE: On the subject of electrical migration: was this typical of all modules? At what distance from anode to cathode did it occur, and is it typical for all metallurgies -- that is, for all modules?

WEAVER: I will defer that to either Ed (Royal) or Gordon (Mon), because they understand that better than I do.

ROYAL: Gordon (Mon) is going to talk about that this afternoon.

WEAVER: I can answer that to some extent -- no, we have not seen it in all of them. In the ones that we understand have silver, yes, we have seen it.

PROVANCE: Have you observed any phenomena with this discoloration per location -- in other words was it more prominent in one location than in another? The reason I ask that is that sulfur tends to sulfide in areas of high sulfur concentration, so if it is in an industrialized area some of the discoloration, I would think, would be from the sulfiding.

WEAVER: No, I don't think I could correlate that to an area. The site at JPL is the worst urban environment, pollution-wise, that we found. Mines Peak had almost none. Almost no discoloring at all.

SCHWUTTKE: But you lost all of your modules there--

WEAVER: On the last inspection.

PROVANCE: We have seen this quite prominently in other thick-film applications, in microelectronic circuits where silver or platinum-silver compositions will tend to discolor or sulfide very quickly in various areas of high concentration of industry. But much longer periods of time for the same discoloration to occur in very clean areas.

WEAVER: The worst case I have seen of it was at Cape Canaveral at the Florida Solar Energy Center. Very predominant in those modules there.

# FUNDAMENTALS OF METAL-SEMICONDUCTOR CONTACTS

by

Dieter K. Schroder

Arizona State University

Tempe AZ 85287

The metal-semiconductor (m-s) contact is one of the oldest semiconductor devices [1], yet even today it is not completely understood. Schottky [2] originally described the basic device, shown in Fig. 1. It is merely a metal in direct physical contact with a semiconductor with the barrier height determined by bulk metal and semiconductor properties. The fact that real devices do not behave in this simple manner (Fig. 2), is attributed to surface states at the semiconductor surface [3]. The mechanism by which this comes about is shown in Figs. 3 and 4.

Bardeen [3] assumed that there were intrinsic surface states at the semiconductor surface prior to metal deposition and that these, if present in a sufficient density, could pin the surface Fermi level to some energy making the barrier height relatively independent of the metal work function. It has been shown [4] that for many semiconductors, the barrier height is approximately  $2/3$  of the bandgap for n-type and  $1/3$  of the bandgap for p-type materials.

The nature of the surface states is not well understood. The termination of the bulk lattice at the surface will introduce dangling bonds, the surface morphology being different from that in the bulk and various impurities on the surface are some of the mechanisms giving rise to surface states [5].

The deposition of the metal alters the nature of these surface states. Recent work by Spicer [6] suggests that in the metal deposition process, defect levels are created in the semiconductor. For a sufficiently high defect density, the surface Fermi level should be pinned to the defect energy level. This is shown in Fig. 5 for GaAs. The location of the Fermi level coincides with the EL2 antisite defect energy levels. This defect is the result of an As atom occupying a Ga site, and it has been suggested [7] that such antisite defects are created at the surface by the deposition process.

Because the exact details of surface states and their role in m-s contacts are not well understood, it is clear that "m-s engineering", i.e. designing the barrier height to a specific value, can in general not be done. The closest to such a realization are silicide-silicon contacts [8] in which the interface is located below the original silicon surface because silicon is consumed in the silicide formation process. This appears to reduce or eliminate surface state related effects. The resulting nearly

linear proportionality between barrier heights and work functions is shown in Fig. 2. For metals, however, it is virtually impossible to make ohmic contacts of the "accumulation" type, although such contacts are preferred because of their low barrier heights. A good example is shown in Fig. 6 for Al/n-Si [9]. The Schottky argument would predict a barrier height of 0.2V, while in reality it is observed to be 0.6-0.7V.

This raises the question "how do we make good ohmic contacts?" The energy band diagrams of a m-s contact with increasing semiconductor doping and constant barrier height are shown in Fig. 7. As the doping concentration is increased, it becomes progressively easier for electrons to tunnel from the metal to the semiconductor and from the semiconductor to the metal, because tunnelling depends chiefly on the width of the barrier. The higher the tunnelling probability the lower the contact resistivity. This is clearly shown in Fig. 6. An additional factor that helps to reduce the contact resistivity is barrier lowering [10], shown in Fig. 8.

An ohmic contact is characterized by a contact resistance, related to the contact resistivity in a complicated manner as a result of the current flow. The front contact of a solar cell is as shown in Fig. 9. The current flows through the thin n-surface layer into the contact causing current crowding at the edge of the contact. To first order, the voltage in the diffused layer under the contact decays exponentially with a characteristic transfer length,  $L_T$  [11]. It depends on both the contact resistivity,  $\rho_c$ , and the sheet resistance,  $R_s$ , and is a measure of that part of the contact that is active in the current flow from the diffused layer to the metal. Once the current is in the metal, it of course spreads out due to its low resistivity.

The expression for the contact resistance is given in Fig. 10. It incorporates both geometrical factors as well as  $\rho_c$  and  $R_s$  [12,13]. Fig. 11 indicates that for typical sheet resistances of 30-100 ohms/square, typical of solar cells,  $L_T$  can be very short. For  $\rho_c = 10^{-4}$  ohm-cm<sup>2</sup>, it is only 10 $\mu$ m, so that even if the contact is 100 $\mu$ m wide, only 10 $\mu$ m around the edge participates in the transfer of current from the diffused layer to the metal. The normalized plot of Fig. 12 shows the contact resistance multiplied by the length of the contact as a function of the contact width, L. It clearly shows that when L exceeds  $L_T$ , the contact resistance is constant and making the contact wider does not result in lower contact resistance. Widening the contact will, however, reduce the grid line resistance but will also increase shading of the cell.

What contact resistance values are required for solar cells? The series resistance of solar cells is the sum of several components, as shown in Fig. 13. Clearly all of these must be optimized, but here we are only concerned with the front and back contact resistance. A first order calculation in Fig. 14 assumes (i) the power loss due to series resistance is 5% [14], and (ii) the contact resistance contributes 10% of the total resistance, i.e. 0.5% of the power loss. The calculated contact resistivities are  $10^{-3}$  ohm-cm<sup>2</sup> for conventional one-sun applications and  $10^{-5}$  ohm-cm<sup>2</sup>

for concentrator 100-sun applications. The requirements for the back contacts are less severe because the contact area is equal to the cell area. This is shown in Fig. 15.

Experimentally determined contact resistivities for Si [15, 16, 17] and GaAs [18] are shown in Figs. 16 and 17. Values for p-Si are less than those for n-Si, because the barrier heights are lower. Limiting values of around  $10^{-8}$  ohm-cm<sup>2</sup> are approached in both cases. The required values of  $10^{-5}$ - $10^{-3}$  ohm-cm<sup>2</sup> for n-Si are consistent with typical solar cell surface concentrations of  $1-2 \times 10^{20}$  cm<sup>-3</sup>. Most of the data points in Fig. 16 are for Al contacts that are well sintered for optimum resistance. Such low values may be difficult to achieve with plated and silk-screened contacts unless special attention is paid to ensure good, intimate contact between the metal and the semiconductor. Low contact resistance and high open circuit voltage places two conflicting requirements on the doping concentration of the n-layer, as shown in Fig. 18. In practice, the "higher" requirement has usually been chosen.

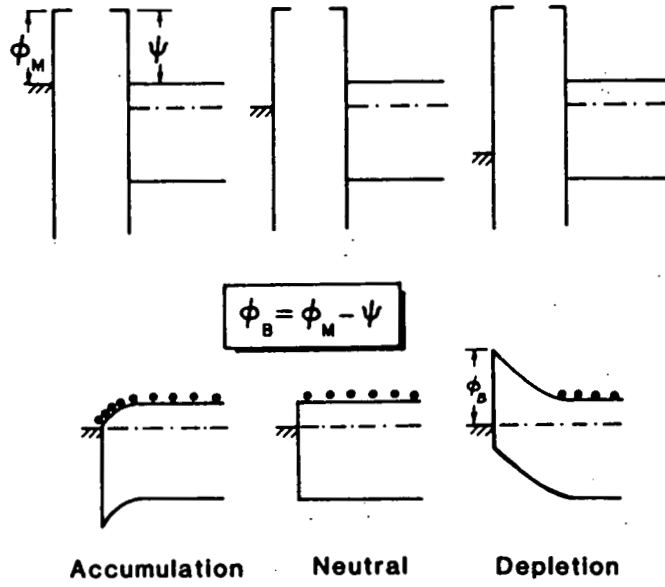
The discussion so far has dealt with a m-s contact that is "ideal" in the sense that there is uniform, intimate contact between the two, even though surface states are present. The surface state problem is overcome by using a heavily doped semiconductor. A "real" contact, however, is not this simple. It may look like that in Fig. 19. Generally there is a layer of oxide or other contaminant between the two with the result that the metal makes random contacts to the semiconductor and alloys non-uniformly [19]. In addition penetration of metal into the diffused layer causes spiking or even penetration of layers of only 0.1 μm thickness. For example, Al/Si often shows a high degree of non-uniformity, generally along the periphery of the contact, which can be eliminated by adding a small amount of Si or Cu to the Al [19]. The contaminant layer may be of little significance if it is sufficiently thin that tunnelling can proceed freely. If it is too thick, then the contact resistance will increase sharply.

It is clear that with proper surface preparation very low resistance contacts can be achieved. For low-cost solar cells, where cost-effective contacting methods like plating and silk-screening are being pursued, care must be exercised to ensure the low resistance contacts required for the cell's performance. This is especially true for concentrator applications where the photocurrent increases and  $I^2 R_s$  losses can become serious.

## References

1. E. H. Rhoderick, "Metal-Semiconductor Contacts", Clarendon Press, New York, 1978
2. W. Schottky, *Naturwissenschaften* 26, 843 (1938); *Z. Phys.* 113, 367 (1939); *Z. Phys.* 118, 539 (1942).
3. J. Bärdeën, *Phys. Rev.* 71, 717 (1947).
4. C. A. Mead in *Ohmic Contacts to Semiconductors* (B. Schwartz ed.), J. Electrochem. Soc., New York, 3 (1969).
5. R. H. Williams, *Contemp. Phys.* 23, 329 (1982).
6. W. E. Spicer, I. Lindau, P. R. Skeath and C. Y. Su, *Appl. Surf. Sc.* 9, 83 (1981).
7. E. R. Weber, H. Ennen, U. Kaufmann, J. Windscheif, J. Schneider and T. Wosinski, *J. Appl. Phys.* 53, 6140 (1982).
8. J. L. Freeouf, *J. Vac. Sci. Technol.* 18, 910 (1981).
9. Y. C. Yu, *Solid-State Electr.* 13, 239 (1970).
10. S. M. Sze, "Physics of Semiconductor Devices", J. Wiley and Sons, New York, 2nd ed., 1981.
11. P. L. Hower, W. W. Hooper, B. B. Cairns, R. D. Fairman and D. A. Tremere, in "Semiconductors and Semimetals"; (R. K. Willardson and A. C. Beer eds.), 7A, 147 (1971).
12. H. H. Berger, *Solid-State Electron.* 15, 145 (1972); *J. Electrochem. Soc.* 119, 509 (1972).
13. H. Murrmann and D. Widmann, *IEEE ED-16*, 1022 (1969).
14. M. Wolf, 15th Photovolt. Spec. Conf. 506 (1981).
15. D. Pramanik and A. N. Saxena, *Solid-State Techn.* 26, 127 (1983).
16. S. S. Cohen, P. A. Piacente, G. Gildenblat and D. M. Brown, *J. Appl. Phys.* 53, 8856 (1982).
17. M. Maenpaa, I. Suni, M. A. Nicolet, F. Ho and P. Iles, 15th Photovolt. Spec. Conf., 518 (1981).
18. N. Baslau, *J. Vac. Sci. Technol.* 19, 803 (1981).
19. M. Finetti, P. Ostoja, S. Solmi and G. Soncini, *Solid-State Electr.* 23, 255 (1980).

Figure 1. Schottky Model



$$J = A^{**} T^2 \exp(-q\phi_B/kT) (\exp(qV/kT) - 1)$$



Figure 2. Barrier Heights

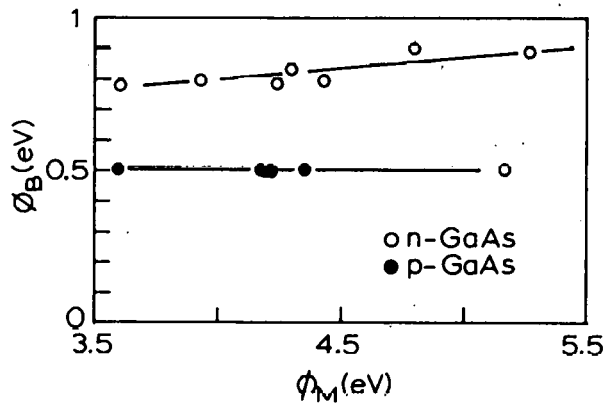
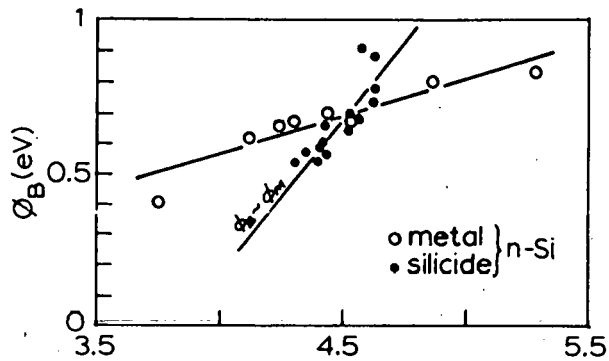
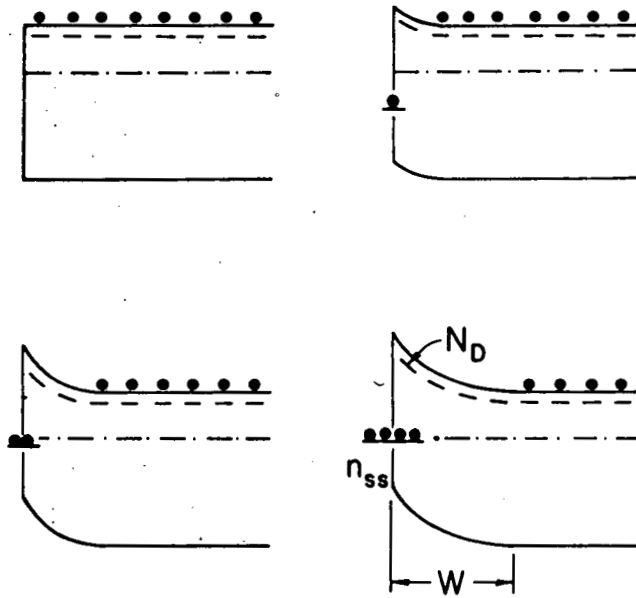
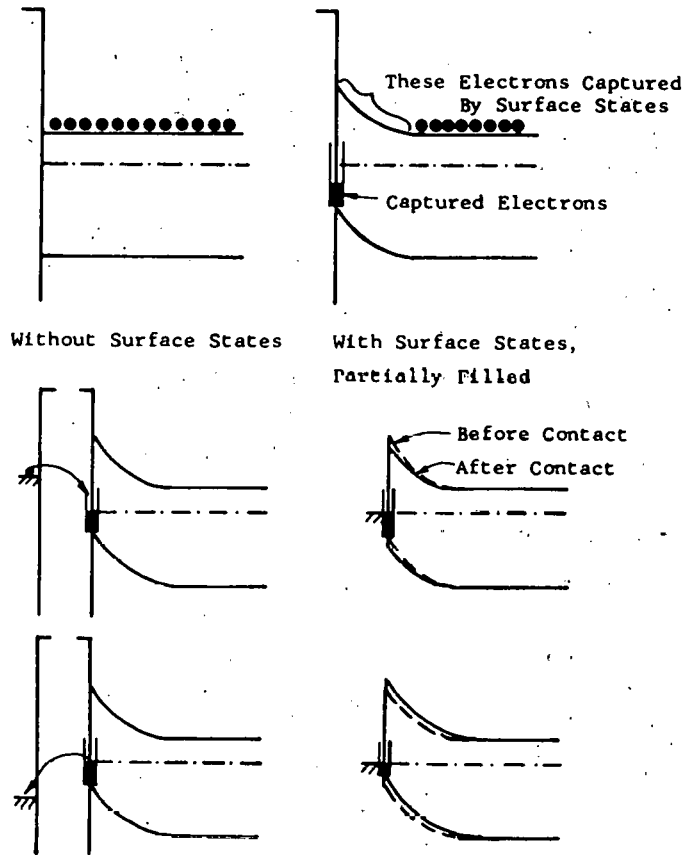


Figure 3. Effect of Surface States



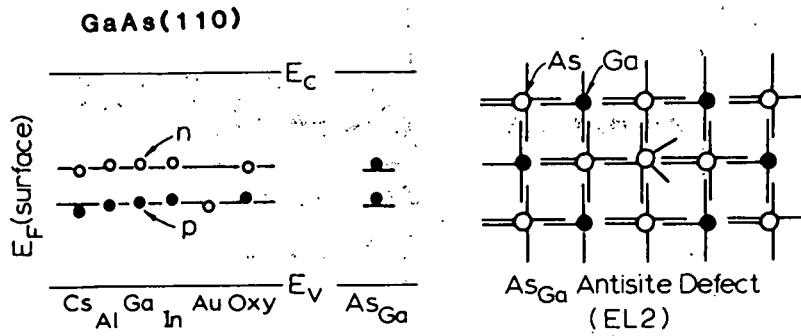
$$n_{ss} = N_D W$$

Figure 4. Bardeen Model



$$\phi_B = S(\phi_M - \psi) + C$$

Figure 5. Spicer Model



- $E_F$  pinning independent of atom
- $E_F$  pinning completed by less than one monolayer of atoms
- Adsorbed atoms disturb surface, creating defect levels

Figure 6. Example: Al-n-Si

$$\phi_M(\text{Al})=4.25 \text{ V}; \psi(\text{Si})=4.05 \text{ V}$$

Hence should get  $\phi_B=0.2 \text{ V}$ ; in reality  $\phi_B=0.6-0.7 \text{ V}$

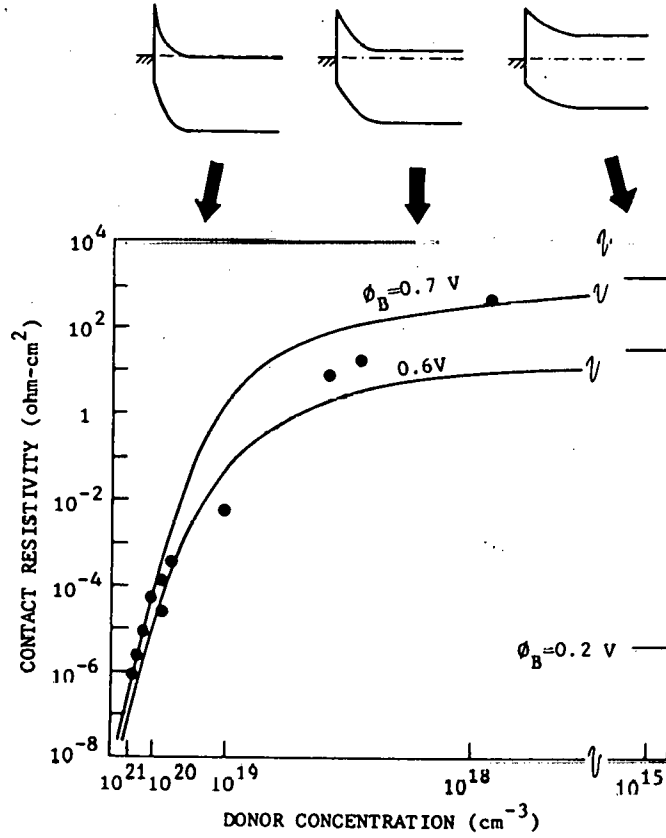
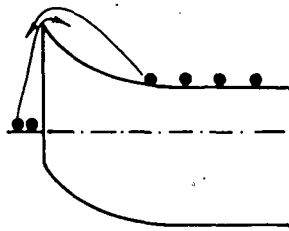


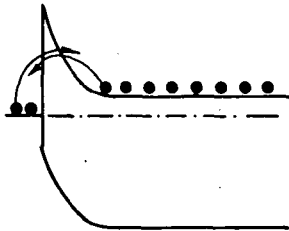
Figure 7. Barrier Width–Doping Concentration



$$\rho_c \sim e^{-q\phi_B/kT}$$

$$\sim 10^3 \Omega \text{ cm}^2 \text{ for } \phi_B = 0.7 \text{ eV}$$

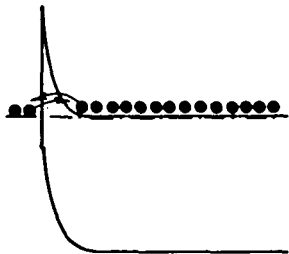
Low  $N_D$  -Thermionic Emission



$$\rho_c \sim 1/N_D$$

$$\sim 1-100 \Omega \text{ cm}^2$$

Intermediate  $N_D$  -Thermionic/Field Emission

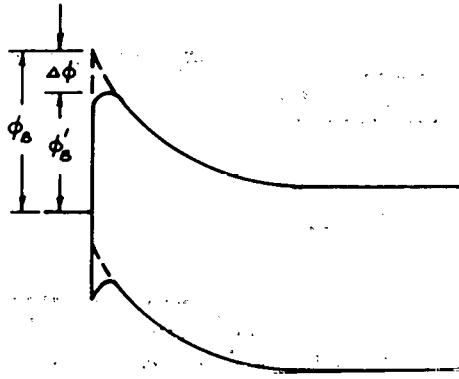


$$\rho_c \sim e^{-\kappa\phi_B/\sqrt{N_D}}$$

$$\sim 10^{-8} - 10^{-2} \Omega \text{ cm}^2$$

High  $N_D$  -Field Emission

Figure 8. Barrier Lowering



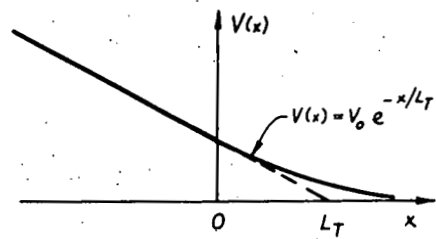
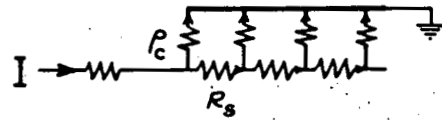
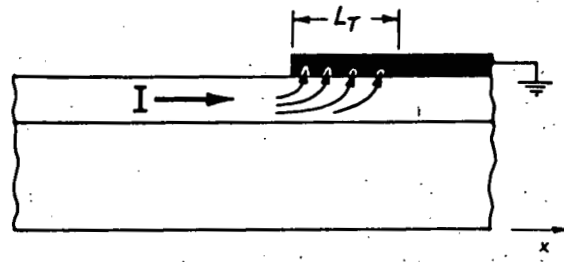
$$\Delta\phi = \left( \frac{qE}{4\pi k_s \epsilon_0} \right)^{1/2}$$

$$E = \frac{qN_D W}{k_s \epsilon_0} \quad W = \left( \frac{2k_s \epsilon_0 \phi_B}{qN_D} \right)^{1/2}$$

for Si:

$N_D$ ( $\text{cm}^{-3}$ )	$10^{18}$	$10^{19}$	$10^{20}$
$\Delta\phi$ (eV)	0.08	0.13	0.24

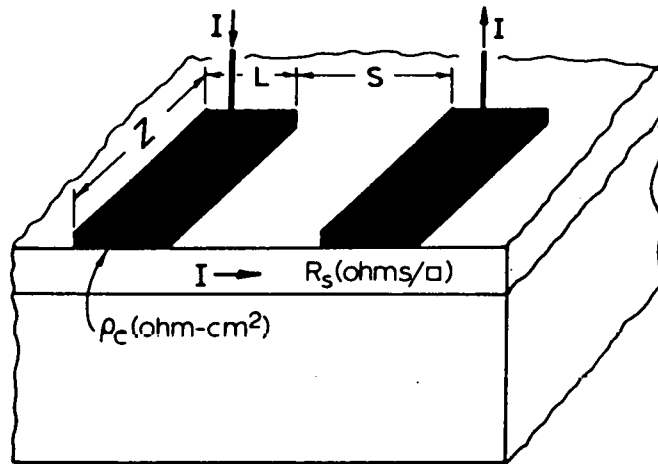
Figure 9. Contact Current Crowding



$$L_T = \sqrt{\rho_c / R_s} \quad (\text{Transfer Length})$$



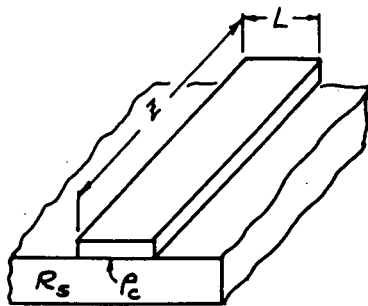
Figure 10. Layer and Contact Resistance



$$R = R_s(S/Z) + (2 L_T/Z) R_s \coth(L/L_T)$$

$R_{\text{layer}}$        $R_{\text{contact}}$

Figure 11. Transfer Length, Contact Resistance



$$L_T = \sqrt{\rho_c / R_s}$$

$$R_c = (L_T / Z) R_s \coth(L / L_T)$$

$$R_c \approx L_T R_s / Z \text{ for } L \geq 1.5 L_T$$

$$R_c \approx \rho_c / LZ \text{ for } L \leq 0.5 L_T$$

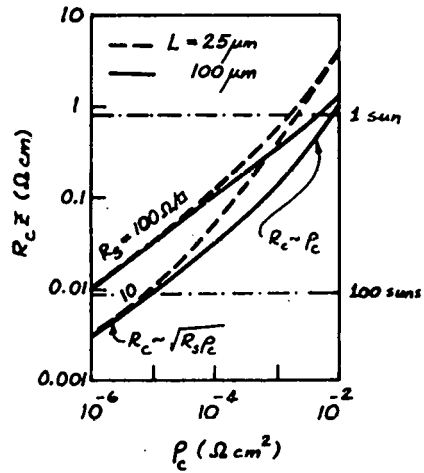
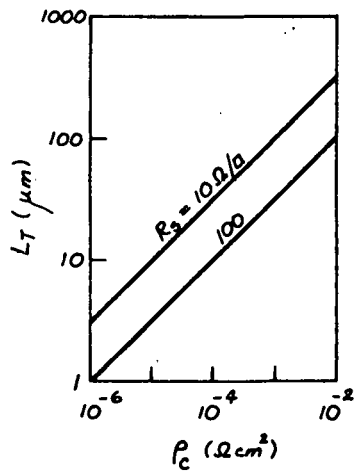


Figure 12. Contact Resistance, Contact Size

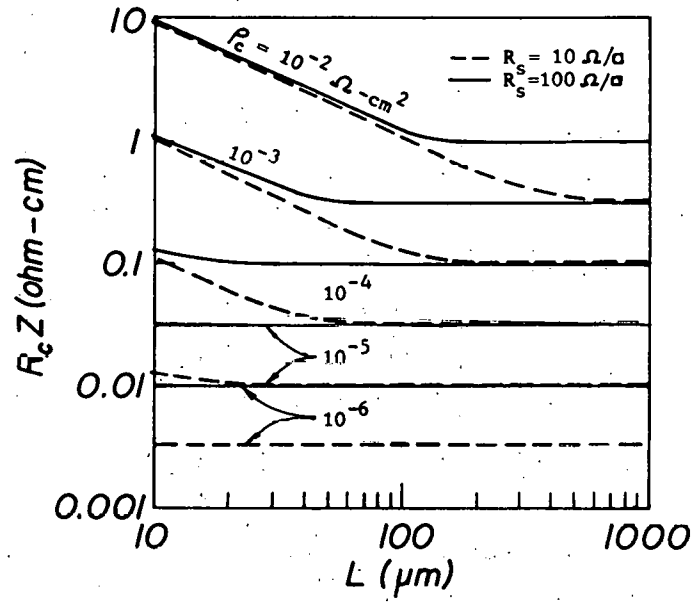
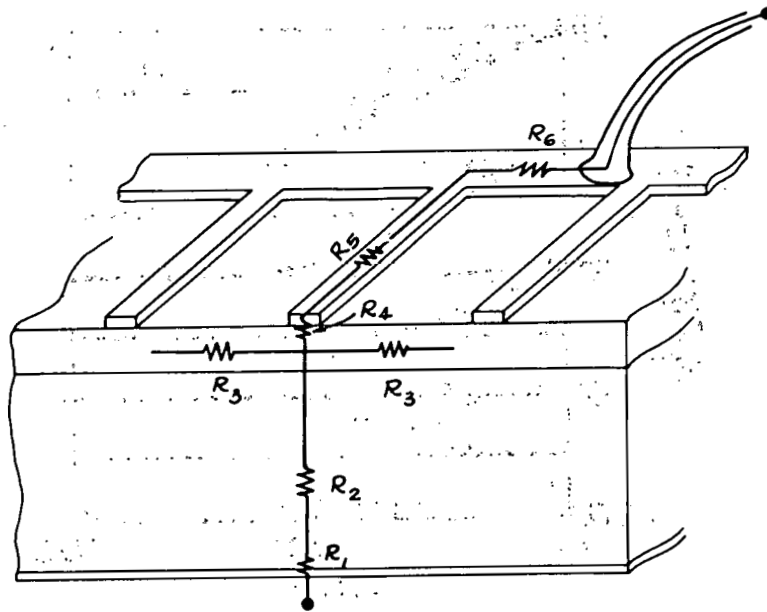


Figure 13: Solar Cell Series Resistance



$$R_s = \sum_{i=1}^6 R_i$$

- |                        |                       |
|------------------------|-----------------------|
| $R_1$ = back contact   | $R_4$ = front contact |
| $R_2$ = bulk           | $R_5$ = grid lines    |
| $R_3$ = diffused layer | $R_6$ = bus lines     |

## Figure 14. Front Contact

### • Case 1

$$A = 100 \text{ cm}^2 \quad J = 30 \text{ mA/cm}^2 \quad V = 0.5 \text{ V} \quad (\text{1 sun})$$

$$\Rightarrow \underline{P = 1.5 \text{ W}}$$

$$\text{Loss due to } R_s : 5\% ; \text{ i.e. } 7.5 \times 10^{-2} \text{ W} = I^2 R_s$$

$$R_s \leq 8.3 \times 10^{-3} \Omega$$

$$\text{Let } R_p(\text{front contact}) \leq 0.1 R_s = 8.3 \times 10^{-4} \Omega$$

$$\text{Let } A(\text{front contact}) = 0.05 A = 5 \text{ cm}^2 \\ = 50 \mu\text{m} \times z \Rightarrow z = 10 \text{ cm}^3$$

$$\therefore \underline{R_c z \leq 0.83 \Omega \text{ cm}}$$

$$R_c z \approx 0.83 \Omega \text{ cm} \quad L = 50 \mu\text{m} \quad R_s = 100 \Omega/\square$$

$$\Rightarrow \boxed{P_c \leq 10^{-3} \Omega \text{ cm}^2}$$

### • Case 2

$$A = 10 \text{ cm}^2 \quad J = 3 \text{ A/cm}^2 \quad V = 0.5 \text{ V} \quad (\sim 100 \text{ suns})$$

same arguments

$$\Rightarrow \boxed{P_c \leq 10^{-5} \Omega \text{ cm}^2}$$

## Figure 15. Back Contact

- **Case 1**

$$A = 100 \text{ cm}^2 \quad J = 30 \text{ mA/cm}^2 \quad V = 0.5 \text{ V} \quad (\text{1 sun})$$

$$P = 1.5 \text{ W}$$

for similar loss due to  $R_s$  as for front contact

$$R_c \text{ (back contact)} \leq 8.3 \times 10^{-4} \Omega$$

but  $A \text{ (back contact)} = 100 \text{ cm}^2$

$$P_c = R_c A$$

$$\Rightarrow \boxed{P_c \leq 10^{-1} \Omega \text{ cm}^2}$$

- **Case 2**

$$A = 10 \text{ cm}^2 \quad J = 3 \text{ A/cm}^2 \quad V = 0.5 \text{ V} \quad (\sim 100 \text{ suns})$$

$$\Rightarrow \boxed{P_c \leq 10^{-3} \Omega \text{ cm}^2}$$

Figure 16. Contact Resistivity: Si

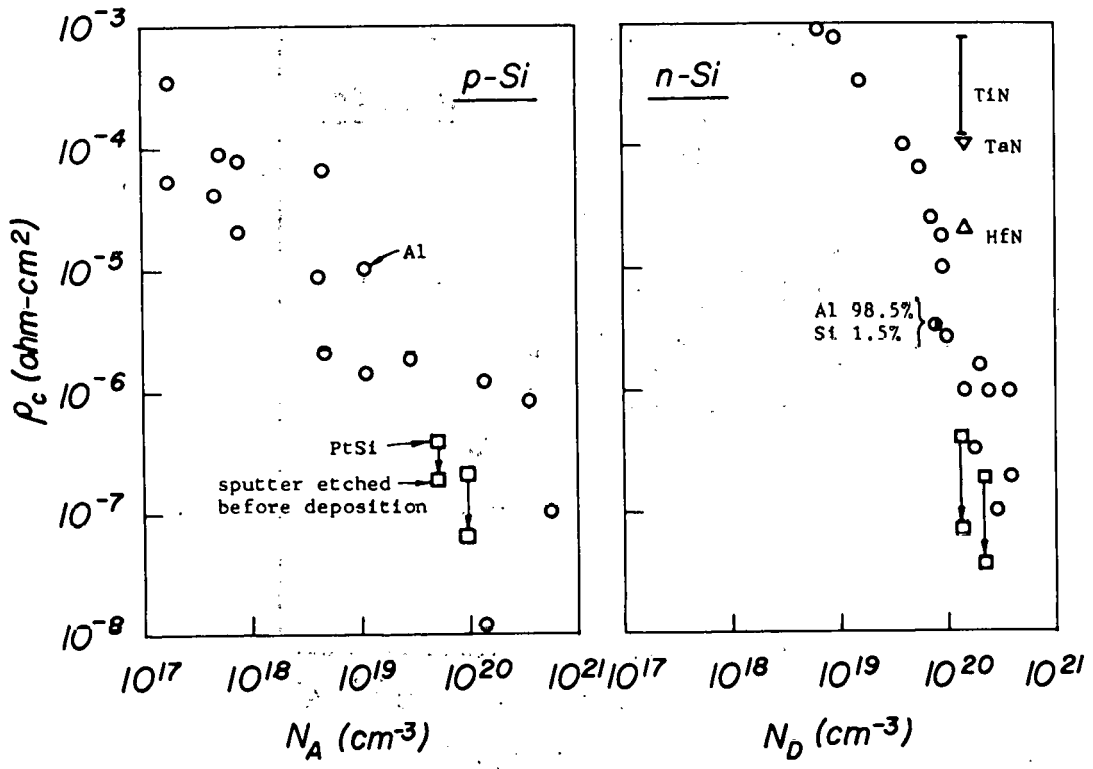


Figure 17. Contact Resistivity: GaAs

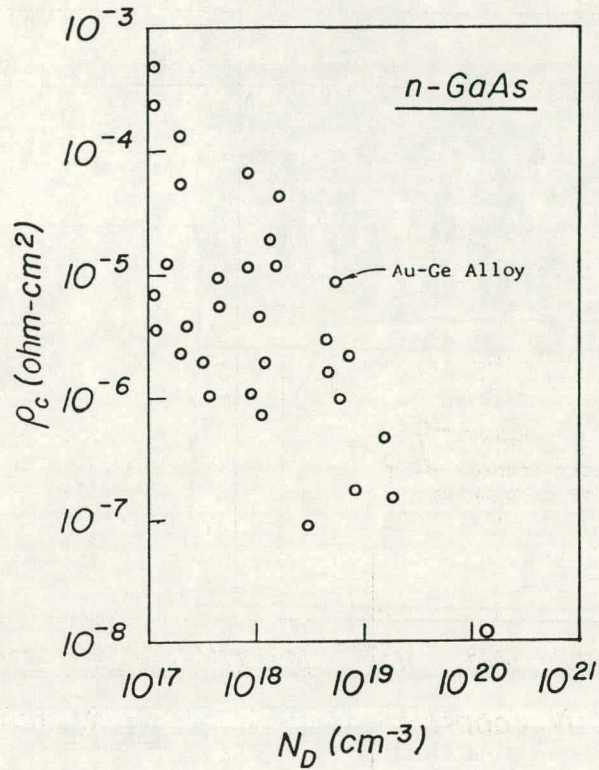
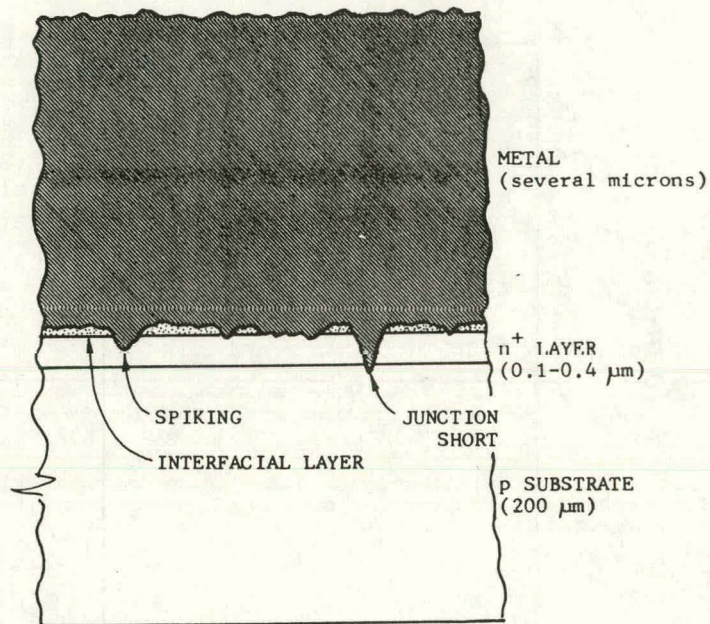


Figure 18. Diffused Layer  $N_D$

- Should be low, because of
  - Bandgap narrowing
  - Auger recombination
  - Increased  $I_{sat}$
  - $N_D \lesssim 1-2 \times 10^{19} \text{ cm}^{-3}$
  
- Should be high, because of
  - Layer sheet resistance
  - Contact resistance
  - $N_D \gtrsim 10^{20} \text{ cm}^{-3}$



Figure 19. "Real" Metal-Semiconductor Contact



- Contact area can be much smaller than metal area
- Interfacial layer must be thin for efficient tunnelling ( $\lesssim 25 \text{ \AA}$ )

## DISCUSSION

HOGAN: Would you comment on the process of annealing, and what might be happening considering gallium arsenide also?

SCHRODER: I think you will see when you read papers and they plot contact resistance as a function of temperature treatment (annealing, for example) that things tend to get better most of the time. Now what goes on? I don't know. Maybe there is an interdiffusion. There can be interdiffusion of metallic species at room temperature. People have found metallic impurities in the semiconductor by not heating it at all, so there is interdiffusion. People are doing a lot of work right now on silicides. I really don't know what the answer is. I don't know what goes on in the contact and I am not sure if anyone else really knows how much interdiffusion really takes place. Does it dope, does it not dope, etc.; we can play all sorts of games, as we heard earlier. If we implant donors or acceptors we can lower or raise the barrier height, and so on, but I think as a rule we don't really understand, not very well anyway.

NICOLET: Would you project the viewgraph with the contact resistivity values? I can give you an upgraded number for titanium nitride.

SCHRODER: This was from a paper two years ago.

NICOLET: We have done Ti-nitride on n as well as on p up about where you have hafnium nitride. About half way; it is  $3$  or  $4 \times 10^{-5}$  and it is the same for n and p. That value is 2 after you anneal by  $400^\circ$  or so. If you don't have it before, it is worth noting that in n on p there is a shift in the value height that has to do with certain states, which goes away by annealing and that, we think, comes because we use RF sputtering. If we did that with dc it probably would be less. We have better numbers. It's still high on the rest of these things, but it is more where hafnium nitride is.

SCHRODER: But you don't really need these values for conventional solar cells. I think if you are here you are fine.

NICOLET: Well, up to 30 times concentration of these values --

SCHRODER: Right, exactly. I think if you can do  $10^{-4}$ ,  $10^{-5}$ , reproducibly, there is no problem. I think it is only when you start moving up to here that you are going to run into problems.

QUESTION: Excuse me, is that using transmission line?

NICOLET: This problem -- this will be published in Solid State Electronics -- the difficulty with making good measurements on these layers is that you have to include the sheet resistivity to the metal layer also. You have to take a double transmission line model -- we can do that in the beginning, learn quite a lot from difficulties -- so we got numbers that attributed voltage difference to the contact resistance while it was due

to the metal. So if you cover that with additional metal to get rid of this or you apply models that include the effect, you get the same result. This is why we are fairly confident that these numbers now are real, honest-to-God numbers for the measurements we have made.

SCHRODER: The measurements are not trivial for these contact resistivities. There was a paper recently that dealt with polysilicon to silicon in which certainly the resistance of the poly becomes very important, and you ought to take that into account, just like you said for the metal, which we normally think of as infinitely conducting. It really isn't.

WOLF: Since you essentially make the entire surface degenerate to make a good ohmic contact -- there was an old method used some decades ago, of mechanically damaging the surface heavily to make a good ohmic contact. Is that a somewhat related method, to essentially make the surface degenerate too?

SCHRODER: I thought about that a little bit and I think what is happening is you have created an enormous number of recombination centers. Normally an ohmic contact is a region of infinite recombinations. That is how we define it from a device viewpoint. So if you, in truth, introduce an enormous number of recombination centers by mechanically damaging the surface, I am not sure I would rely on the reliability of the ohmic contact.

**SESSION II: METALLIZATION SYSTEM DESIGN**

**Dale R. Burger (Jet Propulsion Laboratory), Chairman**

**(The following pages by D.R. Burger were not presented orally, but were handed out at the beginning of Session II, and serve as an introduction to it).**

THIS PAGE  
WAS INTENTIONALLY  
LEFT BLANK

## GETTING THE CURRENT OUT

Dale R. Burger  
Jet Propulsion Laboratory

### INTRODUCTION

Progress of a photovoltaic (PV) device from a research concept to a competitive power-generation source requires an increasing concern with current collection. The initial metallization focus is usually on contact resistance, since a good ohmic contact is desirable for accurate device characterization measurements. As the device grows in size, sheet resistance losses become important and a metal grid is usually added to reduce the effective sheet resistance. Later, as size and conversion efficiency continue to increase, grid-line resistance and cell shadowing must be considered simultaneously, because grid-line resistance is inversely related to total grid-line area and cell shadowing is directly related. Finally, large devices often require bus bars to handle the generated current efficiently.

A PV cell grid design must consider the five power-loss phenomena mentioned above: sheet resistance, contact resistance, grid resistance, bus-bar resistance and cell shadowing. The requirement for competitive power generation adds processing and material cost considerations to the above purely physical concerns. The design of PV cell metallization systems must therefore balance these factors along with other factors such as reliability, materials and end use.

### BACKGROUND

Although cost, reliability and usage are important factors in deciding upon the best metallization system, this paper will focus only upon grid-line design and substrate material problems for flat-plate solar arrays.

Extensive literature is available on analyzing power losses associated with the grid patterns on rectangular PV cells (References 1 through 7). There has been only one computer program released (Reference 8) and one paper presented (Reference 9) that focused on optimal (minimum power loss) grid-pattern designs for round or rectangular cells with more than two design variables.

The computer program (Reference 8), CELCAL (see Appendix A), is a FORTRAN program that treats all inputs as variables and calculates a point solution for each input data set. Optimization must be done manually by iteration. Calculation of the sheet-resistance power loss is by sectional integration (Reference 10). This method is an approximation to the more exact but difficult solution of Poisson's equation for the potential as a function of position (Reference 3). The error introduced by this approximation is small. Another attribute of the CELCAL program is the ability to handle up to three bus bars, which may be either coplanar or multilevel\*.

---

\*J.R. Davis, Westinghouse R&D Center, private communication.

Daniel, Burger and Stone (Reference 9) (Appendix B) use nonlinear optimization, a modified Newton-Raphson method, for interactive computer optimization. This program is written in APL and is presently available only at the Jet Propulsion Laboratory (JPL). When documentation is completed, this APL program will be submitted to the NASA Computer Software Management and Information Center (COSMIC) data bank. This program also uses a sectional integration approach; however, it provides a more precise calculation of round-cell power losses and has sensitivity analysis capabilities.

Considerable analytical effort has been expanded in the development of PV-cell grid lines. These efforts have largely been focused upon single-crystal silicon cells, based on wafers cut from Czochralski-grown ingots. High wafer costs have resulted in the development of numerous competitive PV devices. Using these devices for power production will pose some interesting problems.

### NEW CHALLENGES

At least three new PV materials are being investigated for power production: amorphous silicon, gallium arsenide and copper indium diselenide. Amorphous silicon (a-Si) has been introduced to the world in solar-powered calculators and wrist watches. Japan now manufactures at least two megawatts per year of a-Si cells for the consumer-product market. These cells are typically only 1% to 3% efficient. Some small research a-Si cells have shown 10% conversion efficiency, but larger devices are usually only 5% to 6% efficient. Part of the problem with a-Si is its very high sheet resistivity. A transparent conductive coating (TCC) is required to lower the sheet resistance, adding another element to the metallization design problem. Some TCCs have shown a contact resistance problem with a-Si. An additional problem with a-Si is its thermal sensitivity. Many metallization systems use a sintering process with temperatures exceeding the allowable a-Si range.

Gallium arsenide (GaAs) has a very high operating temperature range and a reasonable sheet resistivity. Why, then, is there a problem? Compound semiconductors contain, by definition, more than one elemental component and thus present a greater range of possibilities for inter diffusion, reaction and compound formation. In particular, GaAs is now attractive only as a power generator due to its high service temperature, which permits its use in PV concentrator cells. These cells combine high current densities with high temperatures and thereby impose severe conditions on the metallization system.

A more recent power system contender is copper indium diselenide. Appropriate metallization systems for this material are being investigated.

Other materials, such as cadmium telluride and zinc phosphide, are possible future contenders.

The field of metallization systems design for photovoltaic application will remain very active for at least the next decade as the world gradually converts to renewable energy sources.

## REFERENCES

1. Wolf, M., Proc. IRE, 48, 1246, 1960.
2. Handy, R.J., Solid-St. Electron. 10, 765, 1967.
3. Wyeth, N.C., Solid-St. Electron. 20, 629, 1977.
4. Moore, A.R., RCA Review, 40, 153, 1979.
5. Jacobs, B., de Mey, G., and Stevens, K., Int. J. Electron. 48, No. 5, 397, 1980.
6. Flat, A., and Milnes, A.G., Solar Energy, 25, 283. 1980.
7. Saha, H., Mukhopadhyay, K., and Biswas, D., Int. J. Electron. 49, No. 4, 313, 1980.
8. Burger, D., CELCAL, NPO-15841, COSMIC, University of Georgia, Athens, Georgia 30602 (in press).
9. Daniel, R., Stone, H., and Burger, D., Proc. Electrochem. Soc. Symp. on Mater.; and New Process. Tech. for Photovoltaics, Montreal (in press).
10. Carbajal, B.G., Texas Instruments, Inc., Annual Report, ERDA/JPL-954405-77/4, March 1979.



THIS PAGE  
WAS INTENTIONALLY  
LEFT BLANK

# A Direct Measurement of Interfacial Contact Resistance

S. J. PROCTOR, MEMBER, IEEE, AND L. W. LINHOLM, MEMBER, IEEE

**Abstract**—A method is described for directly measuring interfacial contact resistance and estimating the degree of uniformity of the interfacial layer in metal-semiconductor contacts. A two-dimensional resistor network model is used to obtain a relationship between the specific contact resistance and the measured interfacial contact resistance for contacts with a homogeneous interfacial layer. Measurement results are given for 98.5% Al/1.5% Si and 100% Al contacts on n-type silicon.

## INTRODUCTION

AS THE critical feature size of semiconductor devices decreases, the physical size of the metal-semiconductor contact regions also decreases causing an increase in the resistance encountered as current passes between the metal and semiconductor. Problems are also encountered with the metallurgies and processes needed to produce reliable, low resistance contacts to regions with shallow junctions [1-5]. Because of these factors, the quality of the metal-semiconductor contacts will have an increased influence on the performance and reliability of integrated circuits.

This paper describes a planar test structure and test method for the direct measurement of interfacial contact resistance while minimizing interferences from parasitic resistances. A relationship is derived between the specific contact resistance and the measured interfacial contact resistance, and a test methodology is presented which allows for an estimate of the interfacial layer uniformity which has been ignored in previous work.

The electrical nature of the contact region is usually described in terms of contact resistance and specific contact resistance. Interfacial contact resistance is used in this paper to refer to the resistance associated with the metal-semiconductor interfacial layer formed during the sintering process and to distinguish it from the term contact resistance as defined by Berger [6]. Interfacial contact resistance (ohms) is defined as the total resistance of the metal-semiconductor interfacial layer encountered as current is forced from one layer to the other. Specific contact resistance (ohms-cm<sup>2</sup>) is defined as the resistance of a unit area of the metal-semiconductor interfacial layer and is expressed as the ratio of the voltage drop across the interfacial layer to the current density through the interfacial layer [7-9]. Specific contact resistance can only be estimated for a uniform interfacial layer.

For planar contacts, (MOSFET source and drain contacts),

a number of methods have been developed for the measurement of contact resistance and the subsequent determination of specific contact resistance [8-12]. The transmission line model (TLM) of the metal-semiconductor contact introduced by Shockley [10] and further refined by Berger [11] is a common method for determining specific contact resistance. Murrmann and Widmann [13] and Berger [11] developed a test structure to determine the "front" and "end" contact resistance as defined by the TLM. A disadvantage of this approach is that the total resistance sensed consists not only of the resistance of the interfacial layer but also the resistance of the diffused layer between the contacts, the resistance of the diffused layer and the metal layer at the contact window, and the resistance of parasitic elements associated with the geometry of the structure.

## A FOUR-TERMINAL CONTACT RESISTANCE TEST STRUCTURE

The four-terminal test structure shown in Fig. 1 allows a direct Kelvin measurement of interfacial contact resistance. The structure is similar to that used by Anderson and Reith [14] and DeVries, Lee, and Watelski [15]. The measurement consists of forcing a known current from probe pad 1 to probe pad 3. Voltage is measured between probe pads 2 and 4 via the voltage taps, which are orthogonal to the direction of lateral current flow through the contact. This test structure allows for an improved measurement of the resistance of the interfacial layer by reducing the effects of parasitic resistances on the measurement. As the measurement is a Kelvin resistance measurement, the probe-to-probe pad resistance is not sensed and neither is the resistance (or voltage drop) in the current and voltage taps up to the contact region. By designing the diffusion taps to be of equal width to the contact window width, the parasitic resistance associated with current-pinch-off as current passes from the current tap into the contact is minimized [9]. Because the voltage taps are orthogonal to the direction of the lateral current flow through the contact, only the average voltage drop across the interfacial layer is sensed. A two-dimensional model of the four-terminal test structure is shown in Fig. 2. The model consists of  $N$  stages of metal resistors  $R_M$ , diffusion resistors  $R_D$ , and interfacial resistors  $R_I$ . For this model  $N = d/\Delta x$  where  $d$  is the contact window length and  $\Delta x$  represents the incremental length of each of the  $N$  stages. In addition, the voltage taps are included in the model and are represented by  $R_{MT}$  and  $R_{DT}$ , for the metal and diffusion taps, respectively. This model is analogous to the transmission line model with a nonzero metal layer resistance. The voltage difference,  $V_2 - V_1$ ,

Manuscript received June 28, 1982; revised July 30, 1982.

The authors are with the Semiconductor Devices and Circuits Division, National Bureau of Standards, Washington, DC 20234.

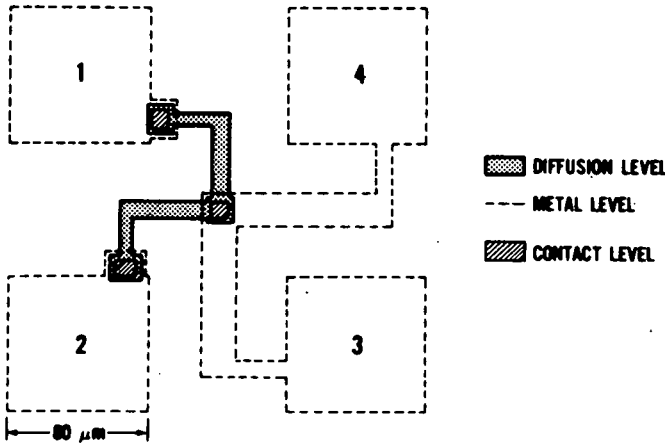


Fig. 1. Four-terminal contact resistance test structure.

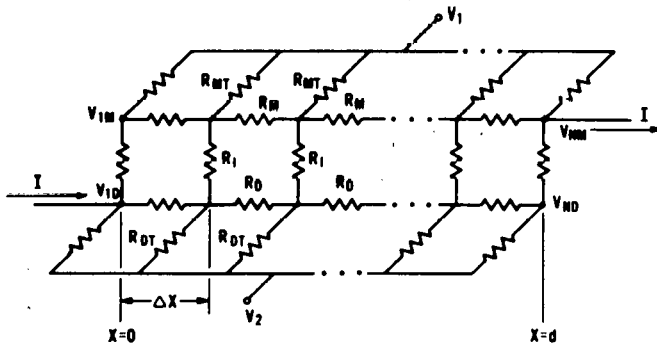


Fig. 2. Resistor network model of the four-terminal test structure.

between the diffusion and metal voltage taps divided by the forced current,  $I$ , represents the measured interfacial contact resistance. The resistance components,  $R_M$ ,  $R_D$ , and  $R_I$ , which represent their respective conductive layers, can be expressed as:

$$R_M = \frac{R_{SM} \Delta x}{W} \quad (1)$$

$$R_D = \frac{R_{SD} \Delta x}{W} \quad (2)$$

$$R_I = \frac{\rho_c}{W \Delta x} \quad (3)$$

where  $\rho_c$  is the specific contact resistance,  $W$  is the width of the contact window,  $R_{SM}$  and  $R_{SD}$  are the sheet resistances of the metal and diffusion layers in the contact region, respectively, and  $\Delta x$  represents the incremental length of each of the  $N$  stages.

This model can be used to determine a relationship between the measured interfacial contact resistance  $R_i$  and the specific contact resistance  $\rho_c$  for a homogeneous metal-semiconductor interfacial layer. Since no current passes out of the voltage taps

$$\sum_{j=1}^N \frac{V_{jM} - V_1}{R_{MT}} = 0 \text{ and } \sum_{j=1}^N \frac{V_{jD} - V_2}{R_{DT}} = 0 \quad (4)$$

where  $V_{jM} - V_1$  and  $V_{jD} - V_2$  are the voltages across the  $j$ th metal tap resistor and diffusion tap resistor, respectively.

The actual voltage difference between the two voltage taps is

$$V_2 - V_1 = \frac{1}{N} \sum_{j=1}^N (V_{jD} - V_{jM}). \quad (5)$$

Also, since all the current entering the structure must pass through the contact,

$$I = \sum_{j=1}^N \frac{V_{jD} - V_{jM}}{R_I} = \frac{N}{R_I} (V_2 - V_1), \quad (6)$$

and thus

$$R_i = \frac{V_2 - V_1}{I} = \frac{R_I}{N}, \quad (7)$$

where  $R_i$  is the measured interfacial contact resistance.

Equation 7 shows that  $R_i$  is dependent only on the resistance of the interfacial layer. This represents a different approach to the measurement of the resistance associated with a metal-semiconductor contact than that of contact resistance as defined by Berger. The resistances due to the diffusion layer beneath the contact and the metal layer above the contact, as well as the resistances of the voltage taps, are not sensed in the measurement. These results indicate that the four-terminal test structure can be used to make a direct measure of the interfacial contact resistance. The specific contact resistance,  $\rho_c$ , can be calculated from the measured interfacial contact resistance,  $R_i$ , and the design contact window area.

## RESULTS AND DISCUSSION

Measurements were made on test chips consisting of the test structure in Fig. 1 replicated with several geometric variations. The test chips were fabricated in a three-mask process. The  $n^+$  phosphorus diffusion resulted in a measured sheet resistance of 6.0 ohms/ $\square$ , as measured by a cross-bridge sheet resistor test structure [16] (also included on the test chip), and a measured junction depth of 3.5  $\mu\text{m}$ , as measured by a groove and stain technique. The diffusion step consisted of a phosphorus pre-deposition at 960°C for 60 min followed by a deglazing step and a 75 min drive-in ( $N_2$ -55 min,  $O_2$ -11 min,  $N_2$ -9 min) at 1100°C. The doping profile for the samples have been assumed to be gaussian with a resultant surface concentration of  $8.5 \times 10^{19} \text{ cm}^{-3}$ . The wafers were subjected to a 5 sec 10% HF etch immediately prior to metallization to ensure a clean contact surface. Two types of metallization were used in the experiment. One consisted of a 98.5% Al/1.5% Si mixture and the other, 100% Al. All wafers were sintered at 425°C for 20 min in 10% forming gas.

Test results with Al/Si metallization are plotted in Fig. 3. Al/Si metallization was used to prevent junction penetration or spiking during high-temperature processing and to give a more uniform interfacial layer [17]. Figure 3 shows measured interfacial contact resistance vs. contact window area for square contact windows with design dimensions ranging from 2.5  $\mu\text{m}$  to 20  $\mu\text{m}$  on a side. A least squares fit of the data shows a linear relation between the measured interfacial contact resistance and contact window area as expected.

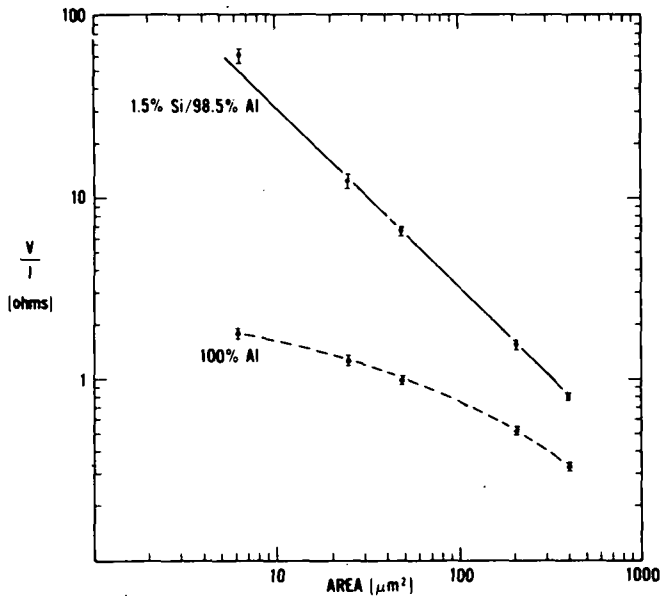


Fig. 3. Measured interfacial contact resistance vs. contact window area for two different metallizations. The solid line is a least squares fit to the 1.5% Si/98.5% Al data.

The specific contact resistance was calculated as  $3.2 \times 10^{-6}$  ohm-cm<sup>2</sup> for these samples. This result is in close agreement with that measured by Naguib and Hobbs [18] for the same surface concentration and similar sintering conditions. Visual inspection of the contact area on devices with the metallization removed confirmed that the interfacial region contained no observable nonuniformities.

Similar test results from samples with 100% Al metallization are also seen in Fig. 3. An obvious nonlinear relation between the measured interfacial contact resistance and contact window area is observed. Visual inspection of the contact area on these devices with the metallization removed showed a high degree of nonuniformity similar in appearance to that reported by McCarthy [19]. The nonuniformities were generally found along the periphery of the contact window and are generally attributed to the dissolution of silicon into the aluminum during the sintering process and subsequent recrystallization of the silicon at the Al/Si interface upon cooling [1].

Test results from a single test structure cannot be used to estimate the specific contact resistance of the interfacial layer unless it has been determined that the layer is homogeneous. By measuring several test structures with each having different contact window area, the degree of homogeneity can be estimated by determining if a linear relation exists between the measured interfacial contact resistance and the contact area. When the interfacial layer is nonuniform, an accurate estimate of specific contact resistance cannot be made. For this case, the interfacial contact resistance for each contact geometry is the only parameter that can be measured.

#### CONCLUSION

A direct measurement of interfacial contact resistance using a four-terminal test structure results in an improved measure-

ment by minimizing measurement interferences. A simple model relates the measured interfacial contact resistance to the specific contact resistance for structures with a homogeneous interfacial layer. Test results from test structures with different contact window areas allow for an estimate of the metal-semiconductor interfacial layer uniformity.

#### ACKNOWLEDGMENT

Portions of this work were supported by the Defense Advanced Research Projects Agency (ARPA Order No. 3882).

#### REFERENCES

- [1] M. Finetti, P. Ostojic, S. Solmi, and G. Soncini, "Aluminum-silicon ohmic contact on "shallow" n<sup>+</sup>/p junctions," *Solid-State Electron.*, vol. 23, pp. 255-262, 1980.
- [2] S. Vaidya, "Electromigration in aluminum/poly-silicon composites," *Appl. Phys. Lett.*, vol. 39, pp. 900-902, 1981.
- [3] M. Morimoto, E. Nagasawa, H. Okabayashi, and M. Kondo, "An Mo gate 4K static RAM fabricated using a novel direct contact technology," *IEDM Tech. Digest*, pp. 655-657, 1981.
- [4] S. Vaidya, "Al/Poly-Si metallization for small geometry, shallow junction contacts and line line interconnects," *Electrochem. Soc. Ext. Abs.*, vol. 82-1, p. 369, May 1982.
- [5] S. S. Cohen, G. Gildenblat, and D. M. Brown, "Ohmic contacts to shallow junctions in silicon," *Electrochem. Soc. Ext. Abs.*, vol. 82-1, pp. 364-365, May 1982.
- [6] H. H. Berger, "Contact resistance and contact resistivity," *J. Electrochem. Soc.*, vol. 119, no. 4, pp. 507-513, 1972.
- [7] C. Y. Chang and Y. K. Fang, "Specific contact resistance of metal-semiconductor barriers," *Solid-State Electron.*, vol. 14, pp. 541-550, 1971.
- [8] A. Y. Yu, "Electron tunneling and contact resistance of metal-silicon contact barriers," *Solid-State Electron.*, vol. 13, pp. 239-247, 1970.
- [9] C. Ting and C. Chen, "A study of the contacts of a diffused resistor," *Solid-State Electron.*, vol. 14, pp. 433-438, 1971.
- [10] A. Goetzberger and R. M. Scarlett, "Research and investigation of inverse epitaxial UHF power transistors," Appendix B, Report No. AFAL-TDR-64-207, Air Force Avionics Laboratory, September 1964.
- [11] H. H. Berger, "Models for contacts to planar devices," *Solid-State Electron.*, vol. 15, pp. 145-158, 1972.
- [12] G. K. Reeves and H. B. Harrison, "Obtaining the specific contact resistance from transmission line model measurements," *Electron. Device Lett.*, EDL 3, pp. 111-113, 1982.
- [13] H. Murrmann and D. Widmann, "Current crowding on metal contacts to planar devices," *IEEE Trans. Electron Devices*, ED-16, pp. 1022-1024, 1969.
- [14] R. M. Anderson and T. M. Reith, "Microstructural and electrical properties of thin PtSi films and their relationships to deposition parameters," *J. Electrochem. Soc.*, vol. 122, pp. 1337-1347, 1975.
- [15] D. B. DeVries, G. Lee, and S. Watelski, "Integrated-circuit process control and development," Technical Report AFAL-TR-73-268, Air Force Avionics Laboratory, August 1973.
- [16] M. G. Buehler, S. D. Grant, and W. R. Thurber, "Bridge and van der Pauw sheet resistors for characterizing the line width of conducting layers," *J. Electrochem. Soc.*, vol. 125, pp. 650-654, 1978.
- [17] P. B. Ghate, J. C. Blair, and R. C. Fuller, "Metallization in microelectronics," *Thin Solid Films*, vol. 45, pp. 69-84, 1977.
- [18] H. M. Naguib and L. H. Hobbs, "Al/Si and Al/Poly-Si contact resistance in integrated circuits," *J. Electrochem. Soc.*, vol. 124, no. 4, pp. 573-577, 1977.
- [19] J. McCarthy, "Failure of aluminum contacts to silicon in shallow diffused transistors," *Microelectronics and Reliability*, vol. 9, pp. 187-188, 1970.

THIS PAGE  
WAS INTENTIONALLY  
LEFT BLANK

# A MICROELECTRONIC TEST STRUCTURE FOR INTERFACIAL CONTACT RESISTANCE MEASUREMENT

NATIONAL BUREAU OF STANDARDS

L.W. Linholm  
J.A. Mazer  
S.J. Proctor

## Outline

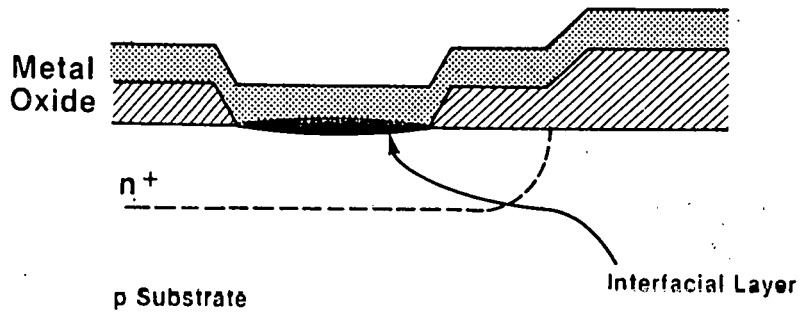
- Introduction
- Metal-Semiconductor Contact Models
- Test Structure and Test Method
- Test Results
- Measurement Interferences

## Objective

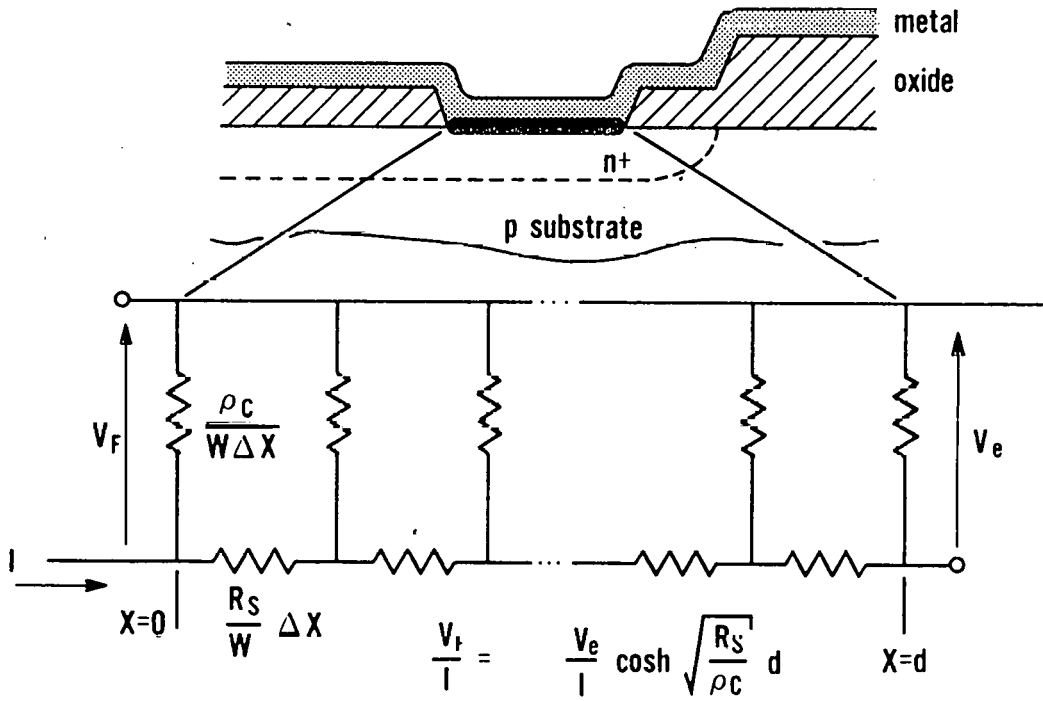
**To develop a microelectronic test structure and test method for:**

- Making a direct measurement of interfacial contact resistance
- Estimating the uniformity of the metal-semiconductor interfacial layer
- Estimating specific contact resistance
- Minimizing measurement interferences

### Cross Section of Contact Window



### Transmission-Line Model



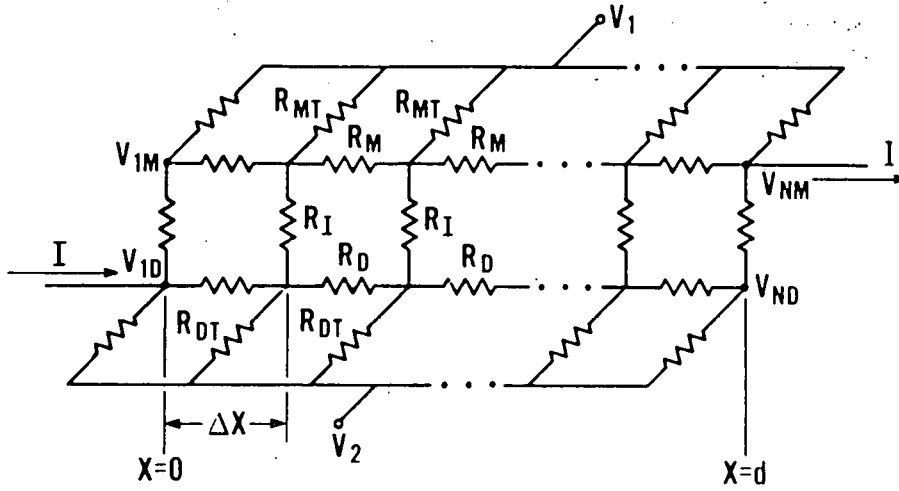
$\rho_c$  - specific contact resistance

$W$  - width of contact window

$R_s$  - sheet resistance of diffusion level

$d$  - length of contact window

## Two-Dimensional Transmission-Line Model for the Interfacial Contact Resistance Test Structure



$$\sum_{j=1}^N \frac{V_{jM} - V_1}{R_{MT}} = 0$$

$$\sum_{j=1}^N \frac{V_{jD} - V_2}{R_{DT}} = 0$$

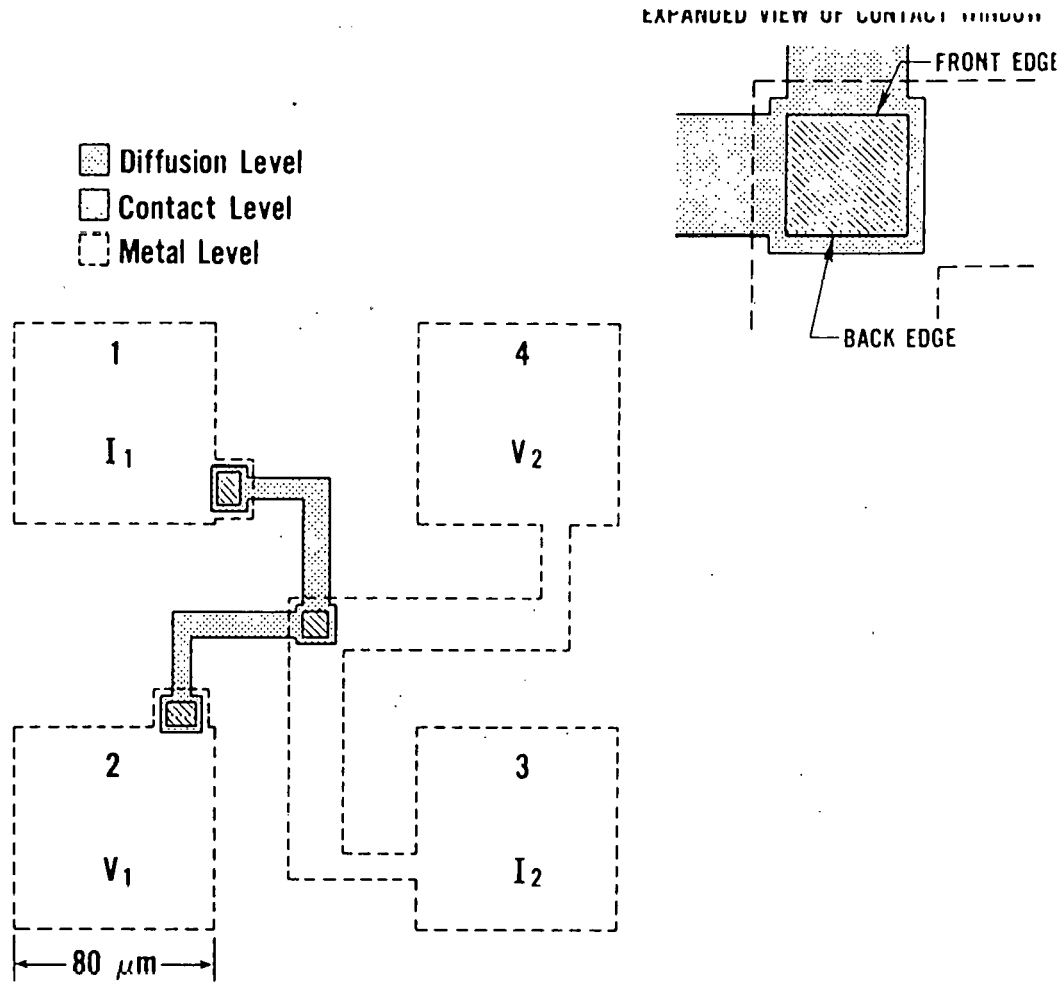
$$V_2 - V_1 = \frac{1}{N} \sum_{j=1}^N (V_{jD} - V_{jM})$$

$$I = \sum_{j=1}^N \frac{V_{jD} - V_{jM}}{R_I}$$

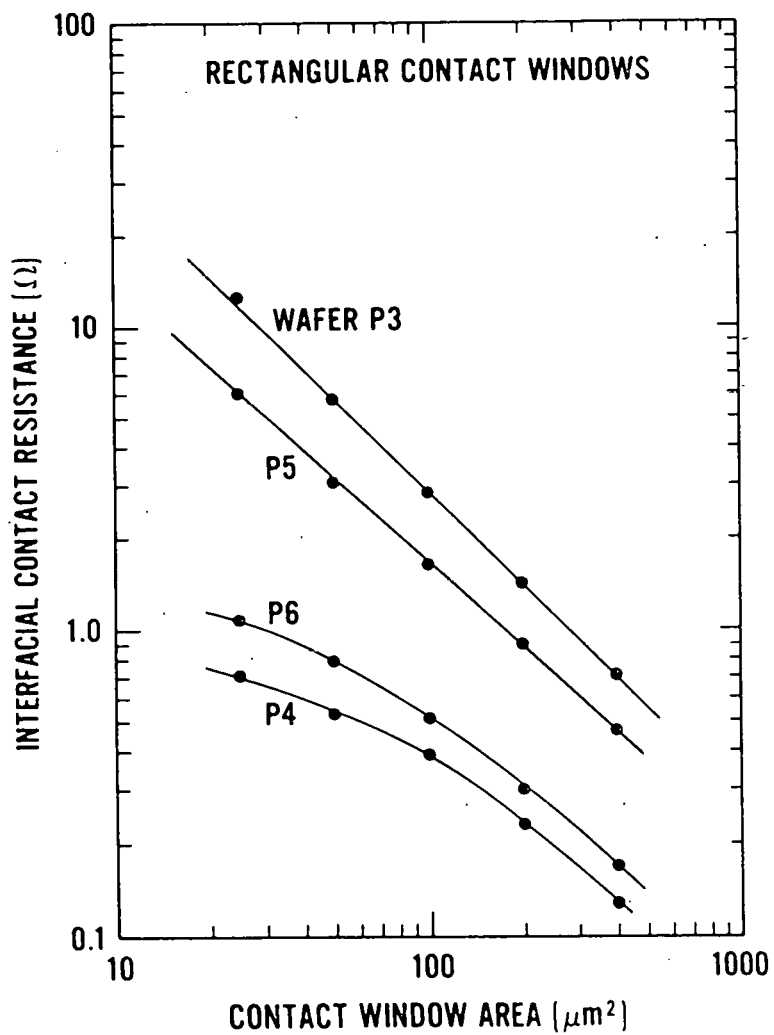
$$\frac{V_2 - V_1}{I} = R_C = \frac{R_I}{N}$$



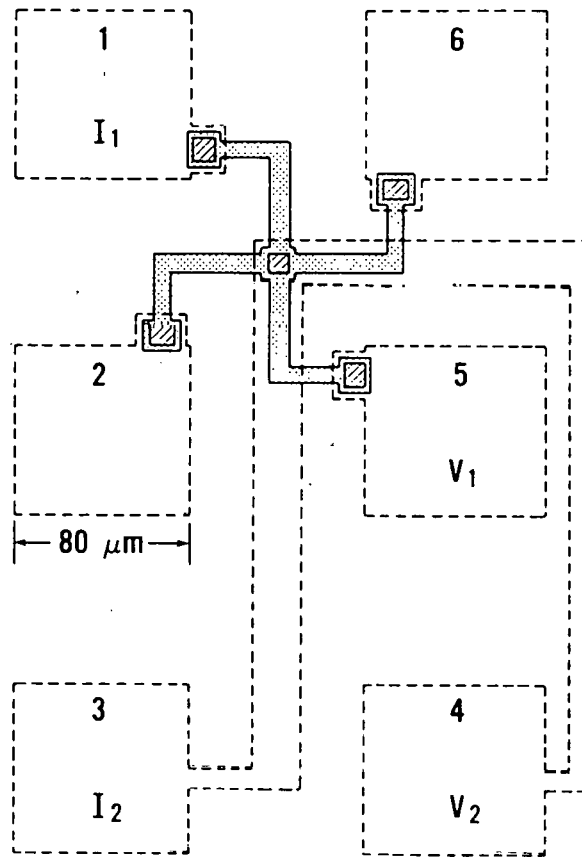
# Four-Terminal Kelvin Test Structure for Determining Interfacial Contact Resistance






# $R_c$ Vs A for Rectangular Windows.

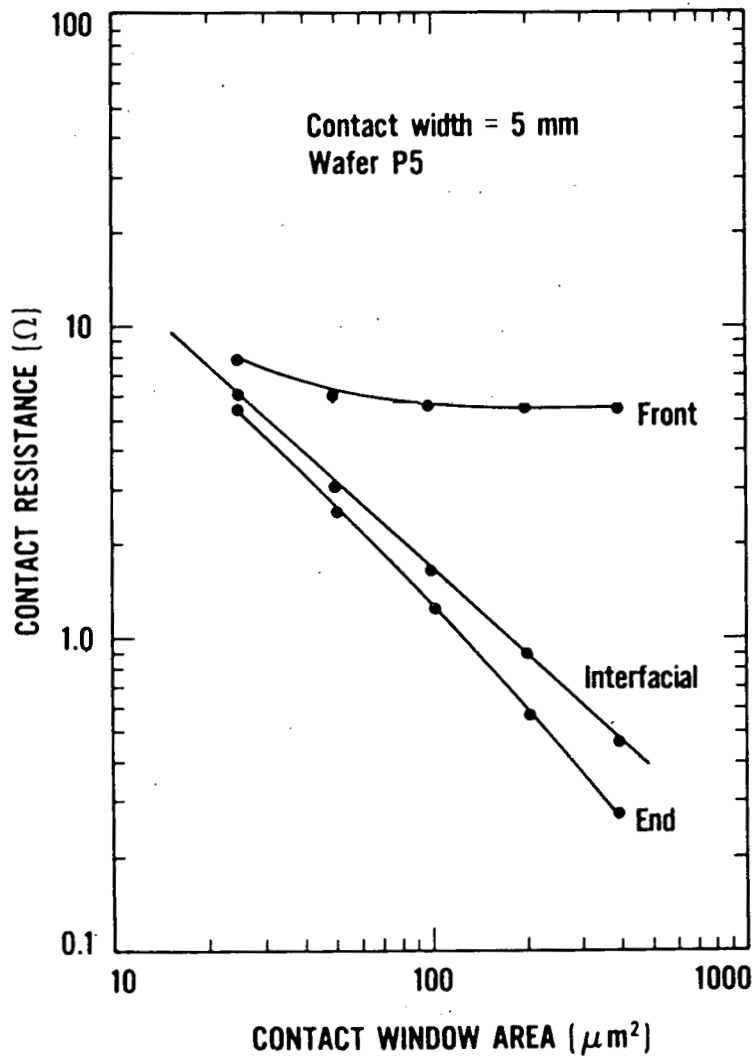


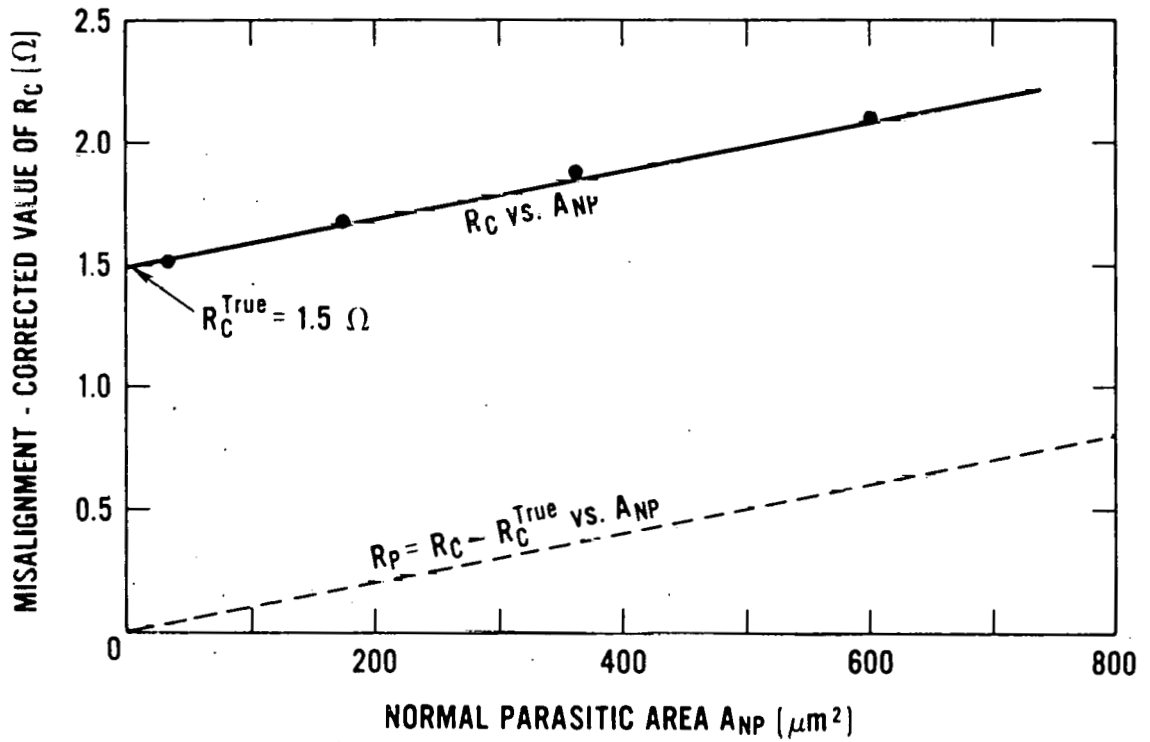
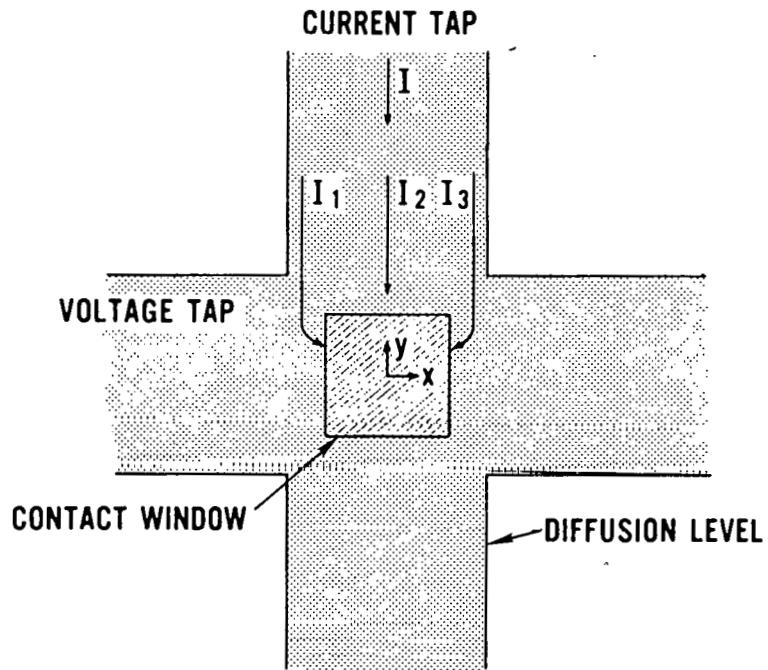
# Six-Terminal Kelvin Test Structure for Determining Interfacial, End, and Front Contact Resistance



-  Diffusion Level
-  Metal Level
-  Contact Level

# Rectangular Contact Windows





## DISCUSSION

SCHRODER: I am referring to the slide that shows the front and the back--

LINHOLM: The test results?

SCHRODER: If you have a contact resistance -- it's the top curve, if someone wants a number, what would you give them?

LINHOLM: I would ask them first what they need, because a lot of people do not differentiate between these quantities. The quantity that most people are interested in, the circuit designers, is the front contact resistance. That's the load they have to drive. Probably the resistance that most of the processing people are worried about is the interfacial contact resistance. That tells them more about how the process is doing. Probably the one measurement that people don't want is the contact end resistance. They really can't use end resistance. I know many cases where that is the resistance they are measuring - but they don't know that.

SCHRODER: How does this measurement compare to the transmission line, for example, or other methods that people use?

LINHOLM: We have looked at structures -- well, the structure reported by Berger in his paper. It was a six-terminal structure with contacts separated by two different resistance lengths. We get general agreement, but we get agreement within a very large margin of errors that we associate with that structure in terms of accounting for what the actual diffusion resistance is. Also, to some extent, the effects of the current crowding as you go into that structure. That structure does not allow you to make a direct measurement of interfacial contact resistance. It allows you to calculate that based on the other measurements you get. But you really have to know the design, the lengths associated with the diffusions on that structure, fairly accurately before you can do that. What troubles us the most with that structure, is one of the numbers you get -- the sheet resistance -- from the measurement. We have a test structure that we have a high degree of confidence in for measuring sheet resistance. When we don't get exactly the same number, that makes this a little suspect.

NICOLET: We have done that and we get the same number. If you measure the end resistance you can find out an additional independent variable, namely, the sheet resistance under the contact.

LINDHOLM: Yes. That is a very good point. There is a difference between the sheet resistance measured elsewhere and the sheet resistance measured exactly under the contact. One can use Berger's method to estimate what that value is.

LAVENDEL: In one of your contact systems that you have discussed, you had, if I remember correctly, platinum-titanium-tungsten-aluminum. What is the tungsten's metallurgical role in that system?

LINHOLM: These are very preliminary results we are getting from American Microsystems; we have a collaborative effort. This represents a metallurgy they are using and I believe that the Ti-tungsten that they are placing there is to act as a barrier for silicon that may be coming from the silicon or platinum silicide under the region, to interface that with the aluminum metallization, which is the prime metal used for interconnects.

## DIFFUSION BARRIERS

Marc-A. Nicolet

California Institute of Technology

Pasadena, California 91125

The choice of the metallic film for the contact to a semiconductor device is usually predicated by considerations of economics, know-how, or precedence. The typical case is that the desired metal is unstable when forming a couple with the semiconductor. One way to try to stabilize a contact is by interposing a thin film of a material that has low diffusivity for the atoms in question. The solution is attractive because it is apparently simple and universal.

The difficulty is that the notion of a diffusion barrier is derived from bulk considerations. The time required to penetrate a layer by diffusion decreases with the square of the layer thickness. In addition, the relevant diffusivity in thin films is typically determined not by bulk diffusion, but by diffusion along extended defects, which can be many orders of magnitude faster than bulk diffusion at the temperatures encountered in device processing and operation. The defects in a film are strongly dependent on the method of deposition used and on the conditions prevailing during deposition. For diffusion barrier applications, the fabrication procedure is therefore as important as the choice of the material. This crucial point is often overlooked.

By their structure, thin-film diffusion barriers can be classified in single-crystalline, polycrystalline, and amorphous. Single-crystalline layers are unpractical, leaving only polycrystalline and amorphous layers as valid options. By their composition, thin-film diffusion barriers can be sub-divided into elemental and compound materials. For electrical contacts, only metallic media apply. Of these, most elemental metal films must be ruled out, because soluble metals dissolve, insoluble polycrystalline metals contain fast diffusion paths, and amorphous metals are not stable at room temperature. Metallic compound and alloys, polycrystalline or amorphous in structure, thus constitute the favored range of materials for electrically conducting thin-film diffusion barriers.

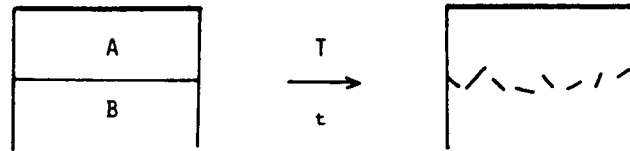


Three types of barriers can be distinguished. The stuffed barrier derives its low atomic diffusivity to impurities that concentrate along the extended defects of a polycrystalline layer. A number of very successful metallization systems are based on that concept. Sacrificial barriers exploit the fact that some (elemental) thin films react in a laterally uniform and reproducible fashion. When a thin film reacts in that fashion on both sides, and when these reactions proceed more rapidly than the diffusion through the film, an effective separation is accomplished as long as the film is not fully consumed in the reactions. Sacrificial barriers have the advantage that the point of their failure is predictable. Several successful sacrificial barriers are described in the literature, and a few new ones are under study at Caltech. Passive barriers are those most closely approximating an ideal barrier. The most-studied case is that of sputtered TiN films. The material has very low diffusivity for many metals, in spite of being fine-grained polycrystalline. The good kinetic properties of TiN are largely independent of the sputtering mode used for its deposition, which suggest that it is the very high melting point of TiN ( $\sim 2400^{\circ}\text{C}$ ) that is the ultimate reason for its success, and not the presence of undetected impurities. TiN is an interstitial alloy, of which there is a fairly large number; a few others of these have also been shown to work well as thin-film diffusion barriers.

Stuffed barriers may be viewed as passive barriers whose low diffusivity material extends along the defects of the polycrystalline host. The same holds for barriers that form by a localized segregation of purposely introduced impurities (e.g. by ion implantation). New possibilities of diffusion barrier synthesis have been demonstrated with this approach. Amorphous metallic films offer another interesting way to obtain low diffusivity films. All amorphous diffusion barriers tested so far have been obtained by sputter-deposition. Both sacrificial and passive barriers can be conceived with amorphous films. Results obtained to date are quite encouraging, but the inclusion of an amorphous compound layer in a metallization system does not by itself suffice to ensure stability, as examples show.

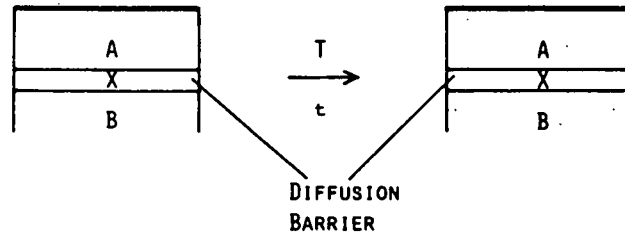
## Problem and Solution

### PROBLEM



METAL FILM ON SEMICONDUCTOR SUBSTRATE IS  
RARELY STABLE - INTERDIFFUSION  
- COMPOUND FORMATION

### SOLUTION WITH DIFFUSION BARRIER



### IDEAL BARRIER X

- LOW DIFFUSIVITY FOR A & B
- STABLE AGAINST A & B
- Laterally uniform & homogeneous
- Adheres to A & B
- Resists mechanical, thermal stresses
- Low contact resistivity
- Compatible with device processing

### COMPROMISING IS NECESSARY

## Difficulties

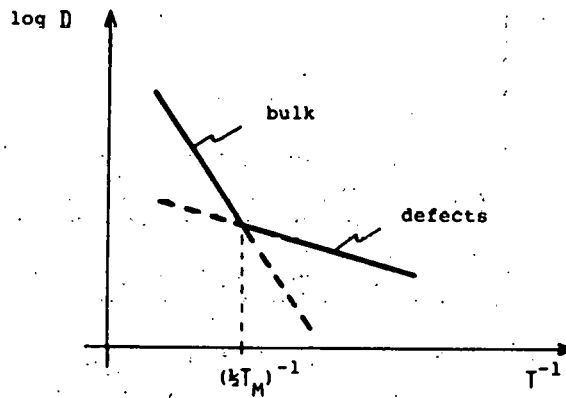
DIFFUSION ACROSS THIN FILMS IS FAST

$$x^2 \sim Dt \quad t \sim \frac{x^2}{D}$$

IF  $t = 10$  YRS FOR 1 MM ( $10^{-1}$  CM)

FOR 1000 Å ( $10^{-5}$  CM)  $t = 3$  SEC!

DEFECTS ENHANCE DIFFUSIVITIES IN THIN FILMS



$D_{\text{FILM}} \gg D_{\text{BULK}}$  FOR  $T < kT_M$

# Defects in Thin Films

FUNCTION OF DEPOSITION METHOD  
- DEPOSITION PARAMETERS

DIFFUSIVITIES =  $f$  (METHOD, PARAMETERS)

TWO PERTINENT QUESTIONS FOR DIFFUSION BARRIERS:

1. WHAT MATERIAL?
2. PREPARED HOW?

ADDRESSING QUESTION 1 IS NOT SUFFICIENT.

## Thin-Film Diffusion Barriers

### STRUCTURE

#### SINGLE-CRYSTAL

Minimal Defects	unpractical
Minimal Diffusivities	

#### AMORPHOUS

No Extended Defects	attractive
Low Diffusivities	novel

#### POLYCRYSTALLINE

Extended Defects	practical
High Diffusivity Paths	problematic

### PRACTICAL BARRIERS

#### ELEMENTAL, POLYCRYSTALLINE

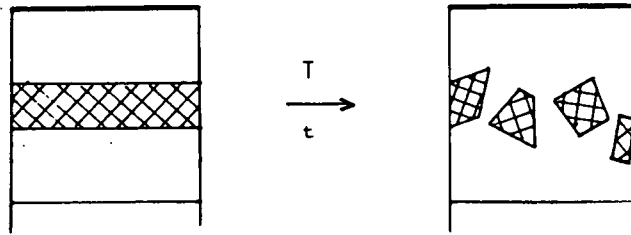
Miscible with A and B	fail
Immiscible with A and B	fail

#### COMPOUNDS, POLYCRYSTALLINE

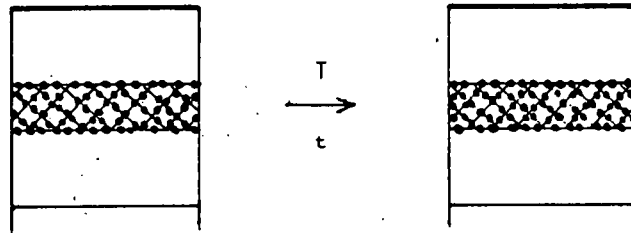
Stuffed Barrier	hold
Sacrificial Barrier	hold
Passive Barrier	hold

COMPOUNDS, AMORPHOUS	hold
----------------------	------

## Stuffed Barrier



PURE BARRIER FAILS



IMPURE (STUFFED) BARRIER HOLDS

### EXAMPLES

<Si>/Ti-W/Au/

<Si>/Cr+Cr oxides/Al/

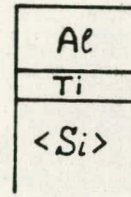
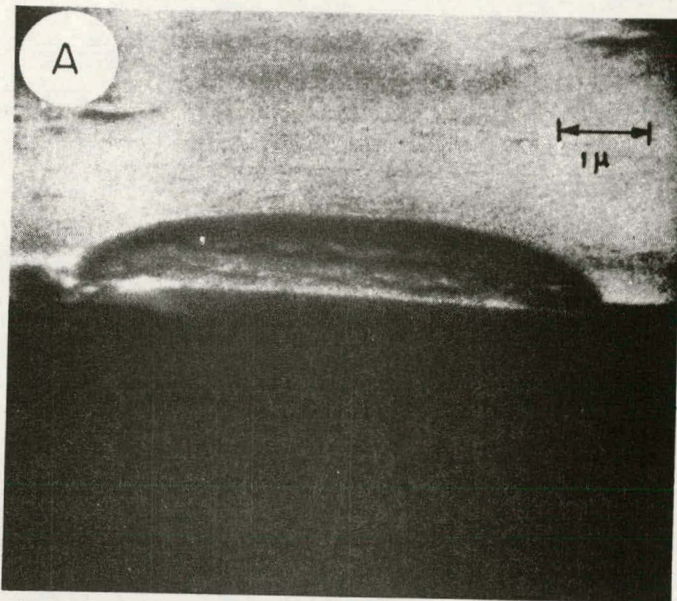
<Si>/Al+Al<sub>2</sub>O<sub>3</sub>/Al/

<Si>/Ta+Ta<sub>2</sub>O<sub>3</sub>/Al/

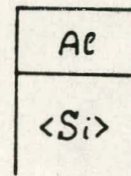
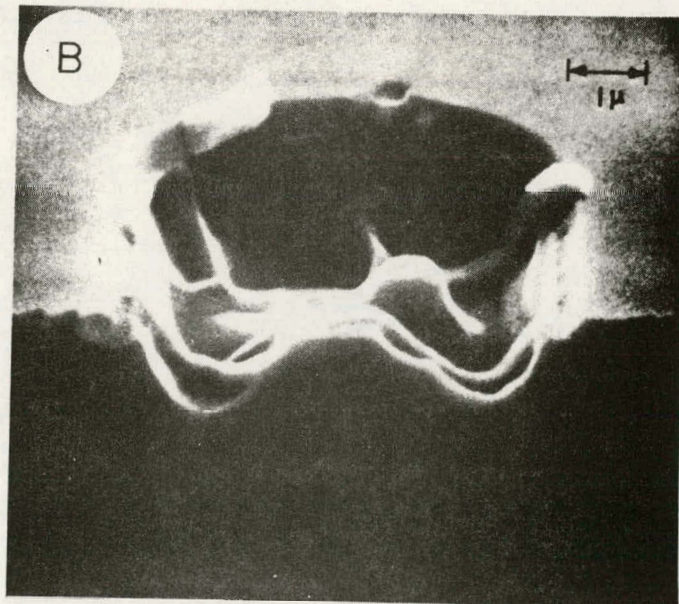
J.E. BAKER ET AL., THIN SOLID FILMS, 69(1980)5.

H.M. DALAL ET AL., U.S. PATENT 4,214,256 (JULY '8

W.K. CHU ET AL., U.S. PATENT 4,206,472 (JUNE 198



*Sacrificial  
Ti Barrier*





H. M. DALAL, M. GHAFGHAICHI, L. A. KASPRZAK, AND H. WIMPFHEIMER,  
IBM

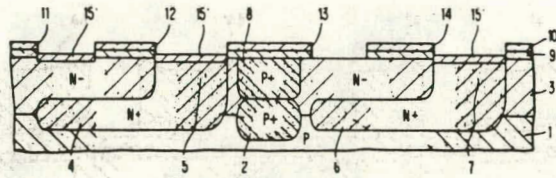
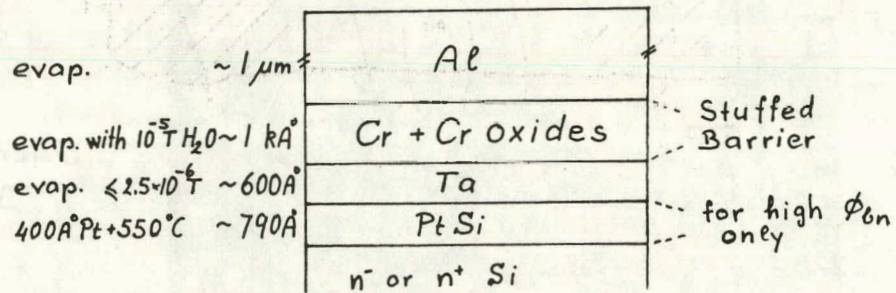


FIG. 1C



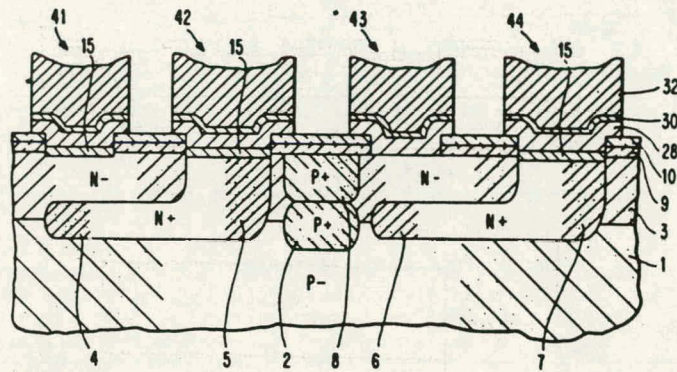
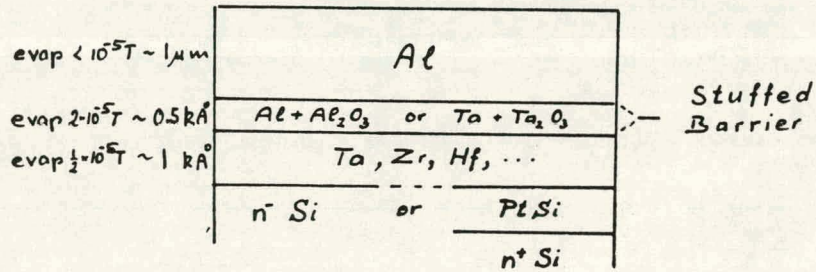
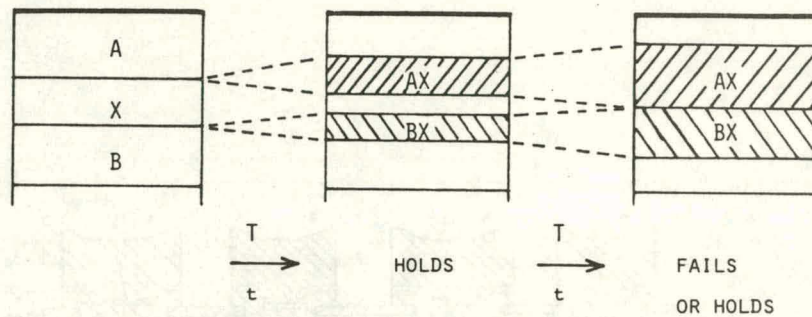


FIG. 1





## Sacrificial Barrier



CONDITIONS ON REACTION OF X WITH A AND B:

- LATERALLY UNIFORM
- REPRODUCIBLE AND CHARACTERIZED
- FASTER THAN DIFFUSION THROUGH A, X, B

### EXAMPLES\*

<SI>/TI/AL/

R.W.BOWER, APPL. PHYS. LETT. 23(1973)99.

<SI>/TA/TAAL<sub>3</sub>/AL/

J.K.HOWARD ET AL., U.S. PATENT 4,201,999 (MAY 1980)

<SI>/PD<sub>2</sub>SI/TI/AL/

G.SALOMONSON ET AL., PHYSICA SCRIPTA, 24(1981)401.

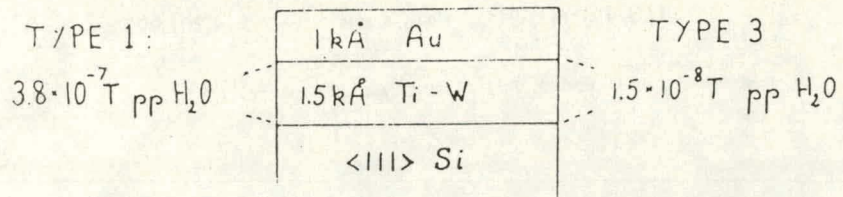
<SI>/PTSI/TI/AL/

<SI>/NISI/CR/AL/

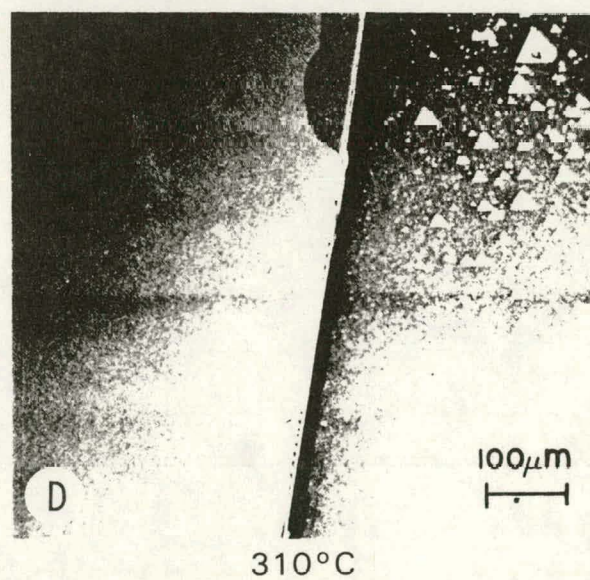
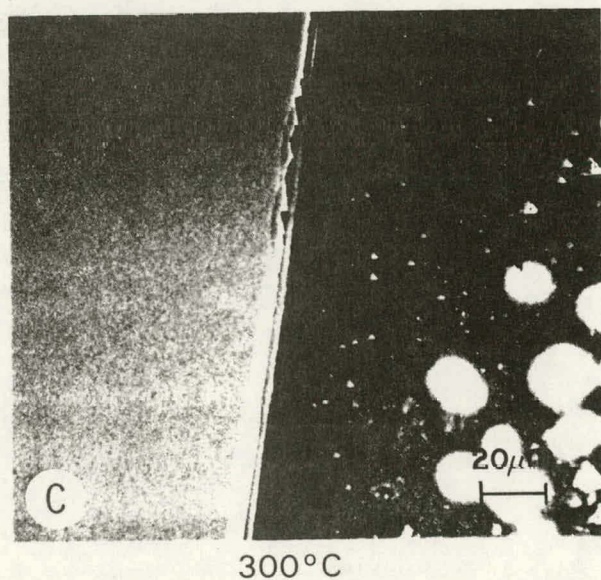
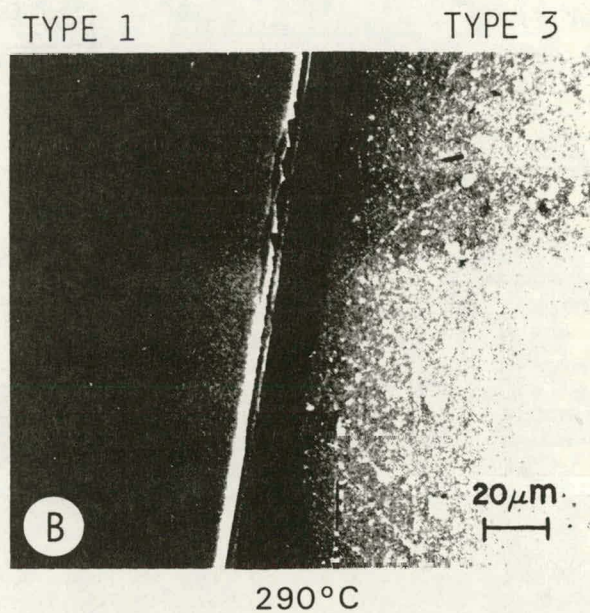
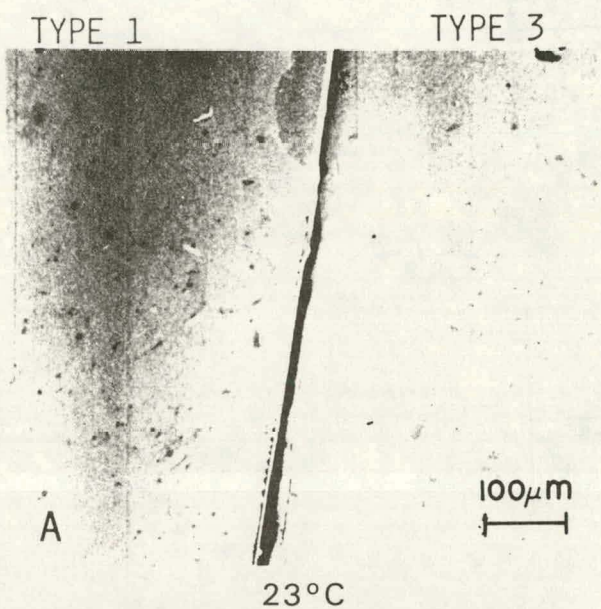
M.BARTUR, (TO BE PUBLISHED).

<SI>/PTSI/CR/AL/

REMARKS: \*STUDIES TESTING BOTH METALLURGICAL AND ELECTRICAL STABILITY.



23°C - 400°C, 6°C/MIN



REF.: J. E. BAKER, R. J. BLATTNER, S. NADEL, C. A. EVANS, JR. AND R. S. NOWICKI, THIN SOLID FILMS, 69, 53 (1980).



J. K. HOWARD, F. E. TURENE, AND J. F. WHITE, I.B.M.

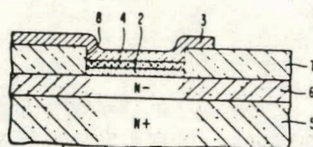
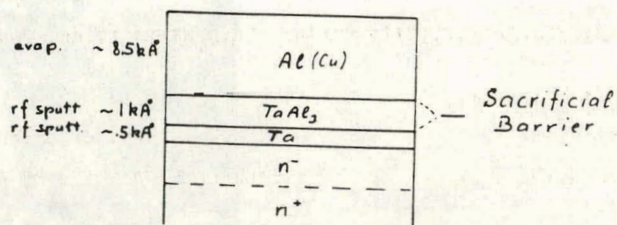
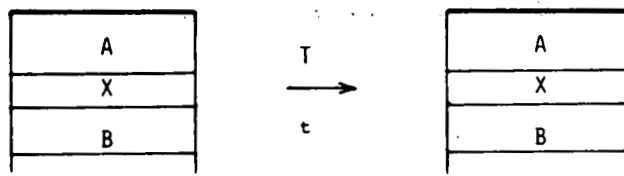


FIG. 1



## Passive Barrier



### EXAMPLES\*

#### STUFFED BARRIERS

#### INTERSTITIAL COMPOUNDS

Ti/TiN/Pt/

<Si>/TiN/Ti/Ag/

<Si>/NiSi/TiN/Al/  
<Si>/Pd<sub>2</sub>Si/TiN/Al/

<GaAs>/Ge-Au-Pt/TiN/Ti-Pt-Au/ R.D. REMBA ET AL. (UNPUBLISHED).

#### IMPLANTED IMPURITY

<Si>/Ni:O/

<Si>/Ni:N/

AN ALTERNATE VIEW OF THEM

C.W. NELSON (1969)

P.R. FOURNIER, U.S. PATENT 3,879,746 (1975).

W.J. GARCEAU & G.K. HERB, THIN SOLID FILMS, 53(1978)193.

N. CHEUNG ET AL., J. APPL. PHYS. 52(1981)4297.

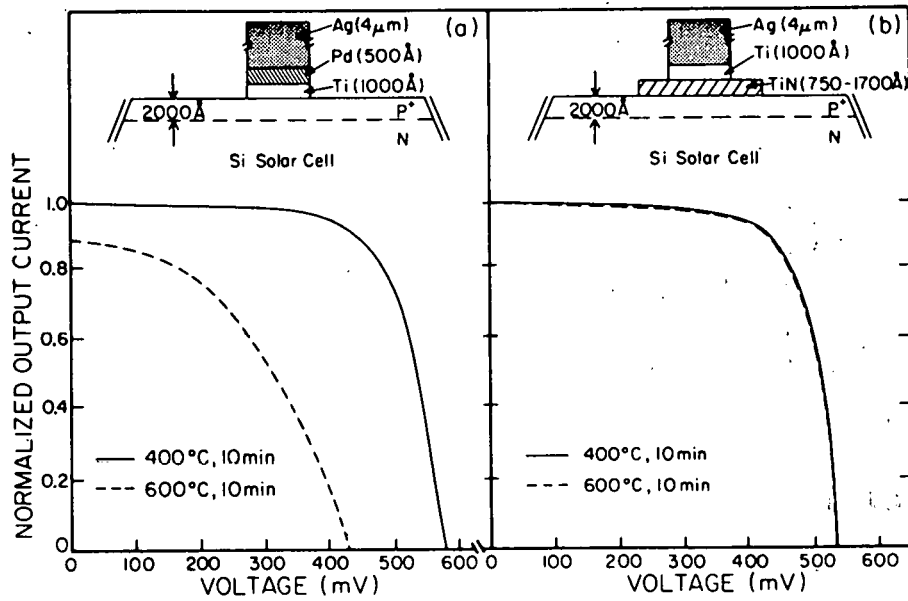
M. FINETTI ET AL. (TO BE PUBLISHED).

D.S. SCOTT, J. VAC. SCI. TECHNOL. 19(1981)786.

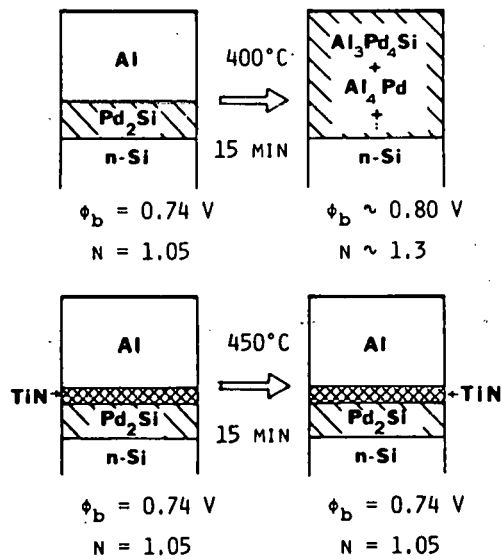
T. BANWELL ET AL. (TO BE PUBLISHED).

REMARKS: \*STUDIES TESTING BOTH METALLURGICAL AND ELECTRICAL STABILITY

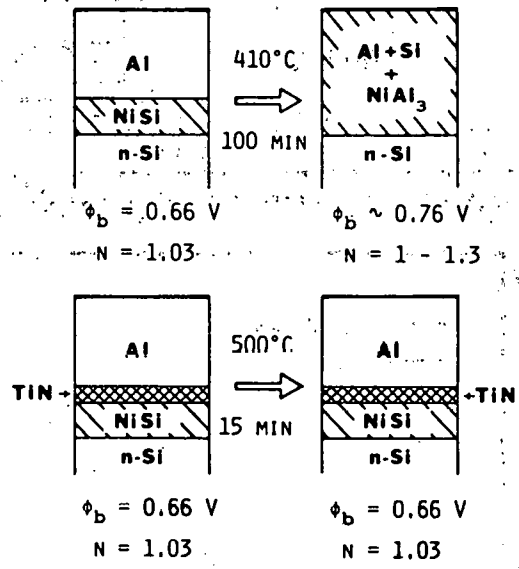




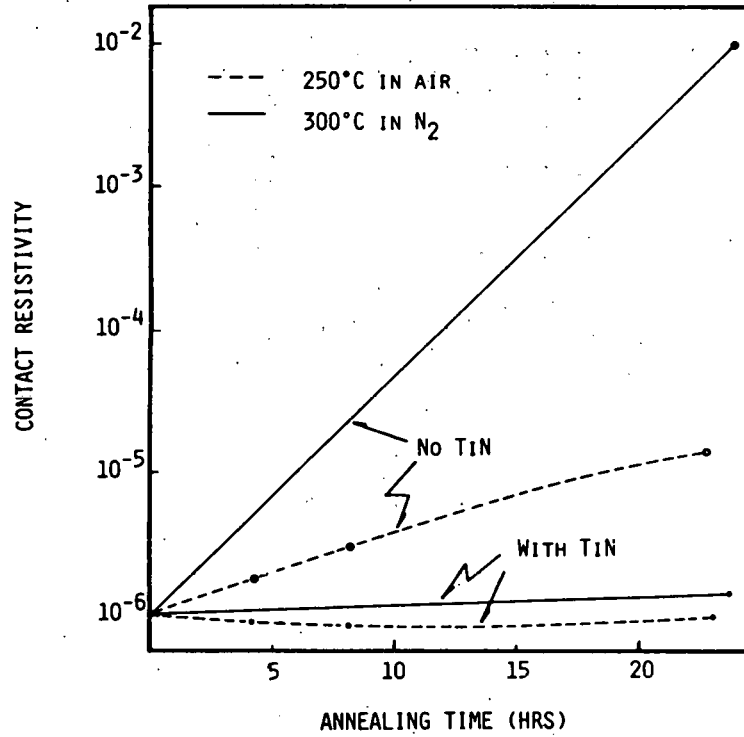
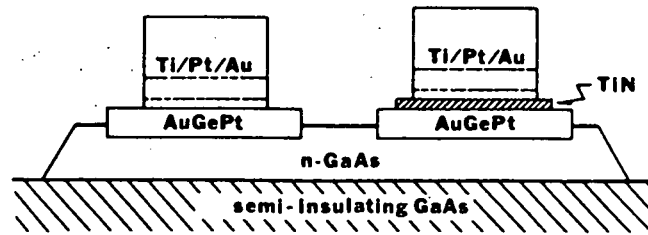
### Al-Pd<sub>2</sub>Si-n-Si Schottky Diode



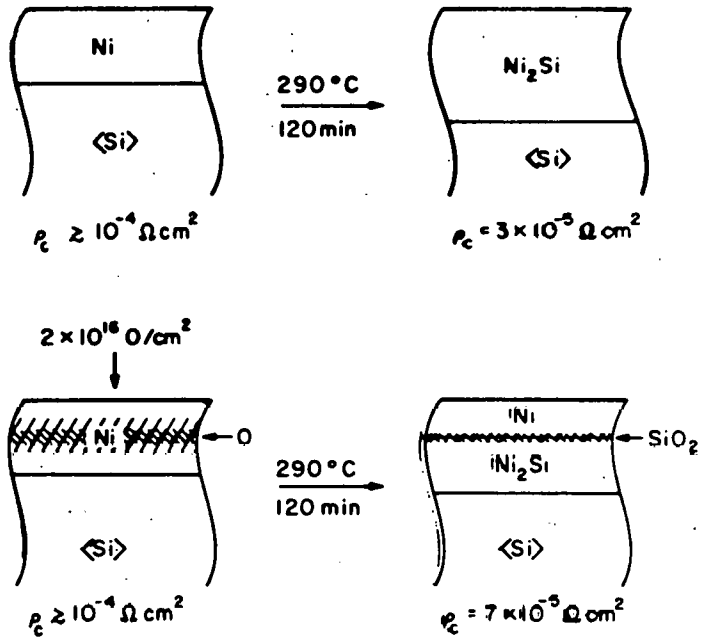
# Al-NiSi-n-Si Schottky Diode



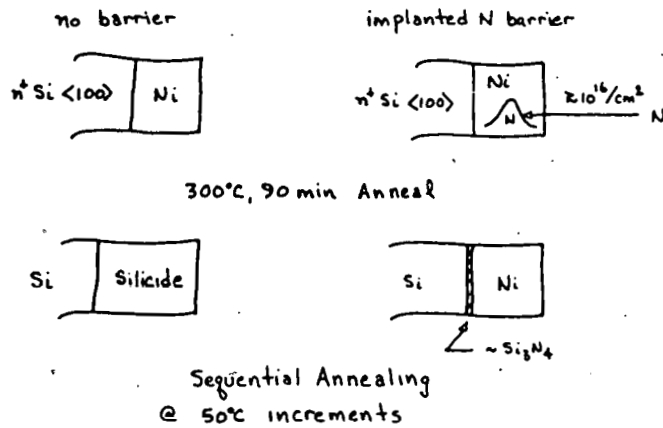
# Ohmic Contacts to GaAs







# Implanted N Diffusion Barrier



phase(s)	$\rho_c$ $\Omega \cdot \text{cm}^2$		phase(s)	$\rho_c$ $\Omega \cdot \text{cm}^2$
NiSi/Ni <sub>2</sub> Si	$1.0 \times 10^{-4}$	300°C 90 min	Ni	$6.3 \times 10^{-5}$
NiSi	$1.0 \times 10^{-4}$	350°C 30 min	Ni	$7.1 \times 10^{-5}$
NiSi	$1.1 \times 10^{-4}$	450°C 30 min	Ni	$6.7 \times 10^{-5}$
NiSi	$1.0 \times 10^{-4}$	550°C 30 min	Ni	$7.1 \times 10^{-5}$
NiSi	$1.1 \times 10^{-4}$	650°C 30 min	non uniform NiSi	$6.6 \times 10^{-5}$

ABBREVIATED TABLE OF RESULTS

# Amorphous Barrier

rf SPUTTERED FE-W

2kÅ	Ag	$\rho_c (10^{-6} \Omega\text{cm}^2)$	
		AS-DEPOSIT.	500°C 30 MIN.
1kÅ	FE <sub>45</sub> W <sub>55</sub>	N <sup>+</sup> SI	0.10
	Si	P <sup>+</sup> SI	2.8
	N <sup>+</sup> & P <sup>+</sup>		1.1

N SI  $\rho_c \sim 71 \Omega\text{cm}^2$ ,  $\phi_{BN} = 0.61 \text{ eV}$

M. FINETTI ET AL., APPL. PHYS. LETT. (IN PRESS).

rf SPUTTERED MULTILAYERS AND 500°C, 4 H ANNEALING

~1.3kÅ	AU	NO DEGRADATION OF I(V) AFTER 400°C, 16 H	AU	"SIMILAR RESULT" 450°C, 8 H
	W-SI		W-SI OR TI-W-SI	
	N<GAAS>		<INP>	

GAAS MESFET

WITH TIW-SI BARRIER: STABLE AT 300°C PAST 944 H (39 D)

WITHOUT TIW-SI BARRIER: FAILS AT 300°C AFTER 360 H (15 D)

W. T. ANDERSON ET AL. THIN SOLID FILMS (IN PRESS).

# Amorphous Barrier: Metallurgical Studies

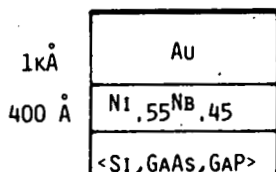
## SPUTTERED AMORPHOUS BARRIERS

	$T_c$ (1 H)
<SI>/NI-NB/AU OR CU/ <GAAS>/NI-NB/CU/ <GAP>/NI-NB/AU/	$Ni_{.57}Nb_{.43} \approx 575^\circ C$
<SI>/Mo-Si/AU OR CU/ <GAAS>/Mo-Si/CU/ <GAP>/Mo-Si/AU/	$Mo_{.60}Si_{.40} \approx 550^\circ C$
<SI>/W-Si/AU OR CU/	$W_{.85}Si_{.15} \approx 700^\circ C$

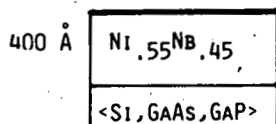
FAILS AT  $T \approx T_c$  FOR SI  
 $T < T_c$  FOR GAAS, GAP

K.J.GUO ET AL., IEEE - 81CH1658-4, P.35 (1981).

J.D.WILEY ET AL., IEEE TRANS. IE-29, No.2, 154 (1982).



$T_c \approx 600^\circ C$  (1 H)  
 FAILS AT  $600^\circ C$ , 15 MIN.  
 DE AT  $600^\circ C$ , 15 MIN.  $\approx 500 \text{ \AA}$



FAILS AT  $T \approx T_c$  FOR SI, GAP  
 $< T_c$  FOR GAAS

B.L.DOYLE ET AL., THIN SOLID FILMS (IN PRESS).

# Summary

## THIN FILMS ≠ BULK

DEFECTS CONTROL KINETICS  
DEFECTS =  $f(\text{FAB. PROCESS})$

## DIFFUSION BARRIERS = $f(\text{FAB. PROCESS})$

MISCIBLE ELEMENTAL BARRIERS      FAIL  
IMMISCIBLE ELEMENTAL BARRIERS      FAIL

## STUFFED BARRIERS

HOLD

Ti/Mo/Au  
Si/Ti+W/Au  
Ta/CR/AL  
TA/AL/AL  
⋮  
⋮

## SACRIFICIAL BARRIERS

HOLD

Si/Ti/AL  
Pd<sub>2</sub>Si/CR/AL  
⋮  
⋮

## PASSIVE BARRIERS

HOLD

TIN  
IMPLANTED IMPURITIES  
AMORPHOUS

THERE IS HOPE

## DISCUSSION

CAMPBELL: Titanium nitride is a passive barrier. Is that the compound titanium nitride?

NICOLET: Yes. It is a compound. It is TiN.

CAMPBELL: Stoichiometric.

NICOLET: In our case it is very close to stoichiometric. It is easy by reactive sputtering. It is easy to produce reactively in stoichiometric form. It is just as easy to produce it reactively in nonstoichiometric form, it is just as easy to produce as in dirt form. As a matter of fact, an interesting idea is why would you not intentionally have a little dirt in Ti-nitride. It might actually make it even better. That is one thing we wanted to try. It looks like heresy. But it is also heresy to apply oxygen to nickel if you talk to the silicon community. I think that there is lots of room to try new ideas in this business. Yes, it is just simple Ti-nitride, however, Ti-nitride isn't simple.

SOMBERG: You mentioned in the beginning that the pure-metal systems like Ti-palladium-silver doesn't work. Could it be that they really are not pure-metal systems, that they are "dirty" systems, that there are other things going on?

NICOLET: Well, that is possible. The Motorola system of electroplated nickel copper, for example, surely has a lot of phosphorus in it and you can make nickel amorphous if you have enough phosphorus in it. It doesn't have to be but it could be. We have looked at this and it is possible. What I was trying to say is if you make things pure the way you write it down, when you say it's nickel, you mean it's nickel not nickel plus a lot of other things. Many things fail. And it is important to make that distinction. Otherwise you will get lost. It becomes black magic and people will not tell you what they do. This is just a sign that it is not understood.

AMICK: Would you comment, please, on the adhesion properties when you implant either oxygen or nitrogen into the nickel and then form this interfacial layer, which is apparently either a nitride or an oxide. What happens to the adhesion properties of that system?

NICOLET: We haven't looked at that much. I will tell you my reluctance to get into this type of question. It is something that I would like very much to consider in our measurements, but I can't conceive of our Caltech graduate students making adhesion measurements.

COMMENT: It is not that expensive.

NICOLET: It's not expensive, but if you can't write down the Schroedinger equations, that is a complaint. If I have someone in industry or elsewhere who would like to collaborate, it would be delightful, but we don't cover that part well, and I don't know how to do it. I know that

I will not get anywhere with this proposition with anybody in my group. I think the way to do that is by collaboration. I think it would be very nice to investigate. The same question for Ti-nitride. Ti-nitride has to be fixed in one fashion or another to have proper adhesion. And that should also be fixed. But I think these things can be resolved.

WONG: Did you, or did anyone else, have any diffusion failure of amorphous alloy?

NICOLET: Yes. Data on diffusion in amorphous alloys are plentiful in bulk. Data on amorphous materials is 20 years old now. A thick compendium. What you really want are the data on diffusion in thin films, that are amorphous. Maybe that is different. There are a number of measurements that were done and they are much more limited. Typically, what people do, they make an amorphous layer and they implant heavy material, like gold. With backscattering you can see how the diffusion takes place. And you see dramatic differences if you compare the same layer amorphized or crystallized. If you have a crystallized layer and implant an amorphous layer and you do the annealing at the same low temperatures the diffusivity is vastly different. That's only half the story, and as we found out with our aluminum layer, you might have very low diffusivity inside but if you have sufficiently thick layers with large diffusivity on the top you might just lose your layer in a hurry. You may not crystallize. It might just be dissolved.

WONG: In this sense, in that example that you showed in the viewgraph, can we do something to saturate the aluminum with whatever -- the iron tungsten, for example -- so that we don't have diffusion during that period?

NICOLET: That would be another idea. Yes, that would be good to try that. Let me just first explain. While we were making these measurements, how frustrating we found it when we failed. But I thought, no, we haven't failed, because it opened our eyes to a lot of problems that are very relevant because you have to recognize this: you have bulk diffusivity in all directions.

## OBSERVATIONS OF SOLAR-CELL METALLIZATION CORROSION

G.R. Mon

Jet Propulsion Laboratory  
California Institute of Technology  
Pasadena, California

The Engineering Sciences Area of the Jet Propulsion Laboratory (JPL) Flat-Plate Solar Array Project is performing long term environmental tests on photovoltaic modules at Wyle Laboratories in Huntsville, Alabama. Some modules have been exposed to 85°C/85% RH and 40°C/93% RH for up to 280 days. Other modules undergoing temperature-only exposures (<3% RH) at 85°C and 100°C have been tested for more than 180 days. At least two modules of each design type are exposed to each environment--one with, and the other without a 100-mA forward bias.

Degradation is both visually observed and electrically monitored. Visual observations of changes in appearance are recorded at each inspection time. Significant visual observations relating to metallization corrosion (and/or metallization-induced corrosion) include discoloration (yellowing and browning) of grid lines, migration of grid line material into the encapsulation ("blossoming"), the appearance of rainbow-like diffraction patterns on the grid lines, and brown spots on collectors and grid lines. All of these observations were recorded for electrically biased modules in the 280-day tests with humidity.

In the temperature-only tests, discoloration of grid line tips was noted in electrically biased modules. Grid line discoloration was observed in both biased and unbiased modules.

The most important electrical observations are I-V curves taken at each inspection period. Changes in the I-V curve can reveal loss of encapsulation transparency (reduced short-circuit current), loss of cells (reduced open-circuit voltage), junction contamination or short circuiting (reduced shunt resistance), and contact and metallization corrosion (increased series resistance).

Other electrical parameters monitored included insulation resistance (decreased significantly), dissipation or loss factor (increased significantly) and cells-to-frame capacitance (generally unaffected).

In an attempt to quantify metallization corrosion, power reductions resulting from decrease of short-circuit current (due to changes in the optical properties of the encapsulant) were subtracted from the observed total power reduction after first correcting for losses due to cracked cells and broken interconnects. The remaining power loss was assumed to result from increases in series resistance, a parameter taken to be indicative of contact (metallization) corrosion. Power loss rate ( $\Delta P/\Delta t$ ) data have been compiled for the various metallization systems and the relative power loss rate ( $\Delta P/\Delta R$ ) was found to decrease linearly with time.



Similar tests are in progress at JPL using 85°C/0% RH, 85°C/85% RH, and 85°C/100% RH environments. Driving voltages for metallization migration are as high as 55 volts, compared with Wyle Laboratories driving voltages of about 5 volts maximum.

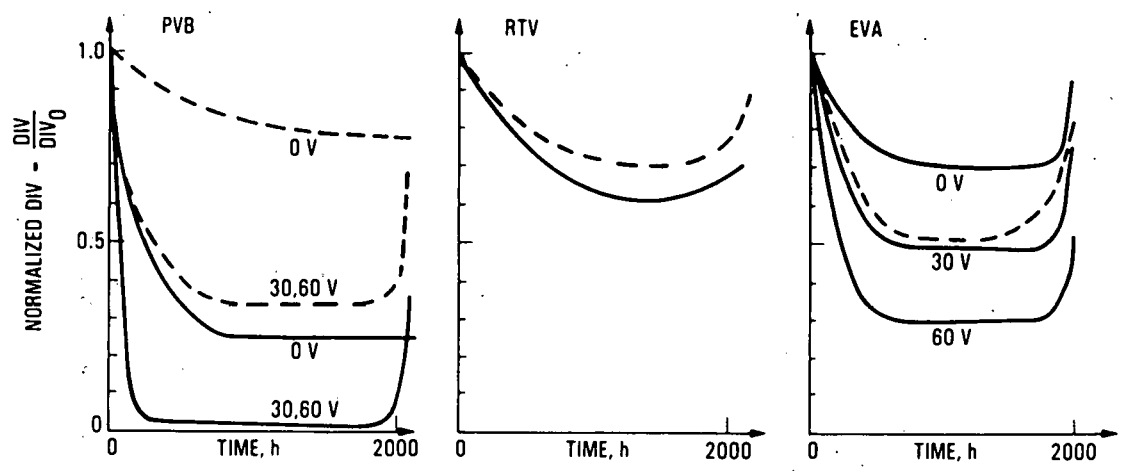
Following the French, we plot time of observation of metallization migration versus the combined variables  $t^{\circ}\text{C} + \% \text{RH}$  to reveal the effect of voltage acceleration.

We speculate about the mechanism underlying the observed phenomena. Photographic evidence indicates that the migration is along electric-field lines and is thus a form of ionic transport driven by potential differences through the encapsulation which, with the absorption of water, becomes an electrolyte. The observed discoloration peels off with the encapsulant--it is in the encapsulant, not on the cell--and is believed to be due in part to oxide-catalyzed reactions within the encapsulation, accelerated by elevated temperature. Investigation of these phenomena continues.

Important conclusions from this study relating to metallization corrosion including the following:

- (1) Ni-solder metallization is extremely stable in the sense that, unlike systems containing silver, no migration has been observed.
- (2) For silver-print metallizations, the power loss observed after 100 hours in an 85°C/85% RH test chamber is equivalent to about 30 years of real-time exposure at 60°C/40% RH daytime conditions.

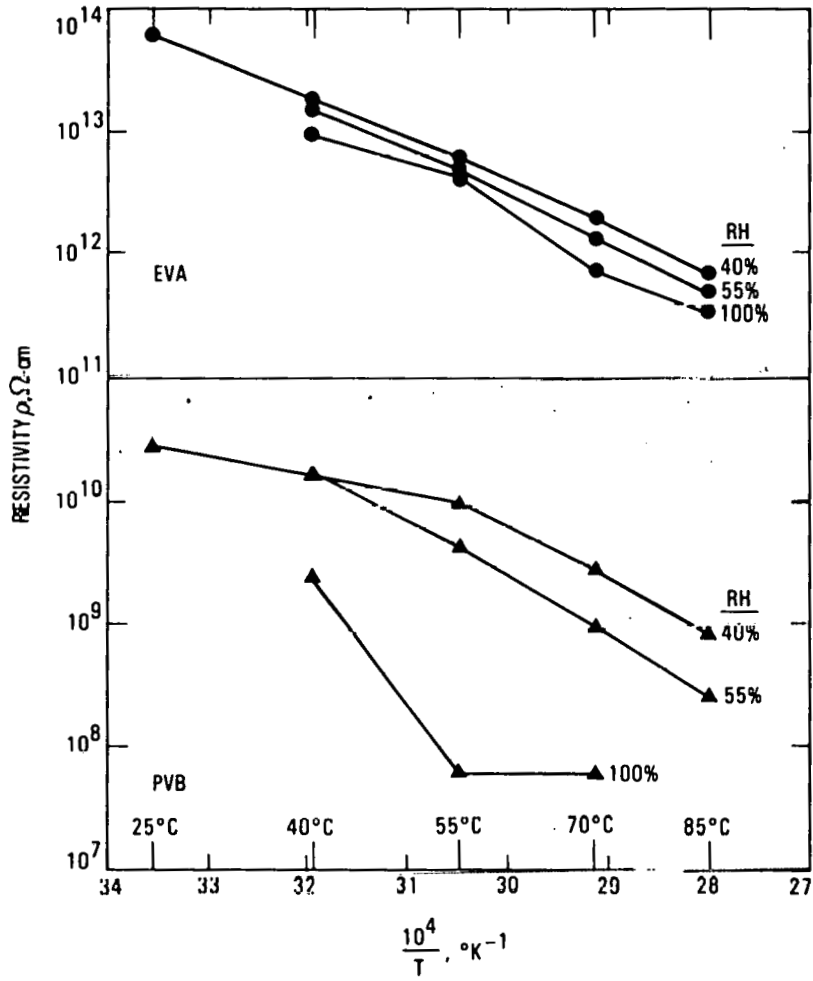
# Discharge Inception Voltage Data (General)



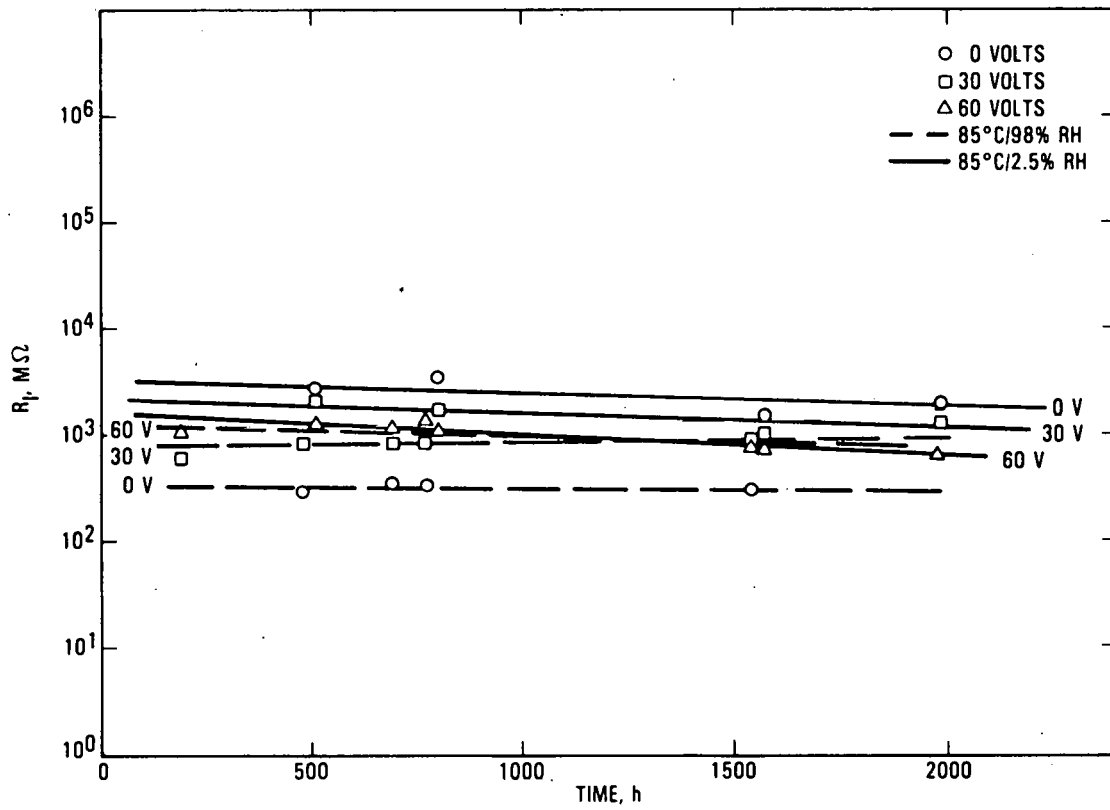
— 85°C/98% RH  
 - - - 85°C/2.5% RH

DIV - VOLTAGE AT WHICH MEASURED  
 PEAK DISCHARGES ARE ≈ 5pC

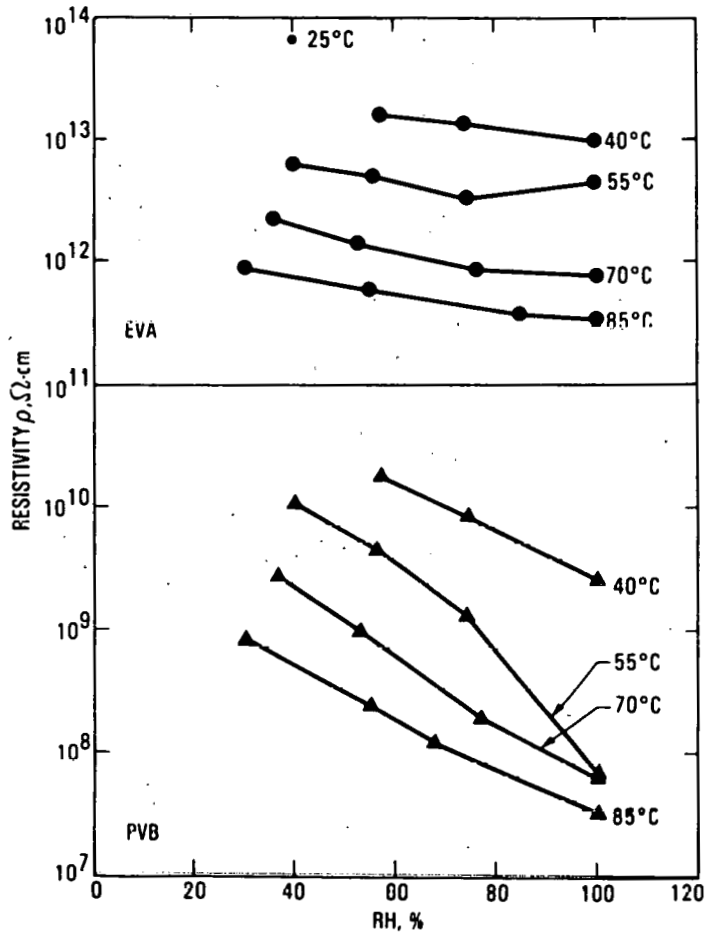
## Resistivity vs Temperature With Relative Humidity as Parameter



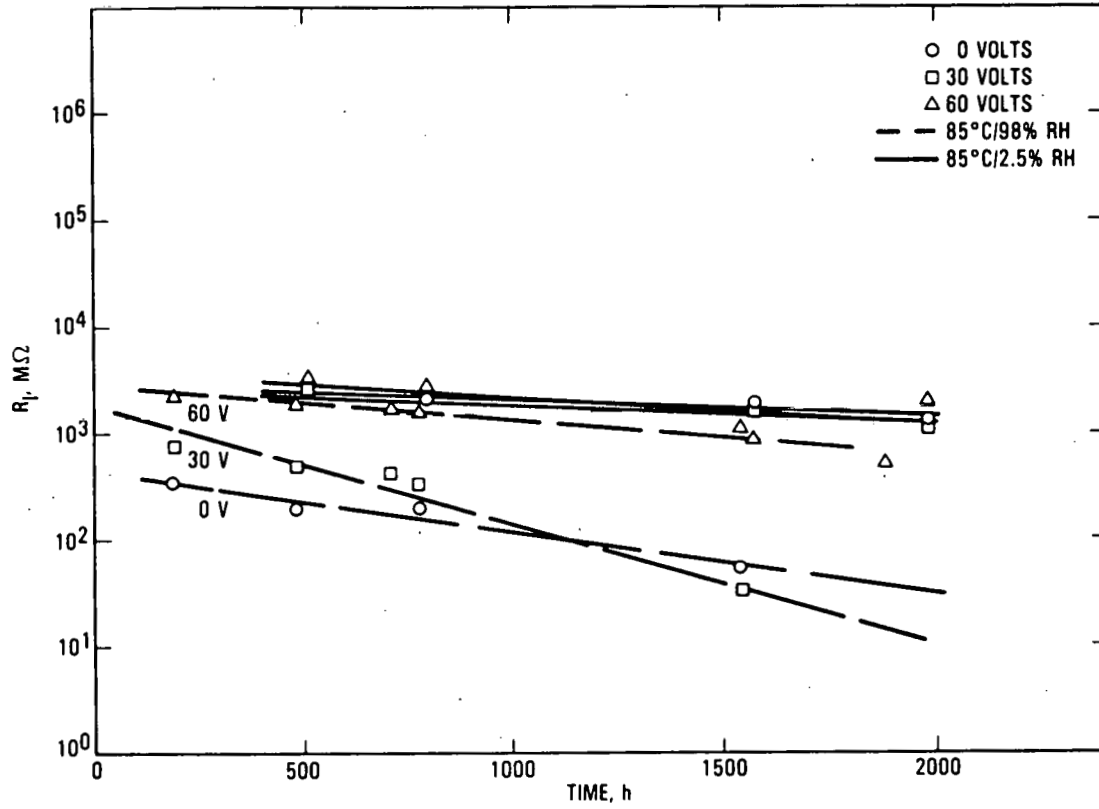
# Insulation Resistance vs Time: EVA-Ag Paste



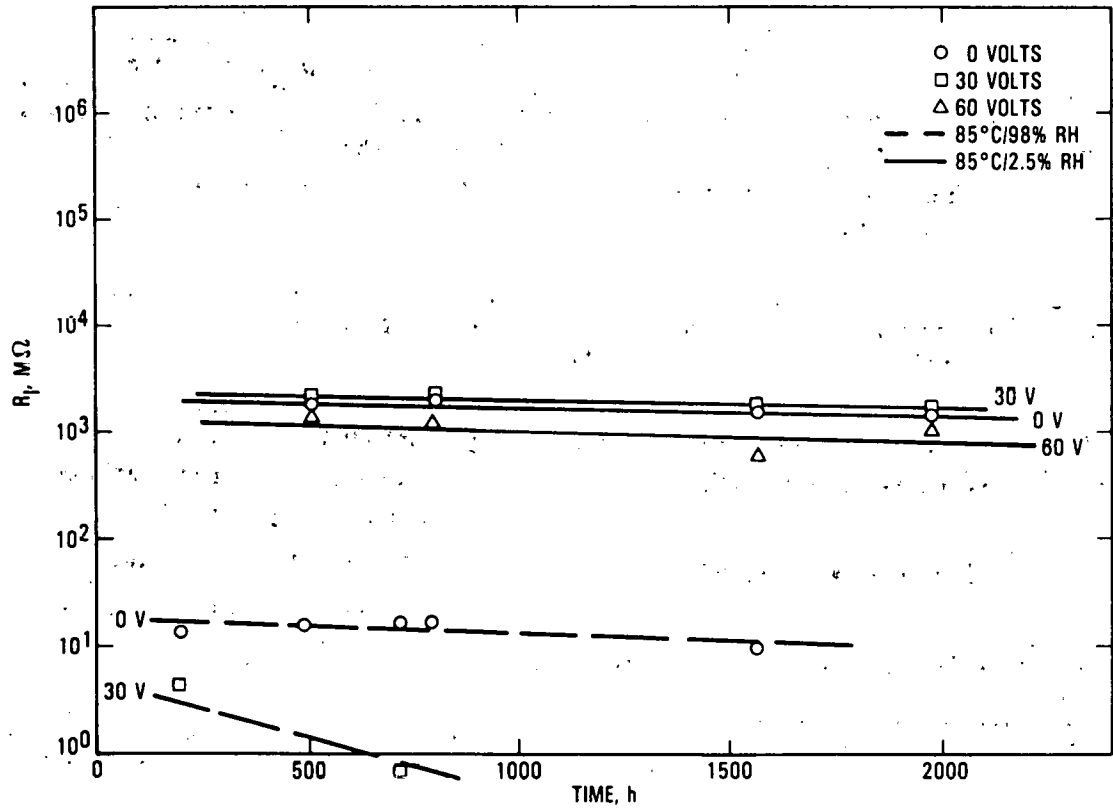
# Resistivity vs Relative Humidity With Temperature as Parameter



# Insulation Resistance vs Time: RTV-Ag Paste



# Insulation Resistance vs Time: PVB-Ag Paste

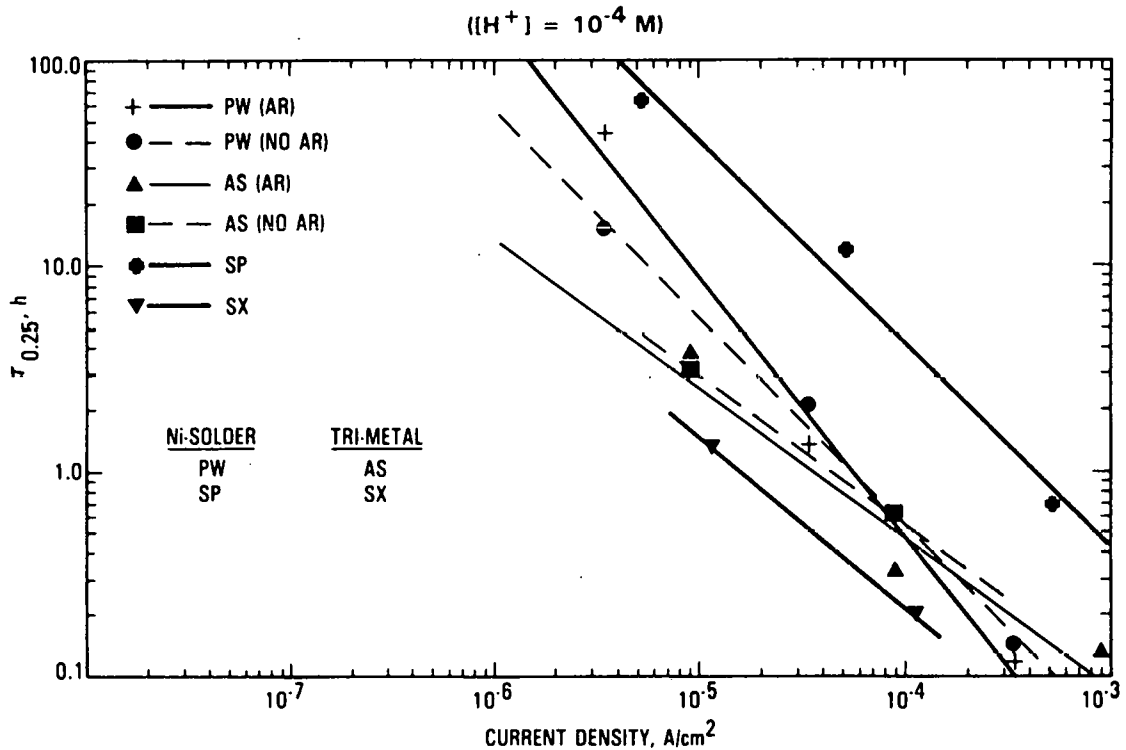


## Observations on Corrosion of Unencapsulated Ag-Metallization Cells in Aqueous Electrolytes

	0.1 Molar HCl, 0.5 h	0.1 Molar NaOH, 0.5 h
<b>Anode Front</b>	<ul style="list-style-type: none"> <li>• Ag dissolution proportional to voltage magnitude</li> <li>• AR coat attacked at 9.0 V <math>\text{Ag} \rightarrow \text{Ag}^+ + \text{e}^-</math></li> </ul>	<ul style="list-style-type: none"> <li>• Ag dissolution proportional to voltage magnitude</li> <li>• Evolution of gas bubbles <math>\text{Ag} \rightarrow \text{Ag}^+ + \text{e}^-</math> <math>4\text{OH}^- \rightarrow \text{O}_2(\text{g}) + 2\text{H}_2\text{O} + 4\text{e}^-</math></li> </ul>
<b>Anode Back</b>	<ul style="list-style-type: none"> <li>• Dissolution of back-surface metallization proportional to applied voltage</li> </ul>	<ul style="list-style-type: none"> <li>• Same as above</li> </ul>
<b>Cathode Front</b>	<ul style="list-style-type: none"> <li>• No observed metallization corrosion</li> <li>• Evolution of gas bubbles <math>\text{H}^+ + \text{e}^- \rightarrow \frac{1}{2} \text{H}_2(\text{g})</math> <math>\text{H}_2\text{O} + \frac{1}{2}\text{O}_2 + 2\text{e}^- \rightarrow 2\text{OH}^-</math></li> </ul>	<ul style="list-style-type: none"> <li>• Severe attack on AR coat</li> <li>• Metallization-silicon bond undermined</li> <li>• Evolution of gas bubbles <math>4\text{e}^- + 4\text{H}_2\text{O} \rightarrow 2\text{H}_2 + 4\text{OH}^-</math> <math>\text{SiO} + 2\text{OH}^- \rightarrow \text{SiO}_2 + 2\text{H}_2\text{O} + 2\text{e}^-</math></li> </ul>
<b>Cathode Back</b>	<ul style="list-style-type: none"> <li>• Metallization-silicon bond undermined</li> </ul>	<ul style="list-style-type: none"> <li>• No observed corrosion</li> </ul>
<b>Control</b>	<ul style="list-style-type: none"> <li>• No observed corrosion</li> </ul>	<ul style="list-style-type: none"> <li>• No observed corrosion</li> </ul>



## Time to 25% Maximum Power Degradation vs Current Density



### Summary: Failure Mechanisms—Causes and Effects

Parameter Monitored	Parameter Variation	Observed Degradation	Probable Mechanism
Series resistance	$R_S \uparrow$	Metallization Dissolution	Electrochemical electrode-electrolyte reactions between metallization and pottant
Short-circuit current	$I_{sc} \downarrow$	Discoloration of encapsulation; reduced optical transmission	Diffusion of metallization into encapsulation resulting in metallization-encapsulant interactions catalyzed by high temperature and moisture levels
Insulation resistance and capacitance	$R_I \downarrow$ $C_I \uparrow$	—	Absorption of moisture
Discharge inception voltage	$DIV \downarrow$	Conducting paths between high-voltage cell and ground, electrical breakdown	Diffusion of metallization from cell to cell or from cell to frame

## MODULE DEGRADATION CATALYZED BY METAL-ENCAPSULATION REACTIONS

B.D. Gallagher

Jet Propulsion Laboratory  
California Institute of Technology  
Pasadena, California 91109

Four major properties are considered to be relevant in determining service life of a photovoltaic module:

- (1) Mechanical: creep resistance, modulus, tensile strength.
- (2) Optical: integrated transmission at 0.4 to 1.1  $\mu$  wavelength.
- (3) Chemical: inertness with respect to metals and other components, retention of stabilizers, etc.
- (4) Electrical: maintaining effective isolation of conductive components.

These properties were measured after exposing polymer specimens to three types of accelerated stress: thermal, ultraviolet radiation and metal catalysts. These conditions give rise to a large number of complex inter-related free-radical reactions that result in the deterioration of polymeric materials.

In all experiments the data were plotted as log % property retained versus time, to yield generally useful graphs of material behavior. The first property to show change is color (yellowing), determined quantitatively by spectroscopy as a percentage of transmittance (T) at 400 nm. The total optical transmittance, however, retains a surprising high value (400 nm to 1100 nm), even with severe yellowing. Specimens retaining only 10% of the original transmittance at 400 nm were still found to have 74% total integrated transmittance. The mechanical properties during aging were, for the most part, unaffected. When physical deterioration was observed, the decrease in elongation at break was the first characteristic to change, followed by the decay of tensile strength. The dielectric strength was found to be the least variable of the properties measured; it retained 100% of the control values in all but the most extreme cases of degradation.

Thermal aging was conducted in the dark in atmospheres of air and nitrogen at temperatures of 60°C, 85°C, 105°C and 130°C. Results show that the candidate potting materials have very good thermal stability, with no life-limiting degradation occurring at 105°C.

For the purposes of this discussion only the data on metal-catalyzed reactions on EVA A-9918 will be presented. All of the other encapsulants tested behaved in a similar or worse manner. The EVA A-9918 consists of five parts: (1) ELVAX 150, the encapsulant; (2) Luprasol 101, the curing agent;

(3) Cyasorb 531, an ultraviolet screen; (4) Naugard P, an antioxidant, and (5) Tinuvin 770, an ultraviolet stabilizer. This material was developed by Springborn Laboratories, Inc., under contract to JPL and is available to the industry.

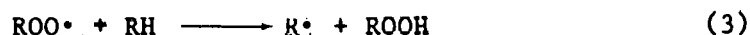
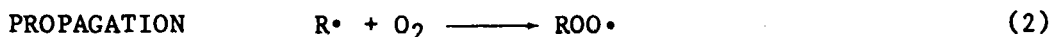
Metal-catalyzed oxidation in the presence of copper was discovered to be the most severe condition examined. The EVA was molded around copper screens and the color (% T at 400 nm) measured after periods of thermal soak at 105°C. The material was found to degrade rapidly and reached end of life at 400 hours. Specimens that had been treated with silane primer demonstrated improved performance and the induction period (before rapid degradation) was moved out to beyond 1000 hours. Similar catalytic reactions have been observed with both  $Ti^{+2}$  and  $T^{+3}$  ions but no reactions have been observed with aluminum, silver, nickel or 60-40 solder up to 1000 hours of 105°C thermal tests.

The postulated mechanisms for the general case and for the metal-catalyzed specific case are:

A. The general case:

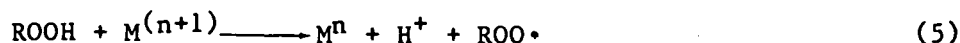
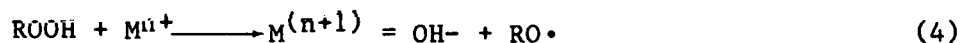


The breaking of the R-R bond to form the  $R\cdot$  free radical is a slow reaction. This step, which requires 80 kcal/mol of energy to break the bond, corresponds to the induction period. Energy can be supplied by heat or light and the unpaired electron in the  $R\cdot$  complex can react with oxygen and/or with some metal complexes.

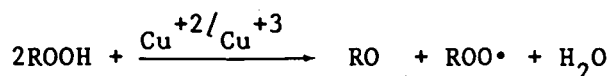


The formation of the  $R\cdot$  in reaction (3) shows this propagation step is autocatalytic and the change in slope of the curves shows it to be quite fast. The formulation of ROOH hydroperoxide is the operative mechanism that allows for redox reactions with multivalent metals to accelerate the production of free radicals and make the system autocatalytic.

B. The metal catalysis case:



to give a summary reaction of



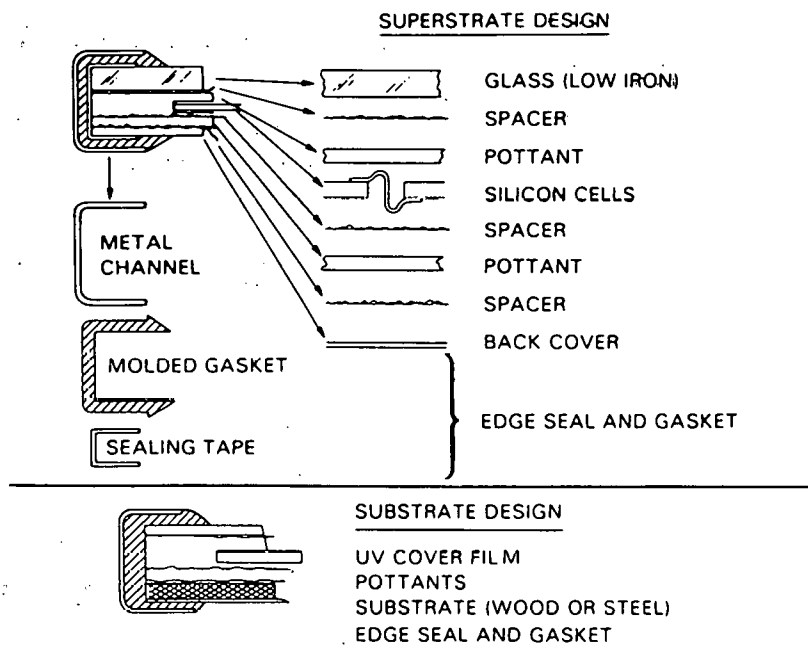
This reaction is quite fast and, as can be seen from the reaction products, is autocatalytic.

General conclusions that can be reached are:

- (1) The first quantifiable property to change is color.
- (2) Observed degradation mechanisms are of the induction-period type.
- (3) Higher acceleration rates are required to assess formulation changes in less time.
- (4) Not all metals catalyze degradation mechanisms; copper and titanium do, but aluminum, silver, nickel and 60-40 solder do not.
- (5) Silane treatment has extended the induction time before autocatalytic degradation but exact formulations for long life have not yet been found.

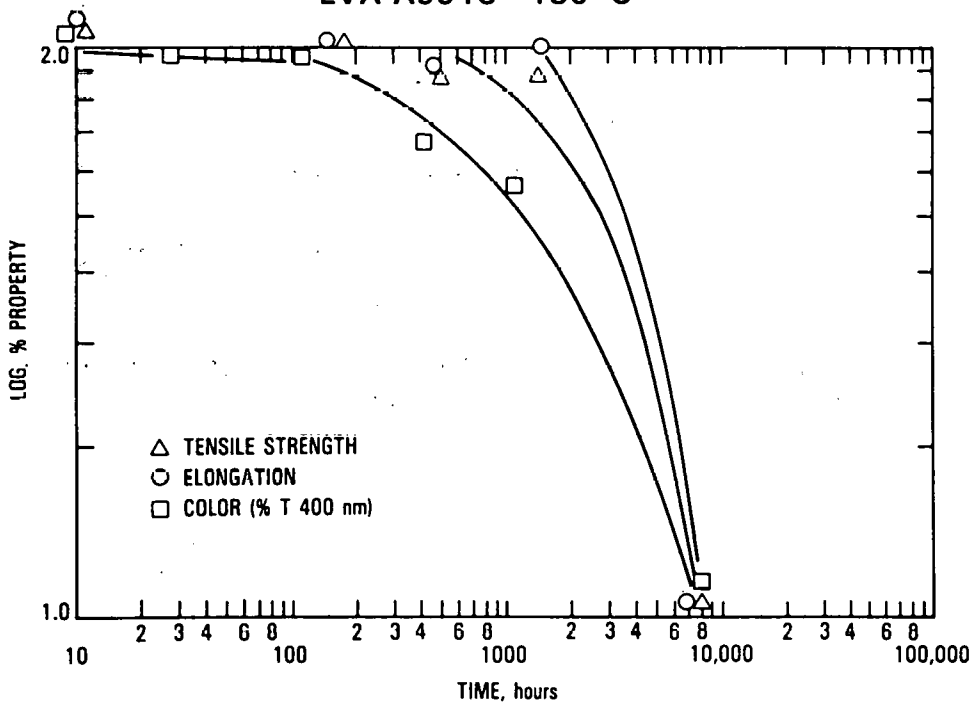
These studies, sponsored by the U.S. Department of Energy through the Jet Propulsion Laboratory, were carried out at Springborn Laboratories, Inc., under the direction of Paul Willis.

# Module Designs



## Thermal Aging

EVA A9918 - 130°C



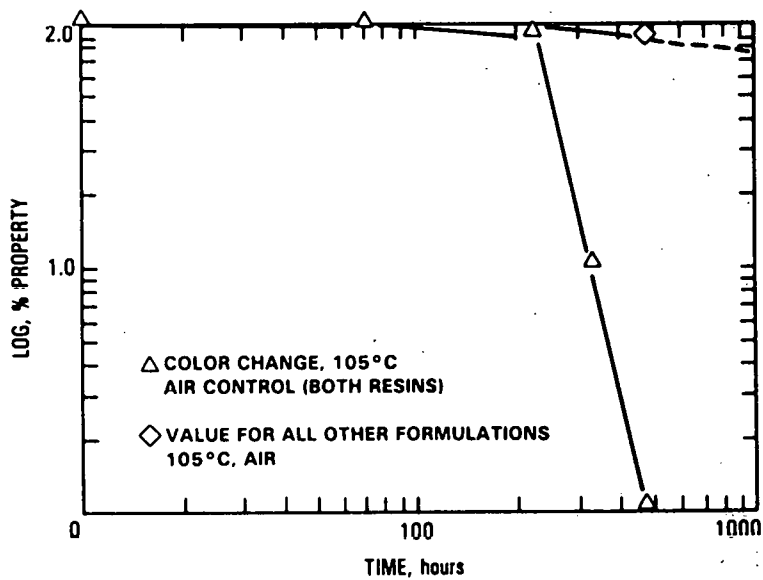
- No change in optical, mechanical, or electrical properties after:  
 90°C: 7200 hours      105°C: 1000 hours

## Metal Deactivation Experiments

- Prepare polymer formulations 0.2 phr deactivator
- Mold over copper screen
- Copper: silane / no silane treatment (Z-6030)
- Thermal age, air and nitrogen
- Monitor % T 400 nm (yellowing)

### Metal Deactivation

(COPPER SCREEN)  
EVA A9918



- EVA controls degraded at 400 hours (coloration and flow of resin away from copper screen)

## Metal-Catalyzed Degradation

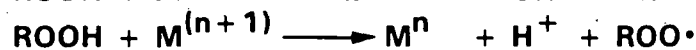
Copper and possibly other multivalent metals  
accelerate oxidation reactions in polymers "pro-oxidants"

### General Mechanisms:

- Initiation:  $R - R \xrightarrow{\Delta} 2 R\cdot$
- Propagation:  $R\cdot + O_2 \longrightarrow RO_2\cdot$   
 $RO_2\cdot + RH \longrightarrow R\cdot + ROOH$

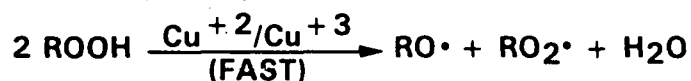
- Metal catalysis:

- Multivalent metals complex hydroperoxides. React through redox mechanisms. accelerates production of free radicals



- Soluble ions are catalytic. Affect propagation rate only.

Sum:



## Conclusions (Results to Date)

### General Observations

- First property to change: color (yellow)
- Degradation: predominantly induction period type, few first order
- Exposure times are long, need higher acceleration to assess formulation changes in less time

### Metal Activation

- Avoid metallic copper in contact with pottant (other multivalent metals?)
- No reactions observed with aluminum, 60/40 solder
- Wash off solder flux (acidic residues, soluble ions)
- Deactivators give improvement (effectiveness?)
- Silane gives improvement (effectiveness?)

## DISCUSSION

SOMBERG: I know that at least one of the modules you showed has not been made for at least three years. Are those typical of all the tests that have been run that you have described?

MON: Initially all we had was Block I, II and III modules, some of which are no longer made. Then we started with Block IV and we are in the process of getting our hands on Block V modules, to put in these chamber too.

SOMBERG: Would you say that the data you have shown are really of Block III and before that?

MON: For the most part, yes. We have had enough time. We have been running Block IV stuff now for about 100 days, if I recall -- well, probably longer than that, since late 1982. About seven months.

SOMBERG: What does that look like?

MON: About as bad as the first group. About as bad as the first three Blocks.

SOMBERG: How many different module manufacturers are in that test?

MON: All the major ones.

SOMBERG: So you are saying Block IV looks about the same as Block III?

MON: Well, yes. When you ask me a question like that, how am I supposed to differentiate between modules that look like this when they all begin to look like this after 70 days and the 85-85 chamber? Yes. EVA is about as bad as PVB as far as degradation is concerned. We are talking about encapsulations rather than metallizations. EVA yellows severely. Especially when in contact with silver metallization. More than PVB, I would think. Maybe not; it is hard to say. The best insulation, from the observations that I see here, is the old silicones. They seem to be much better.

SOMBERG: What about the Block IV cells. What do they look like compared -- not the encapsulation, but the cells themselves. Are you saying that the problem in Block IV appears to be about the same as it was in Block III?

MON: I can't say that.

SOMBERG: Are there any initial indications that it appears that way?

MON: Oh, yes. Like I say, the cells themselves --

SOMBERG: Not the encapsulation of the cells.

MON: No. I haven't seen the cells.



ROYAL: There is another group that is testing cells, with a slightly different approach. The data are not available in that exact same format.

LIVESAY: Have you had the chance to look at that blossoming or that pattern under a scanning electron microscope?

MON: Yes. We are doing that now. What we have discovered there is a lot of silver concentration, of course, right on the metallization. As you probe beyond the metallization, the concentration goes down and as you probe in a lateral direction, the metallization, the silver content also goes down. There is definitely a diffusion.

LIVESAY: What is the microstructure? I have seen things like this, sometimes they are a whisker growth and other times they are dendritic patterns. Do you see that kind of thing?

MON: The microstructure, first of all you see what looks like white puff balls, and stars, and this is formed in the encapsulation but it is right above the metallization. So again that is probably a metallization-catalyzed type of reaction. There seems to be a dark area just off the end of the metallization. There seems to be very little silver content there when we probed for that. It seems to be beyond that. I'm not sure I understand it. It is not doing any quantum jumping as far as I can tell.

QUESTION: There was silver and there is no longer silver?

MON: When you peel the encapsulation off, you can look and see part of the metallization and the blossoming in the encapsulation, and the cell for all apparent purposes is as good as the day it was delivered except that there is probably less silver because we do a dot scan with the EDAX and get a dot map and you can see silver in a decreasing diffusion-like pattern.

WOLF: But you lost silver there?

MON: That's right.

SCHWUTTKE: It would be a migration problem. You have an electromigration problem.

MON: That is correct.

STEIN: Would you clarify that just a bit more? Would you say that the polymer, the encapsulant, is acting as an electrolyte in this case?

MON: Remember, these have been in a humidity chamber.

STEIN: I understand that. If the humidity is absorbed by the polymer then you find silver in the polymer.

MON: That is correct. My interpretation of this is that water vapor has penetrated the encapsulation and has caused it to become an

electrolyte. This happens under the influence of the electromotive forces, as you can see by the bending at the tips, and it is electroytic.

WEAVER: We observed on the PVB encapsulant that it occurred all along the whole collector bar; it occurred in a very short period of time. We installed those last June, but our first cold night with high humidity was in late October, and within one week it showed up. It has not gotten any better or worse since then.

MON: We don't know how long it took for this to occur but this residence has only been powered by solar for about a year.

WEAVER: In my discussion with Neal Shepard, when I called his attention to our problem, he said it occurred very quickly both at the Southwest and the Northeast Residences in a very short period of time. All of a sudden it was there.

MON: This is the Southwest right here.

STEIN: I would suggest that the resistivity of the encapsulant at different relative humidities and temperatures might be a very significant factor here, and should be a means of choosing appropriate materials. If that drops too much, at 85°C or even 100°C, you are in trouble.

MON: Well, we never know these modules in operation will be at around 60°C, the cell temperature, so we are doing accelerated testing and I think we will still be in trouble because I think that the 85°C/85% RH test for, say, 90 days corresponds to probably less than 20 years, in fact I did a back-of-the-envelope calculation one time and it looked like 12 to 15 years.

WEAVER: The concern about high temperature can be brought further forward when you say if I have a weak cell, its temperature will go well beyond 65°C. You will get cells up close to 100°C; if it is a bad cell then you will start heating everything around it.

MON: That right. There will be a reverse bias.

HORN: We've done work where we've seen a similar phenomenon when we do electrostatic-field-assisted bonding of borosilicate glass to a cell. Where we have the glass under high temperature and voltage gradient through the glass and we see a browning halo over the contact grid in the glass. We have actually done analyses of this and it has shown that it is silver migrating into the glass. We have postulated that it is an ion exchange between the sodium in the glass and the silver. By depositing just a few hundred angstroms of SiO<sub>x</sub> through a shadow mask down to that grid line we can eliminate the problem. It might be as simple as putting the AR coating over the contact grid except where you want to make the contact.

MON: Do you have literature on this?

HORN: We published last fall in the IEEE PV Specialist Conference.

MON: I would like to get together with you and get that reference.

WONG: I have two short questions related to this. The first question is, is this blossoming effect happening only under the high humidity and heat condition?

MON: That is correct. Except that we have seen it in the Southwest RES and in various field sites at so called normal field temperatures.

WONG: The second question is, you say the water acts as an electrolyte. Do you mean that the silver will be dissolved in the water, through the water and then deposit at the low potential region?

MON: No, I won't go so far as to say that because I haven't observed that yet. All I am saying is that basically, from that previous picture, it is my contention that it is probably an electrolytic phenomenon. Whether it is actual silver ions or some sort of a -- it could be an electrophore type of thing too, I am not sure that is what you call it. You have a situation where you have either an ion or a polarized molecule following the field line. There is a name for that and I can't remember what it is. But I don't know yet what the mechanism is.

WONG: But it has to be something dissolved in water that can transport through the water. A possible low potential field.

MON: I am sure of that.

WONG: And the driving force has electrochemical potential, do you think?

MON: Yes. I have not seen any deposits on the cathodes. We are looking for that but we haven't seen it. But by the time it gets -- like this gap -- it isn't much of a gap -- but this particular module was accelerated at the difference between those two cells, which is 17 volts. This took 1700 hours, roughly, in that time frame, for this one to turn. So again, I don't know what this translates into in real field conditions. But I do think it is electrolytic. I can't prove it yet.

AMICK: Which is the positive and which is the negative?

MON: The positive one is the bottom one, the one that has the blossom on it.

AMICK: So that is the one where hydrogen would come out if you were electrolyzing the water.

MON: That is correct. This is the cathode.

AMICK: So that is where oxygen would come out? And if oxygen comes out--

WONG: Did you see any bubbles or pockets or oxygen gas in this?

MON: No.

COMMENT: Do you know when Paul (Willis) will be able to make tests with voltage applied?

GALLAGHER: I can't answer that question but I think it is only a matter of time until he is instrumented to do it. I think one of the things that has come out of my being here is my awareness of the fact that the phenomena that we just heard of are very much accelerated by voltage.

COMMENT: Or maybe retarded.

GALLAGHER: Again, there is an activation energy of some sort involved, either positive or negative. Any other questions?

AMICK: Brian, you really should be looking at them in light, too at air mass.

GALLAGHER: I agree, there is another way of looking at this. If you look at the metallic systems that are available, and what Paul (Willis) found: sort of an accidental thing, and he went after it to see what was causing it. Normally one wouldn't worry about the copper if you had the data on nickel because in the course of producing the copper-plated structure it would be very easy and quite economical to give it a nickel flash before you remove it from the plating system, so you wouldn't go after it this way. What happened was that he found a phenomenon he got interested in, and he went after that phenomenon, and then once he started reporting on it he got pushed a little bit to look at some of the other metals to solve it in a different way. He, being a chemist, and very interested in polymers, wants to use that approach, wants to deactivate whatever the metal is in a chemical reaction. In our case, we would just replace the copper with nickel and not worry about it. But you are right, the acceleration factors, now that we know they are present, should be used.

THIS PAGE  
WAS INTENTIONALLY  
LEFT BLANK

# METALLIZATION PROBLEMS WITH CONCENTRATOR CELLS

P.A. Iles

APPLIED SOLAR ENERGY CORPORATION

City Of Industry, California 91749

## INTRODUCTION

Cells used with concentrators have similar contact requirements to other cells, but operation at high intensity imposes more than the usual demands on the metallization.

Table 1 lists the overall contact requirements. We will discuss how concentrator cells can meet these requirements.

## REDUCING RESISTIVE LOSSES

Since concentrator cells operate at high current density, any resistive losses are more severe.

Resistive Loss Modeling (See Reference 1\* for previous references.)

- The procedure used to design concentrator cells is as follows (see Figure 1).
- 1) Select the intrinsic cell design best suited to the planned application -maximize collected current and voltage, minimize reflective and bulk resistance losses. These terms are derived from previous experience gained in optimizing the cell design.
  - 2) Select contacts with low contact resistance, and design a grid pattern using 3-7 below.
  - 3) The various resistive components (contact, front sheet, gridline, bulk) are analyzed as a network of resistors. This analysis generally uses parallel lines for rectangular or square cells, sometimes with the cell divided into quadrants; for circular cells, radial lines are used, often with increasing line density towards the outer edge (bus contact) of the cell.
  - 4) The resistive losses are computed, and transformed into power losses e.g. by taking their ratio to the internal impedance of the cell at the operating intensity  $X$  (this impedance =  $0.9 V_{oc}/I_{sc}$ ). This impedance increases just less than linearly with  $X$  ( $\sim 0.84X$  for  $^xSi$ ,  $^x0.89X$  for  $GaAs$  ), so that the relative percentage loss caused by resistive components increases at this same ratio. The shading loss does not vary with  $X$ , and is determined by the areal grid dimensions.
  - 5) The operating CFF of the cell under concentration is computed by subtracting the total resistive losses from an initial "ideal" CFF.
  - 6) The shading reduces the generated current density to the actual cell current density.

\*P.A. Iles "A Survey of Grid Technology" to be published in Conference Rec. of 16th Photovoltaic Specialists Conference, 1982.

7) Grid line dimensions are selected within the best available state-of-the-art.

The rationale for grid design is to minimize shading losses (at low concentrations up to 10-20X), and then to gradually reduce the resistive losses more at higher concentrations (Reference 1). Figures 2 and 3 show the good agreement obtained between measured and calculated values. The slight improvement in the measured CFF can be explained by slight differences in the assumed and achieved gridline dimensions.

This agreement which has been repeated for many different cell designs, shows that the loss model analysis is valid (especially at low concentrations), even using the simpler lumped resistance assumptions. This adds confidence to use of the same model in designing grid (and busbar) configurations for large area cells, or for cells where low costs limit the choice of grid formation methods. For concentrator cells practical grid formation and deposition techniques have been developed, and generally require the use of photolithographic methods. Of course to obtain high concentrator system efficiency, it is essential to have high cell efficiency.

### INCREASED OPERATING STRESSES

Items 5-7 in Table 1 are especially important under the increased operating stresses for concentrator cells. #5 is important, especially for terrestrial concentrator systems where severe temperature cycling (many times per day) is possible. It also increases the range of bonding methods and conditions which can be used. #6 is important because most concentrator cells operate hot (despite the use of cooling), and there may also be severe temperature gradients between the front and back surfaces of the cell.

Also cells may have to operate at high temperatures for extended periods (say 20 years), and it is considered that additional high temperature stability is required for concentrator cells. Some success has been achieved by using diffusion barriers to minimize interlayer movement; silicon concentrator cells with TiN barriers have survived heating above 600°C for long periods (½-1 hour) with little degradation, and this work continues.

The higher temperatures can also lead to accelerated corrosion rates (#8) when the cell is operating in the field; at present passivating layers (eg. Pd with Ti Ag) are used, but more testing is needed to show that this is not a severe operating problem.

The bonding of interconnects to concentrator cells (#7) involves the use of more massive interconnects (to reduce resistive losses), combined with larger bonding areas on the cells. The back surface must be well bonded to the substrate, to increase heat transfer.

### CONCLUSIONS

Although there are some areas not completely resolved, the results obtained with concentrator cell contacts suggest that the resistive loss models used are satisfactory. The metallization behavior under the increased operating stresses supports the conclusion that for cells operating around one-sun levels, that some of the present metallization systems are adequate. More work is required however, when compromises are required between the metallization methods available, and the cost constraints of the cell or array processing methods.

**Table 1. Cell Metallization Requirements**

#	REQUIREMENT
1.	LOW CONTACT RESISTANCE TO SEMICONDUCTOR (N AND P).
2.	HIGH CONDUCTIVITY TO DECREASE RESISTIVE LOSSES.
3.	EASILY PATTERNED INTO GRIDS.
4.	MINIMUM CHANCE OF GRID ACTING AS FUSE.
5.	GOOD ADHESION
6.	GOOD HIGH TEMPERATURE STABILITY (UNDER SINTERING TO REDUCE CONTACT RESISTANCE, IMPROVE AR COATING, OR UNDER OPERATING CONDITIONS).
7.	EASILY BONDABLE (BY SOLDERING OR WELDING)
8.	MINIMUM CORROSION.
9.	SIMPLE METAL STACK.
10.	COMPATIBLE WITH CELL FEATURES (TEXTURING, SHALLOW xJ).
11.	LOW COST (MATERIALS, DEPOSITION), EASILY APPLIED.
12.	LOW DENSITY TO REDUCE WEIGHT (SPACE-USE).
13.	THERMAL EXPANSION CLOSE TO SEMICONDUCTOR (ESPECIALLY ON BACK SURFACE).
14.	GOOD AT LOW TEMPERATURES (SPACE-CELLS).

### Figure 1. Resistive Loss Modeling

- SELECT  $J_{sc}$ ,  $V_{oc}$ , CELL DIMENSIONS.
- SET-UP RESISTOR NETWORK.
- COMPUTE POWER LOSS COMPONENTS.
- MINIMIZE SUM OF RESISTIVE AND SHADING LOSSES.
- ESTIMATE OPERATING CFF,  $J_{sc}$ ,  $V_{oc}$  AT VARIOUS INTENSITIES.
- SELECT OPTIMUM GRID PATTERN.

CONCLUDE GOOD AGREEMENT BETWEEN EXPERIMENT AND PREDICTIONS.  
INFER THAT BASIC MODEL IS VALID AND CAN APPLY TO ONE-SUN OPERATION, INCLUDING LARGE AREA CELLS.



Figure 2. Curve Fill Factor versus Solar Concentration

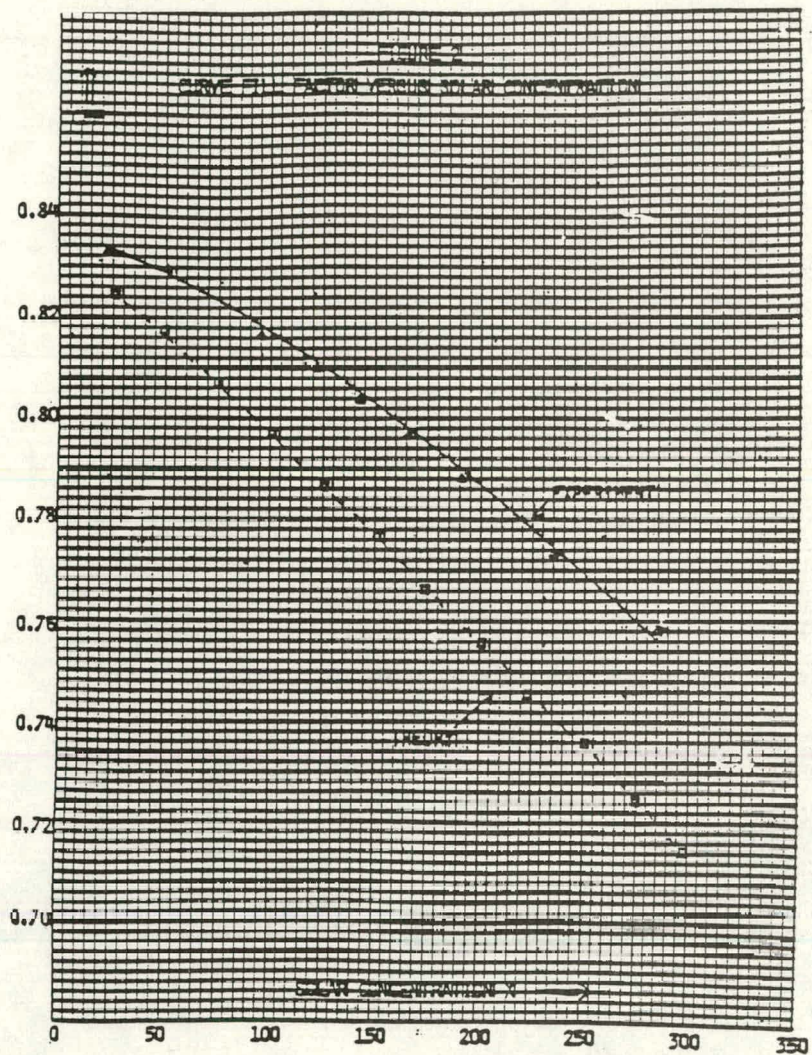
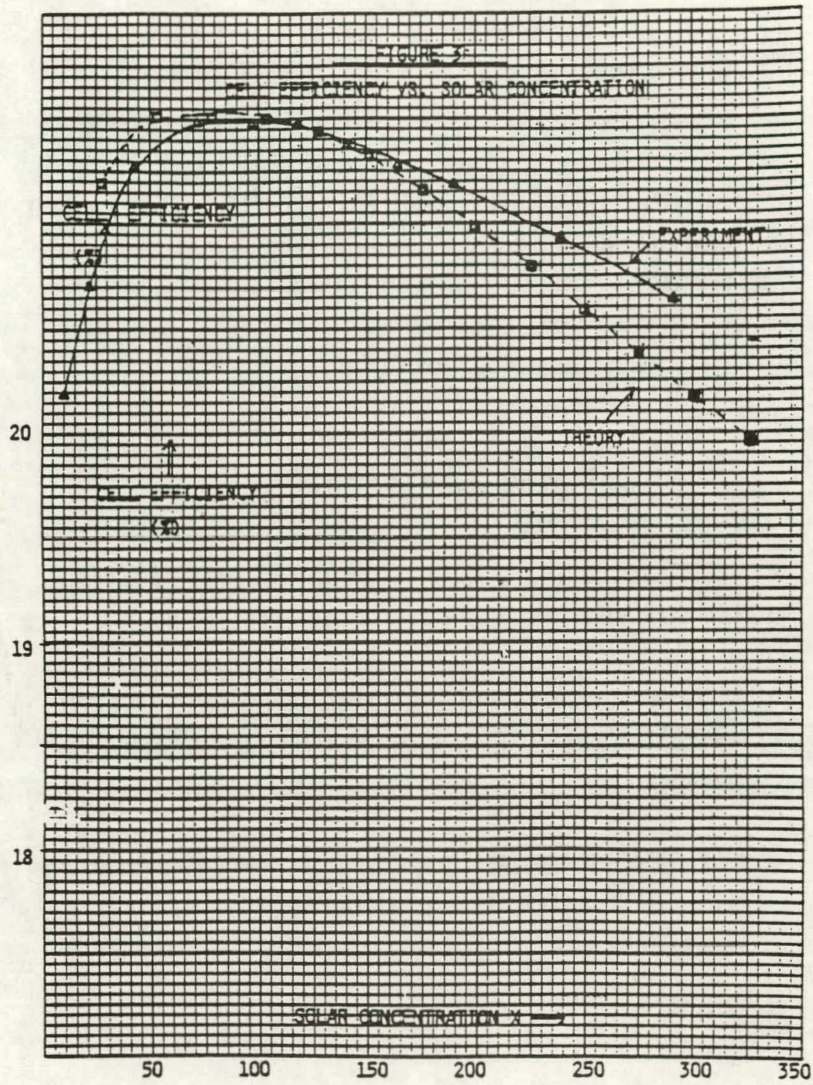




Figure 3. Cell Efficiency versus Solar Concentration





## Figure 4. Increased Operating Stresses

- o ADHESION - FOR TEMPERATURE CYCLING, BONDING.
- o HIGH TEMPERATURE STABILITY
  - PROCESS SINTERING
  - OPERATING CONDITIONS
  - DECREASED CORROSION
- o TESTING DIFFUSION BARRIERS, SIMPLE STACKS AND PASSIVATING LAYERS.
- o BONDING
  - THICKER INTERCONNECTS
  - LARGER BONDING AREA
  - THERMAL CONTACT

## Figure 5. Conclusions

- o RESISTIVE LOSS ANALYSIS IS VALID, SINCE CONCENTRATOR CELLS PROVIDE TEST UNDER VERY SEVERE CONDITIONS.
- o BEHAVIOR OF CONCENTRATOR CELLS UNDER ENHANCED OPERATING STRESSES SUGGESTS THAT HIGH COST CONTACT SYSTEMS HAVE PROMISE.
- o MORE WORK IS REQUIRED FOR LOW COST CONTACT SYSTEMS TO MEET MOST REQUIREMENTS EVEN AT ONE-SUN LEVELS.

## DISCUSSION

WONG: Do you have any grid line patterns available here?

ILES: I don't have any here, you have to know what the concentrator intensity distribution is and what the size is; that's fairly obvious. They are all custom made, there is no such thing as a standard concentrator, there are several linear focus systems in various sizes and several point-focus, so that if you have an intensity and you have some idea of what the distribution is then we can find a pattern close to it. If you are just talking hypothetically we can send you a picture of a thing that looks very pretty with lots of lines on it, but if you have a Fresnel with a 100X lens, which may have a half-inch focused image, that's how we can design a cell with fairly precise dimensions.

BICKLER: Pete, is it true that the concentrator cells are shallow diffusion, slanted toward the blue response?

ILES: Yes, when you do the analysis, when you put the grids close together, the sheet resistance then becomes negligibly small.

BICKLER: Oh, I was going to say, it sounds like a paradox in that there is an advantage to over-shadowing, as you mentioned, in the metallization system to reduce the series resistance. I would assume you draw a parallel with the diffusion depth and that's a lack of transmission or analogous to a shadow, and well worth the --

ILES: That's true, but the scale of the two is so different -- it is typical to say 50X -- you are getting 3% or 4% shadowing and maybe 5% or 6% total resistive loss. If you go to 400X then you slide the shadow mask up to about 10% by putting more lines closer together. Putting the lines closer together is not to reduce the sheet resistance, it is to reduce the power through the grid lines. The grid lines are the more important resistor block.

CAMPBELL: Am I correct that the concentrator cells have a generally lower resistivity base than --

ILES: They generally are, particularly for high concentration, above about 50X or 100X, but they have been good; typically the ones that are made in the range of 0.1 to 0.3 or 0.4 ohm-cm, and have  $10^{17}$  carriers per cubic meter, but there have been some quite good cells made with 1 ohm-cm, with high-quality material, and there have even been some made with 10 ohm-cm but they were thin, they were 2 mils thick, so that the bulk loss was reduced.

CAMPBELL: Other than putting this number into these equations, would this have any effect on the contact pattern?

ILES: No, there is a discrete bulk loss in the equation, even I can calculate that one, but apart from that, no problem, if you want to put it with a web you could easily calculate the pattern.

CAMPBELL: Are not a number of concentrator cells p on n?

ILES: Yes, the ones that Sandia made with great success are p on n; the ones that we make are n on p and p on n. There is a theoretical reason why p on n might be a little better as you go to higher intensities because the Dember effect is assisting you. No one has seen that yet; the resolution of all the other variables hasn't been good enough, but we also haven't seen conductivity modulation in either of them up to 1000X, which is also predicted by theory.

SESSIONS I AND II GENERAL DISCUSSION

GALLAGHER: We have a little time; maybe now would be a good time for people to stop and think a minute about whether or not any questions about the first two sessions have occurred to them.

SOMBERG: I have a question for Gordon Mon: on the two modules you showed in Block III, you said one was PVB, and you thought the one from Applied Solar was EVA. Could you confirm that? Whether it was really EVA or not? I would like to bring out a point of what I am talking about. In some of the early modules, particularly with the printed silver formulations, many people were using a hydrofluoric acid dip to improve the curve shape and I suspect, through my own experiments and talking with others, that the HF was not neutralized. With PVB there is an acid-catalyzed crosslinking that darkens the PVB and that's a result, not of the metal per se, but of the acid in the system. That's why I am wondering if the second was EVA, the yellowing was EVA or was related possibly to acid-catalyzed reaction like in the first one with PVB.

MON: I just can't remember at the moment.

SOMBERG: Well, maybe Peter (Iles) could answer.

GALLAGHER: I might add that regarding the series of viewgraphs that I got from Springborn, I had a very short conversation with Paul Willis. He had looked at the same structures with PVB, and PVB was worse, slightly worse, than EVA. I picked EVA because it was the best of the actors. If you wanted to put them in some sequence of priority, EVA and EMMA were quite good; PVB was next, and I don't think he looked at RTV.

MON: Well, different companies who make modules have seen this problem and they all go to their chemists and they all come up with a different answer as to what is going on. You just brought up this business about hydrofluoric acid washing; well, I have also heard about a similar problem with etching. You know they use hydrochloric acid to etch when using a photoresist and then they don't get rid of the chlorine so that's why it is yellow. ARCO looked at the problem with their modules and they came up with a free-radical theory, that we heard from Gallagher, which caused color centers. I've heard other people with all different types of explanations; they are probably all right for their systems. The problem is that we don't know the detailed composition of all these formulations -- they are proprietary and they aren't going to tell us. So we just have to classify according to broad categories like silver system or nickel system -- we really don't know what other compound metals, or what have you, are in those systems. So we are kind of at a disadvantage.

SOMBERG: I think I brought the point up to separate the issue of metal catalyzed reaction versus something, possibly secondary, that was used in the processing that resulted in the darkening of the PVB.

MON: That could well be.

NAZARENKO: Another problem with polyvinyl butyrals is that they generally have a relatively low glass transition temperature, typically below 60°; now you're working above that temperature, so the material is going to soften and that will enhance moisture penetration.

GALLAGHER: One other thing I might say, you talked about acid-catalyzed reactions. One of the reaction products of the decomposition of EVA should be acetic acid, and they don't see any acetic acid, nor do they smell it. Its odor is the easiest way of finding out whether it is present, so that is why they feel that it is a free-radical reaction and it is the hyperperoxide that is causing the degradation in EVA. I don't know anything else about PVB.

NAZARENKO: There should be some hyperperoxide left at the end of the degradation, and there are very simple tests that you can use -- qualitative tests -- for hyperoxide in even small amounts; that can be easily detected.

GALLAGHER: I am sure that's why they came up with this system.

AMICK: Presumably the stabilizers that are in there would take care of it for a while, and that may be why you have no degradation and then all of a sudden it falls off the cliff. If you change the concentration of those various additives you might delay the onset.

GALLAGHER: Yes, I agree with you wholeheartedly, and you have to remember that this was Paul's (Willis) first cut at it, he's looking at "is this the correct direction to go" and he wasn't lucky enough to fall on top of the cliff and stay there. He did push it out a little bit, but it is the right direction. Anything else? How about the first session?

BICKLER: The first presentations left an impression of the hopelessness of some of these high-efficiency goals that are being expounded. A point that I heard Peter Iles mention -- I don't think it got enough emphasis -- is that a 14% space cell at AMO is not to be compared on the same scale with a 12% terrestrial because of the spectral character going to AM1. Of course, this involves a spectral response to the cells, but you certainly pick up an efficiency point; a 14% space cell is starting to crowd 16% at AM1.

GALLAGHER: What do you use as a correction factor -- 1.18?

ILES: 1.15.

BICKLER: That is the spectral response that Peter (Iles) is familiar with, so somebody's diffused a different junction depth or something there. You know, I don't want to give the impression that 1.15 is a chiseled-in-stone number, but the point is that the goals that have now been set -- I guess I can't speak for the 30 years -- in terms of efficiency are not as bad as they may have appeared to be in the first presentation.

GALLAGHER: I think we have heard a couple of good things today about efficiencies and metallization. Marc Nicolet, for example, when he said "Hey, there is hope." That made me feel good; I think I would like to ask Bob Campbell a question on dendritic web -- nobody has talked sheet

forms, but Westinghouse is running a kind of miniline and doing great things with it, or lots of things with it. Bob, what kind of efficiencies are you getting out of that line right now?

CAMPBELL: The average efficiency with our baseline process at the moment -- liquid boron dopant on the back and gaseous  $\text{POCl}_3$  on the front -- the average efficiencies are about 13.2% in a fairly wide range from around 11 up to about 16.

GALLAGHER: I think that is significant.

CAMPBELL: I should mention these are on  $2 \times 10$  cells,  $20 \text{ cm}^2$  cells.

GALLAGHER: Now, if only ARCO would tell us their distribution. I think the point is, when we started this program many years ago, attempting to get a 10% module was absolutely fantastic and people were really worried about it. The efficiencies that people were getting out of Czochralski cells or the best cells they could make were pretty darned low. We have come a long way.

WOLF: I just came from another meeting last week and we determined that a number of organizations can regularly make over 17% efficiency on some cells, and possibly upward to the low 18% range, but 17% is certainly within existing capability. Also, part of this accomplishment is a metallization level that I think is higher than Ron Daniels explained to us. There are several people who can regularly make metallization patterns that combine shading and (Joule) losses of 5% or  $5 \frac{1}{2}\%$ , and not the 8% that Ron Daniels had on this efficient frontier.

DANIEL: What total area are you describing, since the shading loss described was for  $100 \text{ cm}^2$ ?

WOLF: I was also talking about  $100 \text{ cm}^2$  cells. People can get this quite readily. You have to use strapping over the bus lines. You have to use narrow grid lines. You have to use thicker plating. You can't use sintered matter. You have to use biconductivity metals of the highest conductivity you can get in copper or silver. If you control it you can get 5%, and there are various metallization systems. Copper has been used by some people. It is usually plating; it is not a paste system that gets you to high efficiency.



THIS PAGE  
WAS INTENTIONALLY  
LEFT BLANK

SESSION III: THICK-FILM METALLIZATION SYSTEMS

J. Parker (Electrinx, Inc.), Chairman

THIS PAGE  
WAS INTENTIONALLY  
LEFT BLANK

# EFFECTS OF PARTICLE SIZE DISTRIBUTION IN THICK FILM CONDUCTORS

Robert W. Vest

Purdue University

West Lafayette, Indiana 47907

## INTRODUCTION

The packing of particles for maximum density is a problem of great importance in ceramic processing and powder metallurgy, but it is even more critical in thick film conductors because of the very low compacting pressures exerted during screen printing. The fired film density, and hence the electrical resistivity, is intimately related to the density of the metal compact which exists after the organic constituents of the ink have been removed in the early stages of firing. This green density is even more important if the firing cannot be carried out at a sufficiently high temperature due to limitations imposed by the substrate. The coordination number (CN) and the fractional porosity (P) for the packing of spherical particles is shown on page 2 for various geometries. The case of random packing is of most interest, and previous workers have distinguished two types - dense and loose random packing. The coordination numbers shown on page 2 for these two cases were experimentally obtained as were the porosity numbers. The porosity of 0.363 also given for dense random packing, was obtained by computer simulation.

## THEORETICAL MODELS

A distribution of particle sizes can be used to decrease the porosity associated with packing of monosized spheres. The two primary approaches that have been taken to modeling this problem are shown on page 3. With approach A, a single sphere of the largest possible size is inserted to fill the interstices in the packed bed. Approach B inserts many very small particles to fill the porosity. The methods of modeling with Approach A are given on page 4. Since the experimental coordination numbers obtained for random packing are close to that of body center cubic packing, one can assume BCC and fill all of the tetrahedral sites with small spheres. Since this is a regular geometric packing, the ratio of sizes of the spheres can be exactly calculated as 0.291. The volume fraction of smaller spheres to exactly fill all the tetrahedral sites is 0.129, giving a porosity for the two sized system of 0.219. However, the packing is not really body centered cubic, and the best approach to determining the size and quantity of spheres to add is by computer modeling. The model developed by approach B is described on page 5. If it is assumed that the second size sphere is very small compared to the first, then all of them can go into the porosity of the larger spheres. Since the porosity of any packed bed depends only on the coordination number, it can be assumed that the fractional porosity in each size fraction is the same. With these two assumptions, the volume fraction of the small size can be calculated in terms of the porosity for

packing of the larger size. The final porosity turns out to be simply the square of the porosity of one size. This model can easily be extended to many different sizes of particles as shown on page 6.

The results from applying approach A and approach B to two sizes of spheres are summarized on page 7 for different packing geometries of the large size. The calculations are exact for the simple cubic and body centered cubic packing. The volume fractions and porosities given for the dense random and loose random packings were calculated using the equations on page 5 and the appropriate porosity from page 2 for approach B, and by computer modeling for approach A. For approach B, the ratio between the diameter of the smaller and the larger spheres should be very small, and for the loose random packing, this ratio should be less than 0.006. The origin of this number is described on page 8 in terms of a hypothetical experiment; to start with a layer of small spheres on top of a layer of large spheres, and then mix the two sizes and calculate the change in volume. A parameter  $y$ , which is a function of ratio of particle sizes, is introduced, and an experimental value of  $y$  is utilized to calculate the porosity in terms of the ratios of solid volumes and ratios of solid diameters. This equation is plotted on page 9 as the porosity as a function of volume fraction with size ratio as a parameter. At the optimum volume fraction, the porosity is 0.16 as predicted for loose random packing if the ratio  $d_2/d_1$  is zero. If this ratio is 0.006, the porosity becomes 0.17. Previous researchers have stated that the approach B model can be utilized as long as the ratio of sizes is less than 0.2, but the plot on page 9 shows that the correction at 0.2 is very large. A difficulty with either approach A or B is the uniformity of mixing of the two sizes, and this problem has been addressed by introducing a mixedness parameter ( $M$ ) as described on page 10. Values of  $M$  can only be obtained experimental.

There are some special problems in applying the theoretical models to thick film conductors as listed on page 12. No one has studied the mixedness parameter for roll mill blending of thick film inks, so no values are available for correction factors. For all thick film conductors, at least one additional phase is added in order to develop adequate adhesion to the substrate. Even though the glass frit or base metal oxides are present in small concentrations relative to the metal, they still can influence the packing of the metal particles. The thickness of the films is also a special problem because container effects have been observed in studies of random packing of spheres.

#### EXPERIMENTAL CONDUCTORS

A platinum thick film conductor having the requirements listed on page 13 was needed for a project in the Turner Laboratory at Purdue University. It was decided to try approach B to achieve high density using three different size platinum particles. In order to achieve the desired ratio between diameters of successive size ranges, the smallest size was formed in situ by decomposing a platinum resinate. The variation of grain size with firing temperature of the resinate is shown on page 14. The size 0.02  $\mu\text{m}$  was assumed for particles from this source because that was the grain size corresponding to the temperature at which all of the organics had been re-

moved. The results obtained with eight different inks are given on page 15. The uniformity and porosity of the films were the primary criteria used for judging quality. The optimum volume fractions of three sizes as predicted by the model for approach B is 64-26-10, as given on page 6. This ink did give lower porosity than any of the one or two size inks studied, but was not as good as the last two inks on page 15. These inks had compositions arrived at empirically. The difference in microstructure between the inks at the top and bottom of page 15 are shown on page 16, and it is obvious that selection of particle sizes of the conductor can make a very significant difference in film microstructure.

Another experimental program had the goal to develop silver conductors with the requirements given on page 17. This was for a consumer application, and cost was a very significant factor. The primary criterion used for evaluating various inks was the conductance per gram of silver, or the specific conductance as defined on page 18. If one takes the ratio between the specific conductance of two films, the result is independent of the film geometry. The silver inks were formulated as described on page 19, and the results with 6 different mixtures of particle sizes are given on page 20. Ink 6, which contained only silver particles 17  $\mu\text{m}$  diameter, was not an electrical conductor because the very large silver particles did not sinter during the firing at 625°C for 10 minutes. The ratio of 70-28-2 for the fractions of three different sizes in inks 1, 2 and 3 is close to that predicted by the theoretical model of approach B, but was arrived at empirically. It can be seen from page 20 that ink No. 1 with three sizes of silver particles had a higher specific conductivity of any of the films with only single size particles, but the other two mixtures did not have as high a specific conductivity as two of the monosized inks. The ratio between successive sizes for the three mixed size inks is shown on page 21 along with the specific conductivity ratio. These results reflect the influence of the absolute size of the largest silver particles and its influence on sintering, as well as the effect of the ratio of sizes, particularly between the largest and next largest ( $d_2/d_1$ ). The size ratios for ink No. 1 are close to those calculated for dense random packing by approach A (see page 7).

#### SUMMARY

The conclusions that can be drawn from the studies of particle size distribution in thick film conductors are summarized on page 22. The distribution of particle sizes does have an effect on fired film density but the effect is not always positive. A proper distribution of sizes is necessary, and while the theoretical models can serve as guides to selecting this proper distribution, improved densities can be achieved by empirical variations from the predictions of the models.

## Page 2. Packing of Spheres

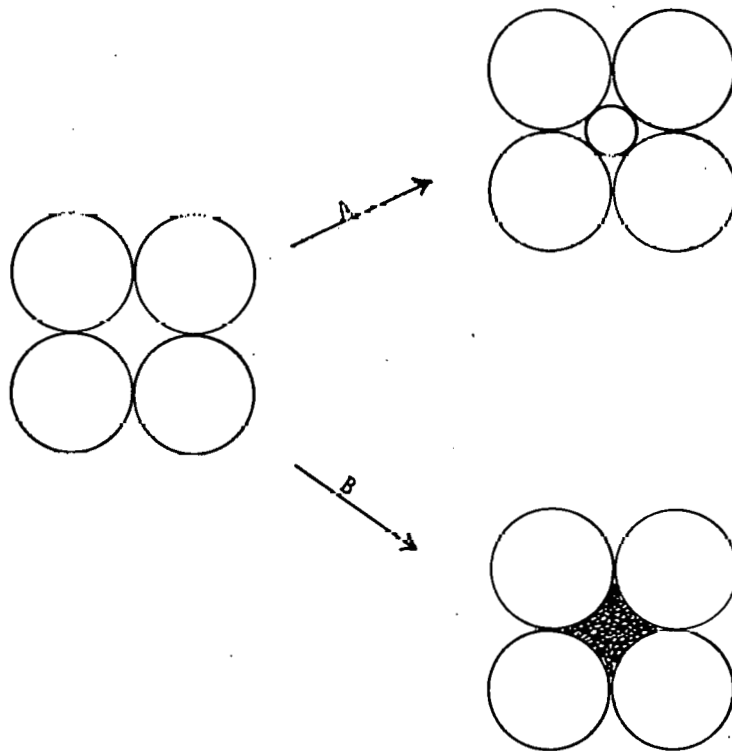
<u>GEOMETRY</u>	<u>CN</u>	<u>P</u>
Closest Packed	12	0.26
Body Centered Cubic	8	0.32
Simple Cubic	6	0.48
Dense Random	8.5 <sup>a</sup>	0.37 <sup>b</sup> 0.363 <sup>c</sup>
Loose Random	7.1 <sup>a</sup>	0.40 <sup>b</sup>

a. J.D. Bernal and J. Mason, *Nature*, **188**, 910 (1960).

b. G.D. Scott, *Nature*, **188**, 908 (1960)

c. C.H. Bennet, *J. Appl. Phys.*, **43**, 2727 (1972).

## Page 3. Two Models for Packing Two Sizes of Spheres



## Page 4. Approach A

1. Assume BCC Since CN = 7.1 - 8.5

N spheres ( $d_1$ ) in BCC packing

6N tetrahedral sites

3N octahedral sites

fill the larger tetrahedral sites with spheres ( $d_2$ )

$$d_2/d_1 = 0.291$$

$$\nu_2 = 0.129$$

$$\text{Porosity} = 0.219$$

2. Computer Modeling

Best Approach



## Page 5. Approach B

$V_1, V_2$  - solid volume of each size

$P_1, P_2$  - pore volume associated with each size

Assume size 2 goes into the porosity of size 1 ( $d_2/d_1$  very small)

$$V_2 + P_2 = P_1 \quad (1)$$

Assume size 1 and size 2 have the same packing. Then the pore fraction will be the same.

$$p = \frac{P_1}{V_1 + P_1} = \frac{P_2}{V_2 + P_2} \quad (2)$$

Combining Eqs. 1 and 2 gives

$$\frac{V_2}{V_1} = p \quad (3)$$

$$\tilde{v}_2 = \frac{V_2}{V_1 + V_2} = \frac{p}{1+p} \quad (4)$$

$$\text{Porosity} = 1 - \frac{V_1 + V_2}{V_1 + P_1} = p^2 \quad (5)$$

## Page 6. Approach B (Cont'd)

Sizes 1, 2, 3, ..., 1, ..., n

Assume  $d_{i+1}/d_i < 0.01$

$$V_{i+1} + P_{i+1} = P_i$$

Assume all sizes have the same packing

$$P = \frac{P_i}{V_i + P_i}$$

Then

$$V_{i+1}/V_i = P$$

And in general

$$\psi_i = \frac{P^{i-1}}{\sum_{a=0}^{i-1} P^a}$$

### Example

3 sizes,  $P = 0.4$

$$\psi_1 = 0.64$$

$$\psi_2 = 0.26$$

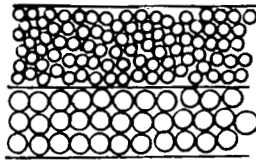
$$\psi_3 = 0.10$$

## Page 7. Two Sizes of Spheres

Packing of Size 1	$\psi_2$		$d_2/d_1$		Porosity	
	A	B	A	B	A	B
Simple Cubic	0.28	0.32	0.73	~0	0.27	0.23
Body Centered Cubic	0.13	0.24	0.29	~0	0.22	0.10
Dense Random	0.17*	0.27	0.22-	~0	0.24*	0.13
			0.6			
			mode =			
			0.26*			
Loose Random	-	0.29	-	<0.006	-	0.16

\*H.J. Frost and R. Raj, Comm. Am. Ceram. Soc., C-19, February (1982).

## Page 8. Approach B: Layered Bed



$$\text{Volume} = V_2 + P_2$$

$$\text{Volume} = V_1 + P_1$$

$$P = \frac{P_1}{P_1 + V_1} = \frac{P_2}{P_2 + V_2}$$

MIX THE TWO SIZES

$$\Delta V_{\max} = V_2 + P_2 = \frac{V_2}{1-P}$$

$$\Delta V = y \Delta V_{\max} \quad \begin{array}{l} y = 1 \text{ for } d_2/d_1 = 0 \\ y = 0 \text{ for } d_2/d_1 = 1 \end{array}$$

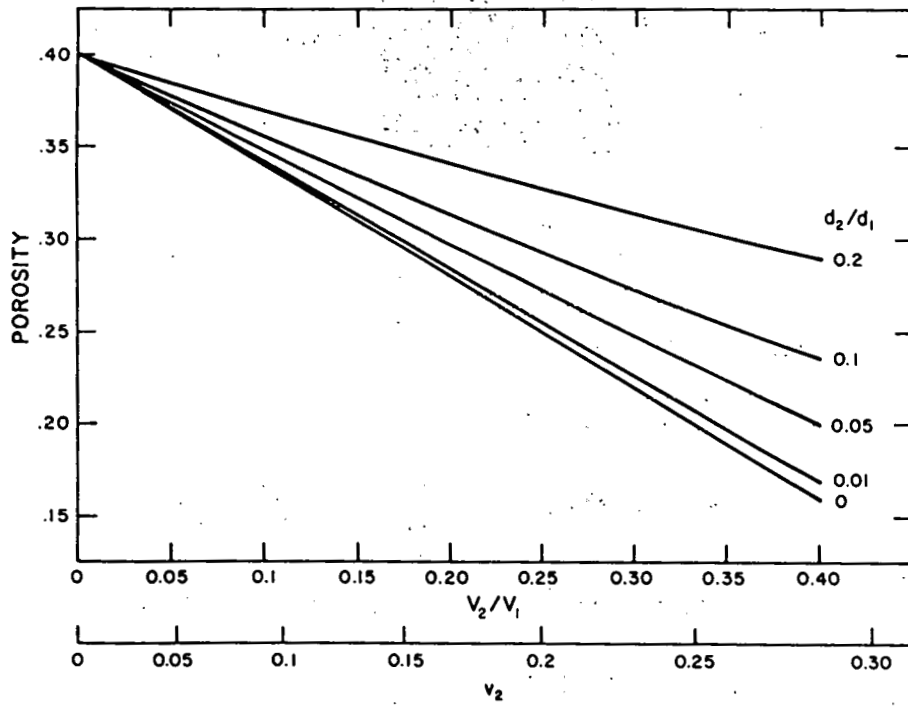
experimentally  $y = 1 - 2.62 (d_2/d_1) + 1.62 (d_2/d_1)^2$

$$\text{Porosity} = 1 - \frac{V_1 + V_2}{V_1 + P_1 + V_2 + P_2 - \Delta V}$$

$$\text{Porosity} = \frac{P (1 + V_2/V_1) - y V_2/V_1}{1 + V_2/V_1 - y V_2/V_1}$$

\*C.C. Furnas, Ind. Eng. Chem., 23, 1052 (1931)

Page 9. Effect of Size Ratio on Porosity With Approach B



## Page 10. Uniformity of Mixing

A problem for Approaches A and B

Introduce a degree of mixedness parameter (M)

$$M = 1 - \sigma / [\nu_2(1-\nu_2)]^{1/2}$$

$\sigma$  = std. deviation of compositional variations

A proposed<sup>a</sup> relationship is

$$B = B_U + M^2(B_m - B_U)$$

where B,  $B_U$  and  $B_m$  are bulk densities of real mixtures, a fully unmixed system, and an ideally mixed system, respectively.

Later work<sup>b</sup> has shown that M and B (or final porosity) are not uniquely related, and a statistical approach must be taken.

- a. D.W. Fuerstenau and J. Fouladi, Am. Ceram. Soc. Bull., 46, 821 (1967)
- b. G.L. Messing and G.Y. Onoda, J. Am. Ceram. Soc., 61, 1 (1978)

## Page 11.

Theoretical studies<sup>a</sup> predict and experimental studies<sup>b</sup> confirm that the maximum corrections due to M occur near the optimum values of  $\nu_2$  predicted by either Approach A or Approach B.

Typical powder mixing techniques give M values of 0.77 to 0.96.

M values for roll mill blending of thick film inks?

- a. G.L. Messing and G.Y. Onoda, J. Am. Ceram. Soc., 61, 1 (1978)
- b. G.L. Messing and G.Y. Onoda, J. Am. Ceram. Soc., 61, 363 (1978)

## Page 12. Special Problems With TF Conductors

Mixedness

Presence of Glass Frit

Availability of Sized Powders

Alloying Reactions

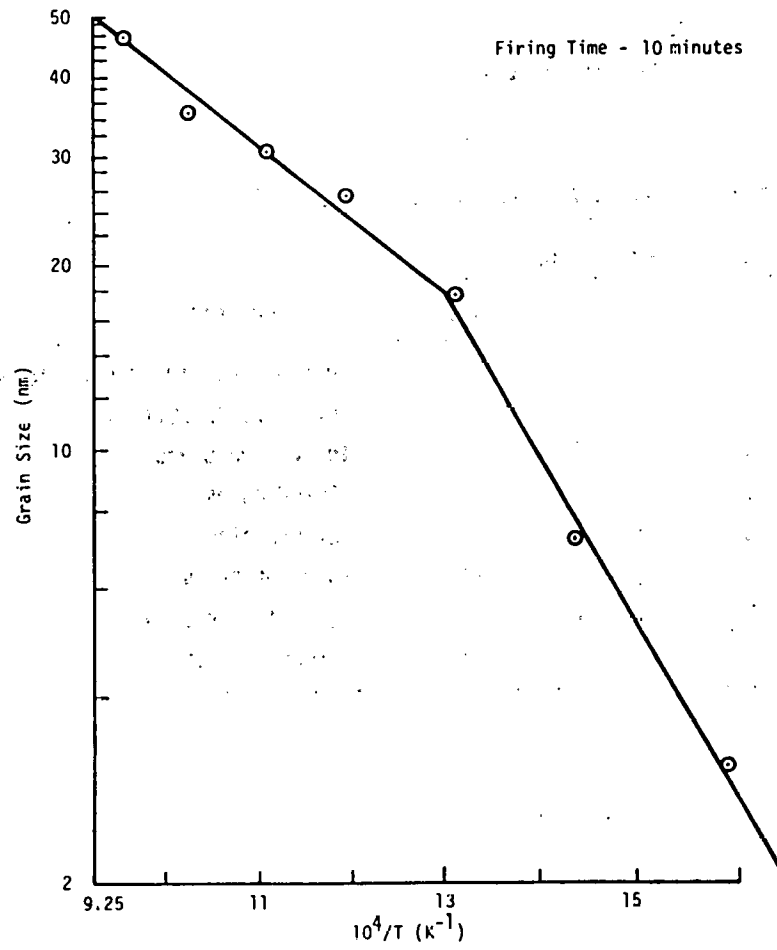
Film Thickness

## Page 13. Platinum TF Conductors

### Requirements

1. No metal other than platinum
2. Single print
3. Highest possible density
4. Highest possible uniformity
5. Fire at  $850^{\circ}\text{C}$  ( $0.55 T_m$ ) on alumina

Page 14. Variation of Grain Sizes With Firing Temperature of Platinum Resinate



## Page 15. Platinum Powders

$d_1$  - 30  $\mu\text{m}$

$d_2$  - 1  $\mu\text{m}$

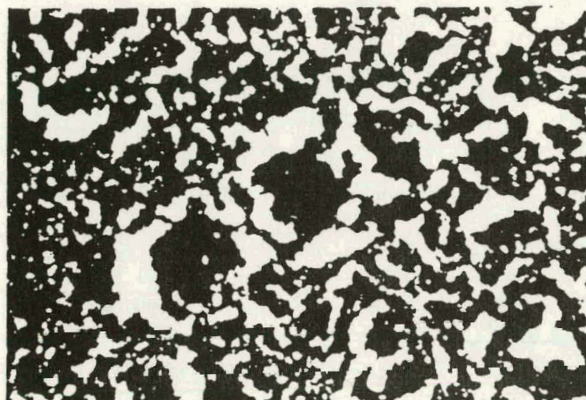
$d_3$  - 0.02  $\mu\text{m}$  (from resinate)

Experimental Platinum Conductors Fired at 850°C.

% Different Sizes			
$d_1$	$d_2$	$d_3$	Remarks
	100		very porous, large open areas
100			very porous, uniform
50	50		large open areas
80	20		closed pores
90	10		low porosity
64	26	10	lower porosity
87	9	4	very low porosity
88	10	2	lowest porosity



Page 16. Experimental Platinum Conductors  
in Transmitted Light (190X)



100%  $d_2$



88%  $d_1$  - 10%  $d_2$  - 2%  $d_3$

## Page 17. Silver TF Conductors

### Requirements

1. Lowest possible cost (highest possible specific conductance)
2. Single print
3. Very uniform films
4. Fire at 625°C (0.73  $T_m$ ) on POS

## Page 18. Specific Conductance Ratio (SCR)

specific conductance -  $SC = \frac{G}{W}$

G = conductance of film

W = weight of film

$$SC = \frac{1}{RW} = \frac{1}{\rho d l^2}$$

$\rho$  = film resistivity

d = film density

l = film length

$$(SCR)_{i,j} = \frac{(SC)_i}{(SC)_j} = \frac{\rho_j d_j}{\rho_i d_i} \quad \text{independent of film geometry}$$

## Page 19. Silver Inks

### Inorganic Constituents

1. 95 w/o silver of various particle sizes or mixtures of different particle sizes
2. 5 w/o glass of composition 72 w/o PbO - 14 w/o B<sub>2</sub>O<sub>3</sub> - 14 w/o SiO<sub>2</sub> sieved to -170 mesh

### Screening Agent

1. 3 w/o ethel cellulose (N-300)
2. 97 w/o  $\alpha$ -terpineol

## Page 20. Composition and Specific Conductance of Silver Films

Ink No.	% of Ag Particle Sizes ( $\mu\text{m}$ )						SC (S/mg)
	.65	2	5	7	11.5	17	
1	2	28		70			3.67
2	2	28				70	1.43
3	2		28		70		1.48
4	100						2.45
5			100				2.13
6						100	0

Page 21. Particle Size Ratios and Specific Conductance Ratios of Silver Films

Ink No.	Size Ratios		(SCR) <sub>1</sub> , Ink no.
	$d_2/d_1$	$d_3/d_2$	
1	.29	.33	1
2	.12	.33	2.57
3	.43	.13	2.54

Page 22. Summary

1. The distribution of metal particle sizes and the absolute sizes affect fired film density.
2. The proper distribution of metal particle sizes gives a higher density film than single sized particles.
3. The theoretical models can serve as guides to selecting the proper distribution of metal particle sizes.
4. Experimental studies are still required.

## DISCUSSION

WONG: I think probably in the real world you make a very fine particle and use coarse particles in your mix, and the very fine particles try to stick together and agglomerate by electrostatic forces, or align, so that is why you never have a mix completely as what you assume in the model.

VEST: That certainly is true. In the platinum case, the second size I said were 1 micron. Well, the 1-micron were the agglomerate size. This was a platinum black, and the ultimate particle size was a few hundred Angstroms. Just because of what you were mentioning: there was agglomeration, and the agglomerate sizes were just about 1 micron. We got this from SEM studies. Yes, that certainly is true.

WONG: In your model you are mixing two sizes, and this small particle size is supposed to fit in the hole. What if you just assumed that there is no mass transport -- no sintering mass transport occurring -- however, if you, from a sintering viewpoint, just use a fine particle size, just a single particle size, would that be better from a sintering viewpoint, from thermodynamics?

VEST: If you can get a high enough compaction to start with and you can go to the proper temperatures, a single-size, a small-enough-sized particle can give you very high densities of sintered mass, but if you have some constraints on your processing, then you can do better with a gradation of sizes. The presence of smaller spheres in the interstices of the bigger ones will enhance the sintering of the bigger ones, because as the smaller ones begin sintering they are also in contact with the big ones and they will attach themselves. So, as they begin to shrink, they give a compressive force to the bigger spheres and make them sinter more rapidly. So you get enhanced sintering of the larger size due to the presence of the smaller size.

WONG: Again you have to assume that the small sizes go into the interstitial sites of the bigger ones.

VEST: That is right. Again, if you are making a large body, using a single size, small size particle has many advantages, but for our conductors we don't want them to change dimensions very much during firing. We want to keep our good line definition, so it is nice to have these big ones there, big particles that are forming the matrix, and then this isn't going to change much. But then if we can fill up the holes in this with smaller ones, enhance the sintering of the bigger ones, then we get closer to what we want.

AMICK: Could you comment on why the 17-micron particles don't work better than the 7 in that silver-ink composition?

VEST: It is because they are too big. The 17 by itself did not sinter; the mix did, and we get a number.

AMICK: You have a bigger ratio difference with the 17 than you did with the 7?

VEST: That is right. You have a bigger ratio difference but you are still not getting as much sintering of the big ones, which constitute the bulk of the silver, with the 17s as you are with the 7s. In other words, these results, I think, are indicative of the fact that you still have very poor sintering of the large particles, so that you have a lot of constriction resistance. You have very small sintered necks between the big particles and so you are getting constriction resistance that is limiting the conductance. The presence of the small particles did exert a force, an influence, in getting sintering but still not as much as you get starting with a 7-micron largest size.

AMICK: Do you alter the ratio to binder for those two different materials? Is there binder in these systems?

VEST: Oh, yes. Well, there was when it was printed. There was a screening agent used for printing.

AMICK: Is there glass also?

VEST: Oh, yes. And it is the same in all of these.

AMICK: The same ratio?

VEST: Yes. The same ratio of metal to binder.

GALLAGHER: In the real world, in some of these soft metals like silver, how close are they to being spherical?

VEST: These particles are very spherical. They are prepared that way; the ones that I used. You can get spheres, you can get flake, you can get all kinds of things.

GALLAGHER: My second question involves flake. I think I have seen somewhere where spherical powders have been mixed with flake. What is the rationale behind that?

VEST: You have these flat plates lying here, and you have little ball bearing between them; you get good contact. That is the rationale I have heard used for the adding the mixture of flake and powder to simply a polymeric binder where you are not firing, really. You get higher pressure contacts when you have the little spheres contacting the flake, so you will get continuity. You will break through the stearate coating that had been on the silvers.

GALLAGHER: Would you care to comment on that stearate coating?

VEST: Well, it is there. It is not a good electrical conductor. Somehow you have to overcome this in order to get good conduction.

GALLAGHER: Do you do it thermally, or is it a trick of the trade? Any reason people don't talk about it?

VEST: I don't know. There are some people here that could probably comment on that but I am not one of them.

STEIN: I think it is a trick of the trade.

GALLAGHER: And here I thought only the plating people had problems and didn't want to talk about it.

LANDEL: Regarding the question that was asked a moment ago about the 17- and 7-micron particles. Does the smaller particle in fact give you a lower sintering temperature? Is it small enough to get particle size effects?

VEST: Well, of course.

LANDEL: The difference between 17 and 7. Does that lower the sintering temperature? If you just take that individual particle size and you work with 17 and you work with 7 --

VEST: I would end up with a larger ratio of sintered neck diameter to particle diameter for the 7 than for the 17 at the 6-25-10 minutes. That was the boundary condition on our process.

LANDEL: Then that is the answer there. The smaller particle size, in fact, is easier to sinter. It has a higher surface energy and therefore it is easier to sinter. Sinters at a lower temperature.

COMMENT: That is really quite a different model from the one that was proposed.

LANDEL: Well, yes. That is an added effect. It would have to be run in.

VEST: Certainly. You see, with the 17s by themselves, there was not sufficient sintering at these conditions to even form a continuous network. Whereas with a 7, there was. Just looking at those results for monosized powders you can tell we have a definite difference in sintering with these different sizes at that temperature.

LANDEL: Do you measure the packing density of the dry powders, and if so, can you use that in your evaluation?

VEST: I would love to. I don't know how. I have looked at the density of the packed powder before sintering. If you very carefully dry, so as to remove all the organics without getting any sintering -- and you can do this, if you are very careful, and then, of course, you have to be very careful in handling because the stuff would fall off the substrate -- but I don't know of a way of measuring the density of that powder compact. You know it has to be somewhat more dense than simple cubic. It is somewhere between there and body-sintered cubic.

LANDEL: For the spheres it would be, ideally, 0.63.

VEST: Yes, if it was closest packed.

LANDEL: Random packing.

VEST: OK, for random packing.

LANDEL: Then someone said that if you get the small particle sizes then the agglomeration drives that up again, or drives that down in terms of packing density, to something like 80.4. You have to trade off those factors.

VEST: Yes. Again we measure things such as dried-film density or dried-film thickness, but that is not something that you can really measure very accurately. You can measure the fired-film thickness quite well. The dried-film thickness doesn't have a smooth surface. You have particles there, so you can use a light section microscope and you try to sit on top of one, but there is a lot of uncertainty in the measurement. Certainly, within what we have measured, it comes down to this loose, random packing. But there is quite a bit of scatter.

STEIN: A further comment on Brian's (Gallagher) question, which really deserves a bit more of an answer. That is, when you try to sinter particles that are coated with stearates or other things, they are not going to sinter very well -- particularly in the instance of people in this room who are firing very quickly for very short times at temperatures in the order of 700°C. Some of the organics can remain at temperatures higher than that, or else need a longer time than a minute or two to be gotten rid of. As long as they are present they will interfere with sintering. In the case of mixed spherical and platelike or flakelike particles, you have some relatively clean particles, you have some relatively dirty particles and you have all kinds of surface things; therefore, you get a combination of decomposition products coming off, sintering occurring simultaneously, and never, never do you have a completely organic burned-out system if you are firing for 30 seconds or one minute or so at 700°C or 720°C, or some such short time at a relatively low temperature. This is particularly different from the thick-film hybrid microelectronics case where they are firing up at 850°C or more, and you have ample time to burn out. Infrared firing is an example that makes this problem very difficult and should you get sintering of the silver, before reaching full burnout conditions, you are going to blow blisters and bubbles.

GALLAGHER: Has anyone ever put a mass spectro on the end of the furnace to see some other decomposition products? Just a general question to anybody.

STEIN: There are all sorts of hydrocarbon fragments. It has not been done at the end of a furnace, but it has been done. You get CO, CO<sub>2</sub>, free-radical type fragments in the methyl and ethyl groups, and all sorts of things coming off. It is a wild mixture. It depends very much on the access of air. How much air you have available.

CALLAGHER: Does that mean that with some of these inks we have to force air into the furnace rather than just have a free air flow?

STEIN: Absolutely.

VEST: The air flow is one of the principal variables in the processing.



SOMBERG: I would like to ask a question of Sid (Stein). You mentioned that some of the organics are still remaining with the spike firing. If I am going through a burnout phase, am I not getting burn out between 300°C and 550°C? I am referring to spike firing at 700°, but I am still going through burnout between 400° and 500°C. Why am I not getting rid of the organics at that point?

STEIN: Because the organics that are closest to the silver surface, in case of the silver, or to any metallic particle surface, are remarkably stable. At least you don't fully get rid of them. That monomolecular layer of materials stays there, well beyond the normal decomposition ranges that one expects.

COMMENT: It is even difficult to remove all the water from the surfaces on the silicon.

LANDEL: Plus, if it is stearic acid you are trying to remove, you are trying to decompose not with an organic but with a metal organic, so you are trying to decompose a salt.

# PARTICLE SIZE EFFECTS ON VISCOSITY OF SILVER PASTES --- A MANUFACTURER'S VIEW

JASON PROVANCE, General Manager and KEVIN ALLISON, Materials Engineer

Thick Film Systems, Division of Ferro Corporation

324 Palm Avenue, Santa Barbara, CA 93101

## I. INTRODUCTION

The electrical performance of single crystal silicon in photovoltaics with thick film silver forming the top metallization grid is well documented. Silver, the major component, however, is often taken for granted. There are several dozen types of silver powders commercially available for use in thick film silver paste (ink) systems. The basic properties of these powders are reasonably well documented. A study was made to characterize some of these powders in actual applications and correlate this information with the viscosity and rheological properties of pastes under shear.

## II. EXPERIMENTAL

A. Materials: Seven commercially available silver powders, representing a cross section of particle sizes and shapes, were selected for investigation in experimental thick film conductor pastes. A glass used in commercial silver paste compositions was also prepared in three powder sizes for study in experimental glass pastes. Pastes were prepared by combining these silver and glass powders with an identical organic screening vehicle and homogenized on a standard three-roll mill. Organic vehicles with varying properties to adjust paste rheology were from the same family of compositions. Solids content was held constant at 80% for each of the silver and glass pastes.

Silver pastes were screen printed by standard methods, subjected to infrared drying at 125°C and fired in a belt furnace at 850°C. This temperature, higher than normally used in actual cell production, was selected to dramatize particle effects on sintered films.

B. Particle Size Analyses: Particle analyses to determine particle sizes, distribution of particles and volume populations were performed with a Coulter Counter, Model TA II. A 50µm aperture, capable of accurate particle measurement from 0.8 to 20µm, was selected as optimum for the cross section of sizes investigated. Tap density data were supplied by the manufacturers of the silver powders.

C. Scanning Electron Micrographs: Micrographs were prepared at 2000X with an AMR, Model No. 1000A Scanning Electron Microscope. For consolidating comparisons, magnifications were reduced, as shown in the figures.

D. Viscosity-Rheology Tests: Viscosity measurements were made with a Wells-Brookfield Micro Viscometer (cone-plate), Model HBT, with a 1.565°C cone. Test temperature was maintained at 25±0.2°C. Rheological properties were computed from viscosity data taken at shear rates from 1.92 to 19.20

reciprocal seconds with a Hewlett Packard Model 9825T Computer which plotted the curves with a H.P. Model 7225A Plotter.

### III. RESULTS AND DISCUSSION

Particle size, particle shape and volume populations have a strong influence on the rheology, and thus the screen printing characteristics of silver pastes. A change in surface area from a change in particle size, shape or population can cause problems in the way the paste prints and contacts the silicon surface. Incomplete line traces or pin holes can occur from pastes which do not allow a full-even print. A paste with a high viscosity is often thought to be the problem source; more likely, a steep slope of viscosity versus shear rate is at fault. That is, viscosity is not responding to shear forces during screen printing. Conversely, a paste with a low viscosity may produce poor grid line quality (line width and definition), not because of absolute viscosity, but because of a flat or shallow slope. This type of paste does not freeze, or set up, quickly enough after deposit onto the silicon.

A. Particle Considerations: Figures 1, 8 and 9 show a variety of silver powders with different sizes and shapes, including finely divided sponge (B), flake (A, C and E), spherical (F), random shapes (D) and random particles with some flake (G). A comparison of particle size distribution curves, weight percent versus equivalent spherical diameter, are shown in Figures 2 and 3 for some of these powders. Volume populations are shown in Figures 4 and 5. The average particle size is important, but differential volume along with particle shape and agglomeration tendencies (revealed in the SEMs) is essential information in selecting the screening vehicle and making rheological adjustments to the paste.

The particle size and differential volume of glass powder, a minor but very important component in silver metallization for application on silicon cells, can be changed by varying the processing time for particle reduction. This is illustrated in Figures 6 and 7. A change in glass particle size will influence adhesion as well as paste rheology. Interestingly, glass particles of optimum size had nearly an ideal, bell shaped population.

B. Particle Effects in Pastes: Silver particles were also characterized from pastes in dried screen prints and sintered (fired) films as shown in Figure 8 for one silver type. Powder clusters, or agglomerates, tended to separate during milling of the paste, revealing truer spherical particle shapes in the dried prints. The spheres tended to retain their shapes in sintered films. Variations in powder lots for the same type of silver are not uncommon. Figure 9 reveals the effects of inadvertent particle size change for silver flake. The acceptable lot (left side) had smaller and fewer large flakes than the unacceptable lot (right side). This is verified by the volume populations in Figure 4. While paste processing tended to fracture and compact flakes from the acceptable lot, the larger and probably thicker flakes in the unacceptable lot retained these characteristics in the dried and sintered films.

C. Paste Viscosity and Slope: The viscosity of a liquid is influenced by a number of extraneous factors, not the least of which is shear force. The response of a thick film paste to shear was shown to have far greater meaning than nominal viscosity. A nominal viscosity can be virtually meaningless if the

slope, or rate of change in viscosity with change in shear rate, is not acceptable. This is illustrated for silver pastes made with Lots C, E and F powders (Figures 10 and 11). The viscosity at a shear rate of  $9.6 \text{ seconds}^{-1}$  for these pastes is nearly the same at 550-600 poise. The viscosity slopes, however, differ from -0.450 to -0.770. Only the slope from paste made with Lot C powders meets a preferred specification from about -0.550 to -0.650. Of the seven silver powder types investigated, pastes from two lots, A and C, met slope specifications. A paste with a slope below this range tended to give poor line definition, lacking recovery capabilities to prevent slumping and moving as it was deposited onto the substrate during screen printing. A paste with a slope above this range tended to lack the necessary flow characteristic to give a full, even print. This condition caused the paste to skip or pin hole during printing. It was theorized that intimate contact of silver particles with the textured surface of crystalline silicon could be inhibited during printing if improper paste flow occurred. Mesh marks were also a product of paste with a steep slope.

D. Paste Adjustment: A lower viscosity at a given shear rate may be achieved by a paste user by adding thinner. This will lower the solids percent, reduce silver content and can lead to electrical and soldering difficulties. While a lower apparent viscosity may be achieved with thinner, a steep slope with attendant printing problems can still persist. Large thinner additions can lower the viscosity slope but cause printed lines to sag or spread. Figure 12 illustrates the adjustment of a paste with an abnormal-high slope (-0.863) by blending in 50% of a paste which contained the same silver powders (Type B) and identical solids; i.e., 80%. This adjusted paste had a slope of -0.548. An "ideal" slope (-0.641) was achieved with the blend of pastes while maintaining the desired inorganic solids content. The viscosity of all three pastes at a shear rate of  $9.6 \text{ sec.}^{-1}$ , the shear rate used when quoting viscosity to the user, was nearly identical at 1000 poise. It was demonstrated from this phase of the study that any number of alterations to the slope could be made to achieve optimum printing performance. Only the organic vehicle was changed to accommodate the characteristics of the silver particles.

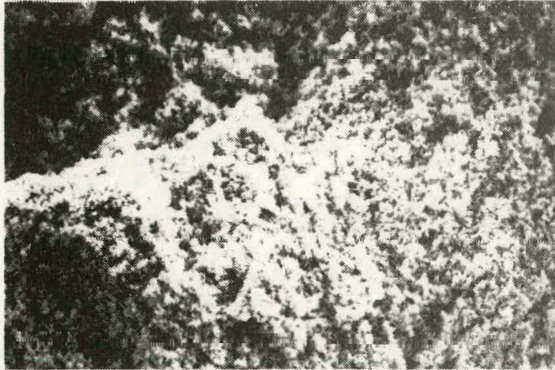
E. Tap Density: A correlation of powder tap density with the slope of viscosity for silver pastes is shown in Figure 13. As tap density increases the slope of viscosity decreases. There was no apparent correlation between tap density and viscosity measured at a single shear rate.

## VI. SUMMARY AND CONCLUSIONS

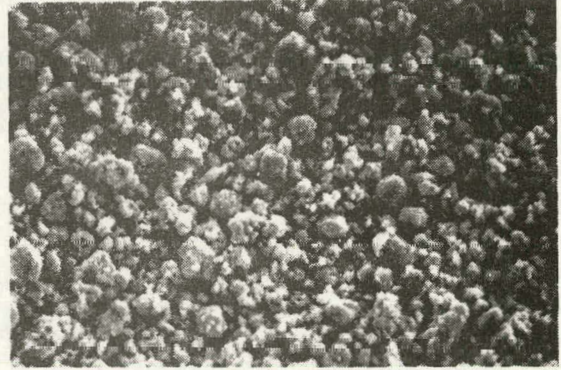
Particles from a variety of silver powders were investigated by scanning electron microscopy and particle size analyses. Particle size distribution curves and volume population graphs were prepared for these silver powders and for glass powders with optimum, extra fine and coarse particle sizes. The viscosity at a given shear rate and slope of viscosity over a range of shear rates were determined for thick film pastes made with these powders. Because of particle anomalies and variations, the need for flexibility to achieve the best printing qualities for silver pastes was evident. It was established that print quality, dried and fired film density and optimum contact of silver particles with silicon, important for cell electrical output, could be achieved by adjusting the slope of viscosity that fell outside of the range, -0.550 to -0.650. This was accomplished through organic vehicle technology that permitted a change in the slope of viscosity, up or down, while maintaining a constant silver and total solids content.



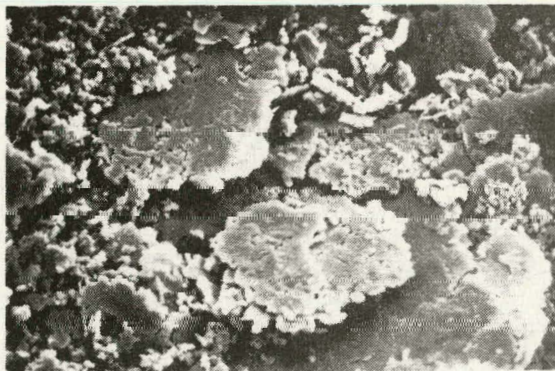
Figure 1. Various Powders Used in Silver Pastes



Type B



Type D



Type C



Type E



Type G

10 $\mu$ m



Figure 2. Particle-Size Distribution Curves:  
Silver Powders

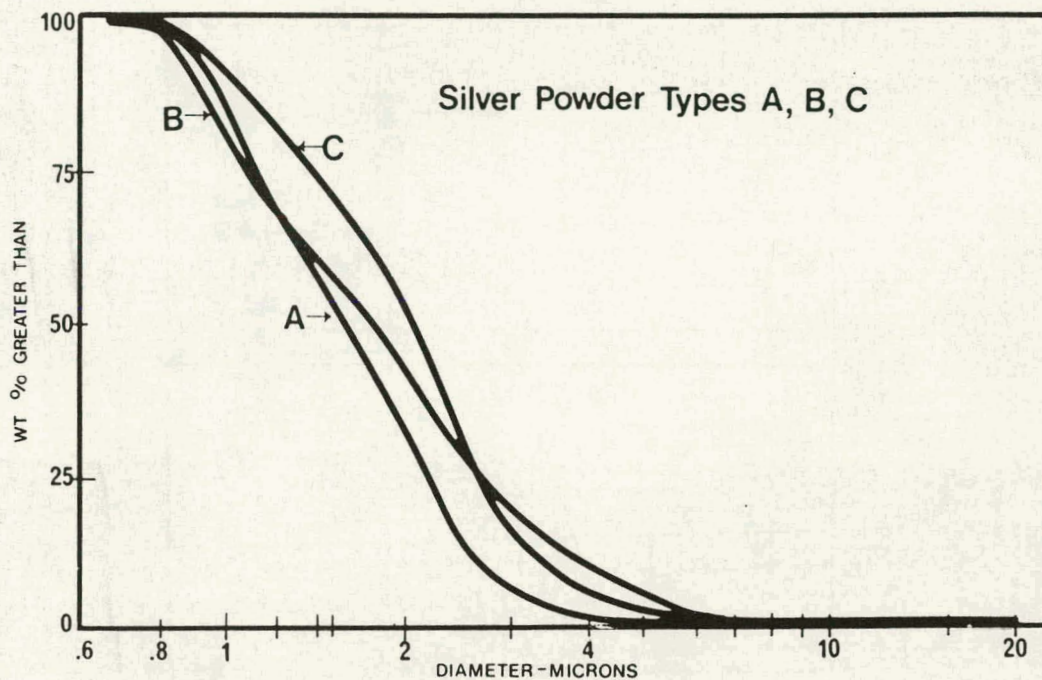


Figure 3. Particle-Size Distribution Curves:  
Silver Powders (Cont'd)

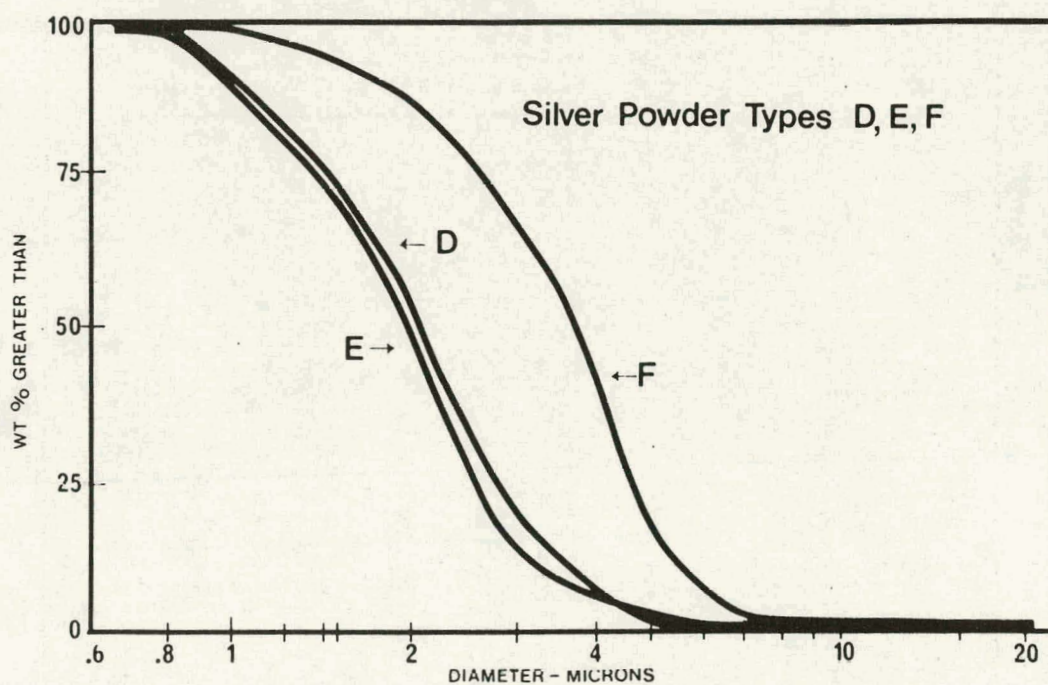


Figure 4. Particle Size of Silver Powders:  
Differential Volume

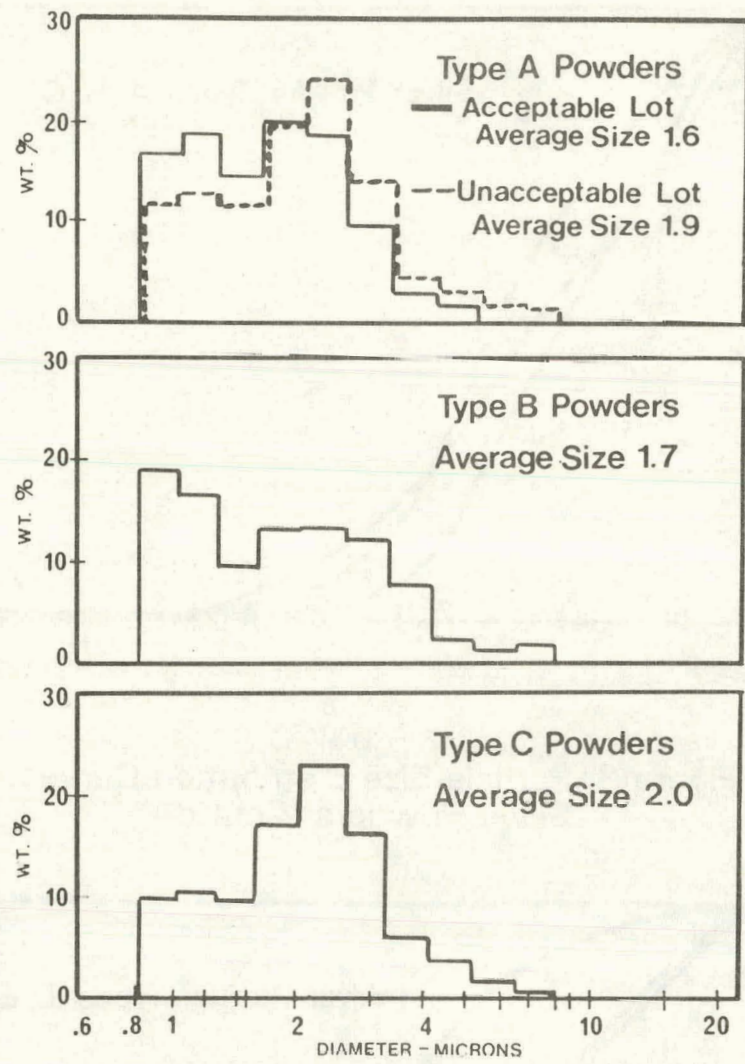




Figure 5. Particle Size of Silver Powders:  
Differential Volume (Cont'd)

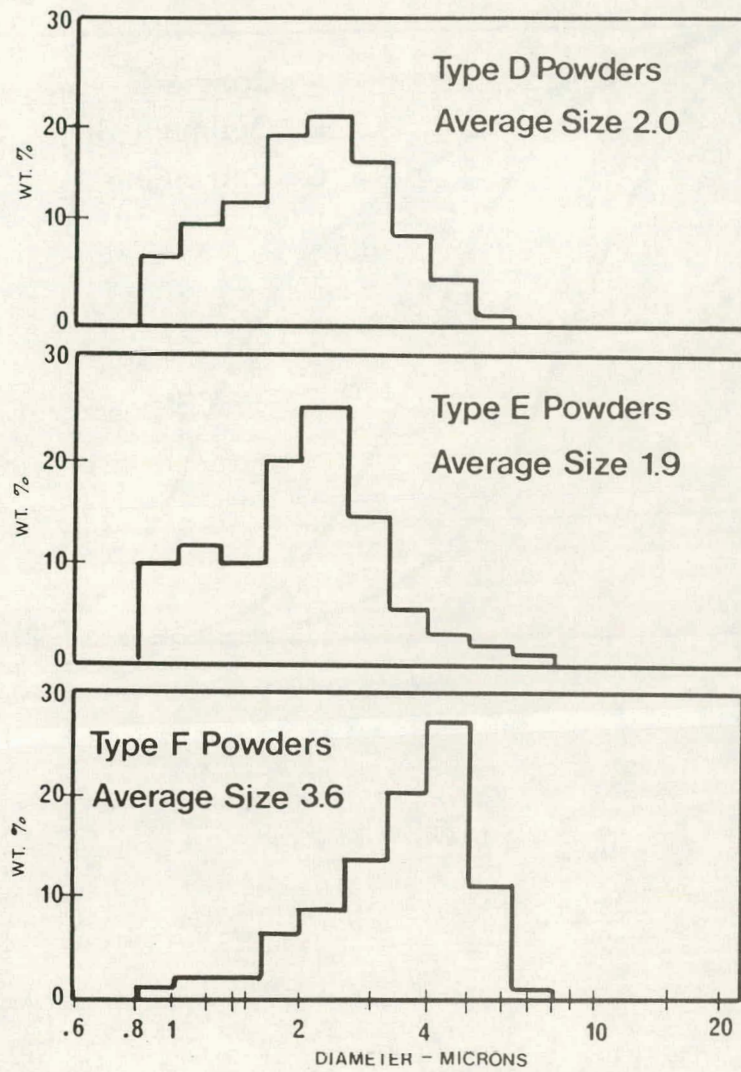




Figure 6. Particle Size Distribution Curves:  
Glass Powders

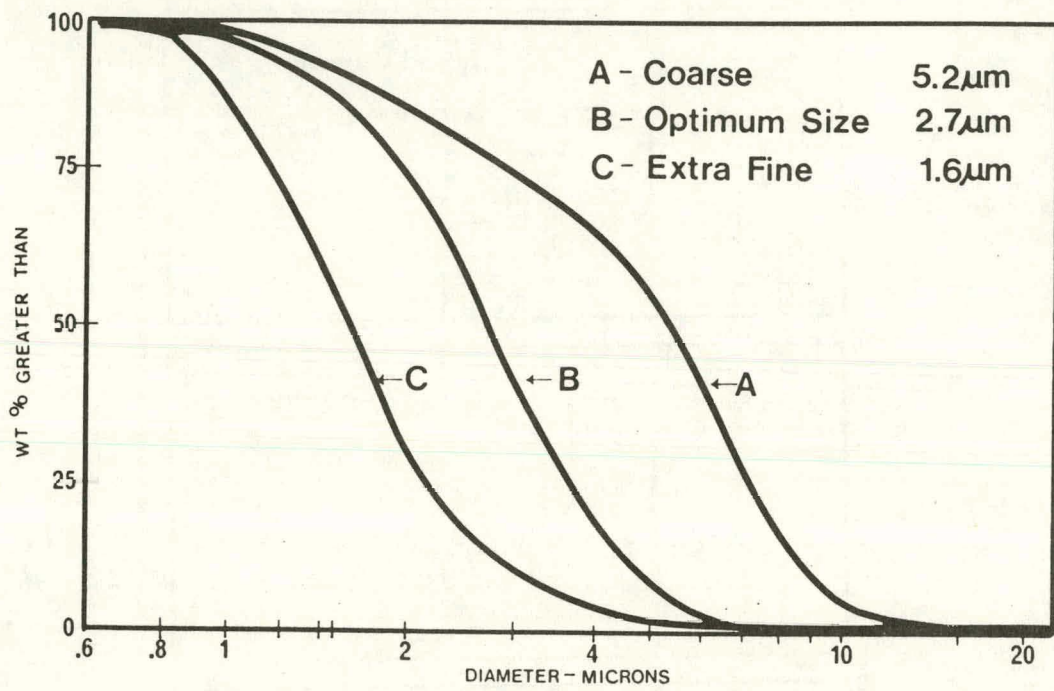


Figure 7. Particle Size of Glass Powders:  
Differential Volume

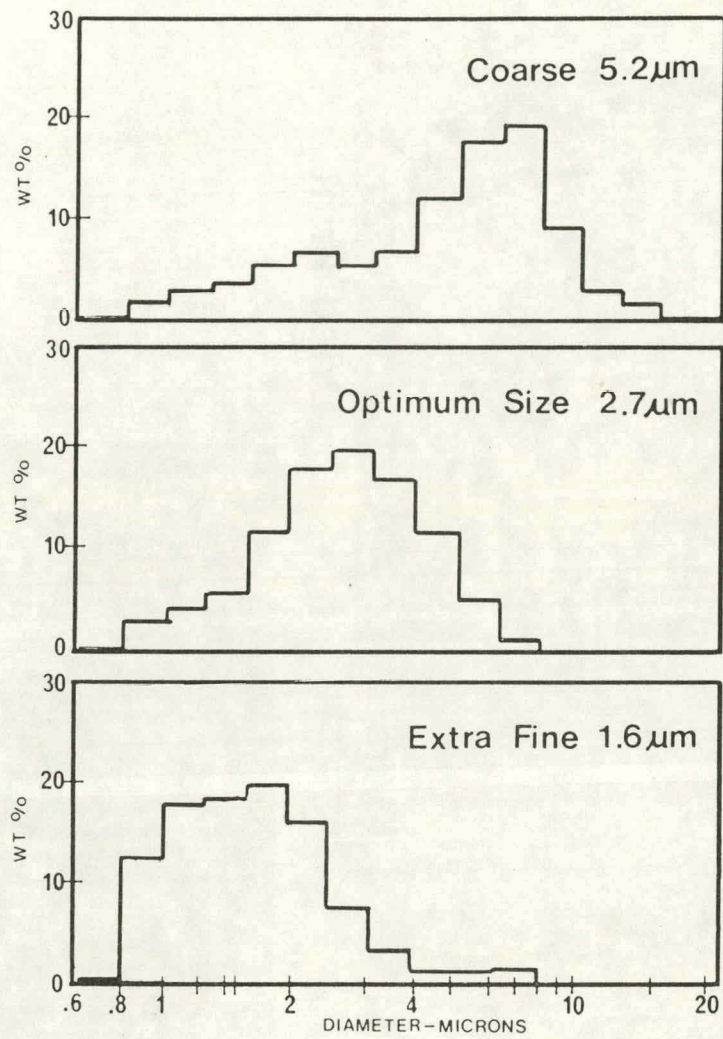
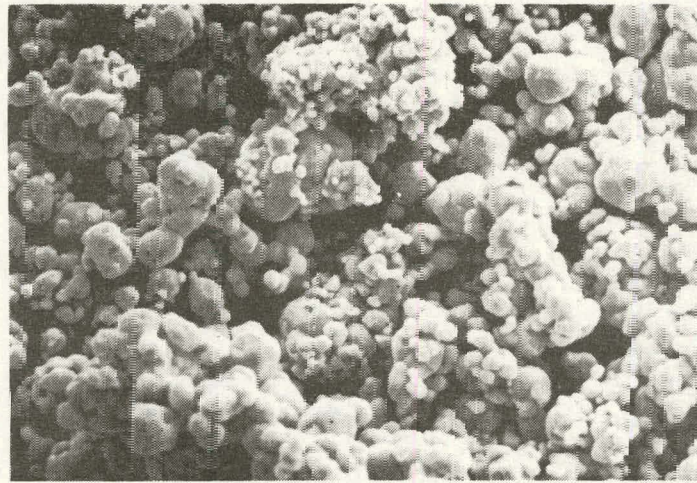


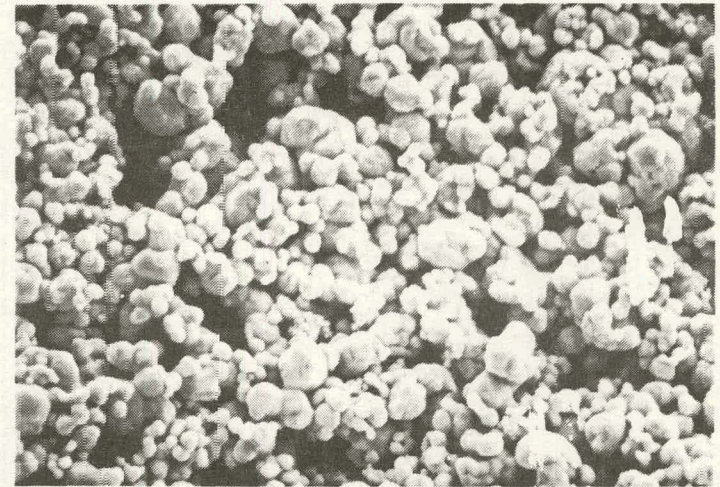


Figure 3. Comparison of Spherical Silver Type F Powder, Dried Print and Sintered Film

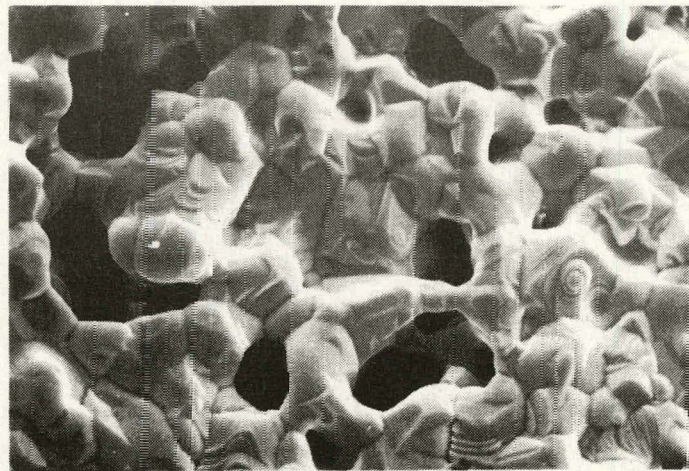


**Powder**

10 $\mu$ m



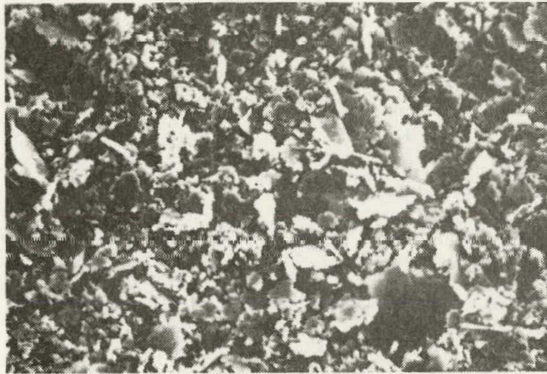
**Dried Print**



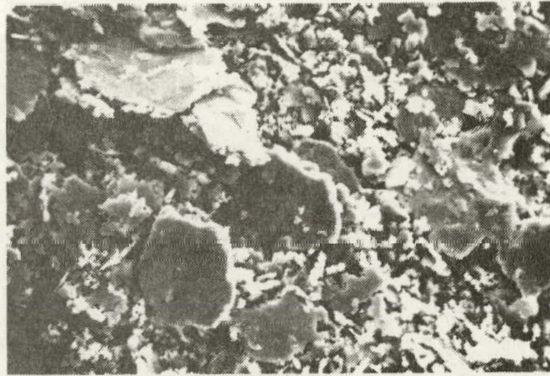
**Sintered Film**



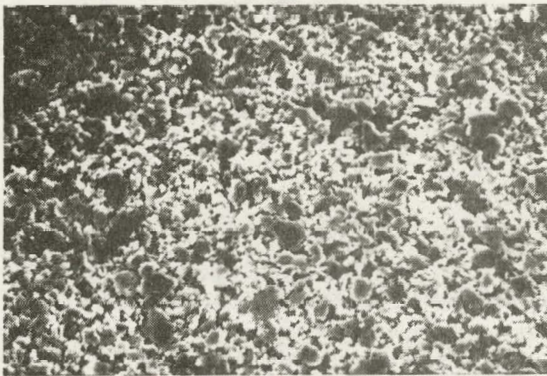
Figure 9. Comparison of Type A Silver Powders,  
Dried Prints and Sintered Films



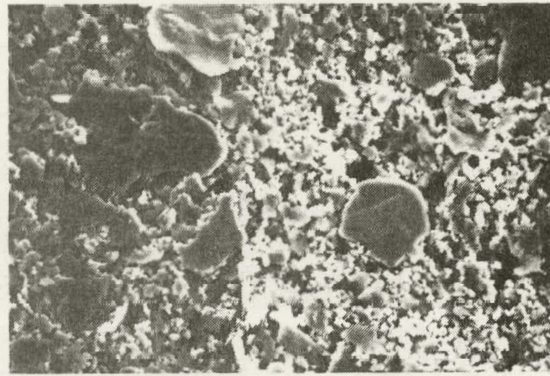
**Powder**



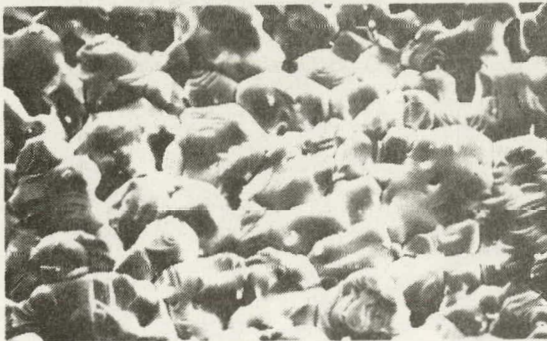
**Powder**



**Dried Print**



**Dried Print**



**Sintered Film**



**Sintered Film**

10 $\mu$ m



Figure 10. Viscosity: Silver Pastes

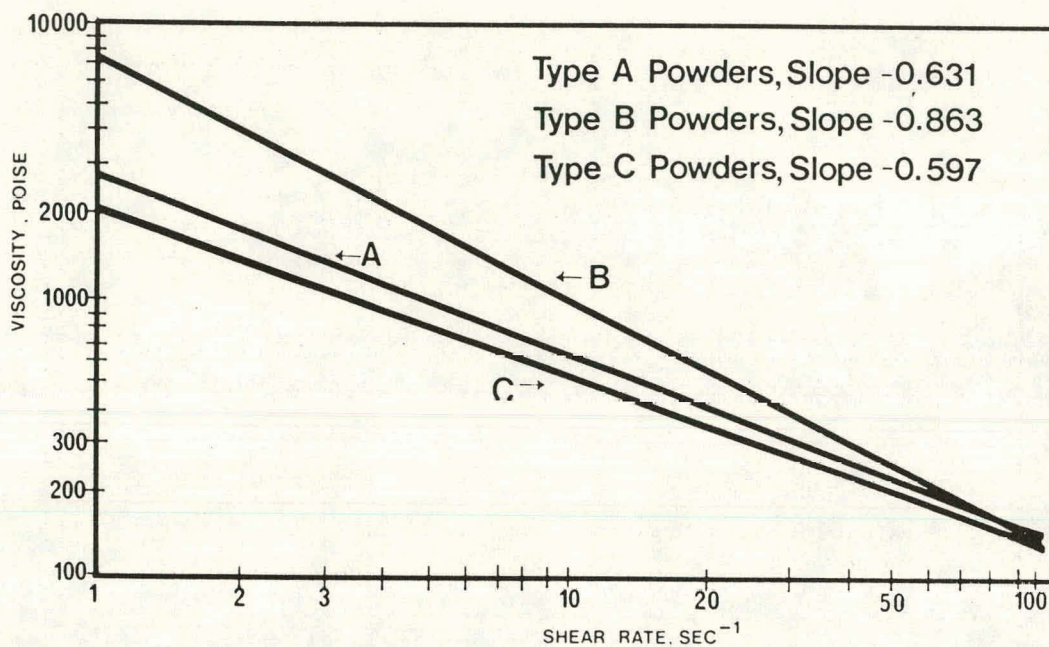


Figure 11. Viscosity: Silver Pastes (Cont'd)

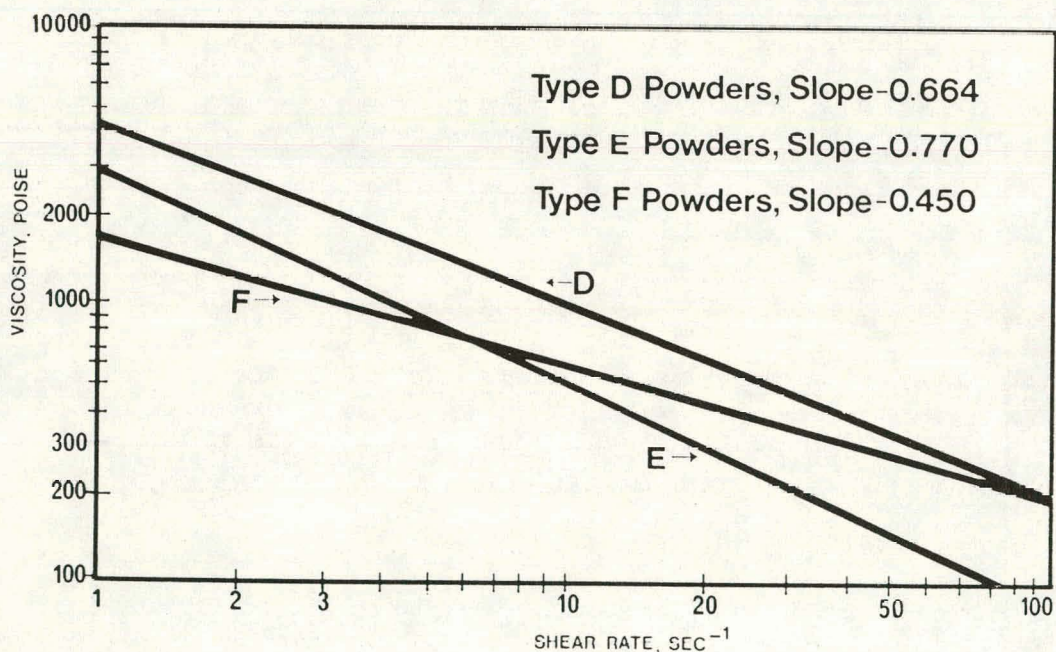


Figure 12. Adjustment of Viscosity Slope for Abnormal Silver Paste

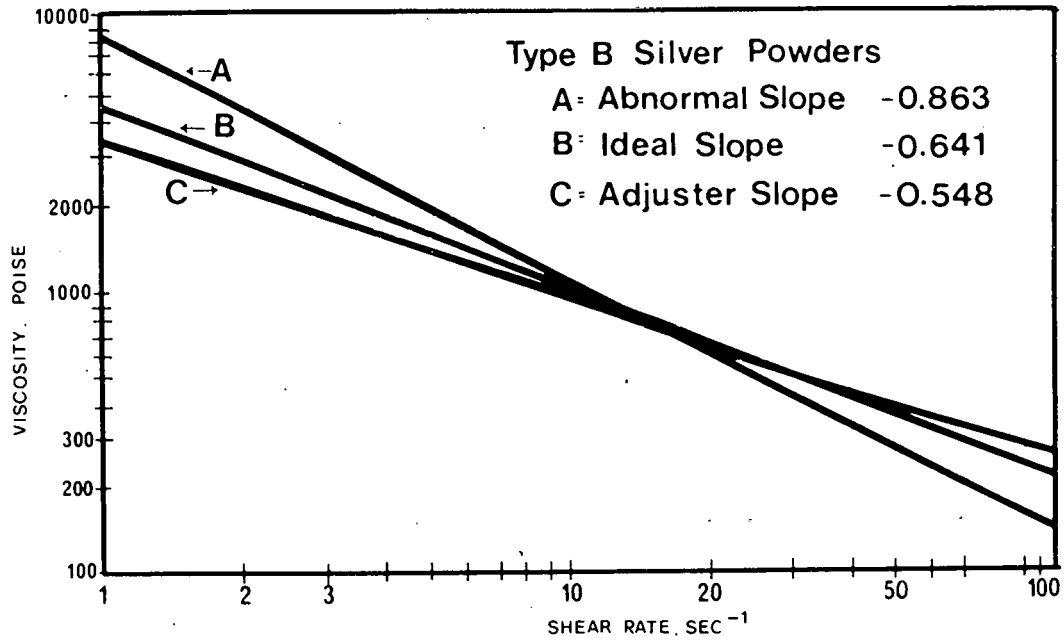
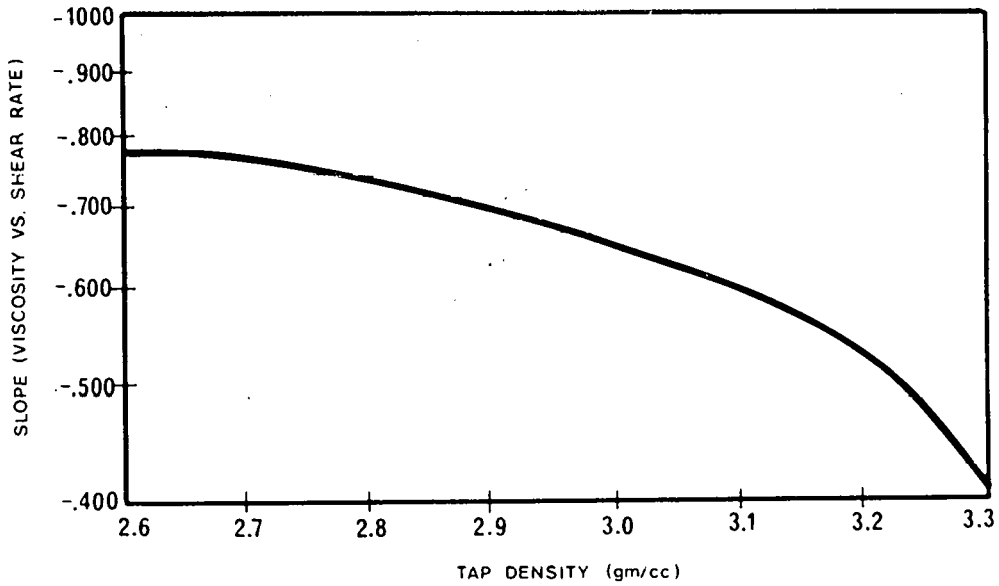


Figure 13. Relationship of Silver Powder Tap Density With Paste Viscosity Slope



## DISCUSSION

SCHRODER: When I think of a metal semiconductor contact, I think of a physical contact, even though the electrical contact may only be an electrical or a physical contact. But the physical contact I think of at least is uniform. Now you showed SEM pictures; if you imagined looking at the interface now of that paste and the silicon, what fraction do you think of a given area is physical contact, never mind electrical contact? Would you kind of guess at that? I know you can't look at it.

PROVANCE: Well, it is strictly one where you have to theorize a bit. You can see what is happening on the top and you sort of flip-flop it over and say is this happening on the bottom, and you have to assume that yes, to some extent, it is. If on top you see a lot of irregular-shaped mountains, peaks, and valleys, then you have to assume that the same thing, to perhaps a lesser extent, is happening on the bottom. The degree of physical contact, I wouldn't want to hazard a guess, I'm not really sure, but in theory the more compact the particles are and the more these particles are separated, and deagglomerated, the greater the contact would be.

GALLAGHER: If I may add to that: in the silver system, you can etch the silver away and you end up with the glass. You can look at that, and we have done it on a Spectrolab contract. One thing you are really not sure of, however, is that glass touching the surface, but you can end up with the footprint of the glass.

QUESTION: What did you see?

GALLAGHER: Depending upon the composition of the structure, and the amount of glass that is added to it, you can see great differences in -- I have two gentlemen here who saw the same SEM pictures that I did. They were taken by Ferro, by the way, and I would guess over 30% to 40% of the area at the most was glass, the rest metal.

QUESTION: Was it physically contacted?

GALLAGHER: It was physically contacted.

QUESTION: And then the electrical maybe even less?

GALLAGHER: I have no idea. We at that particular time formulated some structures that had 5%, 10% and 15% of the total weight as glass.

PROVANCE: The glass plays two roles, or at least two roles. One, of course, is to achieve the adhesion, and the second thing, which is often overlooked, is that glass really is an aid to sintering, within a certain amount of glass. In other words, too much or not enough and you can have problems. There is the thing of optimizing just the right amount of glass and the right formulation of glass for that particular task.

HOGAN: We have done pretty much the same kind of thing, looking at the series resistance associated with glass content, metal content and other things, using the same technique or perhaps the same technique, which is a mercury amalgamation where you can remove that silver. We have discovered, not quite that high, more in the range of 20% to 30%, areas that are not glass-covered between the contacts. That does not mean that the silver is even physically, much less electrically, in contact with that area. It is really hard to say what the electrical coverage is. The interesting thing is, we did some HF etching in experimental work and found that improvements were entirely associated with the etch, so that although there is a dendritic nature to the structure, the majority of the improvement was due to an etching along the edges of the contact -- thereby, we assumed, increasing the silver contact there, the electrical contact. It brings up a point I wanted to make: I think a very important study has to be made with this interfacial area between silicon and the thick-film inks. Contrary to many microelectronics applications, where you are putting it on an aluminum substrate, you are not concerned very much about what the electrical properties are between the substrate and the metal, but here we are very concerned about those kinds of things. The question I had, though, was what percentage of the manufacturers do you feel are doctoring the inks, you know, when you were talking about communications? Is that a problem for manufacturers of the ink products?

PROVANCE: Do you mean which ones do and which ones don't?

HOGAN: Yes.

PROVANCE: I don't know which ones will admit it but I will tell you right now that there is no one in business today making thick-film formulations that don't have some way of making these materials behave. The lesser of the two evils is, don't change the inorganic composition, change the organic part, the part that burns out, and make these materials behave, particularly that slope. Anyone that is not doing that would have an awful problem out in the field because, as I say, these powders are somewhat like fingerprints. No two sets are identical. You can make them pretty close, but you are going to have variations from time to time, and I don't think there is any way of determining if they were absolutely identical. The same number of particles, the same shape, same size, same volume population, you wouldn't know it. In other words, there is no way of defining that precisely, whether you have the exact same number of particles at a given size. So I would say that everyone has his methods of making these materials behave out in the field.

GALLAGHER: How did you designate these powders as A, B, C and D?

PROVANCE: Those are internal designations that we use.

GALLAGHER: But what did you use as your criteria for saying this is powder A, B or C? Are they all made the same way and they came out --

PROVANCE: It was sort of which one came through the door first. That was A and B. There was no rhyme or reason, we simply gave them a letter designation for purposes of identifying them.



GALLAGHER: But they were supposedly made the same way and they were supposed to have the same characteristics?

PROVANCE: Yes, of a given type. The letter number designated the different type --

GALLAGHER: I meant E was supposedly made the same as B, supposedly made the same as C -- they were all spheres?

PROVANCE: Oh, no. A, B, C, D, E, F and G were all different types of powders but we showed one example, supposedly the same type of material from two different lots, and found that indeed they weren't the same. We find that with whatever letter it was or whatever type of silver, the materials do change from lot to lot. Sometimes dramatically, sometimes a little bit but always enough to change, if not absolute viscosity at one shear rate, the slope of viscosity. And that is what we put the emphasis on in trying to adjust that slope back so that the materials will handle the same on a screen printer.

R. VEST: The question was asked a little earlier about how much metal is in contact. That's really not a good question, because it depends on the processing. If you have a printed conductor such as we are talking about here, the amount of glass that is in contact with the substrate as opposed to how high a temperature and how long you fire it -- in general, if you fire high enough and long enough, you will end up with a continuous glass film under the conductor, so you have no metal contact with the substrate. So this is another question that you have to ask: not only how much is in contact, but how much is in contact when we process this particular ink at this temperature for this time. Then it is a reasonable question.

I have one other question. In addition to your slope, you also pick a value at 9.6. I didn't catch what that value was, and why did you pick 9.6?

PROVANCE: That happens to be the mid-point of the five shear rates that we used, and it was simply a matter of convenience. That is what we show in our literature. Almost all thick-film paste manufacturers have a viscosity specification, and it obviously has to be taken at one shear rate. As a matter of convenience, we picked the midpoint of the five that we used, and quote that in our literature. I am the first to admit that that number can be very misleading if you don't have the entire picture of what happens when you shear the material.

R. VEST: What is the range you shoot for at 9.6?

PROVANCE: In the case of conductor pastes, it varies per application and type of metal. In the example I will use, if you are going to go a large screen, such as in the use of making optoelectronic displays, gas-discharge displays, the customer works with large sheets of glass. We found from experience that the squeegee material that pushes the paste through the screen is going to be different than it is on a smaller screen. In microelectronics, most of our pastes are tailored to a relatively small screen, 12-inch-square or smaller, for small devices.

But on a large screen, we have found that you need an absolute viscosity of about 600 poise where on a small screen you need more like 900 to 1000 poise. So at midpoint it varies with the application, and quite honestly, the technology in solar cells is considered somewhat secret. Our customers will sometimes communicate back to us and sometimes they won't. More often than not, if they have a printing problem and we are brought in and can see what they are doing, we can correct it simply by adjusting the organic vehicle so it will print regardless of what size screen they are using or what type of squeegee material they are using.

SOMBERG: Would you care to comment about this previous point I brought up about the presence of organics in, say, solar-cell firing, being aware of the fact that it is spike-fired but it does go through a burnout? Other than metal stearates, things like that, would you comment about the presence or absence of organics through that burnout phase, say through 550° to 600°C?

PROVANCE: In the early going (ceramics), and in the early going of solar cell manufacture (we are talking about maybe four or five years ago) I was a nonbeliever that you could achieve sintering and maximization of adhesion when you peak fire at 60 to 120 seconds. I saw these reports coming, most of them JPL-sponsored, and I said no way can you make thick film work, because I have been in this business for 20 years and we thought we did a marvelous thing when we came from 980°C down to 850°C and brought the cycle time down from one hour to 25 minutes. I became a believer when we went out into the field to one of our customers and printed some parts and set up -- in fact, we turned the furnace on for them. A strange-looking furnace, this IR furnace, which you turn on like a light bulb; it is unconventional, compared with the standard type of furnace, and within an afternoon I was convinced that there was indeed something to that, because I recall I set up three or four profiles from about 500° to 700°C with different times, and one of the early tests which is still used was simply for adhesion, putting Scotch tape down and pulling it off. Before the afternoon was over, I could see that it was certainly passing the Scotch-tape test and it appeared to be a rather dense film. We subsequently went on to study thick-film resistors. In fact, four weeks ago I was in Dallas giving a talk on properties of thick-film resistors fired in an IR furnace, going from the conventional 25- to 30-minute cycle, down to 4, 5 and 6 minutes, which is still long by solar cell standards but much faster than conventional thick film. I can't disagree with Dr. Stein that there is obviously something trapped in there, but it is a negligible amount, we feel, because resistors, especially, are very sensitive to thick-film processing. In this particular series we developed a TCR (temperature coefficient resistance) of 0 to 40 parts per million, and anything that is not right will offset and create an imbalance so that you can't achieve this. Obviously, we are trapping something when we fire in 60 seconds or 120 seconds. I am not sure that anyone has measured just how much. A rough measure would simply be to take a weight with a fine balance to five or six places and fire it and weigh it again. I am not sure that will clear up the mystery, because that still might not be accurate enough to say just how much is coating those particles. It is pretty difficult to imagine that you are indeed burning out an organic binder in a matter of a couple of minutes. When

you consider the shape of those particles, the little crevices and so many places to have binder trapped in there, it is pretty difficult to imagine that you are burning it out clean. Just how much remains, I don't think we know. That is probably something that should be looked into.

WEAVER: Being a field test engineer and not understanding all of this, I was wondering if you used the glass frit, what would happen if you used, say carbon fiber in there with them, because it is more conductive? Would that be detrimental or beneficial, or it wouldn't make any difference?

PROVANCE: Well the glass frit is used to help the sintering processes as well as adhesion. The fiber might help the electrical properties, but you wouldn't get any adhesion benefit from it, or sintering values.

STEIN: There was a question raised before, I think it was from the man from SERI, about the possible modifications to the inks, and it was interpreted as being modifications that the paste manufacturers could make. I would like to suggest also another kind of modification that we have encountered which is done by the customers, and it is highly secret. But basically, in a number of instances we know that people are throwing all sorts of things into the silver pastes on the solar-cell user side. These can have rather dramatic effects. I will give you an illustration. In Europe, some of our customers used one of our silvers, which fires up in the 830° to 850°C region, and it is a totally different system and they insist they like it a lot better than this low-temperature stuff that might peak-fire at 700° + 20. We know that they throw in titanium, in one instance, we know that some others throw in tantalum, we know that a number of other things are used. Coming back then to the basic question of what happens at the interface? Is it a glass contact in part and a silver contact in part? There has to be an interaction between the silver and the silicon, there has to be some diffusion to get good electrical contact. There are probably doping effects due to these additives, and there are very likely new compounds formed at the interfaces, so it is a rather complex picture and it is not an easily answered question. We therefore offer a variety of silvers containing, let's call it dopants, or sintering aids. In fact, if anybody wants it, I am sure that Thick Film Systems or Electro Science Labs will custom-make something with any garbage you want put in it, because we don't understand it.

HOGAN: That was really the intent of my question, because I know it is very easy for a silicon-cell manufacturer to add a little liquid boron dopant to the silver ink and think that is going to do something for his contact. It may or may not. I was just wondering what kind of problems you got into as a manufacturer in trying to straighten out somebody's printing problem when Lord only knows what is in your ink after it's gotten into the plant?

PROVANCE: That is a big problem and as Sid (Stein) says, we will make anything anybody wants. Actually, the manufacturer of the thick film formulation is better equipped and better able to do that because the fine tuning of the screening characteristics as well as the electrical properties can best be done by the person that is making this material.

Once the material is out in the field and altered, it may be altered to achieve a certain physical benefit in the screen printing, or some electrical property, but it could be creating other problems. When a customer does alter these materials, it is generally over a period of time and he has also learned to live with altering this and he makes it work, one way or another. What we are saying is, it is very likely that the thick-film paste manufacturer would be able to achieve this in a shorter period of time and guarantee that it would work time and time again.

AMICK: Do you have any limits, then, to what you would accept in the way of initial ink? Because you know you can tailor that by making up combinations of different binders and then blending, to come within specifications. Are you saying you don't really have any criteria for the original selection?

PROVANCE: Yes. You can live with a certain amount of variation, from time to time, but you can't live with a fired surface that is rough and does not hold line definition. In all cases, all of these powders either experimentally or in production get made into a paste and with full quality control. What we try to do is weed out, as I mentioned earlier, a disaster where you commit several thousand grams of material, or more, to a batch of material only to find that you have made a mistake. You might call it an early warning system. Yes, there are limits as to what we would use. In fact, if the differences between powders are gross, which they were with lot A, shown in the slide, that particular unacceptable lot never make it to manufacturing. What we are looking for is tailoring the small differences, relatively small differences, yet important differences to the slope as well as to the viscosity at a standard shear rate. Yes, there are limits. The use of the vehicle technology, you might say, is a fine-tuning instrument to make the material behave, that misbehaves in the particle state.

NAZARENKO: Just to expand on what was just said, we are constrained on the type of vehicles we can use because the materials are selected so that they offer clean burnout. We try to design the materials so there are no residual carbons or other types of impurities left after the burning cycle. Functional groups on the vehicle will dictate how efficiently these materials are going to be burned out. So there are some limits.

PROVANCE: These binders do burn out rather rapidly and the principle deterrent to them burning out clean, as Sid Stein said, was the fact that you have to watch that you are not melting the glass or sintering the particles to the extent that you capture and freeze these in. But most of these materials have been well researched down through the last three, four or five years and the organic vehicles are better than what they were eight or 10 or 15 years ago. They do burn out pretty quickly so you can, even in conventional firing, come up rather sharply and burn those materials out in a conventional furnace in seven or eight minutes. The old profiles, and I am talking 10, 12 or 15 years ago, used to come up and level off at 500°C and then come on out just to get rid of the binder. It is no longer necessary to do that.

AMICK: Does anyone do microcombustion analysis now to find out how much carbon there is left after binder burnout?

STEIN: We do that.

STEIN: The comment I made earlier was not related to the burning out of the vehicle, which can be handled. It was related to the organics trapped or coated on the surface of the silver particles as Jay (Provance) or anybody else receives them. If they are precipitated particles, precipitated in the presence of a protective colloid, precipitated in the presence of an organic acid with a carboxyl group or precipitated in the presence of some other, heaven forbid, halogenated or sulfonated or other kind of active chemical group. That is very difficult to get rid of and that is present in an extremely minute amount but it can affect the sintering rates. That is what I was talking about.

PROVANCE: That is a very good point, and while I don't want to discuss exactly how we do this, we do make a test for just that sort of thing to keep our suppliers of powders honest, you might say. So we do have some limits on what we will accept in the way of coatings that may or may not be on those particles as we receive them because that can have an overpowering influence on how these materials sinter as well as how our organic vehicles are going to work.

Alexander Garcia III

Spectrolab, Inc.  
March 17, 1983  
Photovoltaic Metallization Systems  
Research Forum

This paper presents the results of efforts to produce a nonsilver metallization system for silicon photovoltaic cells. The system uses a metallization system based on molybdenum, tin, and titanium hydride. The initial work in this system was done using the MIDFILM process. The MIDFILM process attains a line resolution comparable to photoresist methods with a process related to screen printing.

The surface to be processed is first coated with a thin layer of photopolymer material. Upon exposure to ultraviolet light through a suitable mask, the polymer in the non-pattern area crosslinks and becomes hard. The unexposed pattern areas remain tacky. The conductor material is then applied in the form of a dry mixture of metal which adheres to the tacky pattern area. The assemblage is then fired to ash the photopolymer and sinter the conductor powder.

Several compositions of powders were used in this research, the compositions are identified as follows:

TYPE	Mo	Ti	Sn	frit
A DP-E570	19.5	80.0	0.5	0
B DP-E571	50.0	49.5	0.5	0
C DP-E572	70.0	29.5	0.5	0
D DP-E573	49.0	49.0	2.0	0
E DP-E574	48.0	48.0	4.0	0
F DP-F503	19.5	80.0	0.5	5.0

The frit used was a Pb/borosilicate glass.

Initial work using the MIDFILM process was done using only type A paste. It was found that this resulted in cells with a very high series resistance. If the cell was then plated the cell improved. To decrease the series resistance a screen printed process was investigated. The metal powders were formulated into screenprinting pastes by Thick Film Systems using the same vehicle used in silver pastes. After screenprinting the cells are fired in air in an IR belt furnace to burn off the organic components of the vehicle. The cells are then sintered in a pure hydrogen atmosphere.

Paste types A&F gave the best results. Cells were fired at 500-550°C at a belt speed of 18"/min. through a heated zone of 18". The metallization has a blue-grey color which becomes metallic looking after the hydrogen sintering. Sintering was done at 600°C for 90 seconds. Figures 13-16 show a typical Mo/Ti cell as compared to a silver cell (neither are AR coated). Cells produced by this method pass tape pull tests but are difficult to solder to without removing the metallization. Sintering for longer times at higher temperature enhances adhesion but increases series resistance to unacceptable values.

Several different cleaning procedures prior to screenprinting were tried in an attempt to increase adhesion. Figure 17 shows the procedures. All procedures worked equally well (or poorly), procedure D is now used routinely and successfully for silver metallization cells.

CO was used in place of hydrogen as the reducing gas in another experiment. The cells had much higher series resistance as seen in figure 20. Adhesion between the metallization and the silicon was improved but particle to particle adhesion appeared to degrade. Soldering to the cells was impossible under all conditions.

In the next study wafers were coated with indium tin oxide (ITO) prior to metallization. The ITO was applied by reactive sputtering by Applied Film Labs Inc. The thickness varied from 512 to 783A with an index of refraction of 1.95. The reflected color varied with increasing thickness as follows: green bronze, bronze, purple, blue. The cells were reduced using hydrogen at 600°C. The hydrogen firing also reduced the ITO causing a milky appearance on the cells. Air firing of the cell brought back some of the color of the film and improve cell performance as is shown in figure 25. Attempt to fire the cells at 650°C led to severe shunting, figure 24 and 25. The particle adhesion for the ITO cells was still not adequate for soldering.

Future work will include sequential use of hydrogen and CO, and use of other paste additives.

## Figure 2. Objectives

- OPTIMIZATION, EVALUATION AND DEMONSTRATION OF A NOVEL METALLIZATION SYSTEM
- Mo/Sn/TiH SYSTEM
- ITO CONDUCTIVE AR SYSTEMS

## Figure 3. Approach

- SCREEN PRINTING
- AIR FIRING
- REDUCING ATMOSPHERE FIRING
- CONDUCTIVE AR COATING (ITO)

## Figure 4. Metallization Paste Formulations

	A (RH 3659)	B	C	D	E	F
MOLYBDENUM (SYLVANIA 280-325)	19.5	50.0	70.0	49.0	48.0	19.5
TIN (ATLANTIC EQUIPMENT ENGINEERS SN 266)	80.0	49.5	29.5	49.0	48.0	80.0
TITANIUM HYDRIDE (FERRO PLANT FX-41)	0.5	0.5	0.5	2.0	4.0	0.5
LEAD/BOROSILICATE FRIT (THICK FILM SYSTEMS #3347)						5.0

ALL PASTES USE THICK FILM SYSTEMS ORGANIC VEHICLE



Figure 5. Initial Effort I

<u>PREFIRE</u>	500°C			550°C		
BELT SPEED	18"/MIN.	24	36	18	24	36

FIRE 600°C 30 MIN. IN 5% H<sub>2</sub>/95% N<sub>2</sub>

Figure 6.

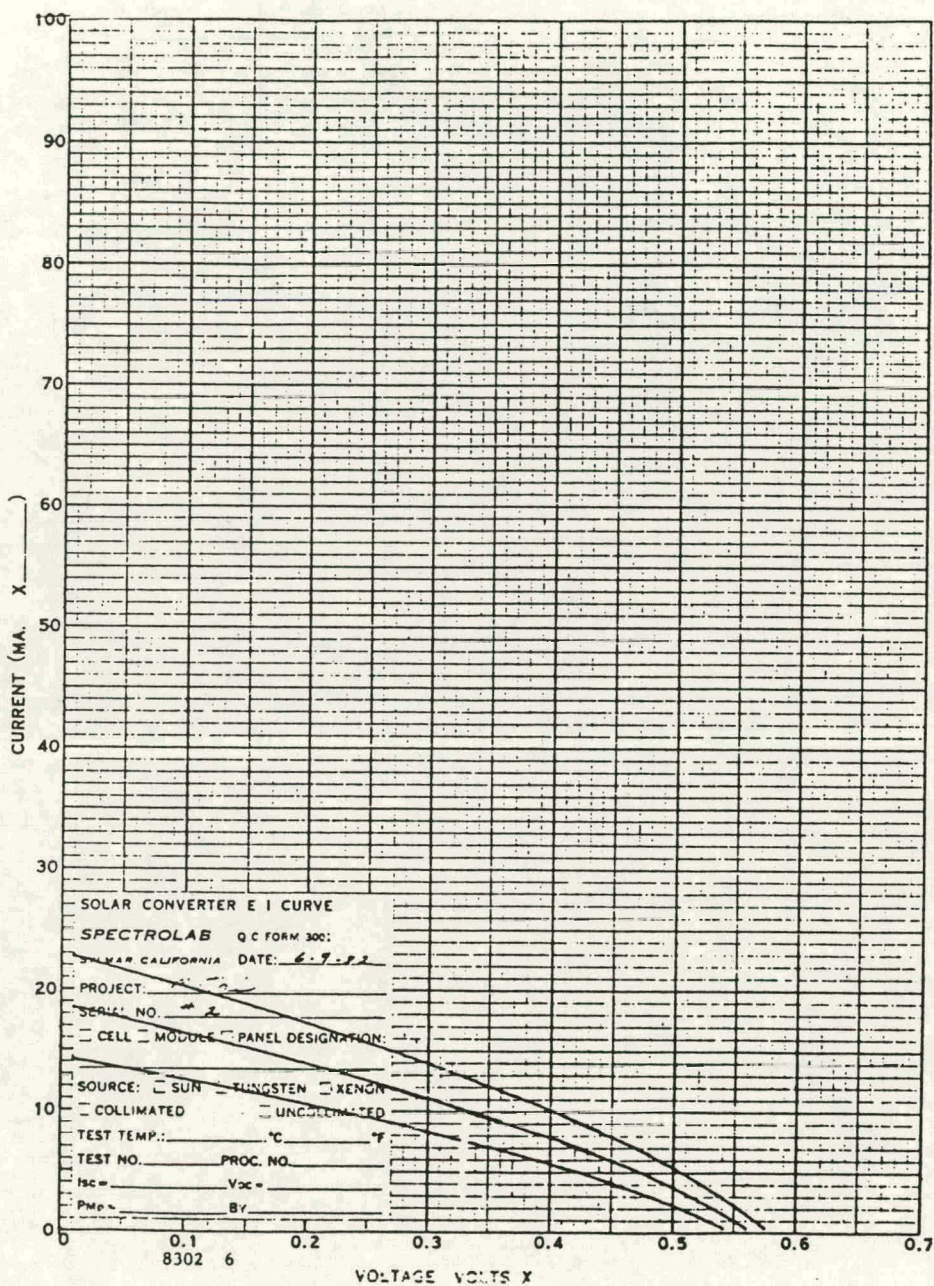


Figure 7. Initial Effort II

PREFIRE

450°			500°	
9	18	24	9	18

FIRE AT 650°C

5% H<sub>2</sub>/95% N<sub>2</sub>

5, 10, AND 15 MIN.



Figure 8.

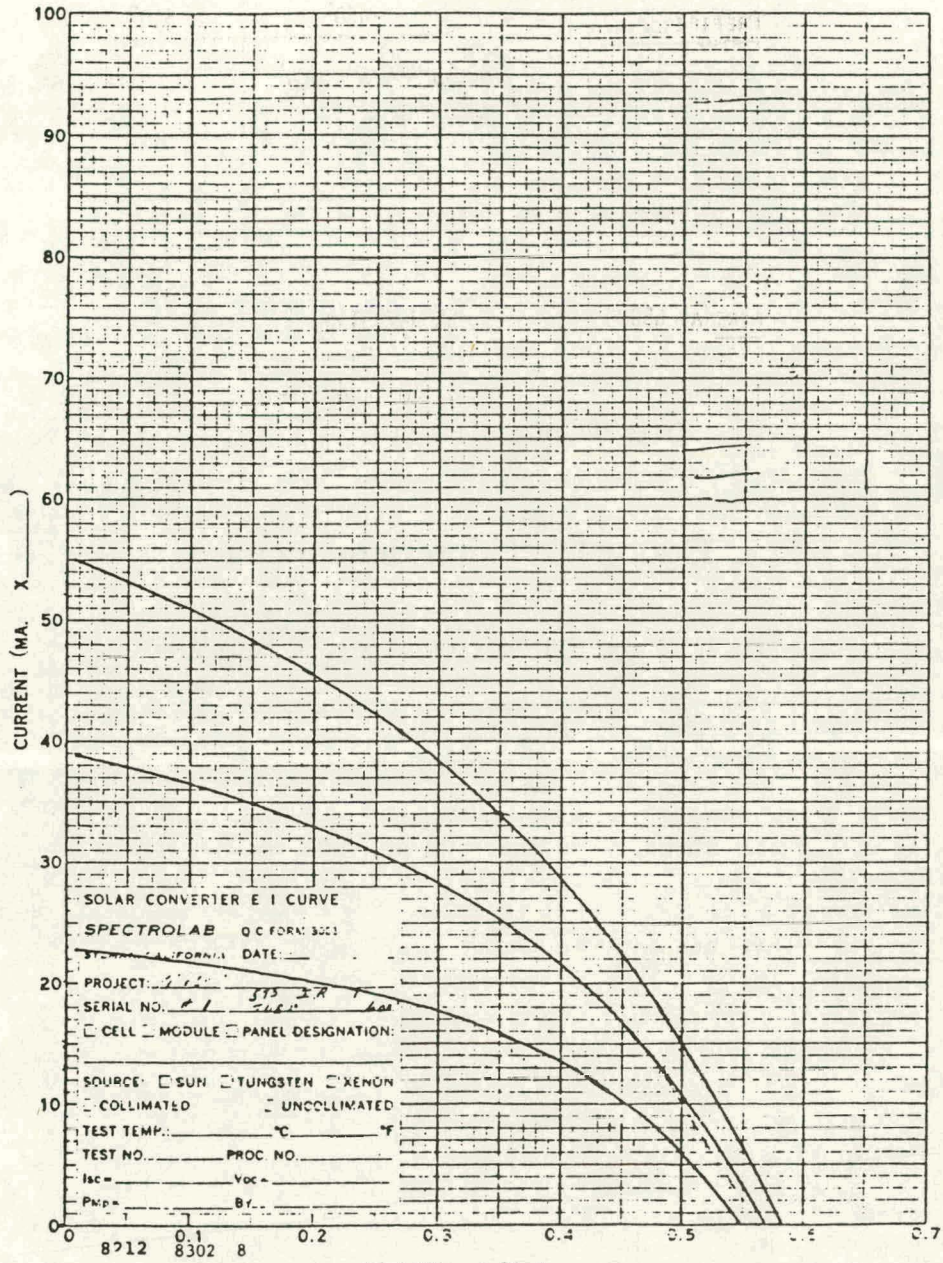


## Figure 9. Initial Effort III

### PREFIRE

400°, 450°, 550°  
AT 24"/MIN.

### FIRE

550°, 600°  
30 MIN., 20% H<sub>2</sub>

CELLS SHOWED METALLIC-LIKE CONTACTS

## Figure 10. Firing Sequences

- 1) 18"/1 MIN. 500°C PREFIRE, 1 MIN. 575°C H<sub>2</sub> FIRE
- 2) 18"/MIN. 500°C PREFIRE, 1 MIN. 600°C H<sub>2</sub> FIRE
- 3) 9"/MIN. 500°C PREFIRE, 1 MIN. 575°C H<sub>2</sub> FIRE
- 4) 9"/MIN. 500°C PREFIRE, 1 MIN. 600°C H<sub>2</sub> FIRE



Figure 11.

Paste Type	Pre-Fire Speed @ 500°	Fire Temp. @ 1 min.	Cell #	V <sub>oc</sub>	I <sub>sc</sub>	I <sub>500</sub>	I <sub>450</sub>
A	9"	575	1	600	701	482	569
A	9"	575	2	598	677	390	490
A	9"	600	3	601	700	469	553
A	9"	600	4	597	696	458	548
A	18"	575	5	603	702	450	543
A	18"	575	7	599	560	286	359
A	18"	600	6	598	701	440	530
A	18"	600	8	602	703	461	550
B	9	575	9	600	687	377	488
B	9	575	11	598	676	297	398
B	9	600	10	600	689	369	478
B	9	600	12	597	644	282	371
B	18	575	13	602	681	345	451
B	18	575	14	602	681	331	438
B	18	600*	15	598	686	409	515
B	18	600*	16	596	692	389	497
C	9	575	20	594	617	194	266
C	9	575	17	589	369	109	150
C	9	600	19	592	668	246	345
C	9	600	18	587	300	90	123
C	18	575	21	597	684	305	415
C	18	575	23	598	667	285	388
C	18	600	22	600	687	350	463
C	18	600	24	596	680	347	458
D	9	575	26	598	684	330	447
D	9	575	25	599	681	320	429
D	9	600	28	598	676	328	435
D	9	600	27	599	678	351	455
D	18	575	31	596	686	346	464
D	18	575	29	598	682	336	448
D	18	600	32	601	691	378	441
D	18	600	30	600	694	393	502
E	9	575	33	596	668	260	356
E	9	575	34	596	639	229	312
E	9	600	35	596	674	265	363
E	9	600	36	598	677	262	417
E	18	575	37	597	672	295	396
E	18	575	38	598	669	286	385
E	18	600	39	597	690	333	440
E	18	600	40	600	685	318	420

Figure 12. Initial Optimization of Paste A

PREFIRE            18"/MIN.            500°C

FIRE                1 MIN.                575°C

COMPARABLE TO SILVER PASTE CELLS

Figure 13. Front Metallization Pattern

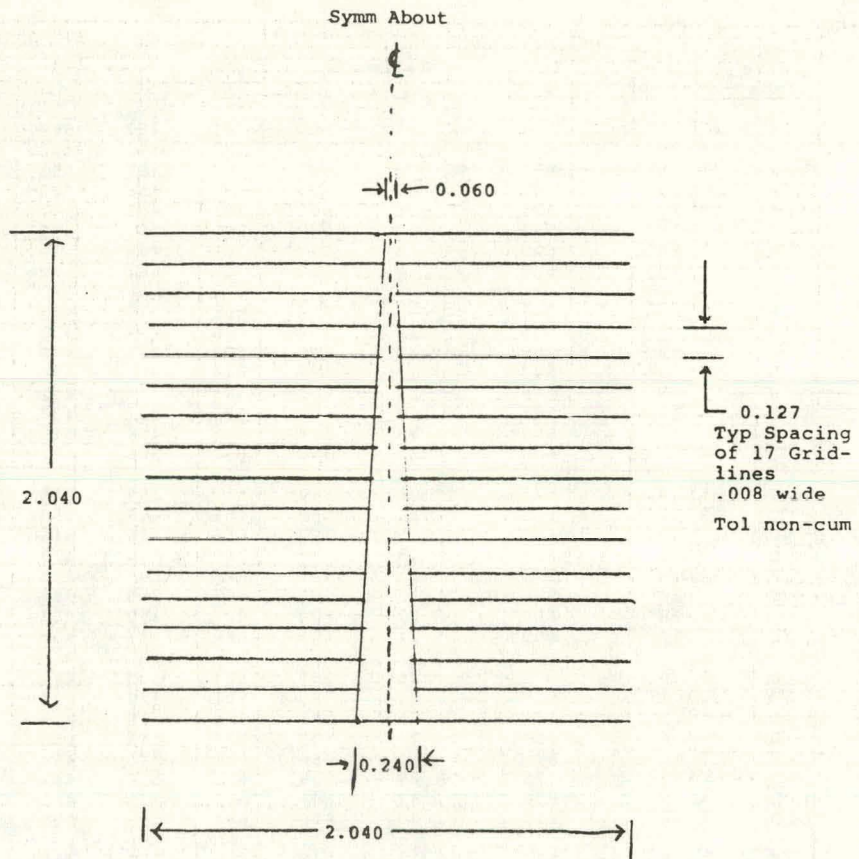




Figure 14.

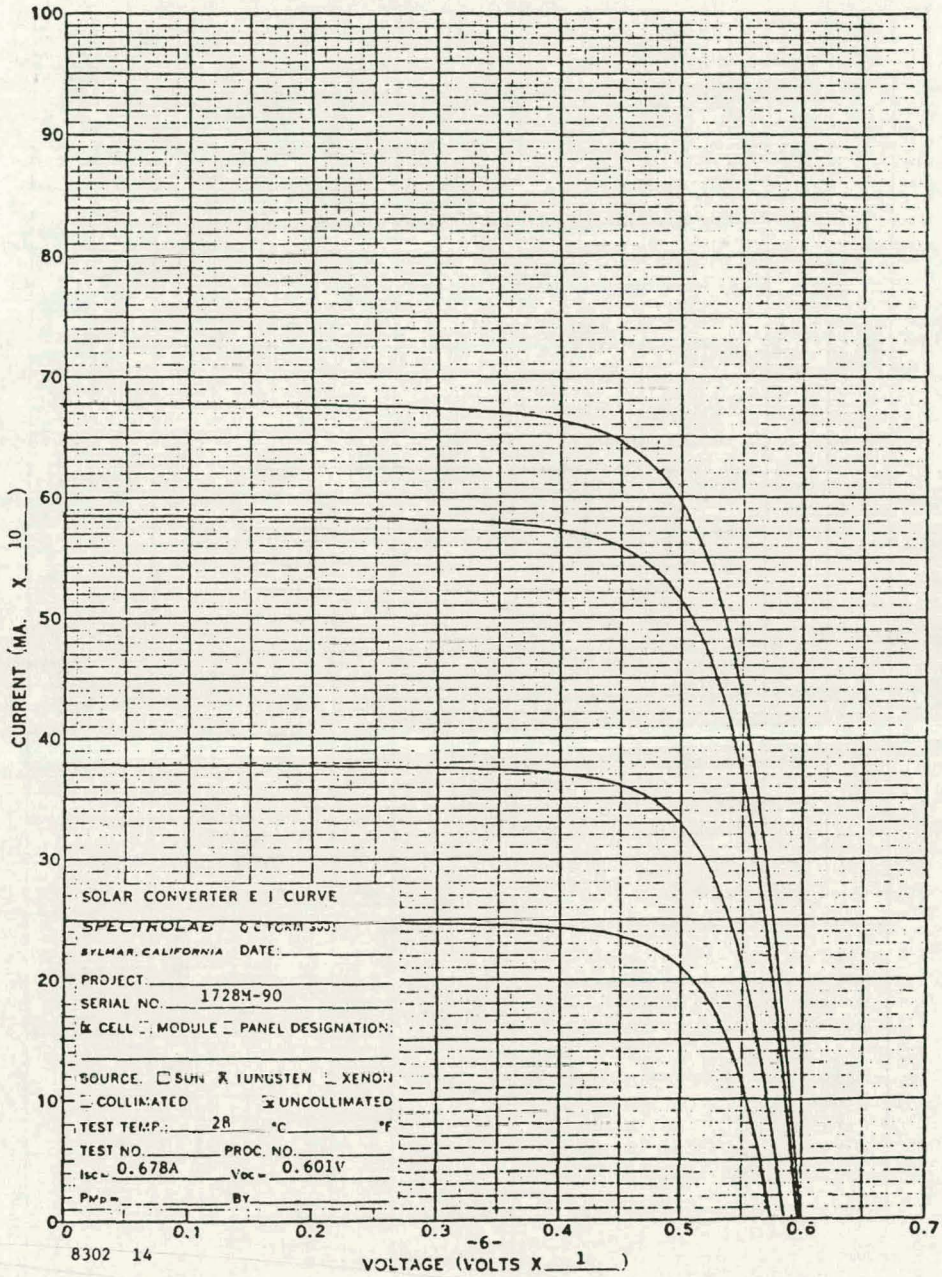




Figure 15.

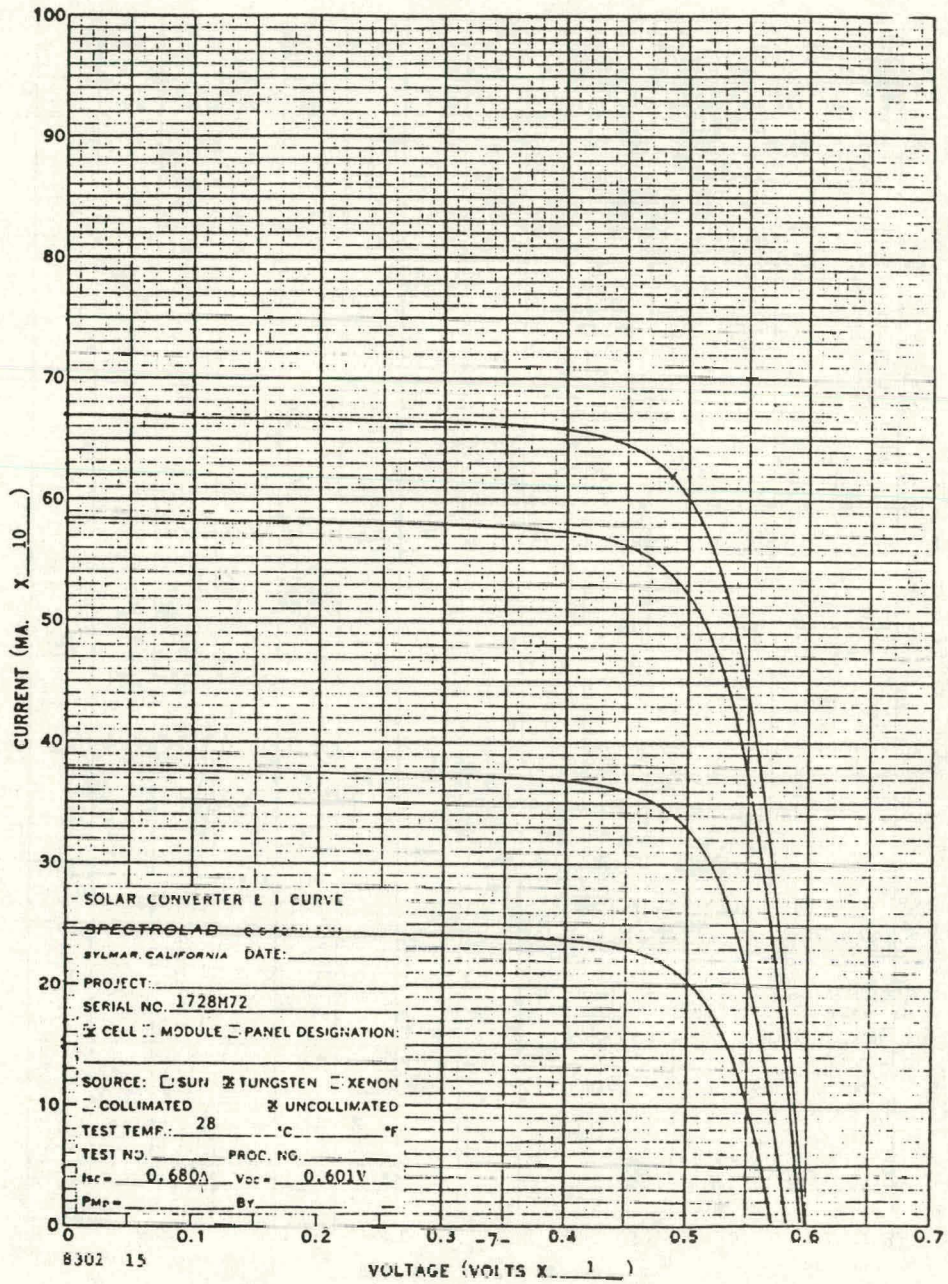


Figure 16. Mo-Sn versus Ag

CELL	$V_{oc}$	$I_{sc}$	$I_{500}$	$P_{MAX}$	FF	E
1728M-90 (Mo/Sn)	.601	.678	.596	.229	.73	10.5%
1728M-72 (Ag)	.601	.680	.600	.302	.74	10.6%

Figure 17. Cleaning Procedures

A	B	C	D
10% HCL 1 MIN.	10% HCL 1 MIN.	10% HCL 1 MIN.	85°C H <sub>2</sub> O/NH <sub>3</sub> /H <sub>2</sub> O <sub>2</sub> 30 SEC.
H <sub>2</sub> O RINSE	H <sub>2</sub> O RINSE	H <sub>2</sub> O RINSE	H <sub>2</sub> O RINSE
10% HF 1 MIN.	10% HF 1 MIN.	10% HF 1 MIN.	
H <sub>2</sub> O RINSE	H <sub>2</sub> O RINSE	H <sub>2</sub> O RINSE	
50% AcOH ~1 MIN.	H <sub>2</sub> O/NH <sub>3</sub> /H <sub>2</sub> O <sub>2</sub> 30 SEC.		
HOT H <sub>2</sub> O RINSE	H <sub>2</sub> O RINSE		
ACETONE 2 MIN.			
MeOH 2 MIN.			
HOT H <sub>2</sub> O 2 MIN.			
H <sub>2</sub> O, N <sub>2</sub> 5 MIN.			

Figure 18. Problems

- POOR ADHESION
- FRIT DOES NOT APPRECIABLY WORK
- SI-POWDER BOND A PROBLEM
- SOLDERING A PROBLEM



## Figure 19. CO as Reducing Gas

- CELLS HAVE HIGHER SERIES RESISTANCE
- PARTICLE TO SILICON ADHESION GOOD
- PARTICLE-TO-PARTICLE ADHESION POOR.

## Figure 20. ITO Studies

- APPLIED BEFORE METALLIZATION
- INDEX OF REFRACTION  $\sim 1.95$
- THICKNESS VARIED 512 - 783 Å
- COLOR GREEN BRONZE - BRONZE - PURPLE - BLUE



Figure 21.

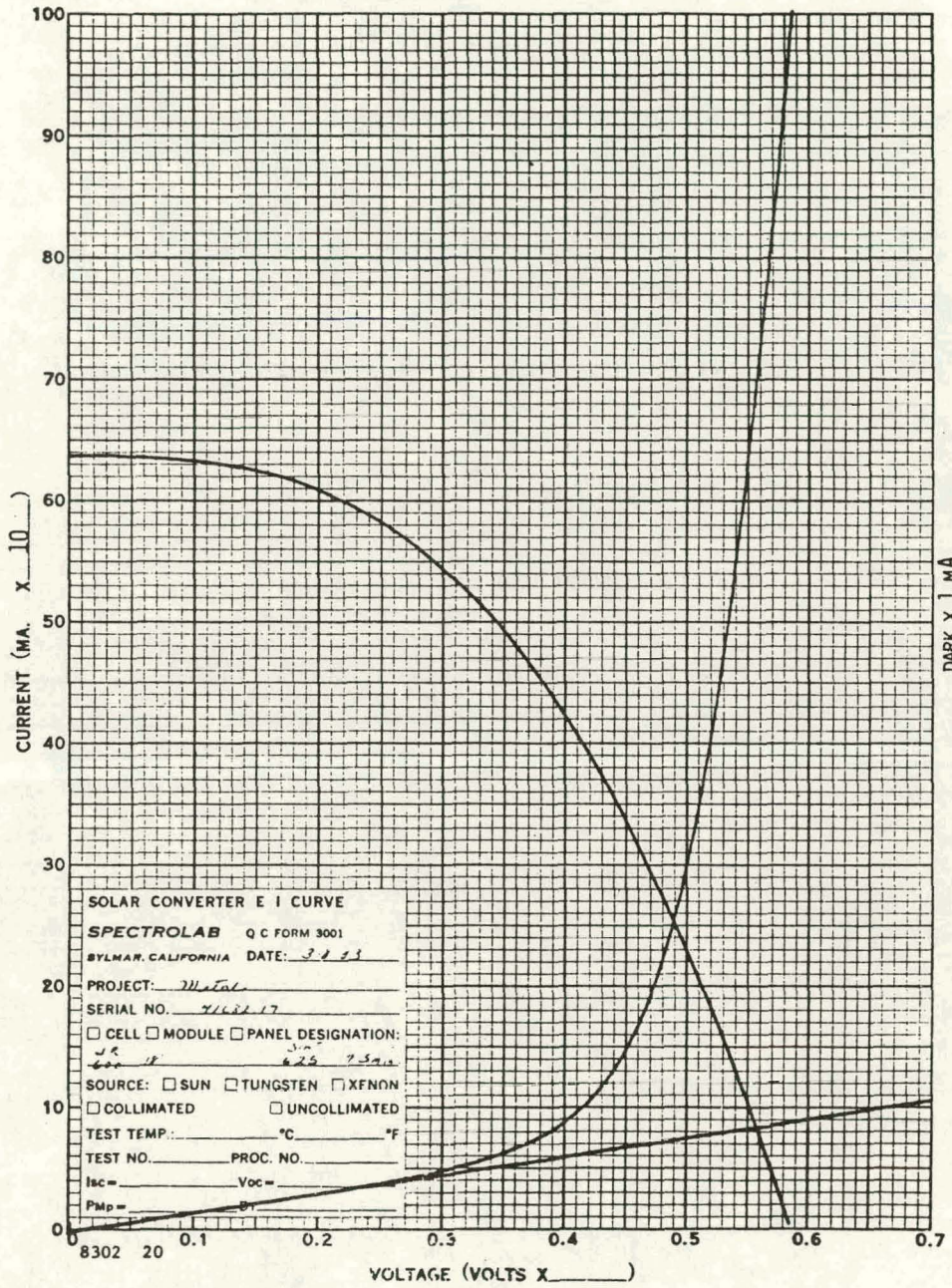


## Figure 22. ITI Results

- GOOD ADHESION PARTICLES - ITO
- POOR ADHESION PARTICLE-PARTICLE  
(REDUCED IN H<sub>2</sub>)
- ITO AR VALUE IS DESTROYED BY REDUCING ATMOSPHERE
- REOXIDATION NECESSARY
- SHUNTING OCCURS ABOVE 600°C



Figure 23.

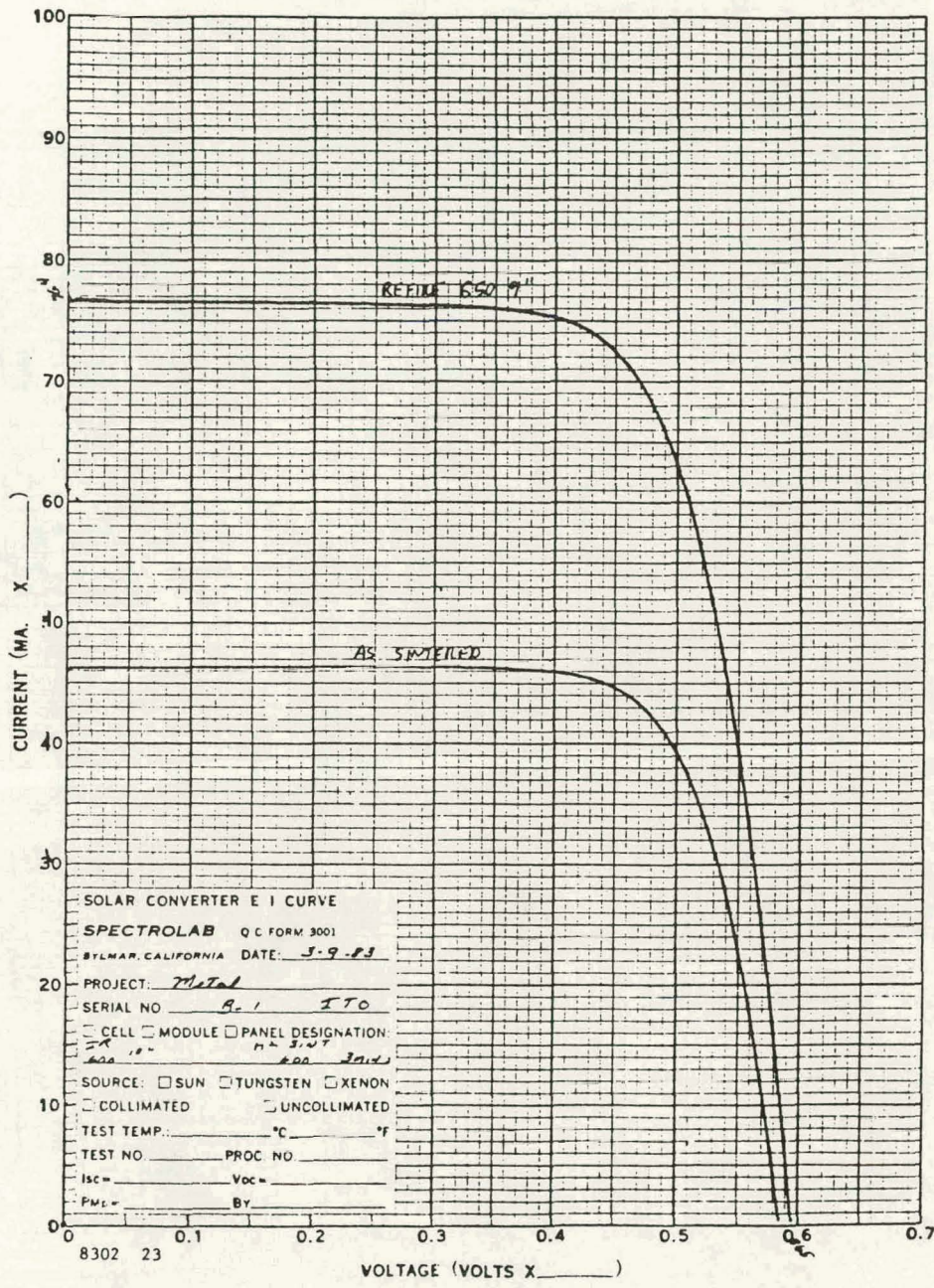




Figure 24.

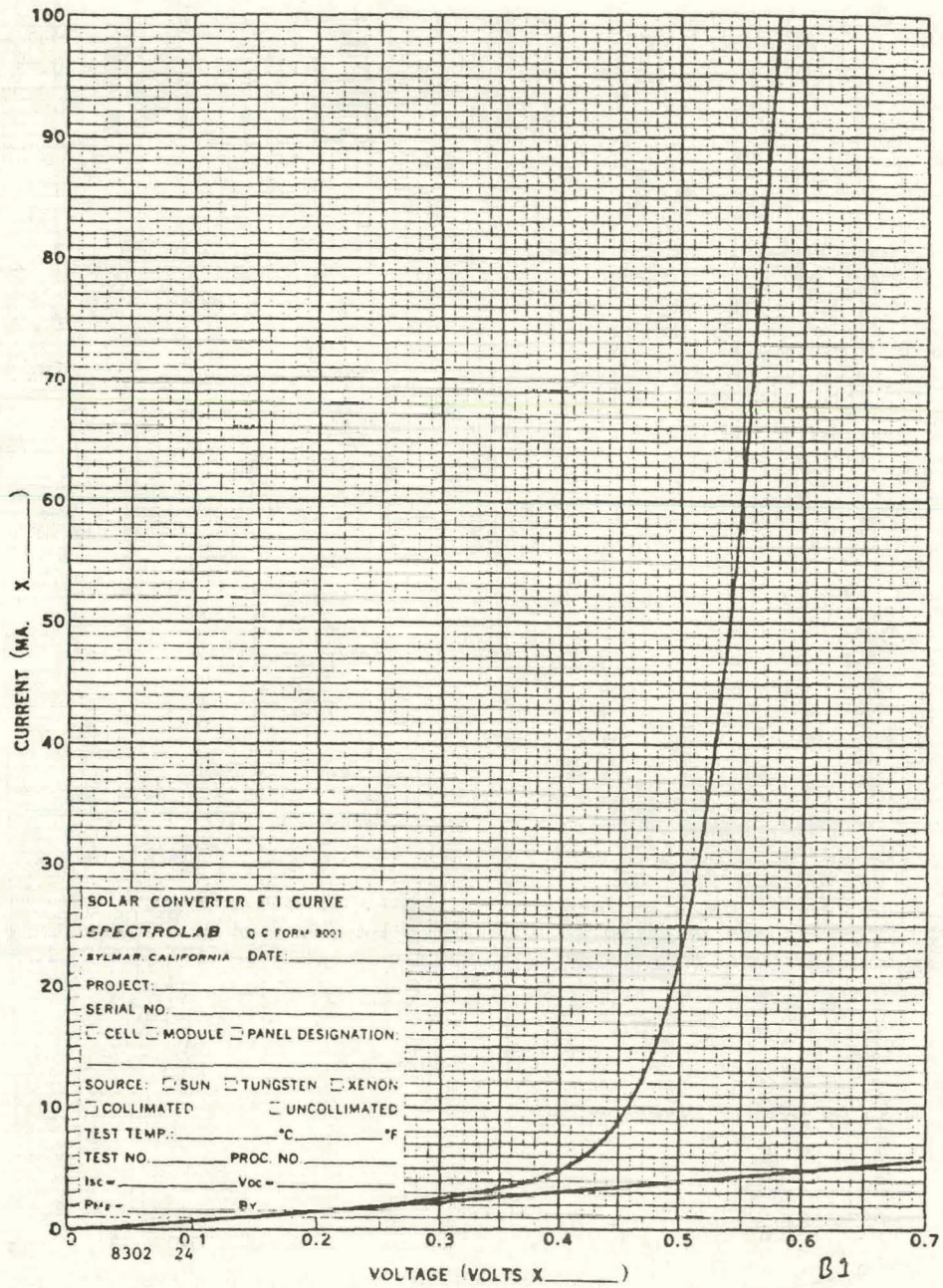




Figure 25.

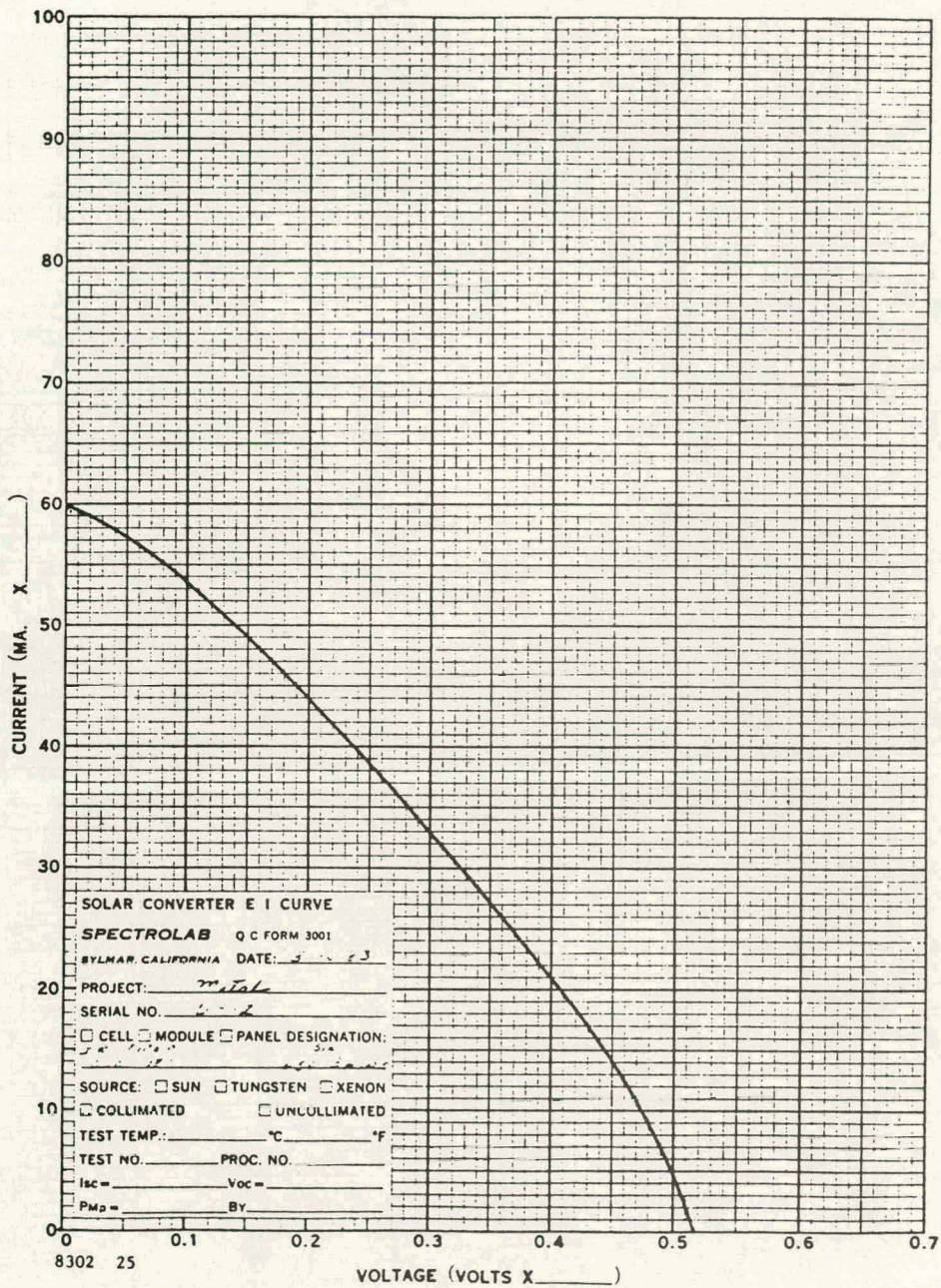
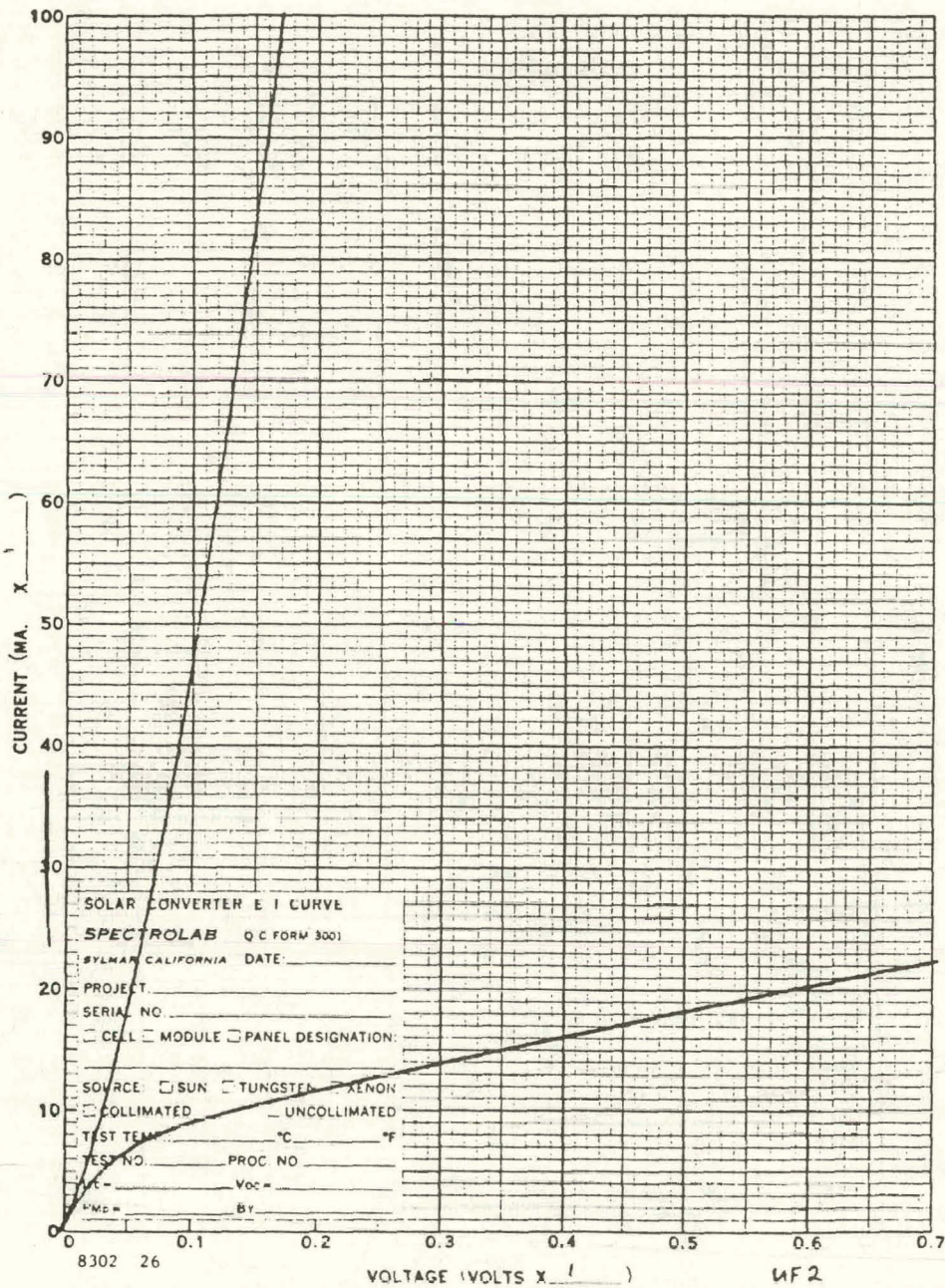




Figure 26.



## Figure 27. Discussion

- CO PROMOTES GOOD SILICON-PARTICLE ADHESION  
POOR PARTICLE-PARTICLE ADHESION
- H<sub>2</sub> PROMOTES BETTER PARTICLE-TO-PARTICLE ADHESION BUT STILL NOT  
GOOD ENOUGH
- PARTICLE-TO-ITO ADHESION GOOD
- ITO EASILY REDUCED AT 600°C IN H<sub>2</sub>
- ITO SHUNTS CELLS AT 650°C

## Figure 28. Future Work

- SEQUENTIAL USE OF H<sub>2</sub> AND CO REDUCTION
- SEM EVALUATIONS
- OTHER PASTE ADDITIVES?

## DISCUSSION

SOMBERG: Did you try any without titanium hydride?

GARCIA: In this study we have not tried them without the titanium hydride. In the mid-film work we did try some without titanium hydride and the results were terrible compared with the ones that did have a little titanium hydride.

SOMBERG: My other question is: when you soldered to the cell, you said there was failure. Were you able to tell where failure was occurring?

GARCIA: It failed in different ways. In cells that were fired in hydrogen, the failure was between the metallization and the silicon. It appeared to just come straight off the silicon. When it was fired in carbon monoxide you divoted the silicon but you didn't get particle-to-particle adhesion; it wasn't very good. It appears you were just making contact with a couple of particles and pulling those out of the silicon, but the particles were not sticking to one another. There wasn't much congruity to the metallization.

LAVENDEL: I might comment on the function of titanium hydride in your system. Believe it or not, I am going back to a problem that I had once with armors. Quite a distance between armors and solar cells, but the problem we were trying to solve at that time was to get to a structure that would be composed of aluminum oxide particles or plates built together with very thin metal films, and lo and behold, one of the best systems was tin titanium hydride. It is because, at these temperatures that you mentioned, titanium hydride decomposes; titanium dissolves in tin and you have a liquid metal that wets and bonds to the ceramic surface, oxide ceramic surface. You say that in the case of hydrogen firing, you don't get a good adherence of your metallization, of bonds of your metallization to silicon. I would propose that you don't get it because you have a very clean silicon surface. If you had traces of silicon oxide on it, then you have that tin-titanium liquid wetting the surface and bonding. If you remove the oxide completely, you don't have bonding. If you use carbon monoxide, you would probably restore very thin oxide film on your silicon and you restore bonding.

GARCIA: Well, one thing we did try was no cleaning at all, which I would assume would leave some oxide on the cell. That didn't help. We also tried putting a big oxide on there by just dipping the solar cells in hydrogen peroxide. I was not sure if that would put oxide on, but I thought it might. That didn't help either. So I am not sure that was the problem.

BEAVIS: Of course when you put it in hydrogen like that, if it is really pure hydrogen, what happens is that the oxide reduces, because there is oxide there anyway in the beginning. Have you tried any with putting water -- in other words, wet hydrogen? That will certainly keep the silicon in the oxidized state. I am not sure what the free energies for tin oxide are, I don't remember right off hand, but it would certainly keep the silicon oxide on the surface if you have water in it.

GARCIA: We have not tried that.

BEAVIS: That is a classic way, by the way, of doing those sorts of things.  
It is just wet hydrogen.

BICKLER: Bernd Ross had concluded that it is the hydrogen occupying the free silicon sites and preventing the chemical bonding to the silicon, it is not the lack of the oxide, carbon monoxide is sufficiently reducing to handle that aspect of the thing but it's occupancy of silicon sites by hydrogen, quite similar to some of these hydrogen involvements with silicon we are seeing in polycrystalline cells.

BURGER: If I remember the original work with the moly-tin systems, wasn't that molybdenum pentoxide and titanium resinate with pure tin?

GARCIA: I am not aware of that. I didn't worry about that.

GALLAGHER: In the original Midfilm program, we used both moly trioxide and moly metal.

GARCIA: This wasn't at the end of the Midfilm contract.

GALLAGHER: That is the one we are talking about, where we used moly metal and molytin.

GARCIA: Yes, we did. But we didn't use a resinate.

GALLAGHER: Yes, there was a resinate in it.

GARCIA: There was? Maybe.

WONG: I have a question for Don (Bickler). This will clear up my mind on the hydrogen business. Are you saying that the free surface of the silicon has a lot of dangling bonds and the hydrogen wants to satisfy those dangling bonds? And becomes stable so that it won't react any more with other --

BICKLER: That is the understanding to date.

AMICK: I would think that picture at 600° is very unlikely because amorphous silicon goes to pieces at something like 500° and you lose the hydrogen at the surface even down at 400° in firing.

BICKLER: Well, it goes through all the temperatures in the furnace. It is still in the hydrogen atmosphere as it comes back out.

AMICK: But at the time you are actually trying to form the bond, it is at high temperatures.

GALLAGHER: Well, actually, Bernd Ross did some nuclear resonance studies with SUNY wherein he not only showed that hydrogen had taken care of dangling bonds at the surface but there was actually hydrogen within the structure to some depth. Depth being in Angstroms.

AMICK: After you come back down to room temperature, I can believe the hydrogen was in there; the question is, whether it's at the surface interfering with something, at the temperature at which you are trying to put it in.

GALLAGHER: I don't know - all I know is that the samples were done in both hydrogen and CO and sent (to SUNY) and he performed this experiment and we got back curves that said there is hydrogen in there and hydrogen absorbs --

BICKLER: He was working with copper; it wasn't molytin. He experienced the same problem and it was because of that experience that Alex (Garcia) --

GARCIA: That is why I went to the carbon monoxide.

TAYLOR: We have been looking at this question also and have looked at systems in which we fire the molybdenum tin and also we have looked at other metallizations in a forming gas-type atmosphere and we have observed the same loss of, or failure to develop, adhesion there even when you go down to very low concentrations of hydrogen in the molecular atmosphere, down below 1% hydrogen.

BLAKE: One of the things we noticed in the study of the effect of hydrogen on adhesion is that we could take silver bonds that were very strong and pass all the tests, expose the bonds to hydrogen at elevated temperatures, and get a complete release with no trace of adhesion. So we felt that hydrogen was insinuating itself between the bond in some way that we were not aware of and causing a release of the bond that we had previously.

SOMBERG: What temperature would it take to do that?

BLAKE: Oh, about 550° and up.

TAYLOR: We have seen that same thing going on in sintered aluminum firing. We fired in a very weak hydrogen atmosphere at 550° to 600° temperature.

BLAKE: It is that observation that caused us to start to do more work with SUNY to find out whether or not hydrogen is present on the surfaces. I don't think it is all that conclusive at this stage. We have to get more work done on it.

GARCIA: I might say that the cells we are firing in carbon monoxide wet the silicon very nicely and on microscopic appearance they looked very good. They look like a very good coating, whereas on the ones where the hydrogen was used, the film was much more rough and appeared to be more particulate in nature, instead of a real film.

HOGAN: Two questions. First of all, what was the series resistance on the cells?

GARCIA: On the good cells, the series resistance was about 30 to 40 milliohms. Bad cells could get up as high as you wanted it. But the cells I showed you, that showed good curve shape, I would say between 30

and 60 milliohms for that cell, which is something we feel is acceptable for that size cell.

HOGAN: The other question was: with the ITO, what was the sheet resistivity as received, and also after you reoxidized?

GARCIA: We didn't make those measurements. I believe that 150 ohm-cm is the number. I'm not sure what it is.

GALLAGHER: Tell them how long you have had them, maybe that would explain.

GARCIA: I did this work last week. So we really haven't done too much work on these films.

HOGAN: That might be something that you would want to look at.

GARCIA: Yes. The thing is, we found that there is sufficient conductivity so that we don't have a problem with series resistance. Just by analyzing the curve shape and everything, we are saying there is enough conductivity. We are more interested, I think, in the adhesion-promoting abilities underneath it than on the conductivity of the cell. It helps, but I don't think that that extra boost in conductivity might make that much difference.

NICOLET: Two questions. What is this system's advantage over the silver system?

GARCIA: Well, in theory, it should be cheaper. We had originally hoped that this could be done using a forming gas atmosphere and could be done in a conventional IR furnace of some sort.

NICOLET: Second question. Did you ever solve the solubility problem?

GARCIA: We have not solved the solubility problem yet.

NICOLET: Why don't you get good soldering? It appears you have plenty of tin.

GARCIA: I don't know. We are still not getting good sintering from particle to particle with good adhesion on the final product.

TAYLOR: Have you done any scanning electron microscope work on these films?

GARCIA: No. That's our next task.

TAYLOR: We did some work with tin-nickel mixtures and in examining those under scanning electron microscope, we discovered that the tin has a terrible propensity for agglomeration. We got real fine tin particles there but you can't find them, they are all in big boulder-agglomerated particles. That agglomeration tendency might be playing some kind of a role in what you are seeing here.

GARCIA: That is possible.

PARKER: Do you know whether you are getting any compounds of molytin that might interfere with your tinning?

GARCIA: I don't know.

STEIN: Did you see any difference in solder wettability between the 80% tin and the very low tin? In other words, does that play a role?

GARCIA: We did try some solder tests to the B through E pastes and they weren't good. I didn't look at them that carefully but they could not be soldered either. The closest to soldering was using the hydrogen firing of the A paste. Then you could actually solder to the metallization and the metallization would stick together even though it wouldn't be on the cell. You could hold it in your hand, and I made a pretty little doodad I stuck on my door.

TAYLOR: How about trying some just pure tin and see if you could solder that?

GARCIA: That's a thought. Try pure tin. I might try that.

# POLYMER THICK FILM CONDUCTORS AND DIELECTRICS FOR MEMBRANE SWITCHES AND FLEXIBLE CIRCUITRY

N. Nazarenko

E. I. du Pont de Nemours & Company, Inc.

Wilmington, DE 19898

## DESCRIPTION OF THE MEMBRANE SWITCH

The membrane switch functions as a normally open, momentary contact, low-voltage pressure-sensitive device. Its design is a three-layer sandwich usually constructed of polyester film. Conductive patterns are deposited onto the inner side of top and bottom sheets by silk screening. The center spacer is then placed between the two circuit layers to form a sandwich, generally held together by an adhesive. When pressure is applied to the top layer, it flexes through the punched openings of the spacer to establish electrical contact between conductive pads of the upper and lower sheets, momentarily closing the circuit. Upon release of force the top sheet springs back to its normal open position.

The membrane touch switch is being used in a rapidly expanding range of applications, including instrumentation, appliances, electronic games and keyboards. Its broad acceptance results from its low cost, durability, ease of manufacture, cosmetic appeal and design flexibility.

The principal electronic components in the membrane switch are the conductor and dielectric.

## CONDUCTIVE INKS

Polymeric conductive inks typically consist of three basic components: conductive metal powder, polymer and solvent. Silver is the predominant metal used. It has the advantages of moderate cost and long-term conductive stability.

The polymer performs three key functions. It binds the conductor to the substrate, provides cohesion of the silver particles and protects the conductor from external chemical and environmental effects.

The role of the solvent in the conductive ink is to dissolve the polymer, control viscosity and wet the polyester surface. The screened ink is generally dried in a hot forced-air oven to remove solvent and bond the polymer to the substrate. Ideally, the solvent must evaporate rapidly from the printed circuit, yet at the same time also must have a limited rate of evaporation on the screen at ambient temperature to minimize viscosity change and screen clogging.



Processing has a pronounced effect on the performance of conductive inks. The processing of a conductor composition can be separated into two broad operations: screen printing and drying. Key parameters that affect printing are ink rheology, squeegee rate and pressure, surface tension, screen materials and residence time on screen.

Rheology is the principal property affecting the printability of polymeric thick films.

Another major consideration is the selection of appropriate screening materials. Various types of screen cloths, mesh sizes, screen emulsions, and squeegees are available. Mesh size governs the coverage area attainable by an ink, and that determines cost. Correlations have been developed that compare the coverage of conductive inks to sheet resistivity.

Air-dried silver inks are governed by a time/temperature relationship. The improvements in conductivity and flexibility that occur with increased temperature are attributable only in part to more efficient solvent removal. To a greater extent, the source of the improvements can be traced to stronger bond formation between polymer and film.

The property specifications and test methods used to evaluate initial and aged performance of polymeric thick films vary with manufacturers and specific applications. Some of the more important conductive ink properties tested for are: resistivity, adhesion, abrasion resistance, flexibility and use temperature.

Retention of these properties after long-term exposure to environmental contaminants and changes is critical to a reliable membrane switch. The impact of temperature/humidity cycling, thermal shock and vibration, moisture, sulfur and salt impurities on aged performance must be minimized under various industry conditions.

Du Pont's new generation of polymer thick film silver conductors, 5005 and 5007, were developed to meet the industry specifications.

Many membrane touch switch products do not require the low resistance supplied by all silver-based conductive inks. To cut costs, manufacturers use products containing less silver. A recent entry into this market is Du Pont 5006, a non-conductive aluminum-based polymeric ink. It was developed specifically to be blended with either Du Pont 5005 or 5007 silvers to give a variable resistance system. The blended product exhibits uniform printability and excellent electrical and physical properties. The operable conductivity range is 15 to 250 m $\Omega$ /sq/mil.

## DIELECTRICS

Current needs for dielectrics in touch switches are to insulate the switch tail from the environment and for construction of crossovers. The dielectric compositions must meet certain performance standards. They must cure to flexible, abrasion-resistant films, with good adhesion to both

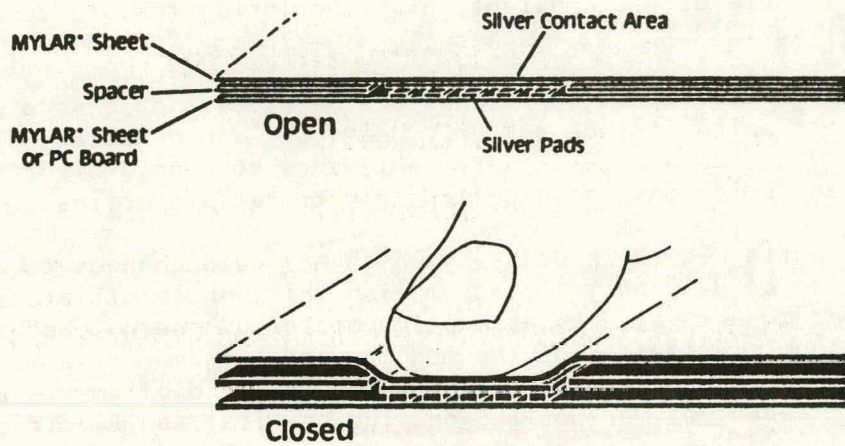
the substrate and to the conductive inks. They must be free of pinholes, have a low dielectric constant, high insulation resistance and high break-down voltage.

Several different approaches can be used to process a polymeric dielectric which include air-dry, heat-cure and UV cure. UV cure systems offer several advantages - very rapid cure at near ambient temperature, no solvent emissions and excellent electrical properties.

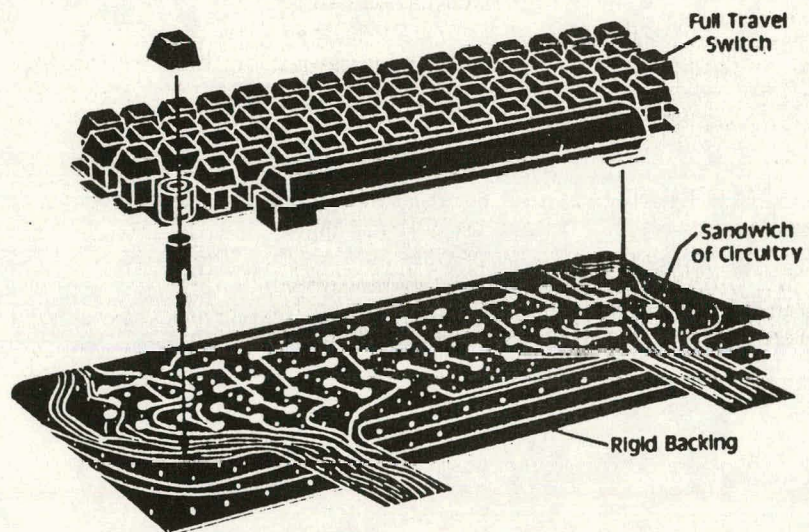
UV curing is the process by which a liquid changes to a solid under the action of UV light. To accomplish this, photoinitiators are used. These become activated by absorption of the UV energy, and in turn, initiate the photopolymerization of the monomer and oligomer, the main constituents of the UV curable formulation. The monomers and oligomers are selected so that the cured polymer has the desired physical and electrical properties.

As with conductors, optimum physical and electrical properties only will be obtained if the dielectric is processed correctly. UV light output and exposure time are the principal variables which govern curing efficiency. Du Pont's 5011, a recently developed UV curable dielectric meets the membrane switch industry property requirements if properly cured.

## Typical Membrane Touch Switch Configuration



## Membrane Switch With Optional Keyboard

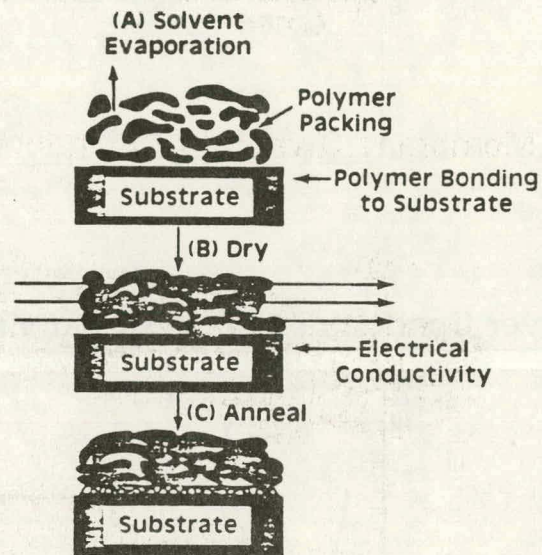




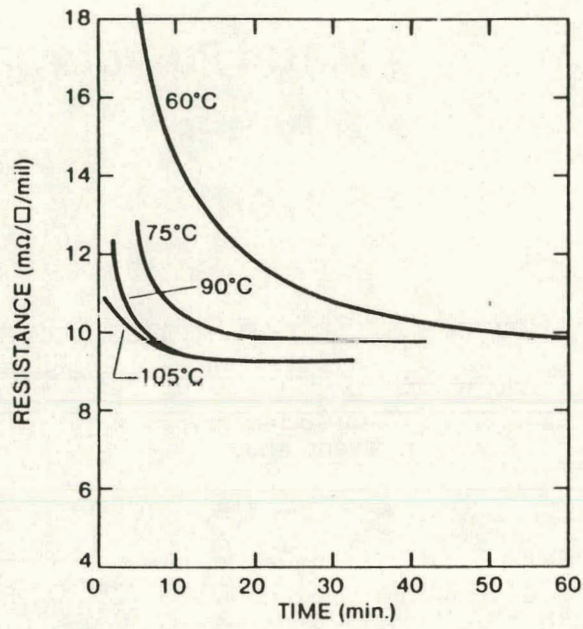
## Key Components of Polymer Thick-Film Conductive Inks

- Metal Powder
- Polymer
- Solvent

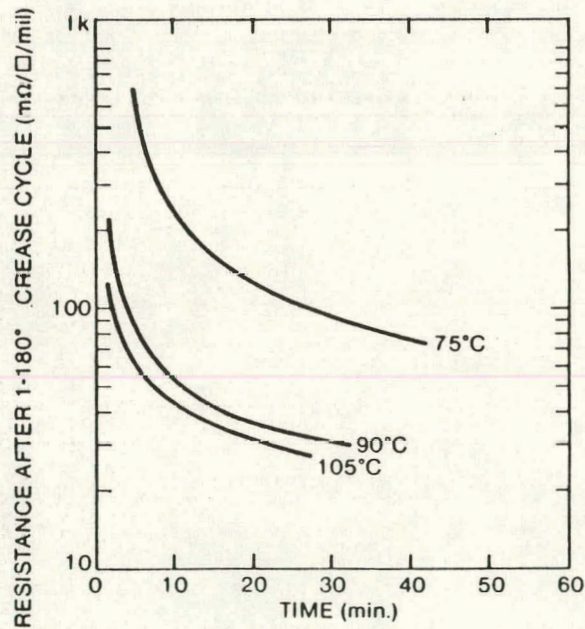
## Air-Dry Process of Screen-Printed Polymer Silver Ink



## 5005 Silver Resistivity vs Drying Conditions

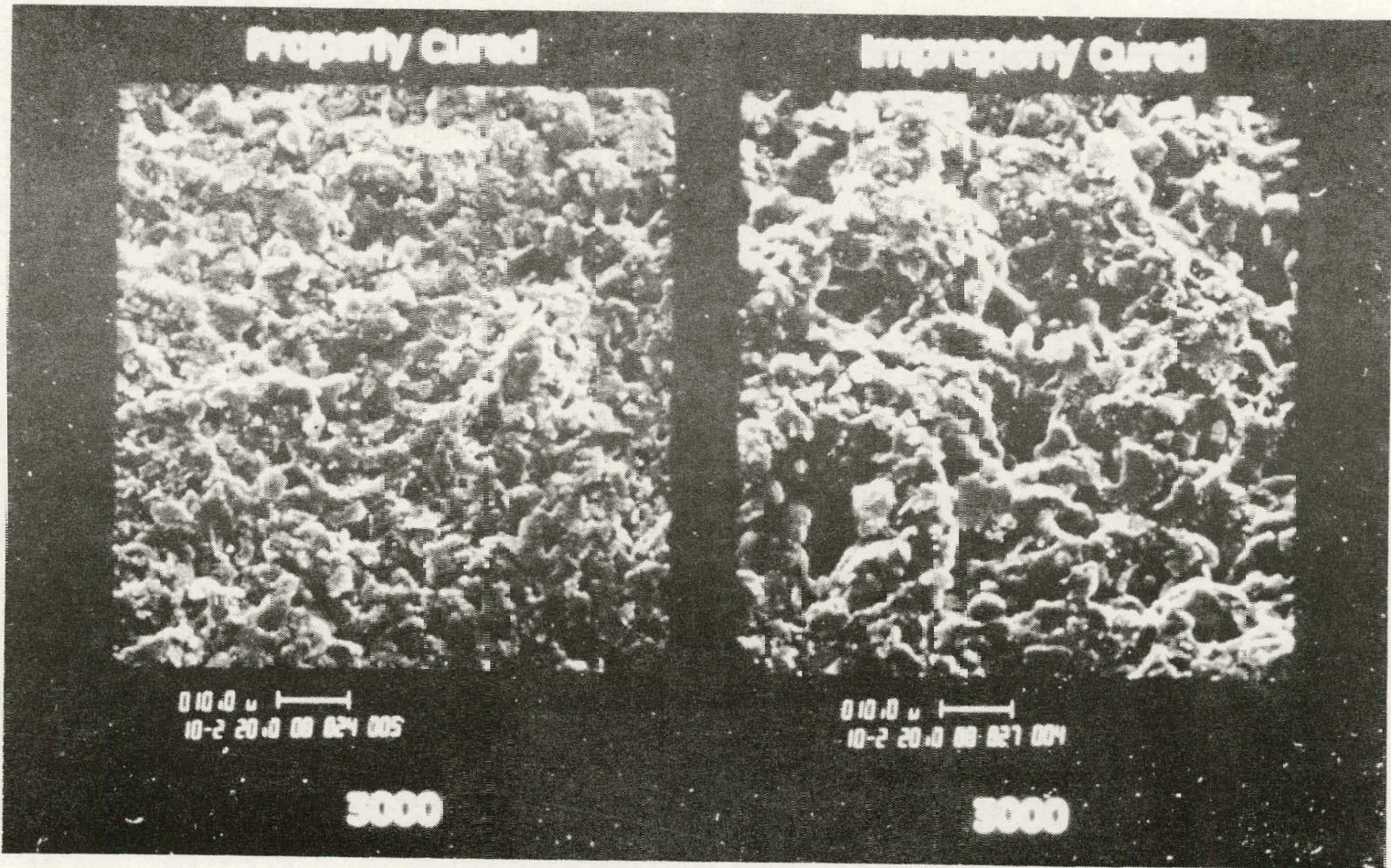


## 5005 Silver Conductor Crease Resistivity vs Drying Conditions



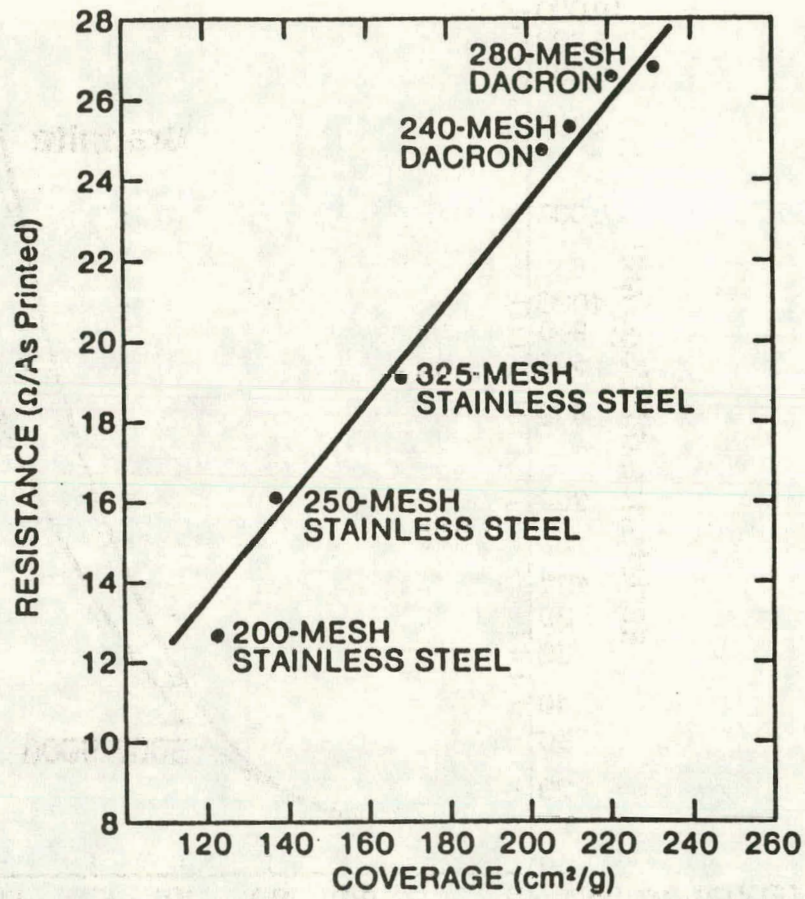


Silver Ink

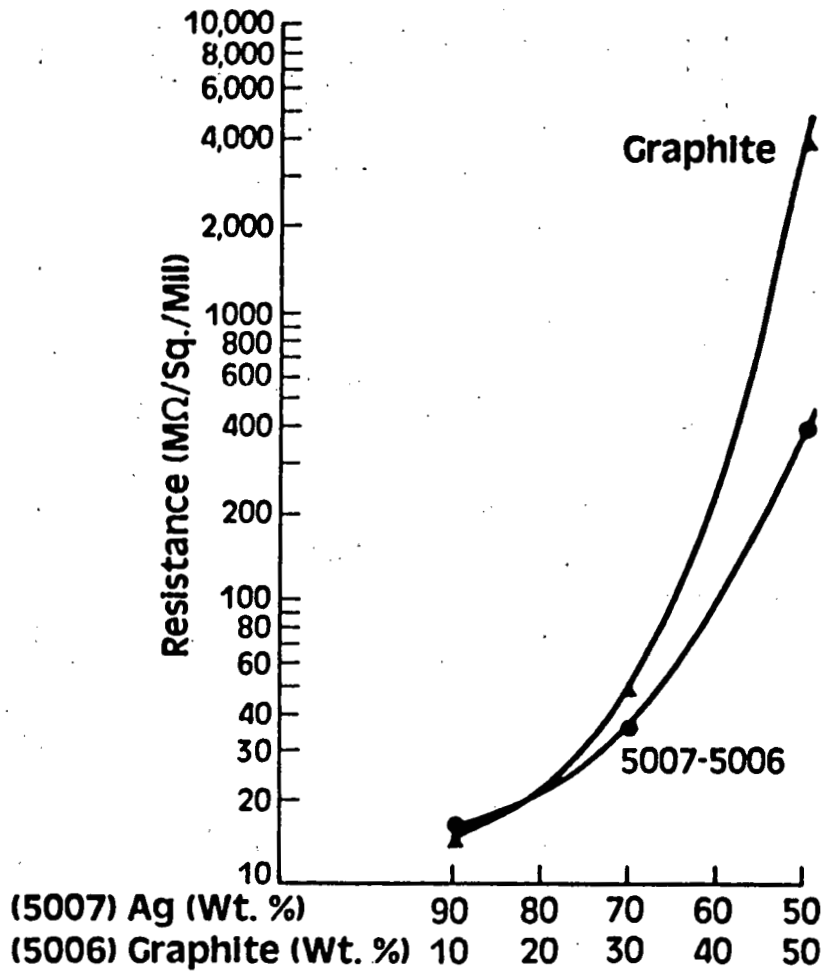




# Resistance vs Coverage of 5007



Blend Curves of 5007-5006 vs Graphite Dried at 120°C 10 min





**Key Industrial Property Requirements  
for Polymer Thick-Film Conductors**

<b>Physical</b>	<b>Test</b>
Sheet Resistivity:	Expressed $m\Omega/sq/mil$
Adhesion:	ASTM D3359-78
Abrasion:	ASTM D3363-74
Flexibility:	ASTM D2176-69
Circuit Temperature Limit:	Tg (DSC)
Contact Resistance:	Mil Std-202, Method 307

<b>Environmental</b>	<b>Test</b>
Thermal Shock:	Mil Std-202F, Method 107D, Test Condition A
Salt Spray:	ASTM B117
Silver Migration:	1000 hr/1V DC/mil gap at 40°C/90% RH
Sulfur:	1000 hr, 500 mg S in 9 liter chamber, 45°C/90% RH
Life at Elevated Temperatures:	1000 hr/85°C
Boiling Water:	2 hr
Humidity:	Mil Std-202E, Method 102 (1000 hr, 60°C/95% RH)

## Performance of PTF Conductors

<u>Processing</u>	<u>Du Pont 5005</u>	<u>Du Pont 5007</u>
Screening equipment	High speed, low temp.	Semi-automatic
Substrates	Polyester, polyimide, epoxy glass, polycarbonate	

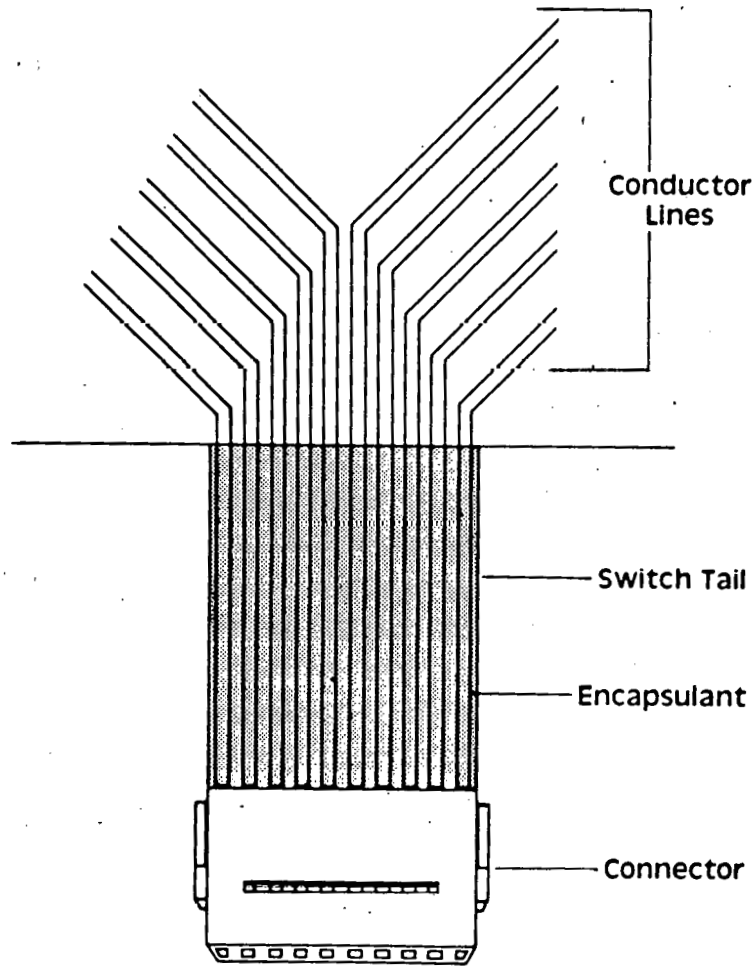
Properties on Mylar® Film                      Governed by time and temperature.

Dry Conditions:	90°C/5 min.	120°C/5 min.
Initial Sheet Resistivity, m <sup>2</sup> /sq/mil	≤15	≤15
Resistivity After Crease Test	90	40
Adhesion (Cross-hatch)	100% pass	100% pass
Abrasion Resistance	≥2H	≥2H
Circuit Temperature Limit	≥70°C	≥70°C

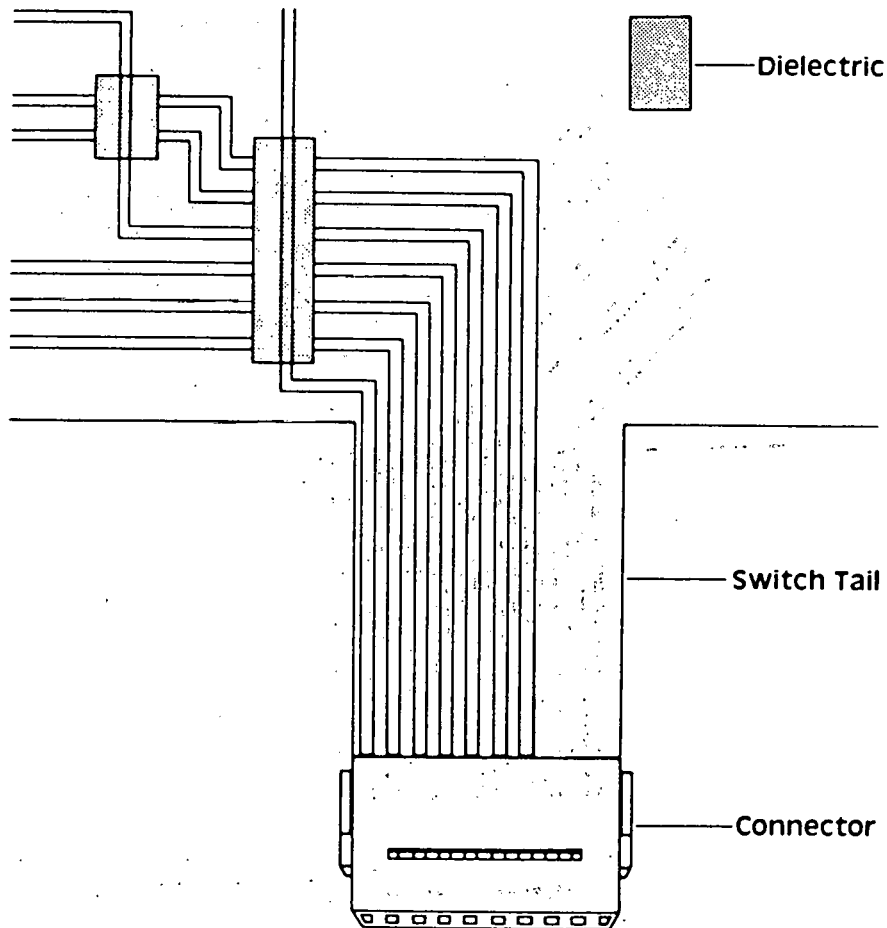
### Environmental Results of 5007 Conductor: Initial Circuit Resistivity = 14.4 ohms

<u>Test</u>	<u>Sheet Resistivity After Test (Ω)</u>	<u>% Change</u>
Elevated Temperature (1000 hr)	14.1	-2.1
Sulfur (1000 hr)	14.3	- .7
Humidity (1000 hr)	14.2	-1.4
Ag Migration (1000 hr)	No migration	N/A
Boiling Water (2 hr)	14.0	-2.8
Salt Spray (500 hr)	13.9	-3.5
Thermal Shock (5 cycles)	14.1	-2.1

# Membrane Touch Switch Termination Tail Encapsulant



## Membrane Touch Switch Insulator to Allow Conductor Crossovers



## Advantages of UV-Curable Dielectric

### Processing

- Rapid Low Temperature Cure
- No Solvent Emissions
- Equipment:
  - Minimal Space Requirements
  - Low Energy Cost

### Physical Property

- Pinhole-Free
- No Solvent Diffusion into Conductor
- Excellent Electrical Properties

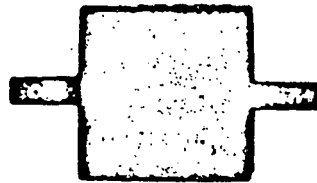
## Key Industry Requirements for Polymer Thick-Film Dielectric

<u>Physical</u>	<u>Test</u>
Abrasion:	ASTM D3363-74
Flexibility:	ASTM D2176-69
Adhesion:	ASTM D3359-78
Pinhole-Free	
Screen Printable	
Low Temperature, Rapid Cure	
<u>Electrical</u>	<u>Test</u>
Breakdown Voltage:	ASTM D150
Dielectric Constant (K):	ASTM D150
Surface Resistivity:	ASTM D257
Dissipation Factor:	ASTM D150

<u>Environmental</u>	<u>Test</u>
Thermal Shock:	Mil Std-202F, Method 107D, Test Condition A
Life at Elevated Temperature:	1000 hr/85°C
Humidity:	Mil Std-202E, Method 102, (1000 hr, 40°C/90% RH)
Salt Spray:	ASTM B117
Ag Migration:	1000 hr; 1V DC/mil gap at 40°C/90% RH
Sulfur:	1000 hr, 500 mg flower of S in 9 liter, 45°C/90% RH

### Effect of Proper vs Improper Cure of Dielectric

Correctly Cured Print



Incorrectly Cured Print



## Performance Results of Du Pont UV-Curable Dielectric 5011 (Properties of Mylar Film With 5007 Conductor)

### Physical

Abrasion Resistance:	≥2H
Flexibility:	No Cracking
Adhesion — (Tape Pull)	
Dielectric to Polyester:	Excellent
Conductor to Dielectric:	Excellent

Odorless

### Electrical

Breakdown Voltage:	>600 V/mil
Dielectric Constant:	<5 at 1KHz
Surface Resistivity:	>10 <sup>11</sup> Ω/sq
Dissipation Factor:	.12%

### Environmental

Thermal Shock (5 cycles)

Humidity (1000 hr)

Surface Resistivity Decreases  
10 to 100 Ω/sq

Salt Spray (240 hr)

\*Capacitance, DF, Adhesion  
and Hardness, Show No Change

Ag Migration (1000 hr)

\*No Ag Migration

Sulfur (1000 hr)

## DISCUSSION

QUESTION: What is the ratio of inorganic constituents to constituents?

NAZARENKO: It has less than 1% -- well, I think it is an inorganic -- it is a pigment to give it color. That is the only reason it is there, and it could be organic. I am not sure exactly what the composition of the pigment is. We have a clear version also, which is 5012, which has no inorganics in it at all.

ROYAL: I think I heard you say that the silver migration problem that apparently went away because there were no ionic impurities that came out -- is that the solution to silver migration?

NAZARENKO: That is one of them, and when I use the term ionic impurities, I am comparing it with a fired system where we have glass frits, and there you have a lot of ionics, which are needed to initiate the silver migration mechanism. In this system we don't use glass frits so we have avoided one potential problem. The other difference is that in fired systems you burn off the organics so you have just metal, sintered metal that is really ready for moisture penetration and reaction. Here we have polymer as a barrier, and because of those two factors we explained, the absence of migration.

WONG: Do people in this area, the thick-film polymer conductor area, usually use thermoplastic polymer?

NAZARENKO: Yes. There are thermoplastics and thermosets. Here we are using thermoplastics because we need flexibility, and thermosets which are crosslinking materials, usually result in a brittle or inflexible product. Thermoplastics are usually more flexible.

WONG: How about from a processing point of view?

NAZARENKO: Also from processing -- crosslinking materials are usually one parts, two parts. The problem with two parts is that they have short pot life. One part usually takes longer to cure than the times that we are indicating here. The industry is driving to faster processing. That is where they see a saving.

WOLF: I noticed that the conductivity in your films is 1/20th of bulk conductivity. It seems the glass-frit, high-temperature-fired inks give you about 1/3 of part conductivity.

NAZARENKO: No. We are talking about 10 to 15 milliohms per square per mil --

WOLF: That makes about 1/20th of bulk conductivity. If you used a bulk conductor you would have 0.6 milliohms.

NAZARENKO: We have polymer in here. So we are never going to achieve the type of conductivity that you are going to get in bulk or fired.

WOLF: I just wanted you to be aware of that.

NAZARENKO: That's right.

WOLF: With solar cells, very high conductivity is necessary.

SOMBERG: People talked earlier about the silver migration problem and people mentioned that possibly what is needed is a coating for the base-metal systems. Would you suspect that the polymers you are using in your system might be applicable to coating a glass inorganic system? Would that be applicable?

NAZARENKO: Possibly. Yes. We have tested the silver migration up to 1000 hours at 60°C/90% RH. I don't know if that is long enough for your application but we feel confident that that silver migration is not a problem.

LANDEL: I didn't get the conditions of that test. What is the voltage applied there?

NAZARENKO: Voltage is applied according to the spacing between the conductive lines. So we did two cases. We did one where the spacing was 8 mils so we applied 8-volt potential. In another pattern we had a 30-mil spacing so in that kind of pattern we used 30 volts. So it is applied to the particular separation.

GALLAGHER: You showed an adhesion test, and you had in parentheses cross-hatched. I am not familiar with that. Could you explain that?

NAZARENKO: This is an ASTM test. It is a Scotch-tape test. But you can semiquantitate it by cutting squares into it, you just lightly etch, say, a grid of 100 squares all the way through, then you put the tape on, and then you pull it off, and then you could count how many squares you pull off. So you can now talk to someone -- otherwise, it is difficult to define what is a pass-test and what is a fail-test.

GALLAGHER: What size are the grids?

NAZARENKO: It depends on your pattern. If you have --

GALLAGHER: Is there any set pattern?

NAZARENKO: No. You just want segments.

HOGAN: Has anyone been successful in utilizing the polymer in thick-film conductor for solar cells?

NAZARENKO. No. I haven't heard of any. The polymer thick-film -- one of the problems with it is that it has poor solderability. Because you have a barrier; you have a layer of organic above the silver particles, say, to wet those silver particles, the silver has to diffuse and get up above this barrier to accept the solder, and that is a problem.

HOGAN: Is there also a barrier at the interface? At the surface -- at the top surface?



NAZARENKO: Yes. At the top surface. So there are ways -- we have a program now going on to try to solve this problem to make these materials solderable. I think you can add to the material system to move the silver up to the surface.

BLAKE: Could you give us a rough idea of the cost per gram of the silver polymer?

NAZARENKO: Again, it depends on the market prices, but at \$10 for silver, it's between 40 and 45 cents.

ADDITIONAL DISCUSSION OF SESSION III

GALLAGHER: Are there any questions from Session III, anything that came to mind for the last speakers?

LANDEL: I have one for the last speaker (Nazarenko) and the audience. What conductivity would be required if you wanted to use such polymeric films for the collectors, and can that be achievable with this sort of system?

GALLAGHER: Do you want to answer that, Martin (Wolf)?

WOLF: My personal feeling is that we need bulk conductivity. So even the sintered silver for the amount of expensive metal you use in this film is basically not good enough. I don't think we can accept 1/20 of bulk conductivity. It would cause much too much shading along with degradation.

GALLAGHER: One other comment I would like to make is, Nick (Nazarenko), I noticed you said you gave those as a function of the thickness in mils. Standard thick films, by the time we fire them, are in the range of about one half a mil, is that correct? Do people buy that? How thick are your films?

NAZARENKO: About a half a mil.

GALLAGHER: Could we just make them thicker before we get to shadowing? Would you buy that?

WOLF: But you are limited by how thick you could go, usually, relative to the width, number one, and number two by process applications. I have my doubts that you can make it 20 times--12 microns thick for line widths of 100 microns.

NAZARENKO: What kind of resistivity are you getting with the fired silver inks?

WOLF: About 1/3 of bulk conductivity.

HOGAN: Just a general question. In light of the new efficiencies, are thick-film contact systems feasible? From the proposed system efficiencies?

GALLAGHER: I think you have to get back to the economics. Agreed that once we get high-efficiency constraints put upon us, we can spend more money on the system but I don't know if we will ever get ourselves to that point in life where we can afford these low conductivities.

HOGAN: You are saying we can spend more money?

GALLAGHER: We can afford more money for the metallization system if we have a 15% module because balance of system costs on the other end are going to go down, so it gives us a bigger chunk of the pot to get there from here. We are rapidly running into that point in life where we can see that we can use an evaporative or sputtered system to obtain a "good"

metallization system; but we don't know what the economics are because nobody wants to spend the money to do the experimentation and development for the required tooling. I don't know how we handle that any more. Somebody has to come up, like an ARCO, and say I am in this business and I am going to spend the money and I am going to make an automated line. And go make the automated line and run it and see what the costs really are. We sit here now and we do things in the laboratory and we make nice cells and we fight very hard to get very large areas and we do get large-area cells with good efficiencies, but we don't make them economically, and we can't produce them in volume.

TAYLOR: On that question, Brian, there are two elements. One is, you have to have somebody who has access to the money to spend but then you have to have somebody who has a conviction that there is a good chance that that will work. And I think that is where a good bit of the problem is, in creating a credibility for an expensive process.

GALLAGHER: I think that is agreed and I think the first speaker this afternoon will give us a feeling for that, won't you, Al (Kirkpatrick)? Because what he is going to talk about is in the same ball park. Somebody had to make a commitment, had to be a champion, it took a lot of money to make the gear when they made it and found out it was worth it. They projected that it would be worth it, and it was worth it.

Anything else on the thick-film session? Remember, all this discussion doesn't die right here. At the end of every session, we can discuss anything that happened earlier, no matter what session it was. At the end of the program, sometime tomorrow morning, we will discuss again, revamp the whole thing if you so desire, so if you get something in your noodle wandering around and you want to find an answer, bring it back.

You had a question?

BLAKE: I was sort of curious as to your personal view on your role in developing base metal inks for thick film systems. Where you thought the research was going to head -- what prospects you saw for it. Because I know for quite a while there had been a number of efforts working very hard on it and up to now nothing has come out that you can actually point to and say this is it. I just wondered where you felt that it was going.

GALLAGHER: When we started at time zero we didn't really have a silver system that was particularly operational. I think we have a silver system that is operational now. I think we have found there were some problems with the systems -- people have always been adding additives but not telling us what they were adding. The program at Spectrolab gave us a cookbook on how to use a silver system. It is available. Looking at thick films, one of the big drivers that drove us in the direction we are going now is the material cost. At that particular time, silver was going up to a pretty high level, so we tried to remove silver (the high-cost material) from the system. With Bernd Ross we have a copper-back system that appears to work. That particular paste isn't available, yet, in industry. The same contract has given us a system that will allow us to put a contact on the back of aluminum fired in

air, used as a back-surface field without removing the oxide of the aluminum, which is a time-consuming and an expensive process. The work we are doing now in the moly-tin system mostly came about because of the rather wide process window we found in it not shunting. That is a very big plus. It looked as if the process window was as wide as a barn door. That is where we are now. The reason for having this Research Forum is to find out, with our dwindling research bucks, where do we put them and how much bang per dollar can we get? You asked me a personal opinion -- it is not going to be my personal decision, it is going to be a consortium of people who have looked at where should we spend this money. That is all I can tell you.

WONG: How good is the conductivity of those systems, what can they achieve, and what conditions we are talking about -- photovoltaic conditions?

GALLAGHER: Well, it looks as if -- you correct me if I am wrong, Martin (Wolf) -- but it looks as if any time we use a thick-film material, no matter what it is, we appear at best to get about a third of the bulk resistivity. Is that correct?

WOLF: The noble metals, the base-metal systems, you don't get anywhere near that, it seems.

WONG: Does it blow up, or what?

WOLF: On the bulk conductor, on the noble-metal systems, you get to about one third of the bulk conductivity; with the base-metal systems it seems people are mostly an order of magnitude below bulk conductivity.

GALLAGHER: Are we that bad?

GARCIA: Seven or eight.

GALLAGHER: About one seventh of the bulk?

GARCIA: No. I'm saying that if silver is 0.6 we are at 7 ohm/cm.

GALLAGHER: Thank you.

GARCIA: The thing with the screen-printing technology as it is today, you cannot get a thin enough line to utilize silver properly, so for that reason it might be OK to use a non-noble system with higher conductivity because it is available to the screen-print system.

GALLAGHER: The other thing, of course, is that we are just now getting to that point in life where we are attempting to use ITO to bridge the gap. Use it as dual layer, additionally, as an AR coating, and we are not attempting to optimize it in work we are doing now. As an AR coating we are attempting to optimize it as a adjunct to the resistances we have now.

WOLF: But the solderability is still the problem.

GALLAGHER: Yes, that is correct.

THIS PAGE  
WAS INTENTIONALLY  
LEFT BLANK

SESSION IV: ADVANCED TECHNIQUES

R. Landel (Jet Propulsion Laboratory), Chairman

THIS PAGE  
WAS INTENTIONALLY  
LEFT BLANK

## IONIZED CLUSTER BEAM DEPOSITION

Allen R. Kirkpatrick

Eaton Ion Materials Systems  
Beverly, Massachusetts 01915

Ionized Cluster Beam (ICB) deposition, a new technique originated by Takagi of Kyoto University in Japan, offers a number of unique capabilities for thin film metallization as well as for deposition of active semiconductor materials. ICB allows average energy per deposited atom to be controlled and involves impact kinetics which result in high diffusion energies of adatoms on the growth surface. To a greater degree than in other techniques ICB involves quantitative process parameters which can be utilized to strongly control the characteristics of films being deposited. ICB is easily amendable to process automation and offers opportunity to utilize film character-process parameter closed-loop control routines.

In the ICB deposition process, material to be deposited is vaporized into a vacuum chamber from a confinement crucible at high temperature. Crucible nozzle configuration and operating temperature are such that emerging vapor undergoes supercondensation following adiabatic expansion through the nozzle. Atomic aggregate clusters, each consisting of roughly  $10^3$  atoms, are formed. The clusters can be ionized by impact ionization and then accelerated toward the substrate by a high potential. It is possible to control average energy per atom from a fraction of an electron volt to more than 100eV. Upon impact, the clusters break up in a manner which converts substantial kinetic energy into surface diffusion energy. A number of advantageous phenomena result.

ICB is being utilized for laboratory deposition of semiconductor device metallization, for dielectric films and for semiconductor materials. In general, very high quality films with remarkable characteristics are achieved. ICB is new technology for which applications development is only beginning and prospective applications to photovoltaic devices are yet to be well defined. One important area which can be specified and is already being addressed involves use of ICB for deposition of the active semiconductor materials for thin film cells. Utilization for metallization systems is another possibility which might be of near term importance.

It should be recognized that ICB is a modified vacuum evaporation process for which economic considerations will be similar to those associated with standard evaporation. Consequently it is reasonable to assume that films to be deposited



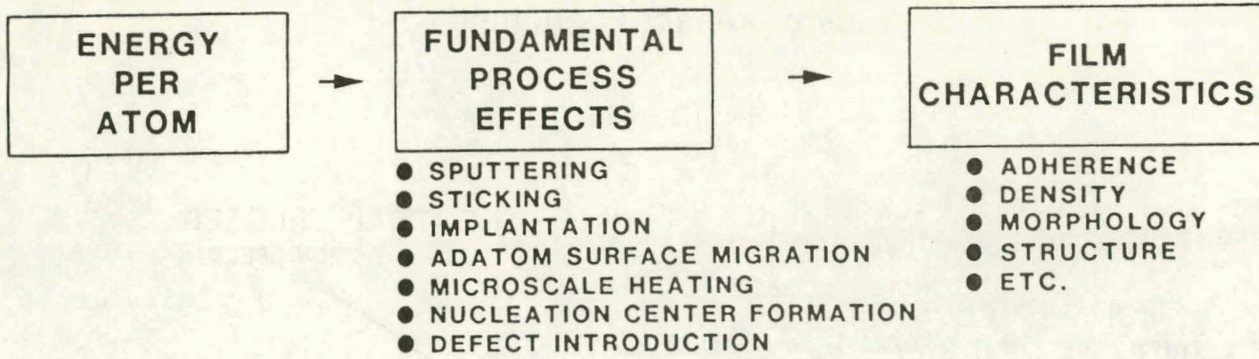
by ICB should be a few microns or less in thickness and probably then must be limited to providing metallization base layers and fine grid patterns. Beyond this constraint ICB offers technical characteristics and process controls which might be very effectively adapted to the needs of advanced photovoltaic metallization systems.

The most important features of ICB relative to deposition of metal films include:

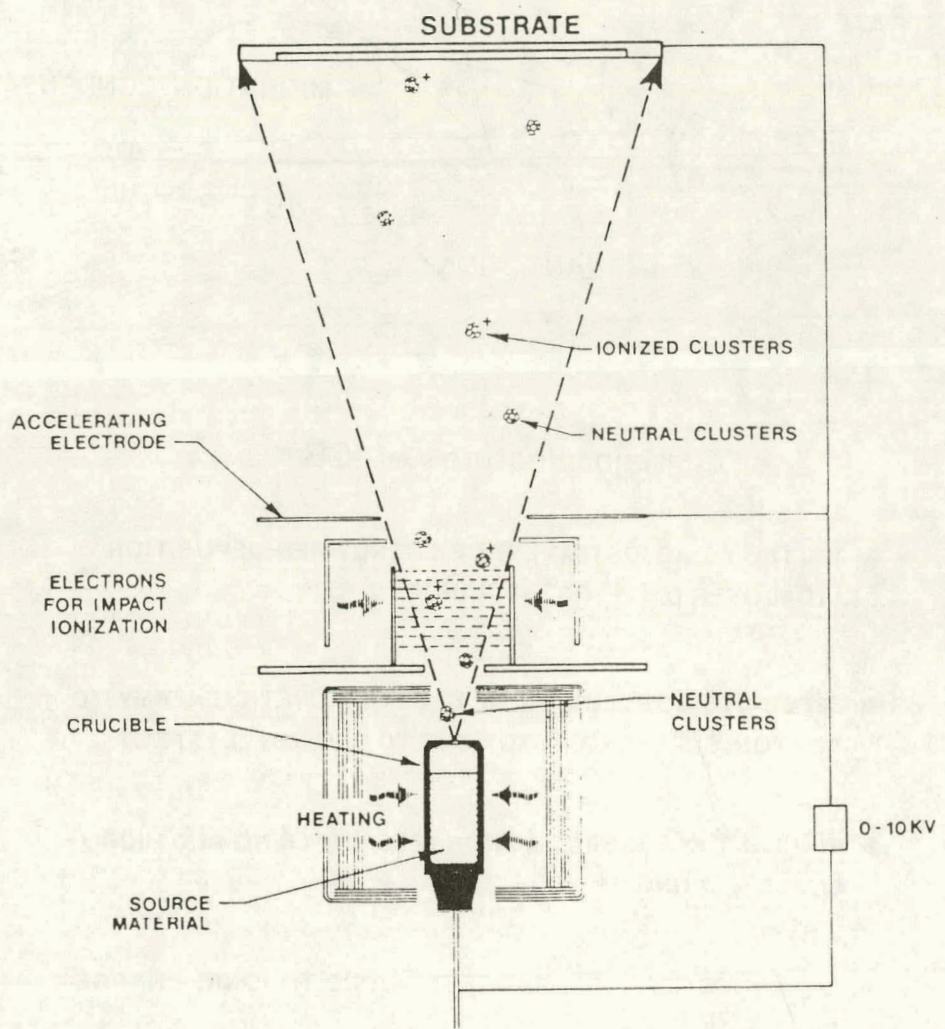
- o Ability to achieve higher quality films onto lower temperature substrates
- o Better process control over film characteristics
- o Spatial directionality of deposition
- o Ease of scale up to very high throughput

Applications if ICB to solve photovoltaic metallization system problems might involve:

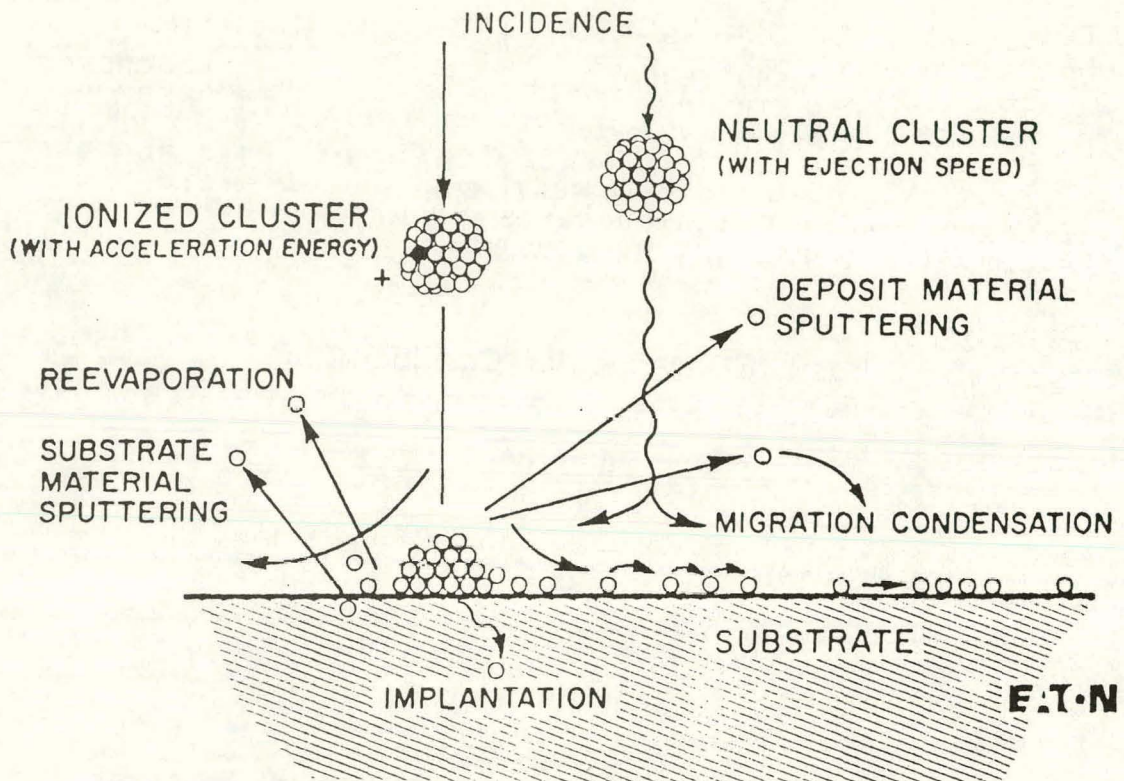
- o Better technical characteristics (structure, adherence, density, morphology, etc.)
- o Lower temperature demands
- o Elimination of interface intrusions with low cost materials
- o Superior long term stability characteristics
- o Compatibility with sequential total device fabrication involving thin film semiconductors and transparent conductive coatings
- o Better compatibility with pattern definition processes
- o Improved material use efficiency
- o Ease of scale up to very high throughputs and total automation



Basic ICB Deposition Configuration



## Cluster Impact Phenomena



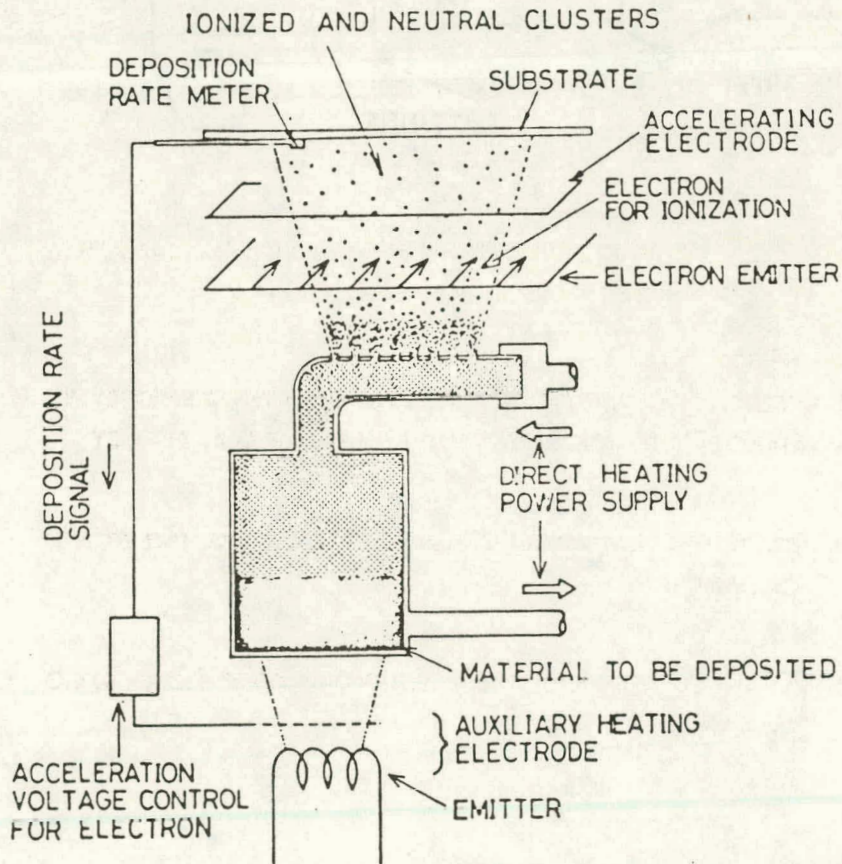
### Major Features of ICB

- ABILITY TO ADJUST AVERAGE ENERGY PER DEPOSITION ATOM OVER 0.01-100<sup>+</sup> eV RANGE
- EFFECTIVE CONVERSION OF CLUSTER KINETIC ENERGY TO ADATOM SURFACE ENERGY DUE TO SNOWBALL EFFECT
- INHERENT CLEANSING ACTION BY SPUTTERING AND MICRO-SCALE HLATING
- ENHANCED REACTIVE PROCESSES DUE TO IONIC CHARGE PRESENCE

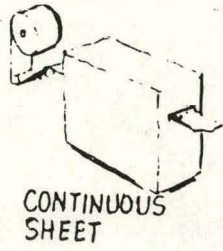
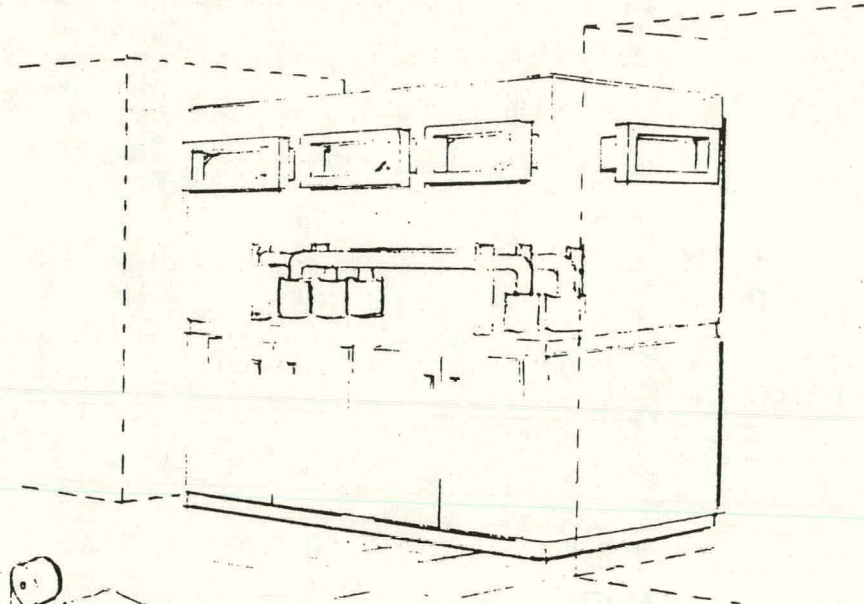


## Materials by ICB to Date

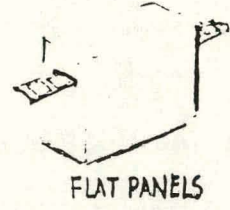
<b>Cu</b>	<b>Si</b>	<b>BeO</b>	<b>Organic Materials</b>
<b>Ag</b>	$\alpha$ -Si:H	<b>GaN</b>	
<b>Au</b>	$\zeta$ -FeSi	<b>ZnO</b>	
<b>Pb</b>	<b>GaAs</b>	<b>SiC</b>	
<b>Al</b>	<b>CdTe</b>		
<b>Au-Sb</b>	<b>ZnS</b>		
	<b>InSb</b>		
	<b>GaP</b>		
	<b>PbTe</b>		
	<b>ZnSb</b>		
	<b>MnBi</b>		



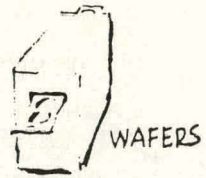
# ICB Production



CONTINUOUS SHEET



FLAT PANELS



WAFERS

## Technical Prospects of ICB for Thin Films

- BULK MATERIAL PROPERTIES
  - CONTROL OF MORPHOLOGY
  - SELECTION OF GROWTH STRUCTURE
  - HIGH T EQUIVALENT PROCESSES AT LOW T
  - PROCESS CLEANLINESS
  - EFFICIENT REACTIVE FORMATION
  - CONVENIENT DOPING
  - QUANTITATIVE PARAMETERS
  - AUTOMATION
  - CLOSED-LOOP CONTROL
  - MATERIAL USE EFFICIENCY
- 
- SCALE UP CAPABILITY
  - VERSATILITY

## Prospective Advantages of ICB for PV Metallization Systems

- BETTER TECHNICAL CHARACTERISTICS (STRUCTURE, ADHERENCE, DENSITY, MORPHOLOGY, ETC.)
- LOWER TEMPERATURES
- ELIMINATION OF INTERFACE INTRUSION EFFECTS WITH INEXPENSIVE METALS
- SUPERIOR LONG TERM STABILITY CHARACTERISTICS
- TOTAL DEVICE FABRICATION COMPATIBILITY
- BETTER COMPATIBILITY WITH PATTERN DEFINITION PROCESSES
- IMPROVED MATERIAL USE
- EASE OF SCALE UP TO VERY HIGH THROUGHPUTS AND TOTAL AUTOMATION

## DISCUSSION

SCHRODER: If you deposit a compound nonreactively I assume you need one crucible per material.

KIRKPATRICK: It depends upon the material. If you have a material like cadmium telluride where the vapor pressures of the two constituents are similar then you can put cadmium telluride into the crucible; but if you want to deposit something like gallium arsenide you need a gallium crucible and an arsenic crucible.

CAMPBELL: Have you ever done any of the refractory metals, like titanium or sodium?

KIRKPATRICK: No. Everyone asks; you have to be able to get reasonable vapor pressure of those metals. Now, I think maybe titanium you can do, but a lot of people ask about tungsten and molybdenum; we make the ion sources out of those metals. It's not out of the question, it depends upon work that has never been done utilizing organometallics, and I think some work will be done on that, but I don't know the answer yet.

BACHNER: What's a piece of equipment like that cost?

KIRKPATRICK: About a half million dollars.

HOGAN: With something like silicon, how do you do the doping?

KIRKPATRICK: You bring in phosphine or diborane as background gas.

HOGAN: What happens if you go to a higher than a 50% cluster ion position?

KIRKPATRICK: Nothing, I think you just end up breaking up some of the cluster and you just don't gain anything, it's just not necessary.

HOGAN: Would it be possible then to directly add a direction to those clusters, to the substrate?

KIRKPATRICK: Yes, because experiments have been done on that, but I think it would be impractical to try and do it now, for real films. I see that as maybe occurring in maybe 10 years or so that you could do directional beaming. It's kind of like ion implantation; when ion implantation first came out 20 years ago, everybody said "Gee, this is the way to do doping, just where we want it." The first machines for that are just hitting the market now. It has taken 20 years for the machine technology to come along and I think the same will be true with ICB.

SCHWUTKE: I would like to congratulate you, if all these things work the way that you explain them, it's a wonderful machine, with a terrific list of all the good things it can do. Would you like to comment on what can go wrong?

KIRKPATRICK: I don't want to be too glib, I don't know what can go wrong. We built machines, more or less, to the instructions of the people in Japan who invented the process and the first several machines that we've

built, the customers were waiting there for them the moment they were finished and they checked them out and took them away and we didn't get any operating experience ourselves. One week ago our own machine became operational, and we now have a laboratory where we are doing our own work. Very soon we will have two machines in there, and people will be invited to come and see this process.

SCHWUTTKE: What is the reliability of the ion sources, how long can the source operate what kind of power do you use, and what kind of crucible material are you using? Would you like to comment on that?

KIRKPATRICK: Sure, can I start with crucible material? Our standard crucible now is POCO graphite, semiconductor-grade graphite cleaned up after machining by high temperature, storage in chlorine gas; for most deposition materials that crucible lasts a long time, and --

SCHWUTTKE: What's a long time? A year, a day, an hour?

KIRKPATRICK: I don't know, nobody's run one long enough to wear it out. If you are doing a metal that doesn't wet the graphite you just keep putting in new charge; if you deposit silicon from that crucible you form silicon carbide on the crucible surfaces and the crucible becomes embrittled and after refilling the crucible about three times, you are better off to throw it away because eventually it will crack. The ion sources are difficult to build. Our first ones have deteriorated after running for a few months, and we have to replace many of the components, but I think there's just engineering experience needed there.

SCHWUTTKE: What are the dimensions of the ion source?

KIRKPATRICK: About the size of a tomato-juice can.

SCHWUTTKE: So you can actually load this thing up, or what? Do you put silicon in it? You can put in a kilo of silicon?

KIRKPATRICK: No, the crucible is smaller. You could build larger crucibles; our crucibles have 10 cc charge capacities, so you can put in 10 cc of silicon.

SCHWUTTKE: And then, theoretically, you could run this machine continuously for how long? Deposition, I mean.

KIRKPATRICK: I don't know. Until the crucible runs out.

SCHWUTTKE: There are there other problems when things are in operation for some time. I try to find out if it can run two minutes or two hours continuously.

KIRKPATRICK: Oh, you can run it two hours continuously, they probably have been run a week continuously and then needed maintenance but I think production machines will run like production ion implanters.

SCHWUTTKE: But you have no real data from Japan.

KIRKPATRICK: Not yet.



SCHWUTKE: We just assume that the machine will do certain things.

KIRKPATRICK: Oh, no. The Japanese complain very loudly when a machine doesn't work.

COMMENT: What about when it does work? They don't complain.

COMMENT: How long have you been in the field?

KIRKPATRICK: We delivered the first of these machines last summer, so total experience on this equipment is what, maybe eight or nine months.

R. VEST: You mentioned that they have done an epitaxial gallium arsenide on gallium arsenide. Now this is also being done by MBE; what's the advantage of your approach?

KIRKPATRICK: There is a lot less experience on ICB than there is on MBE. I can't tell you about relative material quality, but if ICB can achieve the same material quality as MBE, then ICB has practical advantage totally over MBE. This is a normal high vacuum process, and you can scale it to anything you want to talk about; MBE isn't that way and for high-throughput production equipment, one of the things I should have mentioned, this (ICB) is going to be like sophisticated evaporation or sputtering equipment. It uses the same kind of vacuum components, the same sort of chamber, the same kind of mechanical handling. It needs more power supply, so there will be an incremental additional cost, but it is not anything like a factor of 2.

DUTTA: How do you handle patterns? Do you use shadow masks?

KIRKPATRICK: So far we have not patterned anything except by accident by putting things into the cluster stream. You can certainly do patterning by shadow masks, and the patterns are extremely sharp, even when the mask is a long way away from the substrate. I think you can also do very good patterning with this technique using photoresist and liftoff, because you can deposit the film at low substrate temperature and it will adhere, and it will be easy to do a nice clean liftoff afterward.

AMICK: Allen, would you say what the power consumption used or pulled for a small, 2-mm or larger, source?

KIRKPATRICK: On the small one, when you are running silicon and you are running a few hundred Angstroms a minute, the ion source is drawing about 1500 to 2000 watts. On a curtain source I don't know; I know that you would need approximately 3 kW to keep a 2-foot-long tube hot, and I'm not sure how much goes to heating the reservoir.

AMICK: What about vacuum pumps and the use of associated equipment? What's the total input power?

KIRKPATRICK: I'm sorry, I was counting power supplied to the source. It certainly needs the same kind of vacuum support equipment you have with an evaporator. It is very comparable to electron beam evaporation in total power consumption.

SCHWUTTKE: May I ask the last question, without being facetious, did you get any feedback on the films deposited in Japan on the structure? I mean, do they send you samples or anything of that nature?

KIRKPATRICK: They don't send the samples. I think they are pretty good. The first customer is buying a second machine.

SCHWUTTKE: This is too good to be true. If you are right, and you really can do, and have the control they claim you can achieve, and you go basically from amorphous to single-crystal -- I haven't seen any samples yet. I wonder if you've got some?

KIRKPATRICK: Well, in two or three months, you are perfectly welcome to come and get some samples from us.

SCHWUTTKE: I'll have the same problem that I had with Ovshinsky. He has been promising me samples for a year.

LANDEL: Can you add anything about the uniformity of deposition across the deposition area? Particularly, say, with and without the ionization; with the ionization is the way you like to run it.

KIRKPATRICK: The machine that I showed you a photo of is a single-substrate-at-a-time machine. It brings things in on a walking-beam transport system, and the deposition area is a 7 in. diameter circle, and we guarantee that the process that you can measure -- thickness, whatever -- will be uniform to within +5% over a 10-cm square.

MRIG: Do you have any idea of the efficiency of the amorphous silicon being deposited by the Japanese company?

KIRKPATRICK: No, and I don't think we are going to find out.

MRIG: Can this be made into continuous process somehow, or is it going to be a batch process?

KIRKPATRICK: This is very easily a continuous process.

HOGAN: Getting back to definition, did you say there had not been anything done with photoresist, that you know of?

KIRKPATRICK: Nothing published.

HOGAN: My only concern would be the higher energy and possible polymerization of photoresist caused by microheating.

KIRKPATRICK: You do get microheating, but coming from an ion implanter company, I do know the answer to that. Everyone uses photoresist as an ion implant mask. You are implanting at 60 to 200 Kev, you polymerize the surface of the photoresist but it still comes off.

ZWERDLING: Can you provide a background temperature heating of the substrate deposition surface, if you need it, or is it advisable?

KIRKPATRICK: Yes.

ZWERDLING: Can you deposit amorphous metals other than amorphous silicon?

KIRKPATRICK: I believe you can deposit amorphous metals just as easily as you can amorphous silicon.

ZWERDLING: And with regard to metallization would you be able to deposit diffusion barrier material followed by the metal for the metallization of it?

KIRKPATRICK: I wasn't here yesterday, so what are diffusion barrier materials right now?

ZWERDLING: Well, there is a variety of them.

COMMENT: Titanium, as an example.

KIRKPATRICK: I think so, but I don't know.

ZWERDLING: If you could deposit that as well as metal without breaking the process.

KIRKPATRICK: Yes, in the equipment that we presently sell you have a carousel with many crucibles available to you. You can deposit multiple-layer films without breaking vacuum. You only have one ion source, but you can inject different crucibles with different materials.

METALLIZATION WITH GENERIC  
METALLO-ORGANIC INKS

Geraldine M. Vest

Purdue University

West Lafayette, Indiana 47907

WHAT ARE METALLO-ORGANIC COMPOUNDS?

Metallo-organic compounds are ones in which a metal is linked to a long chain carbon ligand through a hetero atom such as O, S, N, P or As. Films formed by the thermal decomposition of these metallo-organics are called MOD films. In order that the products of decomposition contain only CO<sub>2</sub>, H<sub>2</sub>O, and in rare cases nitrogen compounds, and to avoid S containing products, Purdue's Turner Laboratory pioneered the use of a set of metallo-organic compounds for ink fabrication where the linking hetero atom was oxygen. These inks were made from commercially available carboxylates, or synthesized from commonly available reagents. The processing is described on page 3, and the molecular design criteria on page 4. The particular carboxylates or amine carboxylates selected were the octoates or neodecanoates, and they are described on page 5 with examples given on pages 6, 7, and 8. Currently, metallo-organic compounds have been selected for 25 elements as listed on page 9.

WHAT ARE THE ADVANTAGES OF MOD FILMS?

Both the advantages and the problems involved with MOD films are listed on page 11. The chief advantage for metallizing photovoltaic systems is the low firing temperatures; for example, silver films have been fired on silicon wafers at temperatures as low as 250°C.

MOD PROCESSING AND PROPERTIES

The first step in formulating any ink was to assay the precursor materials and thermogravimetric analysis (TGA) results are given on page 15. Low firing silver films are more important in metallizing photovoltaic systems but more work was done on gold and copper films, and they will be discussed first. A very dense gold conductor film of near theoretical sheet resistivity was developed for firing on alumina substrates. The MOD gold films had adhesion and ultrasonic wire bonding properties that were better than conventional thick film gold. The processing of the MOD gold films is described on page 16.

Adhesion is measured in terms of the force required for detachment of two adhering phases. Separation may take place at the interface, or within the interfacial region, or in the bulk of the weaker phase. Different measurement techniques reflect different failure mechanisms and are, therefore, not directly comparable. For this study, the adhesion was measured by

a pull test performed in a similiar manner to the procedure developed by C. Kuo at CTS, by soldering nail head nickel wires to test pads on the substrates. The pretinned nail head wires were clamped perpendicular to the substrates and hand soldered with Indium Corp. of America flux #1 and 70Sn/18Pb/12In solder. The gold pads were not burnished or pretreated before soldering. An Instron Tensil Tester was used for the pull test, and the adhesion expressed in kg. The adhesion was considered to be excellent if the pull strength was 9.5 kg or above. After the pull test was completed, the pads were inspected for the failure mechanism. Each of the tensile test results were classified into the failure modes described on page 17.

The initial tests with gold MOD films showed very low adhesion, and on examining the fracture, it was determined that the solder had completely alloyed with the gold films. These results were not indicative of the adhesion between the gold MOD films and alumina, but rather the adhesion between a Sn-Pb-In-Au alloy and alumina. In order to circumvent this problem, a diffusion barrier layer of Ni or Pt was inserted between the gold and the solder. Metal films of platinum or nickel, approximately 5000 angstroms thick, were sputtered onto the adhesion test pads through metal masks. Before sputtering, the films were cleaned ultrasonically in acetone, methanol, and DI water. The coated conductor patterns were fluxed with Kester 15-44 solder flux and dipped for three seconds in a 60Sn/40Pb solder pot at 200°C. Except for a different solder composition and flux, the previously described procedure for nail head pin attachment was used. Both small pins (diameter 0.05 cm) designated S and large pins (diameter 0.09 cm) designated L, each having a head diameter of 0.127 cm, were used because several of the initial failure modes involved breaking the pins. A summary of the adhesion data for the MOD films is presented on page 18 along with data for Engelhard's conventional mixed bonded gold ink A-3770 and their MOD (mercaptide chemistry) ink A-3725 for comparison.

Wire bonding data for the MOD gold films were obtained using a Kulicke and Soffa Ultrasonic Wedge Bonder. The semicircular loop geometry for attaching Al wires to the gold film is shown on page 19. Twenty five bonds were made on each sample. The test involved putting a small hook through the loop and pulling the wire to failure; the load and failure mode were then recorded. From a side view of the wire loop, the bonded ends look like feet; thus the failure modes were described as a "heel break" or a "foot lift". For a foot lift, the failure occurs by the aluminum wire lifting off of the gold conductor, and it may or may not bring the conductor with it. A heel break refers to a failure mode in which the aluminum wire breaks adjacent to the bonding area where its diameter was reduced during the bonding operation. In general, a heel break is the desirable failure mode because it indicates that the aluminum wire to gold conductor bond was stronger than the aluminum wire after bonding. However, both the mean pull strength and the failure mode are functions of the machine parameters and the bonded wire geometry. The wire bond results for 25 tests on each of the MOD gold films along with the results with conventional thin and thick films are presented on page 21. A summary of the effects of additions to gold in the films is given on page 21, and a summary of the Au film properties is given on page 22.

A screen printable copper ink, developed from an aqueous solution of copper nitrate trihydrate, produced solderable Cu films with good electrical conductivity and adhesion on POS substrates. The chemistry is listed on page 23 and the processing on page 24, and the Cu film properties are summarized on page 25.

Silver inks that could be screen printed or ink jet printed were formulated, and dense Ag films with good conductivity and good adhesion were obtained when they were fired on several substrates. The procedure for making silver neodecanoate is given on page 26, and the processing of screen printable and ink jet printable inks are given on page 27. Substitution of  $\alpha$ -terpineol for xylene was necessary for the screen printable ink because of the high vapor pressure of xylene. A summary of the Ag film properties is given on page 28. It should be pointed out that 1 w/o Pt is adequate for solder leach resistance for conventional thick films, but the MOD films are so thin that 4 w/o Pt was required.

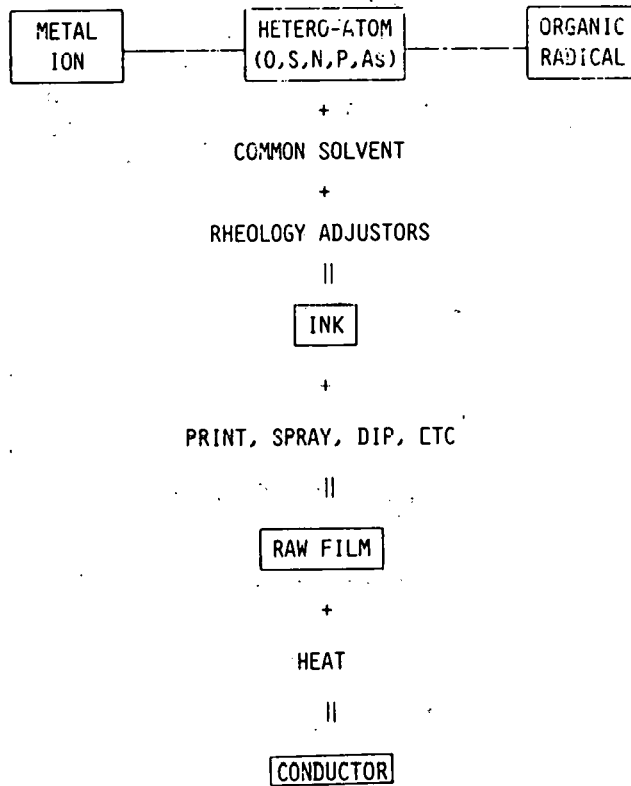
#### WHERE ARE WE?

The metallo-organic inks that have been formulated during the last three years in the Turner Laboratory at Purdue University along with the properties of the fired MOD films are summarized on pages 30 and 31. A great deal of additional work must be done in the area, and we have only scratched the surface of what might be accomplished with low firing temperature metallization.

Page 2.

- 1. WHAT ARE METALLO-ORGANIC COMPOUNDS?
2. WHAT ARE THEIR ADVANTAGES?
3. MOD PROCESSING AND PROPERTIES
4. WHERE ARE WE?

Page 3. MOD Film Processing

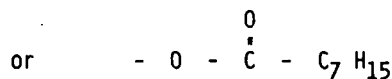
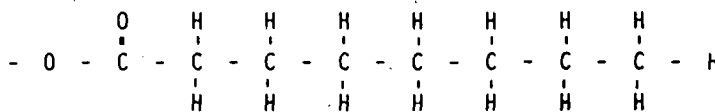


## Page 4. Molecular Design Criterion

1. As the chain length of the organic radical increases:
  - a) the solubility of the compound in organic solvents increases;
  - b) the metal content of the compound decreases.
2. The solubility of the compound increases if the organic radical is branched.

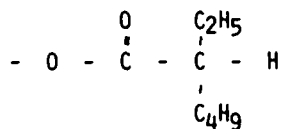
## Page 5.

### NORMAL OCTOATE.



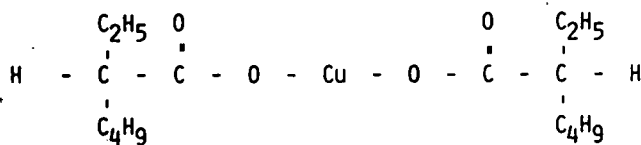
### BRANCHED OCTOATE

#### 2-ethylhexoate

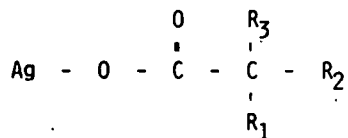




Page 6. Structural Formula for Copper 2-Ethylhexoate

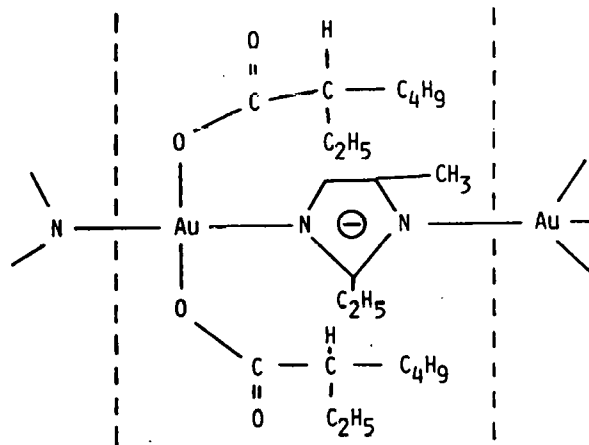


Page 7. Structural Formula for Silver Neodecanoate



The number of carbon atoms in  $\text{R}_1 + \text{R}_2 + \text{R}_3 = 8$

Page 8. Structural Formula for Gold Amine 2-Ethylhexoate



## Page 9. Turner Laboratory Compounds

### 2-ETHYLHEXOATES

Bi, Cd, Co, Cr, Cu, Ga, In, Ir, Ni, Pb, Rh, Ru, Si, Sn, Y, Zn, Zr

### AMINE 2-ETHYLHEXOATES

Au, Pt

### NEODECANOATES

Ag, Ba

### OTHER

B Pyridine  
Pd Acetate  
Sb Butoxide  
Ti 2-Ethylhexoxide

## Page 10.

1. WHAT ARE METALLO-ORGANIC COMPOUNDS?
- 2. WHAT ARE THEIR ADVANTAGES?
3. MOD PROCESSING AND PROPERTIES
4. WHERE ARE WE?

ADVANTAGES	FABRICATION	PROBLEMS
ELIMINATE VARIATIONS IN INGREDIENT MATERIALS.	FORMULATION	LIMITED INFORMATION AVAILABLE ON PURE COMPOUNDS
ELIMINATE VARIATIONS DUE TO BLENDING	INK	LOW INORGANIC CONTENT
VARIETY OF PRINTING TECHNIQUES POSSIBLE	FILM	MORE DIFFICULT TO CONTROL VISCOSITY
LOWER FIRING TEMPERATURE	COMPONENTS	LARGE VOLUME OF VOLATILES
	<u>PROPERTIES</u>	
IMPROVED WIRE BONDING	CONDUCTORS	HIGHER SHEET RESISTANCE
REDUCED LASER TRIM EFFECTS	RESISTORS	RESISTANCE RANGE MAY BE LIMITED
PIN HOLE FREE	DIELECTRICS	DIELECTRIC CONSTANT VALUES MAY BE LIMITED

## Page 12.

1. WHAT ARE METALLO-ORGANIC COMPOUNDS?
2. WHAT ARE THEIR ADVANTAGES?
- 3. MOD PROCESSING AND PROPERTIES
4. WHERE ARE WE?

TO DEVELOP THICK FILM GOLD CONDUCTORS  
TO INCREASE THE RELIABILITY OF ULTRA-  
SONIC ALUMINUM WIRE BONDS.

### APPLICATION

NEXT GENERATION OF HYBRID MANUFACTURING  
TECHNOLOGY.

## Page 13.

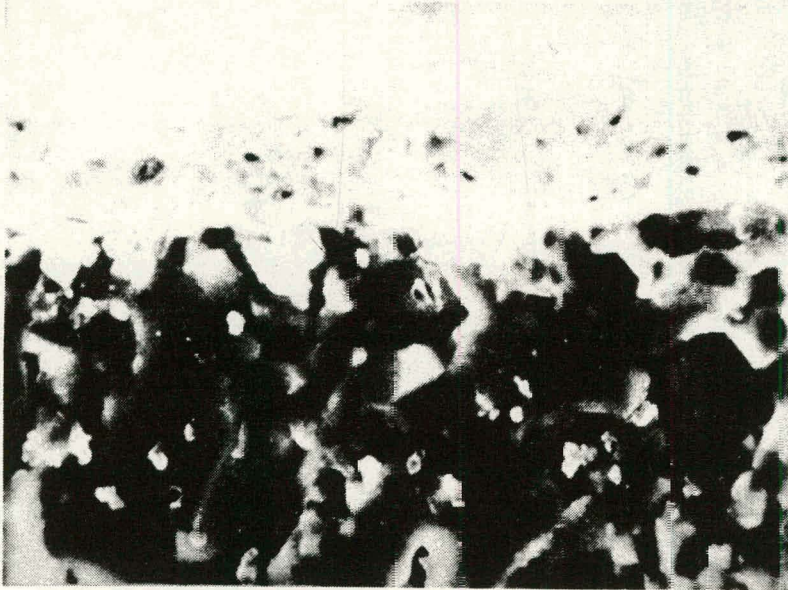
### PROBLEM

TO DEVELOP THICK FILM GOLD CONDUCTORS  
TO INCREASE THE RELIABILITY OF ULTRA-  
SONIC ALUMINUM WIRE BONDS.

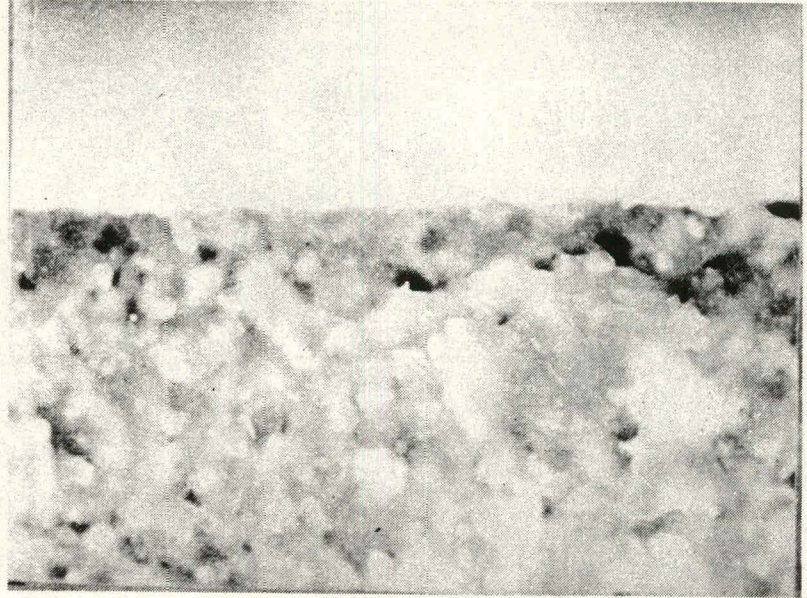
### APPLICATION

NEXT GENERATION OF HYBRID MANUFACTURING  
TECHNOLOGY.

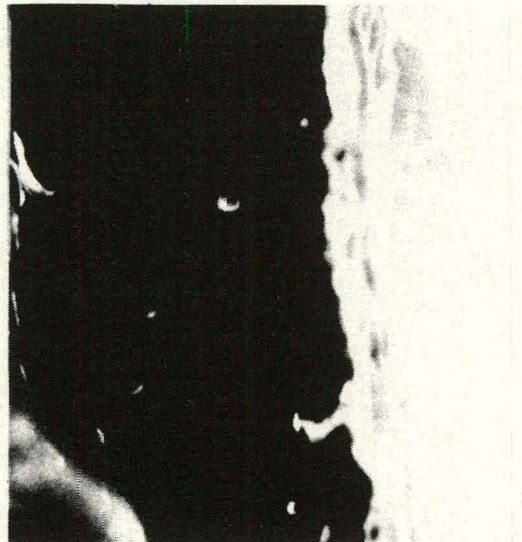




Conventicnal 500X



MOD 500X



MOD 1000X

## Page 15. TGA Results

Saturated solutions heated in air at 10<sup>0</sup>C/min.

Compound	T <sub>decomp.</sub>	w/o Product
Ag neodecanoate	250	15 Ag
Au amine 2-ethylhexoate	600	18 Au
Pt amine 2-ethylhexoate	400	18 Pt
Bi 2-ethylhexoate	350	16 Bi <sub>2</sub> O <sub>3</sub>
Cu 2-ethylhexoate	300	4 CuO
Rh 2-ethylhexoate	225	8 Rh
Pd acetate trimer	225	3 PdO

## Page 16. Processing Gold Films

1. ASSAY MOD PRECURSORS
2. MIX MOD COMPOUNDS +3 w/o PENZOIL'S MINERAL JELLY #20
3. PLACE SOLUTION IN AN OPEN BEAKER AT 50<sup>0</sup>C UNDER A VACUUM OF 67 Pa FOR 24 HOURS
4. SCREEN PRINT WITH AREMCO 3100 ON 3M'S AISIMag 838 SUBSTRATES, 325 MESH S.S. SCREEN
5. BATCH FIRE THE SAMPLES
  - Sequence 1: 10 minutes each at the following temperatures: 120, 350, 500, 850<sup>0</sup>C
  - Sequence 2: same as above except reducing the second temperature to 300<sup>0</sup>C and firing for 20 minutes
  - Sequence 3: IR drying + 850<sup>0</sup>C/10 minutes

## Page 17. Adhesion Failure Modes

- A. Separation of the pad from the substrate
- B. Separation within the solder fillet
- C. Separation between the wire and the solder fillet
- D. Fracture of the substrate
- E. Pin breaks

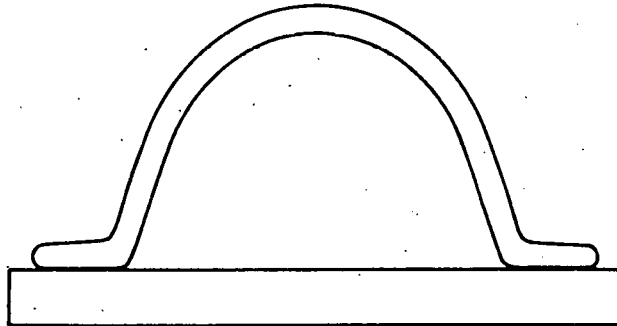
## Page 18. Summary of Adhesion Data

Composition B1	(w/o)*		Barrier Layer	Pin Size	Load (kg)		Failure Mode				
	Cu	Pd			Mean	S.D.	A	B	C	D	E
1.5	-	1.5	Pt	S	9.1	0.6	1	-	-	-	4
			Pt	L	8.1	2.3	10	8	1	-	-
			Ni	L	8.8	1.8	1	1	-	-	-
1.0	-	1.5	Pt	S	7.0	1.1	9	1	-	-	-
			Pt	L	7.2	2.8	10	-	-	-	-
0.5	-	1.5	Ni	L	10.7	1.9	5	-	-	3	-
0.25	-	-	Ni	S	7.4	1.0	3	3	-	-	-
			Ni	L	8.7	1.0	1	2	-	-	-
-	-	1.5	Ni	S	3.1	1.5	6	-	-	-	-
1.5	0.1	1.5	Ni	L	9.5	1.2	3	7	-	2	-
1.0	0.1	1.5	Ni	L	7.6	1.8	3	5	3	12	2
0.25	1.0	-	Pt	S	7.3	1.2	9	1	-	3	-
A-3770			Ni	L	5.9	1.8	12	-	-	1	-
A-3770			none	L	5.9	1.5	10	-	-	3	-
A-3725			Ni	L	4.2	1.2	11	-	-	-	-

\*Inks also contained 0.1 w/o Rh, balance Au.

## Page 19. Ultrasonic Wedge Bonder

MODEL 484  
KULICKE + SOFFA  
S/N 1904



FOOT TO FOOT

LINEAR DISTANCE =  $.125 \pm .001$  cm

BONDED WIRE HEIGHT  $\approx .035$  cm

Al WIRE (1 w/o Mg) 25  $\mu$ m THICK



## Page 20. Aluminum Wire Bond-Test Results

Firing Sequence	No. of Layers	w/o Bi*	Pull Strength (g)		Failure Mode	
			Mean	S.D.	H.B.	F.L.
#2	2	0.5	5.24	1.89	3	22
#2	2	1.0	5.24	1.79	9	16
#2	2	1.5	6.26	1.27	1	24
#2	2	2.5	6.78	1.03	19	6
#2	3	0.5	7.16	1.45	8	17
#2	3	1.0	9.58	1.28	20	5
#2	3	1.5	9.16	2.23	8	17
#2	3	2.5	8.28	1.15	25	-
#4	3	1.5	7.28	1.07	25	-
			8.04	1.23	25	-
#4	3	1.5	8.32	0.95	22	3
Conventional thin film			11.18	1.03	25	-
Conventional thick film			7.9	1.3	24	1

\*All inks also contained 0.1 w/o Rh, 0.1 w/o Cu, 1.5 w/o Pt, balance Au.

## Page 21. Additions to MOD Gold Films on Alumina Substrates

Rh AT LEAST 0.1 w/o Rh IS NEEDED FOR FILM FORMATION.

Cu ADDITIONS OF 1.0 w/o Cu DOUBLE THE  $\rho_s$  WITH NO SIGNIFICANT EFFECT ON ADHESION WHILE ADDITION OF 0.1 w/o IMPROVED ADHESION AND AI WIRE BONDING PROPERTIES WITHOUT DRASTIC EFFECTS ON  $\rho_s$ .

Pt EITHER Pd OR Pt IMPROVES ROOM TEMPERATURE WIRE BONDING AND ADHESION PROPERTIES WITHOUT SIGNIFICANTLY CHANGING THE  $\rho_s$ . SINCE Pd OR Pt ALSO IMPROVE THE SOLDER LEACH RESISTANCE OF Au FILMS  $\approx$ 1.5 w/o WAS ADDED.

Bi BISMUTH INCREASES ADHESION AND WIRE BONDING PROPERTIES AND THE OPTIMUM MAY BE 1.5 w/o Bi.

## Page 22. Au Film Properties

1. Raw materials are pure generic materials - anyone can fabricate films from the formulas.
2. Films can be conventionally processed.
3. Films have better adhesion and wire bonding properties than commercial thick film.
4. The film resistivities approach that expected for pure gold.
5. The microstructure shows that the films are very dense and thickness measurements show that the films are 0.5  $\mu\text{m}/\text{layer}$ .

## Page 23. Chemistry of the Copper Ink

COMPOUND	w/o
Cu nitrate trihydrate	67.4
water	28.8
methyl cellulose (4000 CP grade)	2.2
boron oxide	0.9
Ross Chem's Foam Burst 370	0.7

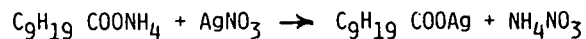
## Page 24. Processing Copper Films

1. The  $B_2O_3$  was added to the water. The methyl cellulose was then added, and several hours were necessary for it to dissolve. Next the Cu nitrate was added, and after it dissolved the Foam Burst was added. The ink was allowed to stand for one day.
2. The ink was screen printed through a 165 mesh S.S. screen on POS substrates.
3. The best firing sequence was to air dry at  $50^{\circ}C/1$  hour + air dry at  $230^{\circ}C/20$  minutes + fire in a 4%  $H_2/96\%$   $N_2$  atmosphere at  $650^{\circ}C/20$  minutes. The samples were cooled to  $100^{\circ}C$  before they were removed from the  $H_2/N_2$  atmosphere.

## Page 25. Cu Film Properties

1. A one layer film ( $8 \mu m$  thick) fired on POS gave  $14 m\Omega/sq/25 \mu m$ , another two layer film ( $9.9 \mu m$  thick) fired on POS gave  $19 m\Omega/sq/25 \mu m$ .
2. For room temperature aging, the sheet resistance increased by  $\approx 0.5\%$  in the first few hours, remained constant for times to 400 hours, increased to 5% after 1000 hours, then remained constant to 2000 hours.
3. Samples were dip soldered with 63% Sn - 37% Pb at  $250^{\circ}C$  - films were completely tinned.

## Page 26. Synthesizing Silver Neodecanoate



1. The acid was added to base and stirred, a clear solution resulted.
2. The  $\text{AgNO}_3$  plus some  $\text{H}_2\text{O}$  was added and stirred and a white cloudy ppt resulted.
3. Xylene was added ( 25 cc for 10 g acid) and 2 immisible liquids were formed.
  - Liquid 1 is  $\text{C}_9\text{H}_{19}\text{COOAg}$  in xylene
  - Liquid 2 is  $\text{NH}_4\text{NO}_3$  (aq)
4. The liquids were poured into a stoppered funnel and the bottom liquid was removed. This more dense liquid was the  $\text{NH}_4\text{NO}_3$  (aq) solution.
5. The top solution was filtered and additional xylene was removed by bubbling air through the solution until a saturated solution was obtained.

## Page 27. Processing Silver Films

1. After adding  $\alpha$ -terpineol to a mixture of saturated xylene solutions of both Ag neodecanoate and Pt amine 2-ethylhexoate the solvents were exchanged.
2. Ethyl cellulose in  $\alpha$ -terpineol was added to adjust the rheology for screen printing.
3. The ink was screen printed through a 325 mesh screen on various substrates.
4. The ink was dried at 150°C/10 minutes then fired at 150  $\rightarrow$  350°C for various times.

### INK JET PRINTING

1. Saturated xylene solutions of Ag neodecanoate and Pt amine 2-ethylhexoate were directly printable.
2. The alumina substrates were preheated to 30°C and most of the xylene was removed during the printing.
3. The substrates were heated to 210°C/10 minutes then fired at 250°C/10 minutes.

## Page 28. Ag Film Properties

### Screen Printing

1. Silver films have been successfully printed and fired on alumina, POS, ITO, glass and Si at temperatures as low as 250°C.
2. These films pass the "Scotch Tape" test for adhesion.

### INK JET

1. Films have been successfully fired on alumina substrates at 250°C/10 minutes.
2. Lines have been printed as narrow as 7 mils on AlSiMag 838 through a 3 mil orifice on the ink jet printer.
3. A film with composition 4 w/o Pt/96 w/o Ag remained after 30 seconds in 63 Sn - 37 Pb solder but if the Pt was reduced to 2 w/o solder leaching was observed.
4. Sheet resistance values as low as 0.06  $\Omega$ /sq have been obtained.

## Page 29.

1. WHAT ARE METALLO-ORGANIC COMPOUNDS?
2. WHAT ARE THEIR ADVANTAGES?
3. MOD PROCESSING AND PROPERTIES
- 4. WHERE ARE WE?

## Page 30. Where Are We

### Au

A MOD gold ink containing Rh, Bi, Cu, and Pt or Pd has been developed for screen printing on alumina substrates and produces a very dense film with near theoretical sheet resistance. The MOD gold films had adhesion and ultrasonic aluminum wire bonding properties that were better than conventional thick film golds.

### Cu

A screen printable copper ink was developed from an aqueous solution of copper nitrate trihydrate, boron oxide and methyl cellulose that produced solderable Cu films with good conductivity and good adhesion when fired in a reducing atmosphere on POS substrates.

## Page 31. Ag

1. Silver inks that could be screen printed were formulated from Ag neodecanoate, Pt amine 2-ethylhexoate, ethyl cellulose and  $\alpha$ -terpineol.
2. Silver inks that could be ink jet printed were formulated from a xylene solution of Ag neodecanoate and Pt amine 2-ethylhexoate.
3. The MOD inks were fired in air as low as 250°C to produce a Ag film.
4. Adhesion was good on all substrates investigated - alumina, POS, ITO, glass, silicon.
5. Fired films containing 4 w/o Pt/96 w/o Ag were solderable.

## DISCUSSION

WONG: You mentioned, I am referring to silver, about 250°C becomes a safe temperature. Is this the TGA data?

G. VEST: Right. Fired at 10° per minute.

WONG: OK, so 10° per minute is the heating range. What is the equilibrium deposition temperature?

G. VEST: We really haven't done that much with silver, but I do know that we fired, in air, just putting it in the furnace for 10 minutes at 220° and we got a silver film.

WONG: OK. Again, what is the sheet resistivity at that temperature -- 60 milliohm per square?

G. VEST: No, that was on the silicon; we just printed it very quickly on the silicon. I didn't know how to calculate how many squares and I was measuring it with a ruler, so it's about 60 milliohms per square, but that was very, very thin, it may be 1000 to 1500 Angstroms; again, I was measuring it with a ruler, so I hate giving very accurate sheet resistivities.

WONG: You think it is possible to go even lower than 220°C?

G. VEST: I don't know, we haven't tried.

WONG: Are you going to try?

G. VEST: Yes. My students say they were trying 210°C, but that's today.

NICOLET: I am very curious to know what scientific logic or inspiring intuition led you to pick rhodium to create a uniform thin foil rather than osmium or molybdenum or whatever.

G. VEST: We really haven't tried to optimize and look at some of those. Just like bismuth for chemical bonding, we wanted something that worked that had a small amount of foreign material in there. A lot of the literature had rhodium; we just picked it. It's the only one we've tried.

SOMBERG: Would you care to comment about the adhesion properties of silicon relative to what we know about thick-film materials, since there is no frit to bond the silver to the silicon? Would you expect anything different from that system?

G. VEST: With the silver, I don't know why, but it seems to bond to whatever we've tried without adding either any form of glass frit or metallo-organic to make an equivalent of a glass, or putting any chemical binders in there. It's great, but I don't really know why, and I'm just not that familiar with it. This is the first we've ever worked with silicon, as such. I did not clean the wafer; we are going to try



that when I get back. There were Monsanto wafers in a nice little supposedly clean container. We borrowed one, I guess we got one from the Physics Department or the E.E. Department; we just did this on Tuesday, just to see if we could get it to adhere, so it's probably dirty silicon. We haven't done any work with silicon.

TAYLOR: Were these Monsanto wafers epitaxial wafers with a smooth surface?

G. VEST: Yes. I have one, if you would like to see it.

GALLAGHER: Have you ever mixed any of these precursors with a standard thick-film ink and blended it to see, for example, in the problem we have with Spectrolab, that you would get adhesions to the substrate?

G. VEST: Yes, as you'll remember, Bob (R. Vest) was talking this morning about making the platinum ink. The lowest particles -- well, you couldn't call it particles, I suppose there was a platinum, a commercial resinate in there.

GALLAGHER: I meant silver, excuse me.

G. VEST: No, no, we've never had any funding on silver. The only reason why we've ever done anything is just that with the ink jet, it was cheaper than gold.

STEIN: Silver metallo-organics are often used in silver thick-film systems along with particles.

GALLAGHER: That's a standard technique?

STEIN: Yes.

GALLAGHER: We never knew they were there.

STEIN: Sorry?

GALLAGHER: We never knew they were there, they were just there.

STEIN: Yes. I don't know who you were talking to, but they are there.

G. VEST: We have played around a little bit. I shouldn't say we've done nothing, because we did do a silver film for an industrial application, though we did wind up having some silver metallo-organic in there.

WOLF: I notice that your prints were rather thin but close to bulk conductivity, and your copper prints were rather thick but in an order of magnitude away from bulk conductivity. Was it very spongy or what, have you noticed anything about those copper films?

G. VEST: No, we really haven't looked at them. The copper-film work was just done to test feasibility with using those solution inks to see if we could make a film. We didn't proceed with that any further.

PROVANCE: One of the severe limitations of the Midfilm process is that it puts the film down too thin to withstand the leaching effects of the solder.

I'm wondering if you have done any tests with the silver, or any other metallization to see what the solder leak resistance might be of these films.

R. VEST: We really haven't done that much work with the silver.

PROVANCE: That might be one of the areas for fruitful further research, because the process is very interesting, but in actual application in the field that is one of the very important criteria. We found that once you go below that minimum thickness on any of these printed films you begin to lose both adhesion, because of the leaching effects of the solder, and the solder leaching system resistance. In other words, the film becomes part of the solder.

G. VEST: We did stick the silver film down into some solder for 30 seconds and they stayed there, but that was just a quick, dirty test. Again, had we had funding in silver -- maybe we will get that.

LANDEL: How much of the metallo-organic can you get into your system?

G. VEST: With the ink jet printer, that is a drop on demand, and again it will be computer-controlled. You could make them as thick as you would like to have them.

LANDEL: That's multiple coating. How much silver can you get in the original ink itself?

G. VEST: We have about 15%, but with the ink jet printing, which probably will be the great application for the silver, we mix up 15 weight percent silver in the xylene solution. We preheat the substrate; by the time the drop has arrived at the substrate, the bulk of the xylene is gone, so we will have, very shortly thereafter, silver neodecanoate. I forget what weight percent silver is in that.

LANDEL: But why isn't it 5%, why is it 18%? Why don't you have more in there?

G. VEST: We have to get the silver neodecanoate soluble in xylene.

LANDEL: Have you tried another solvent?

G. VEST: No, we haven't.

LANDEL: Because the decanoate would be relatively insoluble in the xylene, and straight chain hydrocarbon would be a much better solvent. I think there are some things that I would be happy to discuss with you in terms of calculating loading effects. It should be possible to make better than first-order calculations as to what is a good solvent for a given metallo-organic system.

G. VEST: I will say that the reason why we use silver neodecanoate in xylene is that is what GTE sold, and we really didn't want to start synthesizing this. We purchased it that way.

LANDEL: I have some papers from JPL, on other subjects, that would be very useful in optimizing the system. So you ought to be able to increase your concentration of the metallo-organics by quite a bit.

G. VEST: That would be very interesting.

SOMBERG: What are your intentions as far as further work with this is concerned? You mention you didn't have any funding. Maybe Brian Gallagher is the person to talk to here, but it seems very promising.

G. VEST: If we get money, we would be delighted to do whatever we are asked, to study any application. It does seem promising, it just doesn't have much data.

WONG: I'm thinking of the other side of your technique. Regardless of solubility, what is the practical limit for you to lay down a thin film with your technique? What is the thinnest film you can deposit, uniform thin film?

G. VEST: We have always been worrying about how thick we can make, how thin, I really don't know right now. We can get the solubility in xylene; you can add quite a bit of xylene. I really don't know. I have never gone that way. At least, you would have to have a few molecules of silver neodecanoate to decompose, and again as they decompose they fire off the silver an atom at a time. I don't really know what the limit is for making the thinnest film. That would be interesting to work on.

WONG: Do you really need 4% of platinum to get decent solderability --

G. VEST: We tried two and that didn't quite work, so we tried four. We have made two quick attempts. We are just playing around with the silver. We haven't put anything in it.

STEIN: First, I'll make a comment about the question on solderability. You don't need any platinum for solderability, you need it for solder-leach resistance. You can solder to pure silver very readily, too readily. The other question that Wong asked about thin film: you can drop the thickness of these films in an almost infinitely continuous fashion. You can see it go through quarter wave length of light; you can get interference patterns; you can go down to discontinuous films. It is completely controllable.

WONG: In other words, you can make transparent, mechanical films.

STEIN: If you sandwich them, yes, but not by themselves. If you sandwich silver film of this sort between two dielectric layers and make a transparent film.

## DRY ETCHING OF METALLIZATIONS

DAVID BOLLINGER  
VEECO INSTRUMENTS  
PLAINVIEW, NEW YORK

The production dry etch processes from the perspective of microelectronic fabrication applications are reviewed. While for semiconductors, the term "metallization" is generalized to include all conductors, particularly doped polysilicon, the only actual metals extensively used in the large volume semiconductor applications are aluminum based. Aluminum in these applications is in the form of an alloy with silicon (usually 1%) and/or copper (up to 4%) and sometimes in conjunction with a barrier metal such as titanium to prevent diffusion of silicon. Consequently, recent work in dry etching of metals has been concentrated on developing reliable production processes for the aluminum based metallizations. And, only within the past two years, has dry etching of aluminum emerged from the laboratory into production, primarily because of progress in Reactive Ion Etch mode plasma systems, (discussed below) along with the associated gas chemistries.

For dry etching, applications are to thin films with thicknesses usually less than 2 microns and with a pattern defined by a photo resist mask. Dry etching provides the advantages of (1) eliminating disposal of hazardous chemicals, (2) etching materials that are difficult to wet etch, and (3) etching patterns with vertical walls, that is, etching anisotropically. Anisotropic etching is essential to advanced microelectronic devices because: (a) undercut limits line width sizes and corresponding "packing density", (b) loss of cross-sectional area of a conductor causes increased resistance, and (c) a negative slope type undercut, as tends to occur if aluminum etching is not fully anisotropic, makes step coverage by a subsequent layer difficult. For a dry etch application, etch quality criteria which should be considered are: the degree of anisotropy, etch selectivity (with respect to mask and underlying layer), etch uniformity, residue after etching (compare figures 1 and 2) corrosion after etching (a critical consideration with aluminum), thruput requirements, and process reliability.

The major dry etch processes used in the fabrication of microelectronic devices, given in figure 3, can be divided into two categories - Plasma processes in which samples are directly exposed to an electrical discharge, and Ion Beam processes in which samples are etched by a beam of ions extracted from a discharge. The plasma etch processes can be distinguished by the degree to which ion bombardment contributes to the etch process. This, in turn is related to capability for anisotropic etching. Reactive Ion Etching (RIE) and Ion Beam Etching are of most interest for etching of thin film metals. RIE is generally considered the best process for large volume, anisotropic aluminum etching.

### Barrel Type Plasma Etchers

The Barrel Type plasma etch configuration, schematic in figure 4, is usually

a quartz cylinder into which wafers are loaded concentric to the cylinder axis. An RF discharge, with fields applied external to the reactor vessel, fragments the gas into chemically reactive species. A shielding screen may be used to prevent the ionized gas from reaching the wafers. Etching is then primarily, or entirely, by neutral, chemically reactive species. The advantages of barrel type reactors are their high throughput at a low capital cost. The disadvantages are that etching is purely chemical, and therefore isotropic, and that materials for which bombardment is needed to contribute to the etch process (eg.  $\text{SiO}_2$ ) are difficult to etch.

#### Plasma Mode and RIE Mode Plasma Systems

Plasma Mode and RIE Mode planar electrode configurations, figures 5 and 6, have two important differences: (1) RIE operates at a lower pressure ( $< 200$  microns), and (2) for RIE, the wafers sit on a capacitively coupled, RF driven electrode, while for the plasma mode, wafers are on a grounded electrode. In the RIE mode, wafers being etched can take on an average negative self bias voltage with respect to the plasma and, as a result, energetic ion bombardment (in the range of several hundred eV as opposed to less than 50 eV for Plasma mode operation) can contribute to the etch process. The energetic ion bombardment provides the RIE process with its anisotropic etch capabilities (figure 7). Anisotropic etching is possible in the Plasma mode but such processes are much more dependent on polymerization processes to protect the pattern sidewall from undercut than in RIE processes.

As with the barrel etch process, in Plasma mode and RIE chemically reactive species are created by the RF discharge. However, etch mechanisms, and hence etch characteristics, differ as a result of the degree of ion bombardment. In RIE processes for Aluminum, the chemically reactive species are chlorine species produced by fragmentation of molecules containing chlorine (ie.  $\text{BCl}_3$ ,  $\text{CCl}_4$ ,  $\text{Cl}_2$ ,  $\text{SiCl}_4$ ). The surfaces which are etched, those parallel to the electrode to which the wafers are affixed, continuously undergo ion bombardment which cleans the surface of native oxide, or any other reaction inhibiting layer (figure 7). Directional etching can then proceed by the reactive chlorine species forming aluminum chlorides which, having a low vapor pressure, can be pumped away.

Fully automated, cassette-to-cassette, load locked Plasma and RIE mode systems are available. Plasma mode systems, by virtue of their higher operating pressure can have much higher etch rates, thus single wafer at a time as well as batch systems are made. Figure 8 shows the Veeco DV-40 cassette-to-cassette, load locked RIE system for large volume aluminum,  $\text{SiO}_2$  and polysilicon etching.

#### Ion Beam and Reactive Ion Beam Etching

Ion beam etching is accomplished by a collimated beam of ions which is extracted from a discharge by a set of grids (figure 9). Substrates to be etched are affixed to a target plate which must perform the multiple functions of: (1) heat sinking the wafers being etched to prevent overheating, particularly of resist, (2) tilt at an angle with respect to the incident ion beam to give control over the pattern sidewall characteristics, and (3) rotate in the ion beam to symmetrically average the affect of the tilt on the

pattern being etched. Ion beam systems operate at a low pressure, about  $1 \times 10^{-4}$  Torr, to eliminate ion beam - gas molecule collisions in the etch chamber from affecting the etch process. Vacuum pumping by means of a diffusion or cryopump is needed, when using reactive gases cryopumping is generally not acceptable.

For inert gas Ion Beam Etching, in which argon is commonly used, the etch process is purely mechanical sputtering. The sputtering rate is a function of the binding energy between the atoms in the surface being etched. In the case of Reactive Ion Beam Etching, reactive species can chemically change the bonding of the surface atoms thus changing the etch rate. When using the reactive gas  $\text{Cl}_2$ , formation of weaker Al-Cl bonds on the surface can enhance the etch rate from the pure sputtering case of 400 Å/min to over 1,000 Å/min. When  $\text{O}_2$  gas is used, stronger aluminum-oxygen bonding will depress the etch rate to less than 100 Å/min. The advantages of Argon ion beam etching are that: (1) Any material can be etched, in particular, chemically inert materials such as Ni-Fe (bubble memory and thin film magnetic head applications) and gold (high frequency transistor applications). (2) Combinations of materials, alloys and layers can be etched in a single step. (3) Pattern size that can be etched is limited only by the lithography. A characteristic making this process useful for etching electron beam written master chrome glass masks. And, (4) The slope of the pattern sidewalls can be controlled to give good step coverage for subsequent layers. Reactive Ion Beam Etching adds the capabilities of etch selectivity and higher etch rates.

Some of the capabilities of ion beam etching are shown by figures 10-12. In argon ion beam etching bubble memory patterns, figure 10, the aluminum conductor pattern can be etched with a sloped wall to provide step coverage for the subsequent dielectric layer. The Ni-Fe layer must be etched with spacings of less than 1 micron and with vertical walls to give well defined magnetic domains. Tantalum silicide ( $\text{TaSi}_2$ )/polysilicon double-layer "metallizations" which are of interest to replace doped polysilicon to give lower resistivity can be etched anisotropically in a single Reactive Ion Beam Etch process, figure 11, whereas anisotropic etching through both layers is difficult with Plasma and RIE processes, figure 12.

Ion Beam Etching has been used for lower throughput, "specialty" applications in which there are particularly demanding etch requirements. For a large ion beam etch system (eg. Veeco 10" Microetch, figure 13) an application in which 5,000 Å of Ni-Fe or 1 micron of gold are etched, the throughput would be about twenty-five 3" diameter or fifteen 4" diameter wafers/hr. Presently, ion beam etch systems with fully automated wafer handling are not available.



Figure 1. RIE Pattern in 1.2-Micron Al and 2000 Å Over SiO<sub>2</sub> (Photo Resist in Place)

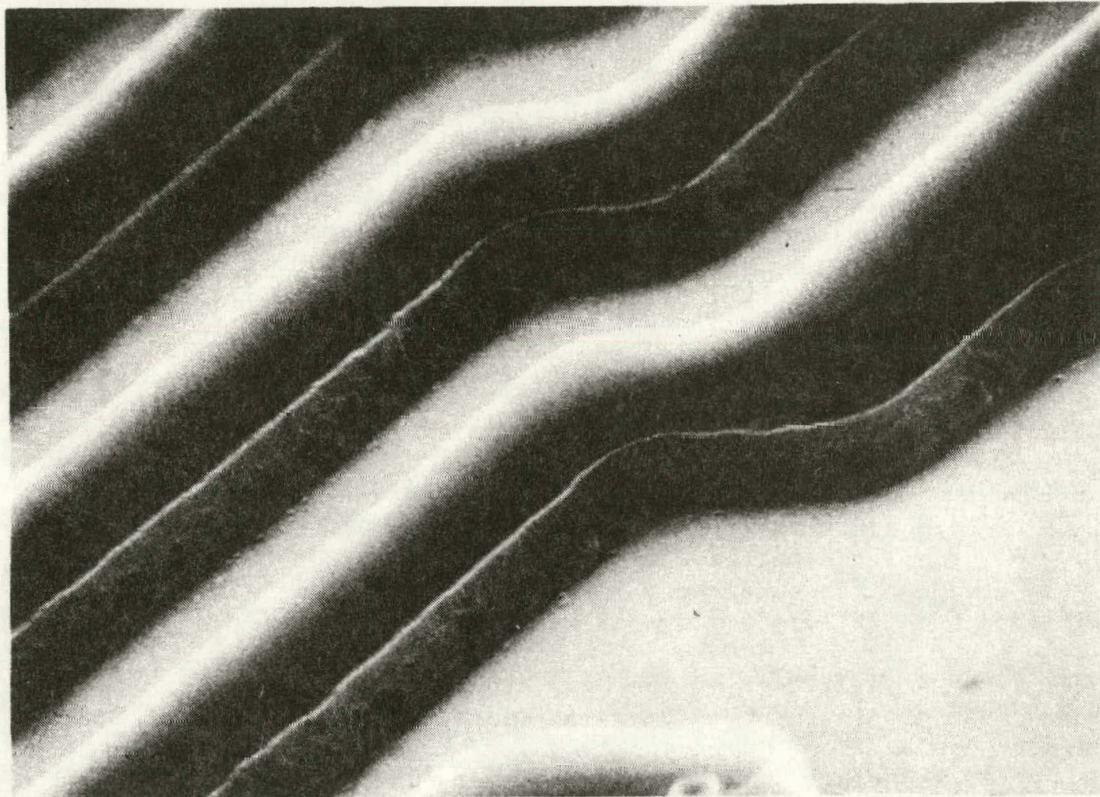




Figure 2. Plasma-Etched Pattern With Residue

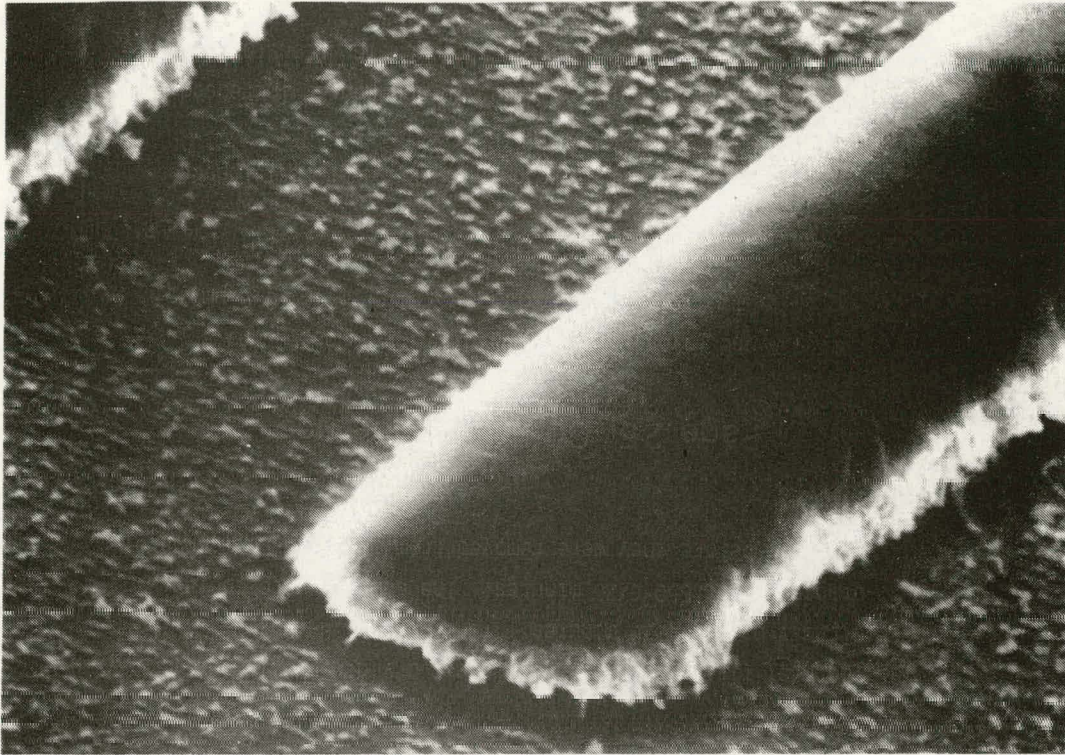




Figure 3.

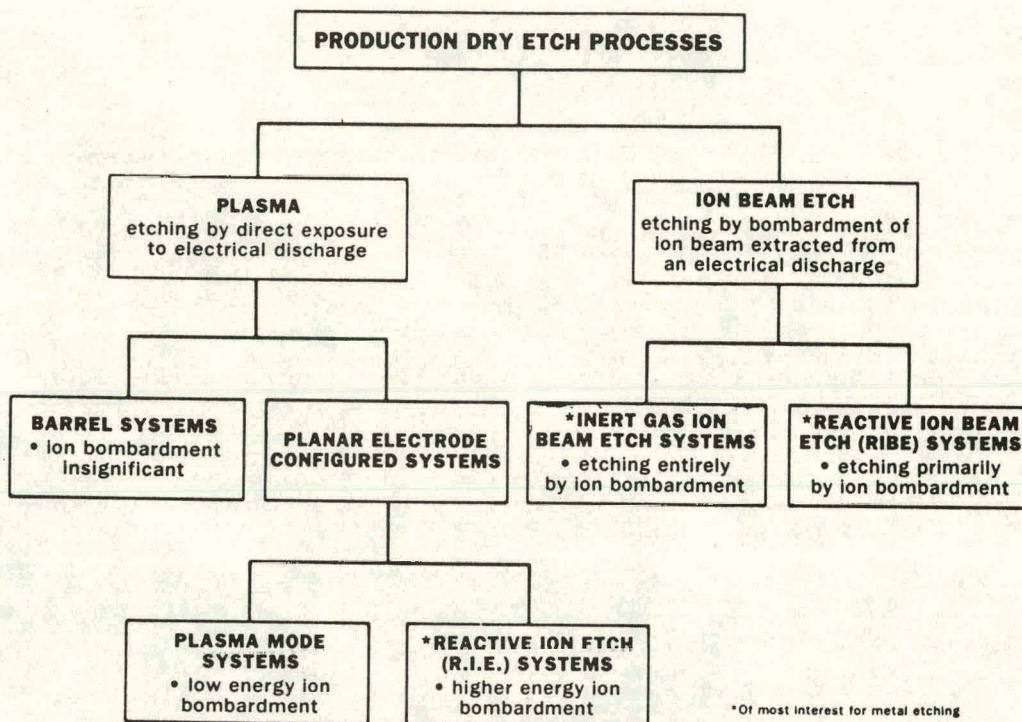


Figure 4. Barrel-Type Plasma-Etch Configuration

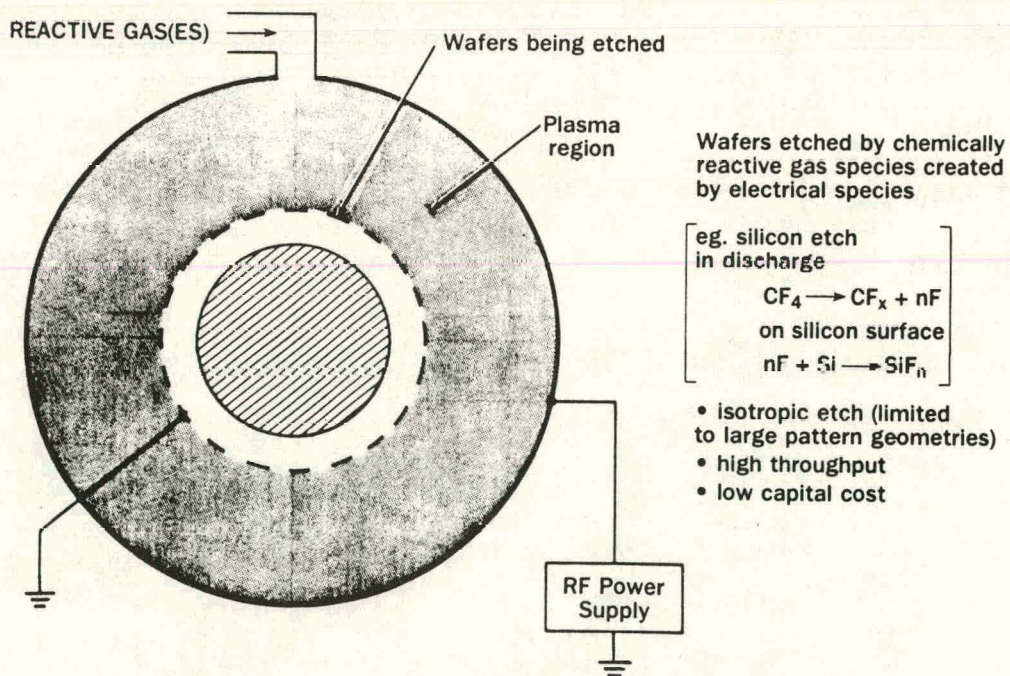


Figure 5. Plasma Mode Type Etch System

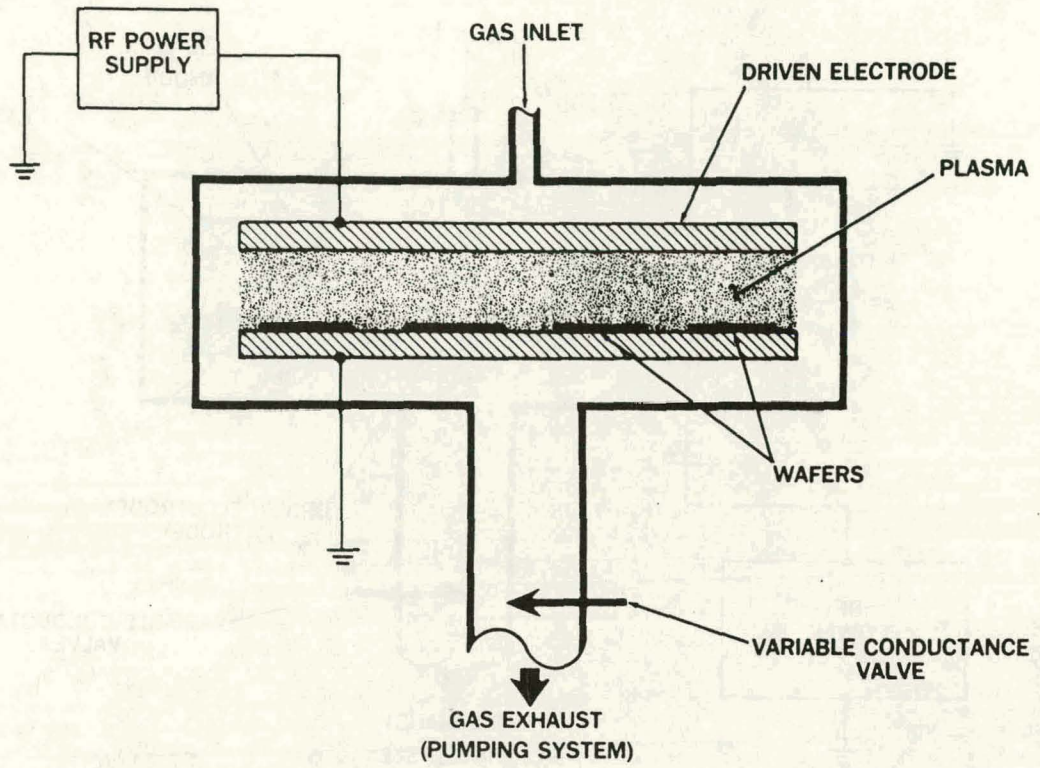




Figure 6. Reactive Ion Etch Chamber

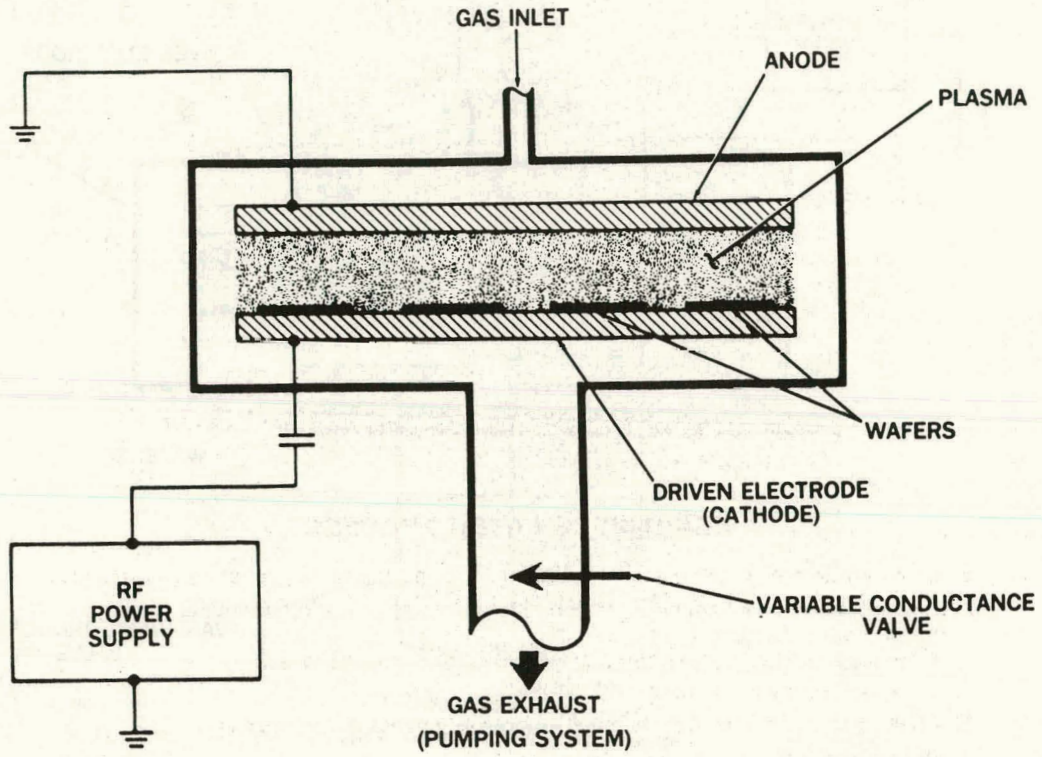
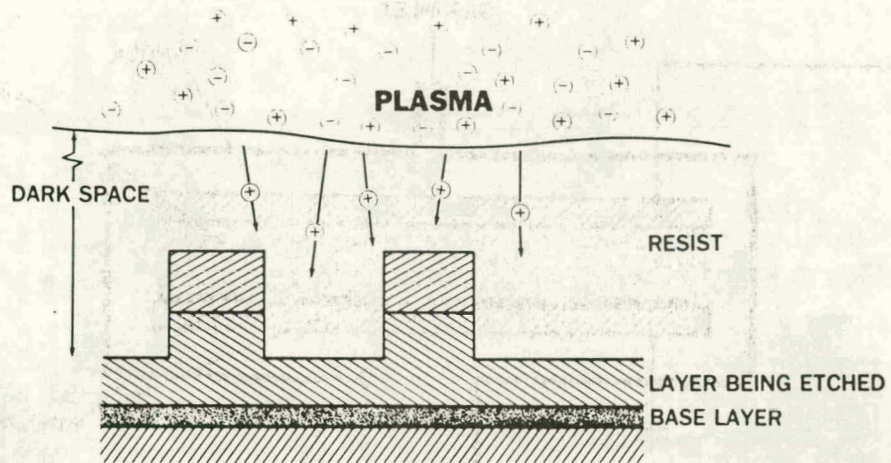


Figure 7.



### REACTIVE ION ETCH PROCESS

1. RF discharge breaks up molecules creating ions and chemically reactive gas species
2. Horizontal surfaces "activated" by ion bombardment allowing chemical attack by reactive species.
  - anisotropic etch results from directional ion bombardment.
  - ion energy in range of 100 - 500eV.
3. When base layer reached, chemical selectivity results in low etch rate.
4. Etching stopped.



Figure 8. Veeco-Kokusai Reactive Ion Etch System

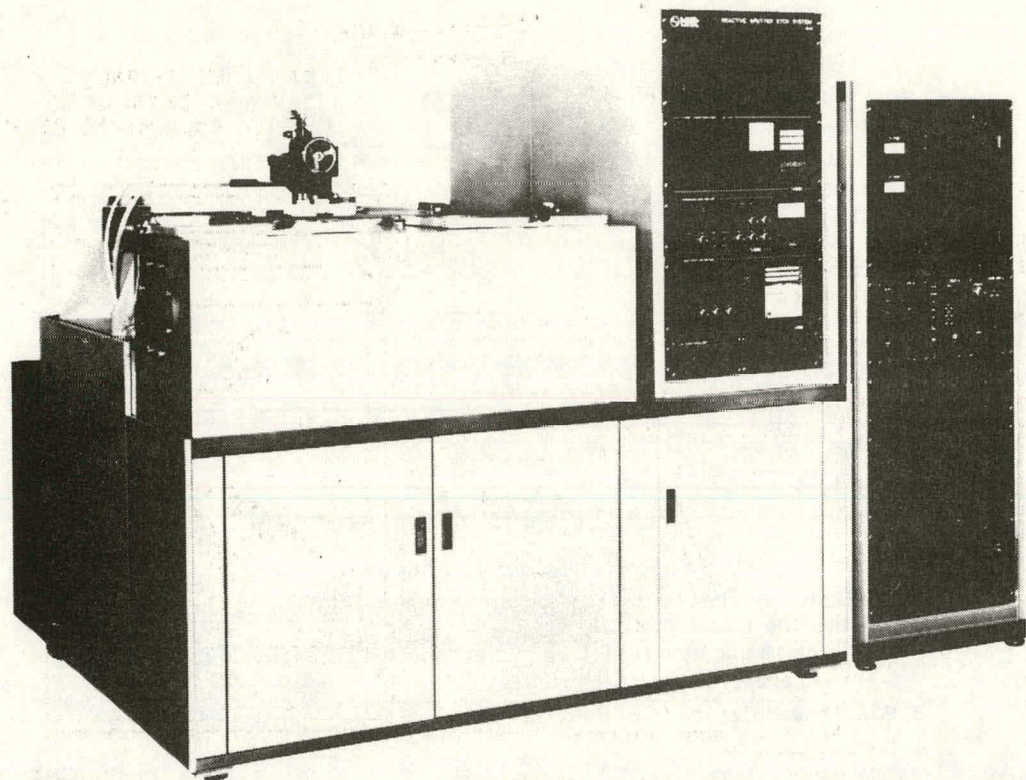


Figure 9. Production Ion Milling System

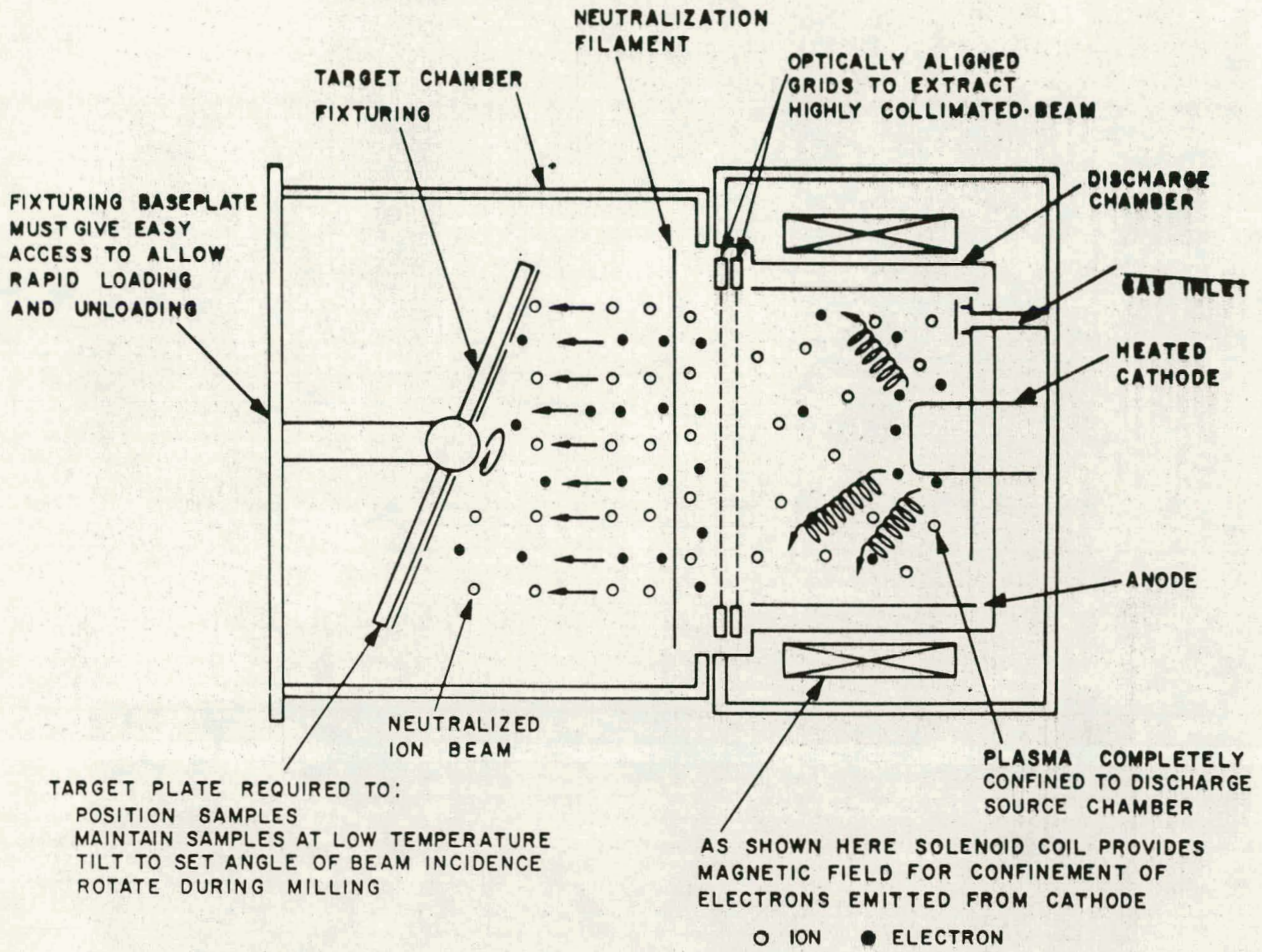




Figure 10. Bubble Memory Device Pattern Cross Section

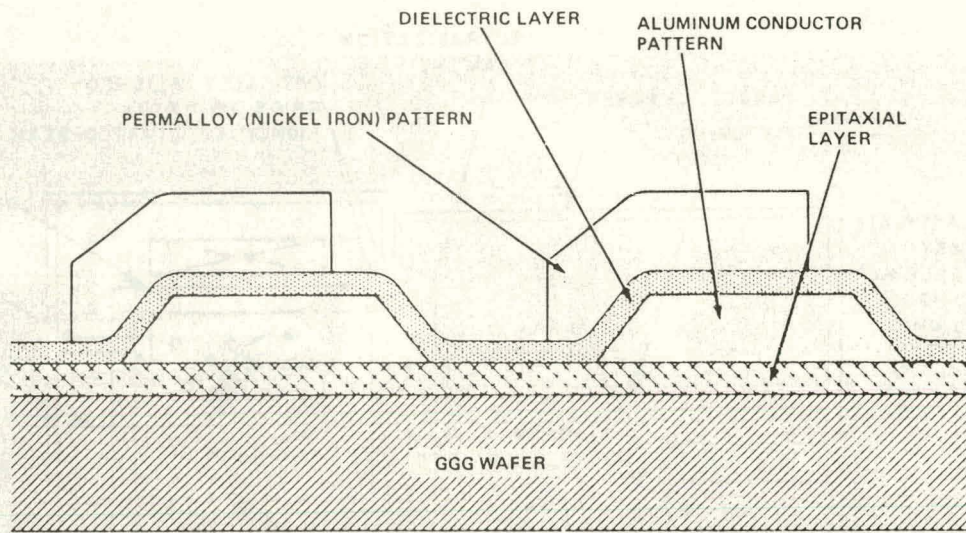


Figure 11. Reactive Ion-Beam-Etched TaSi<sub>2</sub>-PolySi Structure

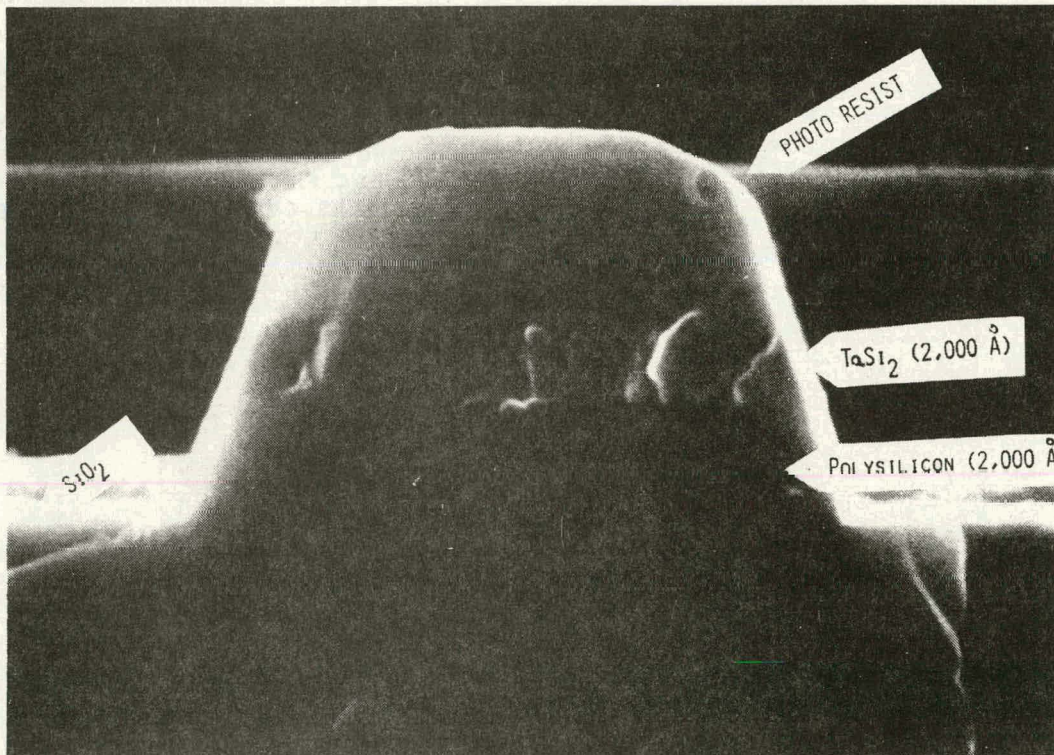




Figure 12. RIE of TaSi<sub>2</sub>-PolySi (Using SF<sub>6</sub> Gas)  
Showing Undercut into PolySi Layer

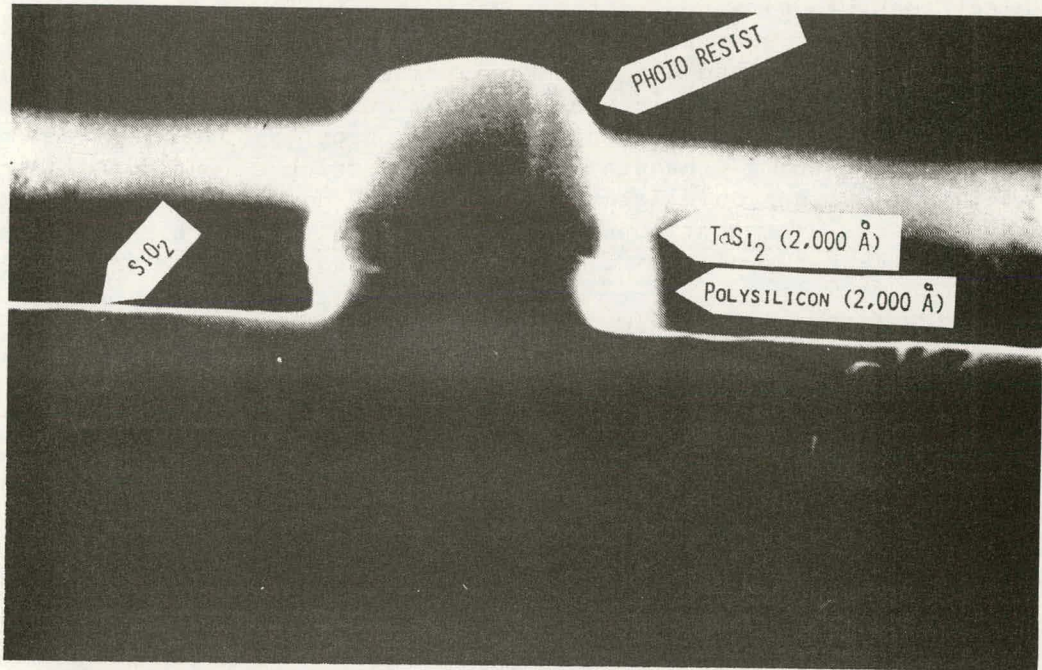
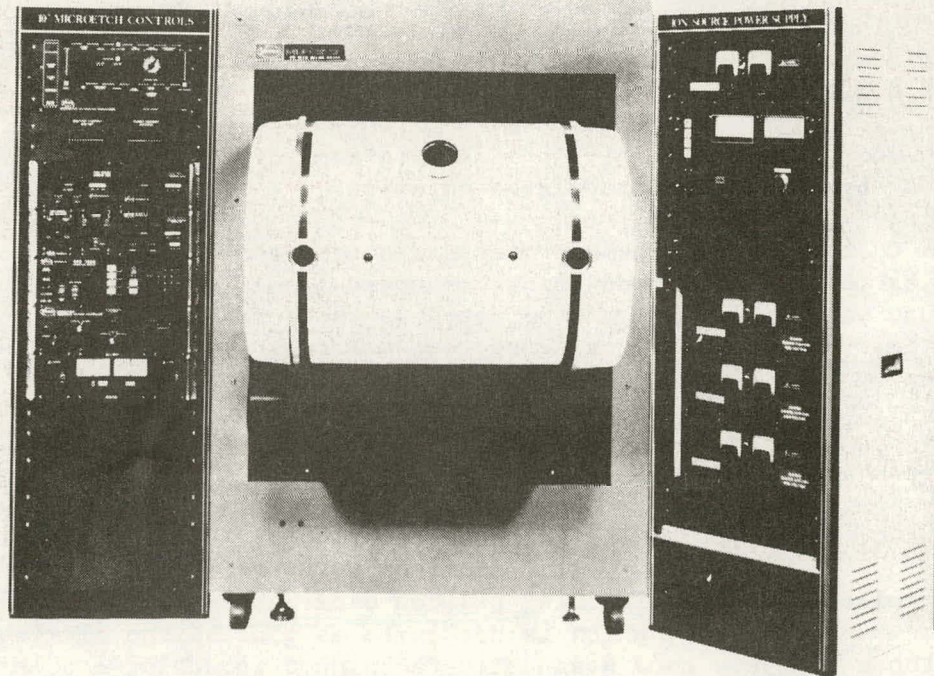


Figure 13. Veeco 10-in. Microetch Ion-Beam Etch System





## DISCUSSION

GALLAGHER: Have you, in your travels, ever done any etching using shaped electrodes, to give you patterns without using photolithographic processes? For example, in our system, which you may or may not be familiar with, we had one of our contractors etch silicon nitride. We were using silicon nitride basically as an AR coating in this application and he wanted to make rather gross patterns, in relation to what you are doing, through the silicon nitride at the top of the solar cell, so that he could later plate contacts down in there and make his top contact. The gentleman who did some of it is sitting over in the corner. I just wondered if you had any history or knowledge of it.

BOLLINGER: Veeco hasn't done any direct etching without masking. We haven't done any specifically that I'm aware of. Both direct-writing etching and single-ion-beam etching were done through a mask, but not on a wafer directly.

GALLAGHER: Bob (Pryor), can you tell us a little bit about the conclusions Motorola reached on that?

PRYOR: We've used basically the parallel-plate type of method in the reactive ion mode, with a mechanical mask to actually shadow the impinging beam and etch where you want to etch without applying photoresist or any other kind of resist. That was the process developed on one of the former JPL contracts that we had. It works very successfully and worked quite well down to things on the order of about 1 mil in terms of line widths, which for our application is the size we were interested in.

BOLLINGER: Do you use a plate or something to shadow?

PRYOR: Yes, in effect, to put a shadow plate with a grid pattern in between the plasma and the substrate. It masks the accelerated ions and it works quite well.

AMICK: Can you say whether it is possible to monitor the progress of the etching by looking at the plasma emission?

BOLLINGER: Oh, yes. For plasma processes, a very good diagnostic tool, as well as for detecting end point, is optical emission spectroscopy, because you can look at a line, such as when etching aluminum or monatomic excitation lines. And the amount of the light emitted is basically proportional to the etch rate.

AMICK: Have you worked out any reactive ion etching techniques for diagnostic purposes using plasma emission?

BOLLINGER: Oh, yes. It is used in those techniques; in a reactive ion technique it works very well. Aluminum works very well; it's particularly good. In etching silicon dioxide you usually monitor the carbon monoxide line, which is not quite as good as the aluminum line, but those are very good diagnostic techniques for doing etching as well as monitoring end point.

AMICK: Are those built into the equipment?

BOLLINGER: It is built into the Veeco reactive ion system. In other equipment it would be an option, but it is an easily added option.

CAMPBELL: Is it safe to say that both the plasma mode and reactive ion-etching mode are line-of-sight etching?

BOLLINGER: You mean by the ions?

CAMPBELL: Yes.

BOLLINGER: I would guess it would be a line of discussion some people would agree with that with the plasma mode, because of the higher pressure and the many collisions suffered by ions in going through the sheath. But there has to be a directional aspect, certainly because it can give an isotropic etching, so it certainly would be safe to say that for the reactive etch mode people might argue it, but there is that aspect for plasma certainly.

CAMPBELL: So there would be "load factors" involved in both those cases. In other words, your etching has to be some way facing the beam.

BOLLINGER: Oh, yes. The beam is really formed in there, actually with the plasma and that cathode sheath, that dark space I mentioned, that forms around everything you put in a plasma. If you turn it in an angle it's going to form at an angle with respect to it, and you are going to get normal ion bombardment. You can't tilt it and get ion bombardment at another angle.

BURGER: Is there any area limitation in something like plasma planar reactors? For instance, you know you may make them 24 inches around because you are used to 24-inch bell jars. Why not 48-inch, or something like that?

BOLLINGER: I don't think there is any limitation. Very large systems have been made. For commercial sales they haven't done very well because of initial capital. I know of a company in Japan that made a 100-inch-diameter system and couldn't sell any because it was too big, but it can be done.

BURGER: Basically you would still get good process control and expect to turn out a good quality product.

BOLLINGER: Yes, you could. It would, of course, depend on making sure that the gas flow gave even etch gradients.

BURGER: It was the gas glow that was worrying me.

BOLLINGER: That would be a problem. The bigger you get the more deterrent it is, but it can be done. It has been done, I'm not sure how successful very large diameters are, but I'm sure it could be done.

SCHRODER: Which technique is the most used in IC production today?

BOLLINGER: If you just say silicon device production, it depends on the size. If you don't worry about anisotropic, certainly the barrel reactors are the most commonly used today. Most of IC production is 5 microns and in that range, but for the newer devices, so-called VLSI (Very-Large-Scale Integration), reactive ion etch and plasma mode are used almost exclusively.

SCHRODER: Ion beam is hardly used for the large application, is that right?

BOLLINGER: For the large-throughput applications, ion beam just doesn't have the throughput, and the plasma mode and the RE mode systems can handle the semiconductor materials well, so ion-beam equipment has not been developed for high throughput at this time.

# LASER ASSISTED DEPOSITION

Subhadra Dutta

Westinghouse R&D Center

Pittsburgh, PA 15235

## INTRODUCTION

Metallization of semiconductor devices is conventionally accomplished by a multistep process involving photolithographic pattern definition, metal film deposition, and liftoff or etching. Laser-assisted pyrolysis and photolysis techniques have recently emerged as novel, maskless, one-step processes for well-resolved, localized metal film growth on semiconductor substrates. Infrared, visible, or ultraviolet lasers have been used to deposit metal films on selected substrates, either thermally, as in laser chemical vapor deposition (LCVD), or non-thermally by photodissociation or organometallic vapors.

### Laser-Assisted Thermal Deposition

Chemical vapor deposition (CVD) of metals is conventionally performed by resistively or inductively heating an appropriate substrate in a reactive atmosphere, with pyrolysis reactions at the substrate surface providing the basis for film growth. Pulsed or CW lasers of suitable wavelengths may be used to selectively heat localized areas of substrates which absorb at these wavelengths. The use of a laser as a heat source for chemical vapor deposition (LCVD),<sup>(1)</sup> particularly for photovoltaic metallization systems applications, offers several distinct advantages: (1) the spatial resolution and control required for maskless production of fine line metal grid structures; (2) localization of the heating to a shallow, surface layer, resulting in limited distortion of the substrate; (3) the possibility of cleaner films due to the small volume heated; and (4) the ability to interface easily with laser annealing<sup>(2)</sup> and laser diffusion<sup>(3)</sup> of solar cells.

Allen and Bass<sup>(4)</sup> have used a CO<sub>2</sub> laser to deposit nickel on quartz substrates from gaseous Ni(CO)<sub>4</sub>. LCVD metal film thicknesses tend to be self-limiting, with a maximum thickness of 550 Å being obtained for nickel. Electroplating or electroless plating techniques may have to be employed in order to build up the requisite film thickness for solar cell applications.

Visible or ultraviolet lasers may also be used to selectively heat the substrates. Excimer lasers, which operate at ultraviolet wavelengths, may be more effective than long-wavelength lasers for LCVD applications, as silicon has a direct bandgap transition at ultraviolet wavelengths. As a result, the ultraviolet radiation is absorbed much more strongly at the silicon surface and does not penetrate as deeply into the substrate, resulting in precisely localized heating. Other advantages of excimer lasers include: (1) greater electrical efficiency resulting in lower fabrication costs; (2) low coherence, alleviating interference problems such as speckle; and

(3) a typically high transverse mode structure, producing a beam of uniform intensity over a large area.

### Photodissociative Metal Deposition

One of the most exciting new techniques for metal film deposition that has recently emerged is laser-induced photodecomposition of gas-phase organometallic compounds. The fundamental difference between this technique and laser chemical vapor deposition is that, instead of relying on localized substrate heating and subsequent pyrolysis reactions at the substrate surface to achieve film deposition, the photons non-thermally sever bonds in gas-phase organometallic molecules, liberating metal atoms which condense on the laser-illuminated regions of the substrate, forming a film. This technique is capable of very high resolution patterned film deposition for two reasons. Firstly, the deposited metal linewidths are independent of the substrate absorption or thermal conductivity, resulting in finer resolution and greater uniformity over the entire substrate due to the insensitivity to local variations of thermal conditions. Secondly, the ultraviolet lasers that are generally used in this technique have considerably smaller diffraction-limited spot sizes than visible, or infrared lasers, resulting in deposited linewidths as small as 0.7 micron.<sup>(5)</sup>

Ehrlich, Deutsch and Osgood<sup>(5)-(8)</sup> have performed a variety of experiments on photodissociative metal deposition using both pulsed (excimer lasers, 1-100 mJ, 10 ns) and CW (frequency-doubled Ar<sup>+</sup> laser, 10  $\mu$ W - 3 mW) UV lasers. In one of their most interesting experiments,<sup>(6)</sup> a two-step process was used to deposit Cd, Al, and Zn patterned films from metal-alkyl vapors. In the first step, called pre-nucleation, a focused UV laser was used to irradiate the substrate in the requisite pattern, photodissociating a thin, adsorbed layer of metal-alkyl molecules. The laser was then defocused to illuminate the entire substrate, causing film growth to occur selectively in the pre-nucleated regions. These experiments also indicated that films of one metal, e.g., Al, may be grown on nucleation centers of a second dissimilar metal, e.g., Zn. This is of particular interest for solar cell applications, where a two- or three-metal system often has to be employed for diffusion barrier and galvanic buffering purposes.

Draper<sup>(9)</sup> has deposited both Cr and Mo using off-resonance laser-induced dielectric breakdown of metal carbonyl vapors with a pulsed CO<sub>2</sub> laser. Solanki et al.<sup>(10)</sup> used a pulsed copper hollow cathode laser at 260 nm, utilizing the multiphoton absorption that occurs at this ultraviolet wavelength for carbonyl molecules, to deposit Cr, Mo, and W films. The laser was operated at 150 mW peak power with pulse widths of 120  $\mu$ s. In another set of experiments, Coombe and Wodarczyk<sup>(11)</sup> used KrF (249 nm) and XeCl (308 nm) excimer lasers to induce the localized deposition of Zn and Mg films from the pure metal vapors. The laser pulses used in these experiments were typically 20 ns in duration and carried energies of up to 20 mJ (KrF) or 5 mJ (XeCl).

### Conclusions

Applications of laser-based processing techniques to solar cell metallization will be discussed. Laser-assisted thermal or photolytic maskless deposition from organometallic vapors or solutions may provide a viable

alternative to photovoltaic metallization systems currently in use. High power, defocused excimer lasers may be used in conjunction with masks as an alternative to direct laser writing to provide higher throughput. Repeated pulsing with excimer lasers may eliminate the need for secondary plating techniques for metal film buildup. A comparison between the thermal and photochemical deposition processes will be made.

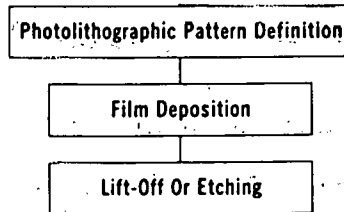
#### REFERENCES

1. C.P. Christiansen and K.M. Lakin, *Appl. Phys. Lett.* 32, 254 (1978).
2. R.T. Young, R.F. Wood, J. Narayan, and C.W. White, *Laser and Electron Beam Processing of Materials*, eds. C.W. White and P.S. Peercy, Acad. Press (1980), p. 651; R.T. Young, *Lasers and Applications*, 2, 33 (1983).
3. T.F. Deutsch, J.C.C. Fan, G.W. Turner, R.L. Chapman, D.J. Ehrlich, and R.M. Osgood, Jr., *Appl. Phys. Lett.* 38, 144 (1981).
4. S.D. Allen, *IEEE J. Quantum Electron.* QE-15, 43D (1979); S.D. Allen and M. Bass, *J. Vac. Sci. Technol.* 16, 431 (1979).
5. D.J. Ehrlich, R.M. Osgood, Jr., and T.F. Deutsch, *J. Vac. Sci. Technol.* 21, 23 (1982).
6. D.J. Ehrlich, R.M. Osgood, Jr., and T.F. Deutsch, *Appl. Phys. Lett.* 38, 946 (1981).
7. T.F. Deutsch, D.J. Ehrlich, and R.M. Osgood, Jr., *Appl. Phys. Lett.* 35, 175 (1979).
8. D.J. Ehrlich, R.M. Osgood, Jr., and T.F. Deutsch, *J. Electrochem. Soc.* 128, 2039 (1981).
9. C.W. Draper, *J. Phys. Chem.* 84, 2089 (1980); *Met. Trans.* 11A, 349 (1980).
10. R. Solanki, P.K. Boyer, J.E. Mahan, and G.J. Collins, *Appl. Phys. Lett.* 38, 572 (1981).
11. R.D. Coombe and F.J. Wodarczyk, *Appl. Phys. Lett.* 37, 846 (1980).

## Potential Advantages of Laser Deposition Techniques for Photovoltaic Systems

- High Resolution
- Maskless Process
- Clean And Contamination - Free
- In-Situ Sintering
- Low Contact Resistance
- Low Cost

A Conventional Metallization System Employs a Sequential Multistep Process:



Laser-Assisted Metallization Techniques Are Essentially One-Step Processes:



## Photovoltaic Metallization System

### Screen Printing

- Electroplating Not Required
- Poor Resolution
- Limited To One Metal — Ag
- Possibility Of Low Shunt Resistance, Low Lifetimes
- High Contact Resistance

### Photolithographic Definition

- Better Resolution
- Variety Of Metals (Diffusion Barrier)
- Electroplating Required
- Multistep Process

### Laser-Assisted Deposition

- Submicron Resolution
- Variety Of Metals
- Electroplating May Not Be Required
- One-Step, Maskless Process

## Laser-Assisted Deposition Techniques

### Pyrolytic Deposition (Thermal)

- Laser Chemical Vapor Deposition (LCVD)
- Laser Deposition From Solutions

### Photolytic Deposition (Non-Thermal)

- Laser Photodissociation Of Vapors
- Laser Photodissociation Of Solutions



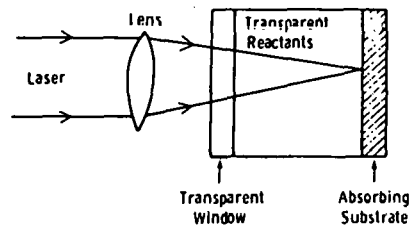
# Pyrolytic Deposition

## Laser Chemical Vapor Deposition (LCVD)

C. P. Christiansen and K. M. Lakin (1977)  
Electrical Engineering Department  
University of Southern California

S. D. Allen and M. Bass (1979)  
Center for Laser Studies  
University of Southern California

W. Roth, H. Schumacher, and H. Beneking (1983)  
Institute of Semiconductor Electronics  
W. Germany



Schematic of LCVD Apparatus

S. Dutta  
I.I. - m. 2. 3-11-83

Dwg. 7779A96

## Advantages

- **Spatial Resolution And Control — Maskless Process**
- **Limited Distortion Of Substrate**
- **Possibility Of Cleaner Films**
- **Convenient Interfacing With Laser Annealing And Laser Diffusion Of Solar Cells**

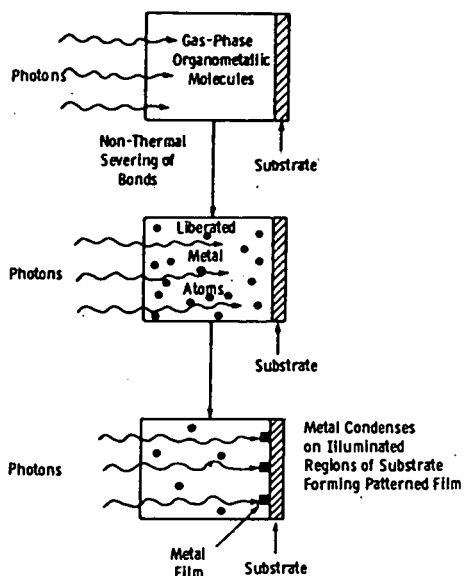
## Disadvantages

- **LCVD Metal Film Thickness Self-Limiting — Require Electroplating**
- **Direct Laser Writing Relatively Slow Process**

# Photolytic Deposition

Laser-Induced Photodecomposition of Gas-Phase Organometallic Compounds:

This Technique is Fundamentally Different from Thermally Based Laser Processes



S. Dutta  
I.L.-m.z. 3-11-83

Dwg. 7779A94

## Laser-Induced Photodissociation Experiments Performed by:

D.J. Ehrlich, T.F. Deutsch, And R.M. Osgood  
(1979-1982)

M.I.T. Lincoln Laboratory

### Lasers

- Pulsed Excimer Lasers  
 $\lambda = 157\text{-}350\text{ nm}$   
 Energy = 1-100 mJ  
 Pulse Width = 10 ns,  
 Repetition Rate = 1-150 Hz
- CW Frequency-Doubled Ar<sup>+</sup> Laser  
 $\lambda = 257.2\text{ nm}$   
 Power = 10  $\mu\text{w}$  - 3 mW

### Encapsulant Gases

Cd (CH <sub>3</sub> ) <sub>2</sub>	Fe (CO) <sub>5</sub>	CF <sub>3</sub> I
Zn (CH <sub>3</sub> ) <sub>2</sub>	W (CO) <sub>6</sub>	SnCl <sub>4</sub>
Sn (CH <sub>3</sub> ) <sub>4</sub>	Cr (CO) <sub>6</sub>	
Ga (CH <sub>3</sub> ) <sub>3</sub>		
Bi (CH <sub>3</sub> ) <sub>3</sub>		
Si (CH <sub>3</sub> ) <sub>4</sub>		
Ge (CH <sub>3</sub> ) <sub>4</sub>		
Al <sub>2</sub> (CH <sub>3</sub> ) <sub>6</sub>		

## Two-Step Deposition Process

### Prenucleation:

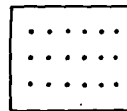
1. Substrate Exposed To High Pressure (~ 20 Torr) Of  $Zn(CH_3)_2$
2. Chamber Evacuated To  $\ll$  1Torr
3. Focused CW Laser Beam ( $\lambda = 257.2$  nm) Scanned Across Substrate In Requisite Pattern Forming Zn Nucleation Centers

### Film Growth:

1. Chamber Filled To 10 Torr Of  $Zn(CH_3)_2$
2. Substrate Flood Illuminated Using Defocused Laser Beam
3. Film Growth Occurs Selectively In Prenucleated Regions

Films Of One Metal, e.g. Al, May Be Grown On Nucleation Centers Of Another Metal, e.g. Zn

Prenucleation



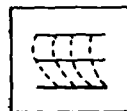
Nucleation Centers Formed  
(Invisible)

Flood Illumination



Localized Film Growth

Over-Exposure



Film Growth In  
Non-Prenucleated Regions

## Other Laser-Induced Photodeposition Experiments

R. Solanki, P.K. Boyer, J.E. Mahan,  
And G.J. Collins (1981)

Colorado State University

Pulsed Copper Hollow Cathode Laser

$\lambda = 269 \text{ nm}$   
Power = 150 mW  
Pulse Width = 120  $\mu\text{s}$

Cr, Mo, And W Films Deposited From  
Metal-Carbonyl Vapors

R.D. Coombe And F.J. Wodarczyk (1980)

Rockwell International

Pulsed KrF Excimer Laser

$\lambda = 249 \text{ nm}$   
Energy = 20 mJ  
Pulse Width = 20 ns

Pulsed XeCl Excimer Laser

$\lambda = 308 \text{ nm}$   
Energy = 5 mJ  
Pulse Width = 20 ns

Zn And Mg Films Deposited From  
Pure Metal Vapors

C.W. Draper (1980)

Western Electric Research Center

Pulsed CO<sub>2</sub> Tea Laser

$\lambda = 10.6 \mu\text{m}$   
Energy = 4-5 J  
Pulse Width = 170 ns

Cr And Mo Films Deposited From  
Metal-Carbonyl Vapors

## Advantages

- Possibility Of Depositing Two Or More Dissimilar Metal Films Over Each Other
- Higher Resolution Obtainable Than With Thermal Techniques
- Defocused, High Power, Pulsed Excimer Laser May Be Used With Mask For Faster Deposition
- Repeated Pulses For Film Buildup

## Advantages of Excimer Lasers

- Direct Bandgap Transition → Strongly Localized Heating At Silicon Surface (For Thermal Deposition Techniques)
- Greater Electrical Efficiency → Lower Costs
- Low Coherence → Absence Of Speckle
- High Transverse Mode Structure → Uniform Intensity Over Large Area

## Applications To Photovoltaic Metallization Systems

### Laser Thermal Deposition From Vapors (Or Solutions):

- Clean, Maskless Process
- Possibility Of Interfacing With Laser Annealing And Diffusion Techniques
- Ability To Electroplate On Thin, Laser-Deposited Film For Rapid Metal Buildup

### Laser Photodeposition From Vapors (Or Solutions):

- Possibility Of Two Or Three Layer Metal Deposition (Diffusion Barrier, Galvanic Buffering)
- Flood Illumination Using Mask For Rapid Throughput
- Possibility Of Using Repeated Laser Pulses For Film Buildup

## DISCUSSION

LANDEL: I'm sure there will be a number of questions. Let me exercise the chairman's prerogative to ask a few. You described the nature of the technique, but I'm sure the audience is hungry or thirsting for some information. For example, what has been put down? You talked about the ability to put down lines, in some cases you talked about films, which must be general films. It is not clear when you are talking about a line and when you are talking about a general surface area coverage. Finally, since you talked about thin films at the end of the last talk, you were talking about the problems that could be seen if you tried now to bond to the very thin films. Would you comment on any or all of those? Let me repeat them, let me take them in turn. The quantitative data: what has been put down in thin film or thin lines, since we are talking about metallization systems for cells?

DUTTA: Well, zinc, aluminum. The group at MIT have put down both films and lines, they have done several experiments on this technique and in the review paper they have written on the subject they have listed all of these encapsulant gases, so I assume they have put down all of these materials. They have talked in greater detail about aluminum, zinc and they have written lines, as well as deposited films; they have tried both. They have written lines using focused laser, and they've deposited films.

LANDEL: That wasn't clear. The second one was bonding to these lines. People have been talking about the difficulty of soldering to the various ink lines or lines put down in various ways. For example, the last speaker talked about the possibility of depositing the chemically metallo-organic systems, but those are so thin that she had to take special precautions to keep from simply dissolving them off again. Has anyone tried bonding to these sorts of lines?

DUTTA: You mean electroplating to these sort of lines? No, I have not seen it. There is a paper that this group (MIT) has written on using this metallization technique for MOS FETs, and they were able to measure device characteristics.

HYDE: What kind of deposition rate can you get with these techniques? What speed of layer buildup?

DUTTA: With this pyrolytic technique you are limited by your writing speed because you have to use speed that is compatible with the pyrolytic decomposition taking place at each spot. That makes it a relatively slow technique. I think you approach one micron or several microns a second. It is quite slow. With the photodissociated technique, the deposition rate is linear with the laser intensity and also with the density of organo-metallic gas.

LANDEL: You still have to prewrite, evidently, a nucleation site. Is that true?

DUTTA: That is true.

LANDEL: I think an appropriate question would then be, what sort of writing speed do you have there?

DUTTA: I think you could prewrite the pattern very rapidly -- 2000 cm per second.

SOMBERG: Would you care to comment on the cost of such a system, assuming it is done in a vacuum or some kind of chamber?

DUTTA: If you use an eximer laser -- that is a high-efficiency laser, so it is not as expensive as other laser systems -- I think the initial setting-up cost would be greater -- the initial optimization. All that would be greater than other techniques because it is a novel procedure, and I would assume that if things are properly optimized it would not be all that much more expensive to run.

SOMBERG: Are we talking in the order of, say, a quarter of a million dollars, a hundred thousand dollars? I am talking about the laser with the equipment, with the vacuum equipment.

DUTTA: The vacuum equipment should not be too expensive--a few thousand dollars. The laser would be the most expensive item.

SOMBERG: The other question I have, if I may, is: if you have to use a plating-up procedure on the pyrolytic technique, what is the advantage of the technique if you have to plate up?

DUTTA: You get very much better resolution than in the screen printing technique.

SOMBERG: I am talking about plating -- if you have to plate up, and if you were to use a photolithographic technique, what is the advantage of the pyrolytic technique if you have to plate up anyhow?

DUTTA: What is the advantage of the pyrolytic technique over the photolithographic technique?

SOMBERG: Yes.

DUTTA: You are still using maskless procedure -- the plating, of course, plates onto the metal. You don't have to use a mask during plating, so you are cutting down some of your process steps.

SOMBERG: Thank you.

AMICK: In describing the single-step photodecomposition gaseous organo-metallic technique, you say that after the metal atoms have been freed they will condense on a region of the substrate illuminated by the laser. Why are they so cooperative as to do that?

DUTTA: The laser is focused close to the substrate, so that the dissociation occurs right at the substrate and your dissociation is occurring in the absorbed layer at the surface of the substrate. It is dissociating only where the laser strikes it.

AMICK: If I go back from the substrate a little bit, unless it is a highly converging beam, I will also see dissociation there as well, so I would actually be depositing some metal atoms all over the place, wouldn't I?

DUTTA: That is right.

SCHWUTTKE: I believe that the surface temperature in general where the focused laser beam hits the silicon surface, there you have the proper temperature that the gas dissociates. There you would get the deposition.

COMMENT: That is pyrolytic.

COMMENT: Would you put up that viewgraph? I also had the same problem.

LANDEL: Also your sketch showed a general budding of the area for the order of associations.

DUTTA: Yes, that is the problem with schematics. They are not very precise. This was to just give an idea of what is going on, but I realize it can be confusing. It is very critical to have the right density of the gas. If you have too high a pressure of gas within your cell, then you get decomposition too early on. As your photons enter the cell you get decomposition very close to the window, and so you have composition all over the walls in the chamber. But if you peak the gas pressure at some critical pressure, and you focus your beam so that the maximum intensity is close to the surface, or at the surface, where you have the absorbed layer, then you dissociate the gas at the surface. You don't have that problem.

TAYLOR: I am having problems, also. Let's assume that you are doing your excitation all very close to the surface but when you undergo a dissociation event the metal atom that is liberated is likely to move in any direction--to be moving straight out away from the surface as frequently as it is moving toward it so, it seems to me like you would get a lot of diffusion through the gas phase before it hit the surface and stuck. Your resolution would not be very good.

DUTTA: Well, apparently once you form your nucleation sites then the sticking coefficient is such that when you are flood-illuminating the substrate, then you have very good localization of the subsequently deposited layer. It sticks very well to those nucleation sites. Are you talking about the initial nucleation?

TAYLOR: No. I can understand if you do your pre-nucleation, that route of preparation, then you have sites to which the deposited atoms can stick, but unless you do that pre-nucleation, if you are depending on writing a pattern on a substrate without pre-nucleation, now I think you would have trouble with getting resolution.

DUTTA: Well, people who have not used the pre-nucleation technique have reported lines of one to two microns with just using the one-shot deposition process.



LANDEL: In this case, you are using a line laser that is focused somewhere off the surface, so you are getting presumably gas-phase disassociation, and then that gives rise to what line? How wide?

DUTTA: Well, with the pre-nucleated --

LANDEL: No, not pre-nucleated.

DUTTA: One to two microns.

LANDEL: And how far off the surface are you focusing?

DUTTA: The Bell system researchers don't specify.

LANDEL: I wonder -- in fact, aren't you saying that if you pre-nucleated, this represents some distance of microns for the pressure you have. You must be dissociating through the whole line, whatever your absorption is, but you must have some recombination rate. So you dissociate and recombine, and only if you have a site close do you have deposition. If you have thought about it, it would seem to me, like Bill (Taylor) said, you are going to have things going off in all directions. And furthermore, it means you are going to have a tremendous loss or wastage of the material you have. It dissociates and now you have the methyl radicals and the metal, and it is just floating around in a cloud, and now it is going to deposit all over the place -- unless one is relying on the dissociation and rapid recombination during the length of the mean free path.

DUTTA: Yes.

QUESTION: Doesn't the intensity at the focal point increase the dissociation?

DUTTA: It does. That is why it is important to have the focus close to the substrate.

COMMENT: You have drawn the laser's focus down at the surface, so that you get more dissociation at the focal point of the laser than back in the gas where it is not so intense.

COMMENT: Plus the fact that it really is a surface-absorbed phase; we are really talking about enormous density gradient too.

LANDEL: Well, it is not clear whether it is dissociation of the surface-absorbed phase, or whether it's dissociation in the gas phase.

COMMENT: The point is, if it is out of the surface-absorbed phase, the density there is much higher than it would be out of the gas phase--3 orders of magnitude or something like that.

COMMENT: I'm getting confused back and forth between pre-nucleation and the single -- this particular one is the single step process, is that correct?

DUTTA: Well, this is just a generalized viewgraph, depicting the entire technique. I think the pre-nucleation and the whole technique is just

one technique, but a two-step deposition process in which they pre-nucleate and then flood-illuminate is just breaking down the process into its component parts. I think when you do it one shot, the same thing is happening. The adsorbed layer is being decomposed.

COMMENT: But when done in one shot, this does not represent a flood example, does it?

DUTTA: The localization can be done by either focusing or by using a mask. This was just to generalize the depiction of the technique. I am not specifying how it's being localized.

STEIN: If you look at the second and the third illustrations there, there are two different functions that the photons are performing. One is, you call it liberating the metal atoms, and the other is actually illuminating the substrate. The way I'm assuming this thing is working is that you've really got to attack that substrate with a laser beam, whether you pre-nucleate it or whether you just illuminate it. Whether the gas is photolytic or pyrolytic is not as critical as the fact that you've got to get the substrate very receptive to these available atoms that are going to be deposited. I think that's what you're saying. I am not sure; I wish you would correct me. And once you get that substrate ready, then anything close, any atoms close to it, if they are still atoms, are going to stick. Is that what's happening? I mean, you have two functions for that laser beam shown in the second and third photograph. It seems to me that the last function, the bottom one, is the critical one. You've got to illuminate, you've got to pre-nucleate the surface, to liberate the metal atoms. In fact, you don't want to do much of that away from the substrate.

GALLAGHER: Do you know if anyone has ever made a solar cell and/or laid down metal on a solar cell using this technique?

DUTTA: No.

ZWERDLING: I assume that in this process you have to use wave lengths or photon energies that are capable of breaking the organo-metallic bond. Does that mean you have to choose selected wave lengths for your laser? It is not a thermal process that is breaking the bond and freeing the metal, it is a photolytic process. So you must choose wave lengths, particular wave lengths, for different compounds?

DUTTA: All of the UV wave lengths will do it, some more effectively than others.

ZWERDLING: You're raising the vibrational energy, or the electronic state, to such a point that the vibrations will tear the molecules apart.

DUTTA: That's correct.

LANDEL: You point out that one of the advantages of this was the possibility of having cleaner film. Is there any evidence on whether or not they are cleaner films, than by some other technique? It is a reasonable supposition, but then there are always so many things that can go wrong. Is the supposition borne out in the product?

DUTTA: I think so. The SEM pictures of the deposited films don't show any impurities. It looks very clean, very uniform.

SESSION V: FUTURE METALLIZATION CHALLENGES

G. Schwuttke (Consultant), Chairman

THIS PAGE  
WAS INTENTIONALLY  
LEFT BLANK

## TRANSPARENT CONDUCTIVE COATINGS

S. Ashok

The Pennsylvania State University

University Park, PA 16802

Materials with electrical conductivity and optical transparency are highly desirable in many optoelectronic applications including photovoltaics. Ultra-thin, semitransparent metal films have served the purpose in some situations but they suffer from a number of problems which seriously limit the performance of the resulting devices. In contrast, certain binary oxide semiconductors such as tin oxide ( $\text{SnO}_2$ ) and indium oxide ( $\text{In}_2\text{O}_3$ ) offer much better performance tradeoff in optoelectronics as well as better mechanical and chemical stability. These thin-film "transparent conductors" (TC) are essentially wide-bandgap ( $\approx 3.5$  eV) degenerate semiconductors - invariably n-type - and hence are transparent to sub-bandgap (visible) radiation while affording high electrical conductivity due to the large free electron concentration (up to  $10^{21}$   $\text{cm}^{-3}$ ).

The principal performance characteristics of TC's are, of course, electrical conductivity  $\sigma$  and optical transmission  $T$ , but a suitable figure of merit  $\phi_{\text{TC}}$  for TC's has been shown to be the ratio  $T^{10}/R_s$ , where  $R_s$  is the sheet resistance of the TC [1,2]. It is found that  $\phi_{\text{TC}}$  is much higher for the oxide semiconductors than the corresponding value for thin metal films. The TC's also have a refractive index of around 2.0 and hence act as very efficient antireflection (AR) coatings. For using TC's in surface barrier solar cells, the photovoltaic barrier is of utmost importance and so the work function or electron affinity of the TC is also a very important material parameter.

A large number of processes are available for depositing TC thin films [3], but for illustration the preparation of tin-doped indium oxide ( $\text{In}_2\text{O}_3:\text{Sn}$ ) or the so-called indium-tin oxide (ITO) by a simple spray pyrolysis process and its use in fabricating an efficient surface barrier solar cell on silicon will be discussed at length [4]. It is found that the performance of the cell is strongly dependent on ITO preparation conditions, silicon surface preparation and the nature of carrier transport across the interface.

The method of deposition used for preparing the TC/Si surface barrier cell has drastic consequences on the photovoltaic barrier region and hence on the cell efficiency. To take an extreme example, ion-beam deposited ITO forms a barrier (and hence a good solar cell) on p-type Si, while spray and vacuum evaporation processes yield efficient cells on n-type Si [5]. It has also been found that the angle of deposition of  $\text{SnO}_2$  has a strong bearing on the efficiency of the resulting  $\text{SnO}_2/\text{n-Si}$  solar cell [6]. Similarly thermal annealing can also affect both the bulk and interfacial properties of these TC's.

Thermal [7] as well as photon [7,8] induced stresses can degrade the characteristics of solar cells by reducing the open-circuit voltage  $V_{oc}$ , short-circuit current density  $J_{oc}$  as well as the fill factor FF. Much further study is needed in this crucial area of environmental stability.

A number of problems remain unresolved in the field of transparent conductors, including such basic ones as the role of the 'dopant'. Easy as the preparation of these TC's is, comparing films prepared by different techniques under different conditions is often difficult, requiring thorough material characterization. In terms of fabricating highly efficient surface barrier solar cells, it may be convenient to alter the absorber semiconductor (substrate) surface by shallow ion implantation as done for metal-semiconductor Schottky barriers [9]. With further applications in optoelectronic detectors, and imaging devices, there is currently a great deal of interest in this field and numerous studies are in progress for improving the quality and controllability of the films, as well as basic understanding of this class and materials.

#### References

1. G. Haacke, J. Appl. Phys., 47, 4086 (1976).
2. G. Haacke, Am. Rev. Mat. Sci., 7, 73 (1977).
3. J. L. Vossen, Physics of Thin Films, G. Hass, M. H. Francombe and R. W. Hoffman (Eds.), Academic Press, 1, (1977).
4. S. Ashok, P. P. Sharma and S. J. Fonash, IEEE Trans. Electron Dev., ED-27, 725 (1980).
5. S. Ashok, S. J. Fonash, R. Singh and P. Wiley, IEEE Electron Dev. Lett., EDL-2, 184 (1981).
6. T. Feng, A. K. Ghosh and C. Fishman, J. Appl. Phys., 50, 8070 (1980).
7. G. N. Advani and A. G. Jordan, Solar Energy, 30, 71 (1983).
8. H. P. Maruska, T. Feng, A. K. Ghosh and D. J. Eustace, Proc. 15th Photovoltaic Spec. Conf., IEEE, 1412 (1981).
9. J. M. Shannon, Solid-State Electron., 19, 537 (1976).

1. INTRODUCTION
2. PROPERTIES OF TRANSPARENT CONDUCTORS(TC)
3. TC's IN SURFACE BARRIER SOLAR CELLS - SPRAY ITO/N-Si SOLAR CELL
4. INFLUENCE OF DEPOSITION CONDITIONS ON SOLAR CELL CHARACTERISTICS
5. STABILITY AND AGING OF TC's IN SOLAR CELLS
6. FUTURE DIRECTIONS AND PROBLEM AREAS

## Transparent Conducting Films

DEFN. - VISIBLE TRANSPARENCY AND ELEC. CONDUCTIVITY.

CURRENT INTEREST - PHOTOVOLTAICS, SOLAR THERMAL, OPTOELECTRONICS.

PARAMETERS - TRANSMISSION T, CONDUCTIVITY  $\sigma$

HISTORICAL - CdO(1907), AIRCRAFT WINDSHIELD DEICING(1940's), NESA GLASS.

APPLICATIONS -  
 TRANSPARENT HEATERS  
 DISPLAYS AND IMAGERS  
 HEAT MIRRORS(IR REFLECTORS)  
 ANTISTATIC AND SCRATCH-RESISTANT COATINGS  
 ELECTROCHEMICAL STUDIES  
 TRANSPARENT SUBSTRATES

PROPERTIES -  
 ELECTRICAL RESISTIVITY  
 OPTICAL TRANSMISSION Vs.  $\lambda$   
 ENVIRONMENTAL AND LIFE STABILITY  
 CHEMICAL NATURE, STRUCTURE AND MORPHOLOGY  
 CHEMICAL RESISTANCE AND ETCHABILITY  
 INTERFACIAL AND BULK PROP.(WORK FUNCTION, ENERGY GAP,...)  
 METHOD OF DEPOSITION

TYPES -  
 1. ULTRA-THIN METALS( 50 Å) - Au,Pt,Cu,Ag,...  
 2. WIDE-BANDGAP DEGENERATE SEMICONDUCTORS -  
 OXIDE SEMICONDUCTORS -  $\text{SnO}_2$ ,  $\text{In}_2\text{O}_3$ ,  $\text{CdO}$ ,  
 $\text{ZnO}$ ,  $\text{Cd}_2\text{SnO}_4$ ,...  
 (DOPED OR UNDOPED)



## Thin Metal Films

VACUUM EVAPORATION AND SPUTTERING - PROPERTIES DEPEND ON  
FILM NUCLEATION AND COALESCENCE.

- A. DISCONTINUOUS FILMS - ISLAND STRUCTURE - LOW  
LIGHT SCATTER, ACTIVATED CONDUCTION.
- B. CONTINUOUS FILMS - SIZE EFFECT, EXCESS IMPURITIES,  
INSULATING PHASES.
- C. NUCLEATION-MODIFYING LAYERS - EG.:  $\text{Bi}_2\text{O}_3$  MAKES  
AU FILM MORE CONDUCTIVE.

## Semiconducting Oxide Films

- NO NUCLEATION PROBLEM DUE TO CHEMICAL BONDING AT SURFACE.
- CONDUCTION MECHANISM DIFFERENT FROM THAT OF METAL.
- ALL N-TYPE SEMICONDUCTORS.

- A. BINARY OXIDES - ANION-DEFICIENT (OXYGEN VACANCY)  
ELECTRON CONC. =  $10^{17}-10^{21} \text{ cm}^{-3}$

RELATIVELY EASY TO OXIDIZE OR REDUCE.

- B. DOPED OXIDES - SUBSTITUTIONAL CATIONS OF HIGHER  
VALENCY, OR ANIONS OF LOWER  
VALENCY (EG.:  $\text{In}_2\text{O}_3:\text{Sn}$ ,  $\text{SnO}_2:\text{F}$ ).
  - NO COMPOUND OR SOLID SOLUTION  
OF SUBSTITUTIONAL CATION.
  - CARRIER SCATTERING

IDEAL TRANSPARENT CONDUCTOR (TC)

LOW  $m_e^*$

INSB:  $m_e^* = 0.013 m_e$ . SO  $R_s = 0.5 \Omega/\text{SQUARE}$  @  $T=95\%$   
FOR  $2 \mu\text{M}$  FILM DOPED TO  $10^{19} \text{ cm}^{-3}$ .

BUT BANDGAP  $E_g = 0.17 \text{ eV}$ . TOO LOW!

BANDGAP REQUIREMENT -  $E_g \geq 3 \text{ eV}$ .

## Methods of Preparation of Transparent Conductors

1. VACUUM EVAPORATION
2. REACTIVE EVAPORATION
3. EVAPORATION AND OXIDATION
4. SPUTTERING - DC, RF, ION-BEAM
5. REACTIVE SPUTTERING
6. CHEMICAL VAPOR DEPOSITION
7. SPRAY HYDROLYSIS

## Oxide Semiconductors: Properties of Interest in Solar Cells

### OXIDE SEMICONDUCTORS - PROPERTIES OF INTEREST IN SOLAR CELLS

1. WORK FUNCTION OR ELECTRON AFFINITY - HIGH FOR N-TYPE ABSORBERS, LOW FOR P-TYPE ABSORBERS.
2. WIDE BANDGAP ( 3 eV).
3. LOW ELEC. RESISTIVITY (SHEET RES. 10 OHMS/SQUARE).
4. HIGH OPTICAL TRANSMISSION.
5. INTERFACIAL MATCHING, ABSINCE OF SURFACE DAMAGE.
6. ENVIRONMENTAL AND LIFE STABILITY.
7. REFRACTIVE INDEX.

### FUNCTIONS OF OXIDE SEMICONDUCTORS IN SURFACE BARRIER CELLS-

- A. FORMATION OF PHOTOVOLTAIC BARRIER
- B. PHOTOCURRENT COLLECTION
- C. LOW-RESISTANCE FRONT CONTACT REGION
- D. OPTICALLY TRANSPARENT WINDOW
- E. ANTIREFLECTION (AR) COATING

### PROPERTIES OF IMPORTANT OXIDE SEMICONDUCTORS-

MATERIAL.	$E_G$ (eV)	LATTICE	T(%)	$n$ ( $CM^{-3}$ )	$\mu_n$ ( $CM^2/V-S$ )	$\epsilon$ ( $\epsilon-CH$ ) <sup>-1</sup>
$IN_2O_3:Sn$ (ITO)	~ 3.7	BCC ( $A_0=10.12 \text{ \AA}$ )	0.83	$10^{20}$	75	1200
$SnO_2$	~ 3.5	RUTILE ( $A_0=4.74 \text{ \AA}$ $C_0=3.19 \text{ \AA}$ )	0.85	$8 \times 10^{20}$	10	1300

## Fig. of Merit for Transparent Conductors

$$\phi_{TC} = T/R_s$$

$$\phi_{TC} = \sigma t \exp(-10at)$$

For given  $R_s$

$$\phi_{TC} \propto \exp\left(-\text{CONST.} \frac{\alpha}{\sigma}\right)$$

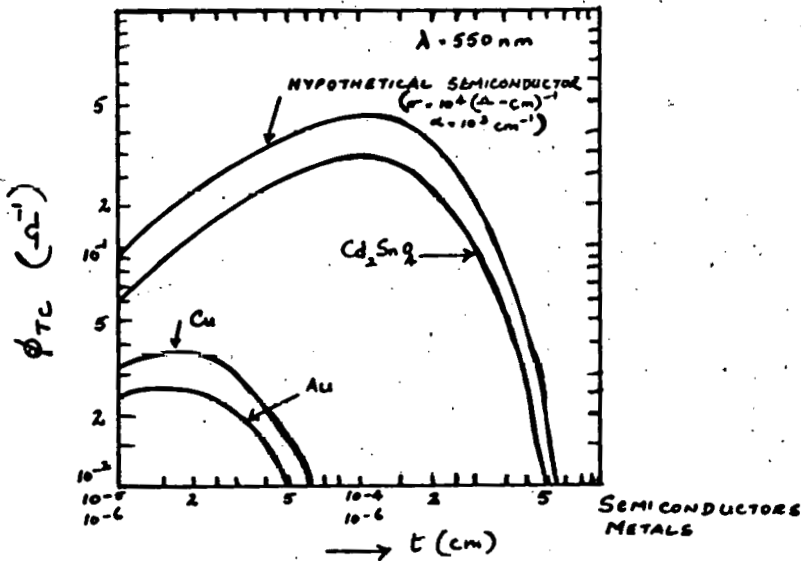
$$\frac{\sigma}{\alpha} = \pi c n v^2 \tau^2 = \frac{\pi c n v^2}{e} \mu^2 m^{*2}$$

Since  $\mu = \frac{e\tau}{m^*}$

$\mu$  = MOBILITY  
 $\tau$  = FREE CARRIER RELAXATION TIME  
 $n$  = REFRACTIVE INDEX  
 $m^*$  = EFFECTIVE MASS

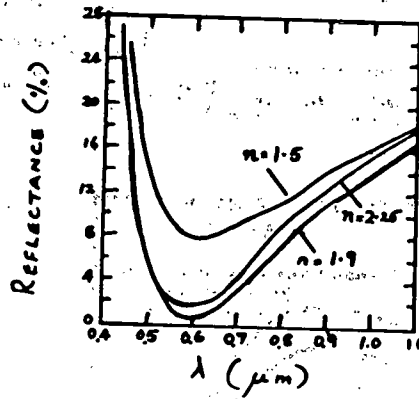
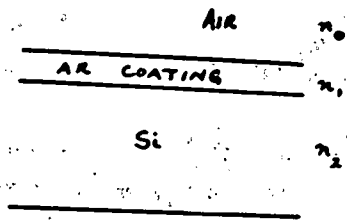
$\phi_{TC} \uparrow$  as  $\mu \uparrow$  OR  $m^* \downarrow$

SINCE  $\mu \propto (m^*)^{-1.35}$



Ref. [1,2]

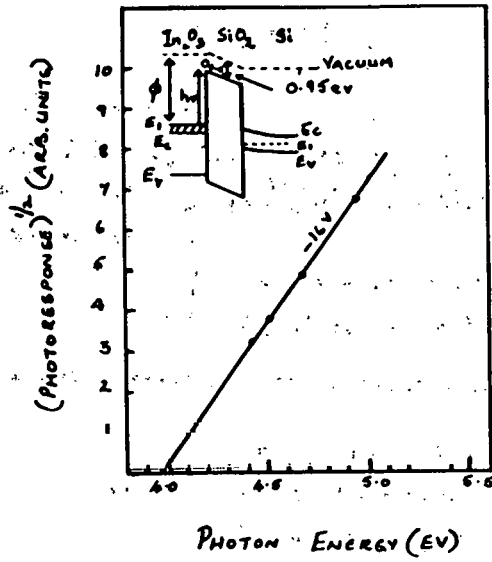
# AR Coating



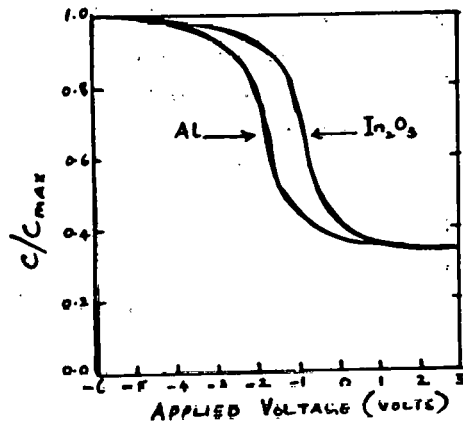
$n_2 = 3.5$  AT  $1\mu\text{m}$   
 $3.75$  AT  $0.75\mu\text{m}$   
 $n_1 = 1.9 - 2.5$

REFLECTANCE MIN. AT  
 $n_1 d_1 = (2m-1) \frac{\lambda_0}{4}$

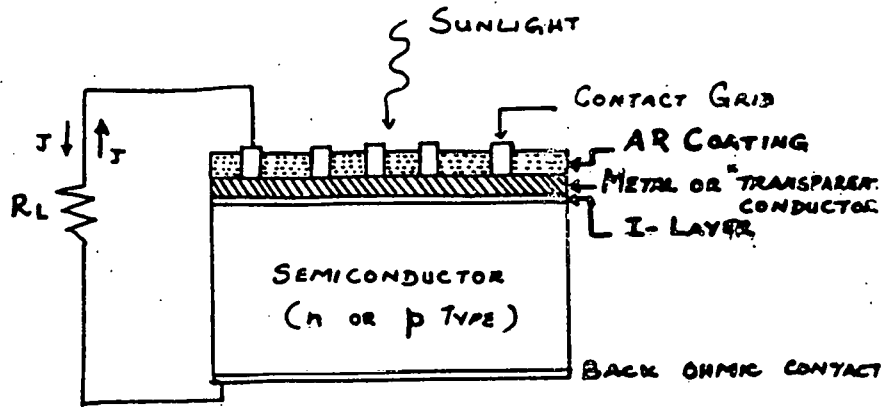
$R_{\text{min}} = 0$  FOR  $n_1^2 = n_0 n_2$



INTERNAL PHOTO-  
 EMISSION MEAS.  
 TO FIND WORK  
 FUNCTION/ELECTRON  
 AFFINITY OF  
 TRANSPARENT  
 CONDUCTOR



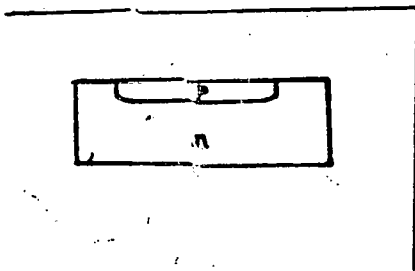
MOS/TCOS  
 CAPACITOR  
 C-V DATA



SCHMATIC OF  
SURFACE BARRIER SOLAR CELL  
(MS, MIS, SIS)

Surface barrier cell -

only one semiconductor, of  
conductivity type, is used as  
absorber; the principal source  
of photovoltaic action is a  
potential barrier existing at the  
surface.



# Surface Barrier Solar Cells

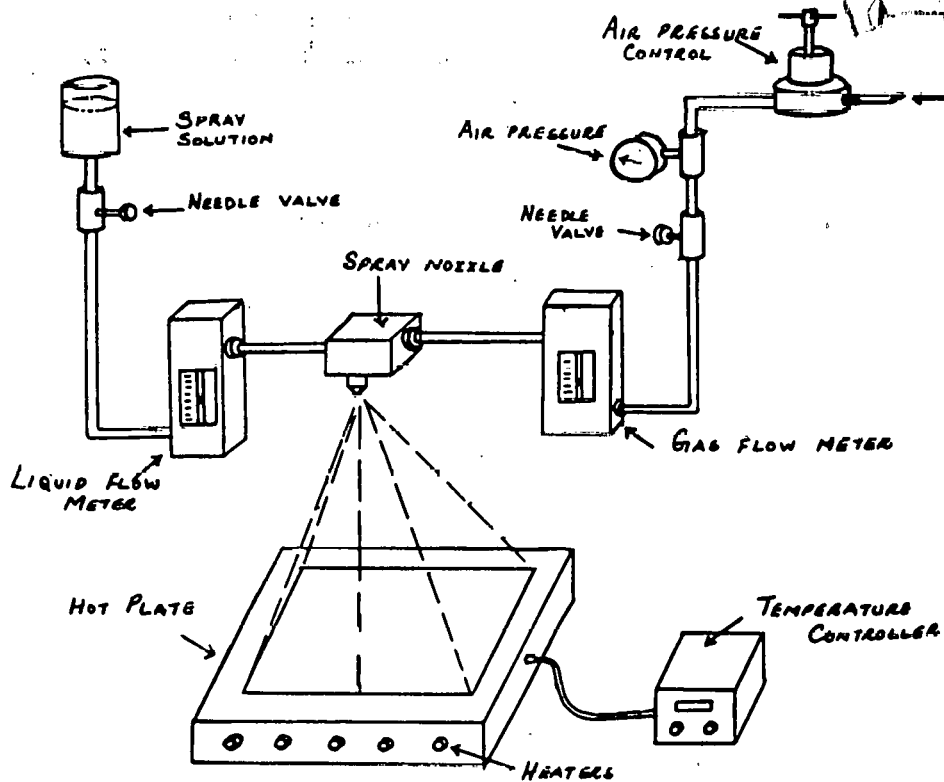
## FEATURES -

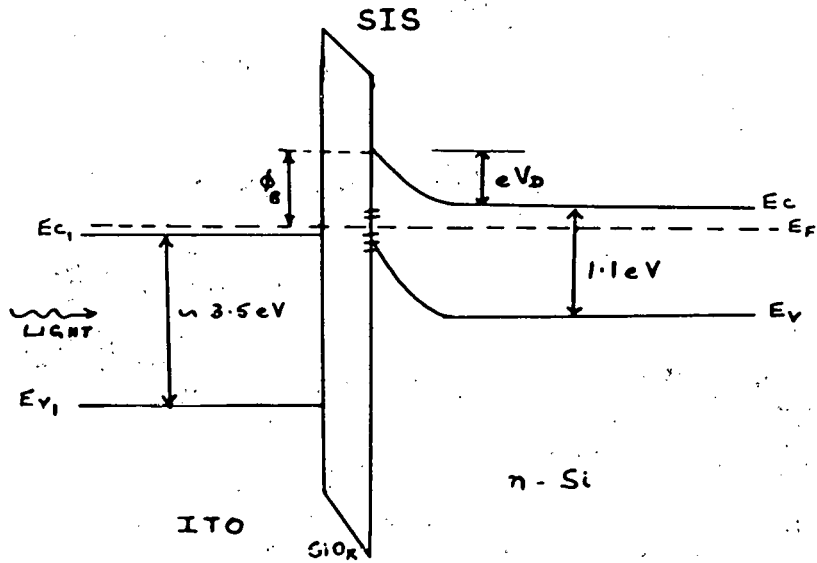
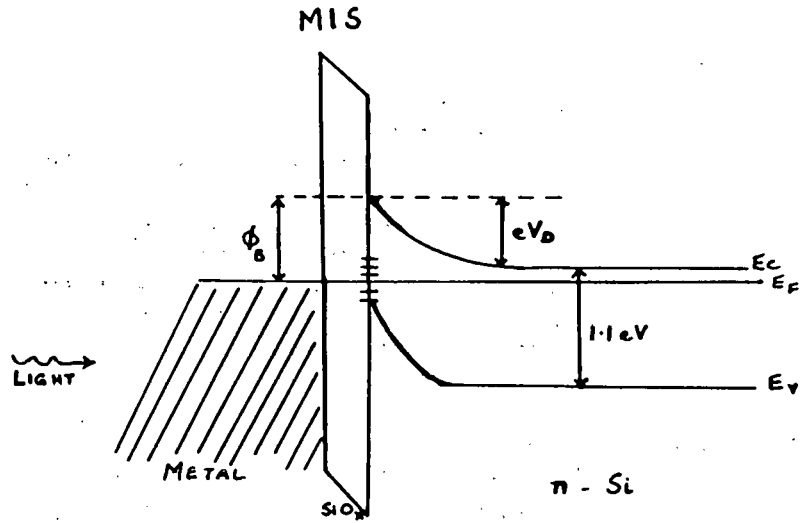
1. SIMPLE FABRICATION
2. LOW TEMP. PROCESSING. SO  
NO MIN. CARRIER LIFETIME DEGRADATION  
(SINGLE XTAL)  
NO GRAIN BOUNDARY DIFFUSION (POLY)  
NO DECOMPOSITION (AMORPHOUS)
3. BETTER BLUE RESPONSE THAN P-N HOMOJUNCTION
4. USEFUL FOR ASSESSING NEW PHOTOVOLTAIC  
ABSORBER MATERIALS

## LIMITATIONS -

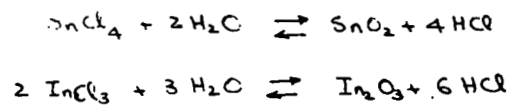
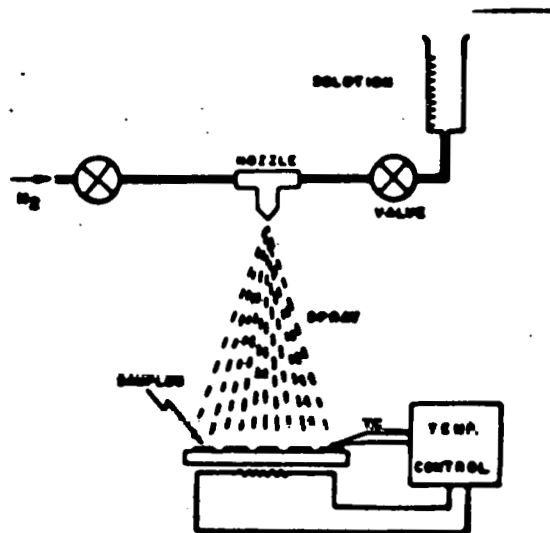
1. LOW  $V_{OC}$  - THERMIONIC EMISSION OR MULTI-STEP  
TUNNELING.
2. SHEET RESISTANCE/TRANSPARENCY TRADEOFF  
( $J_{SC}$  VS. FF TRADE-OFF)
3. STABILITY AND AGING OF THIN FILMS.
4. POSSIBLE PHOTOGENERATED MINORITY CARRIER  
LOSS THROUGH INTERFACE TRAPS)

## Spray Pyrolysis System



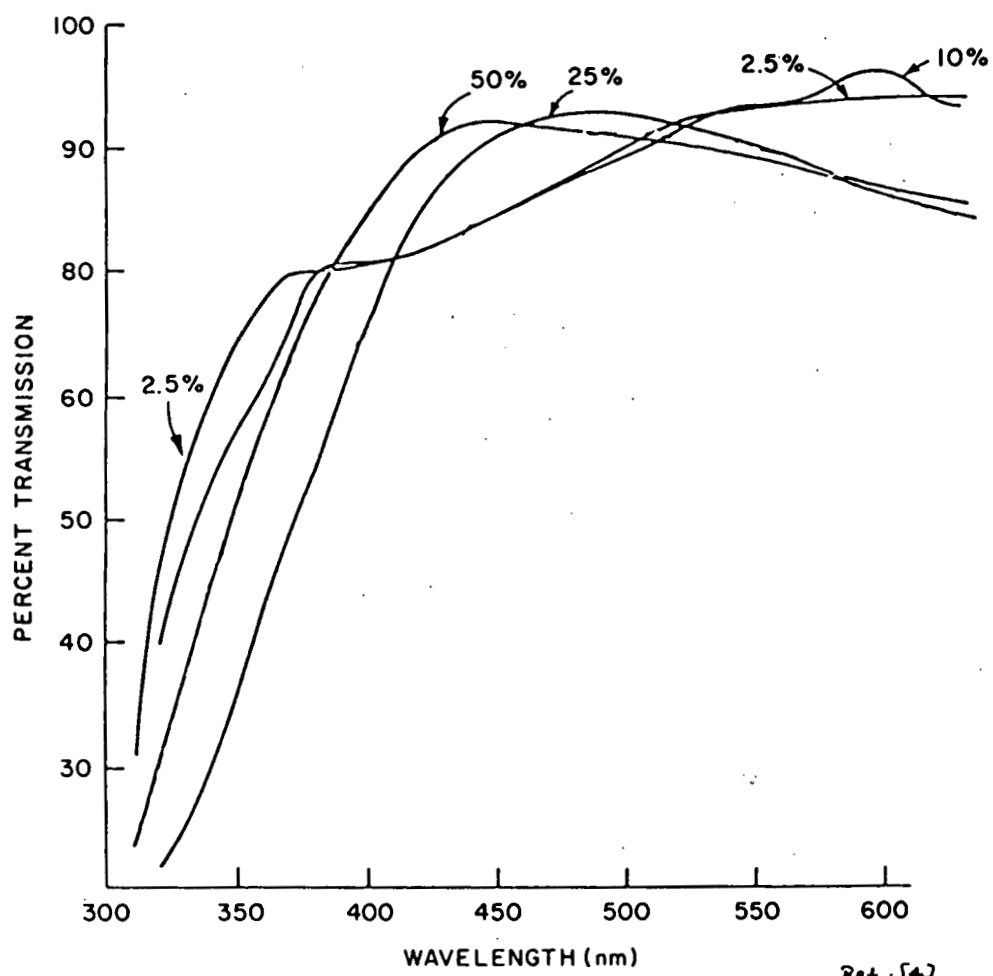






### ITO Resistivity as a Function of Chemical Composition

Weight % of $\text{SnCl}_4 \cdot 5\text{H}_2\text{O}$	Thickness ( $\text{\AA}$ )	Refractive Index	R ( $\Omega/\square$ )	P ( $\Omega/\text{cm}$ )
2.5	4200	1.9	25	$1.1 \times 10^{-3}$
25	4700	2.1	270	$1.3 \times 10^{-2}$
50	4300	2.2	335	$1.4 \times 10^{-2}$

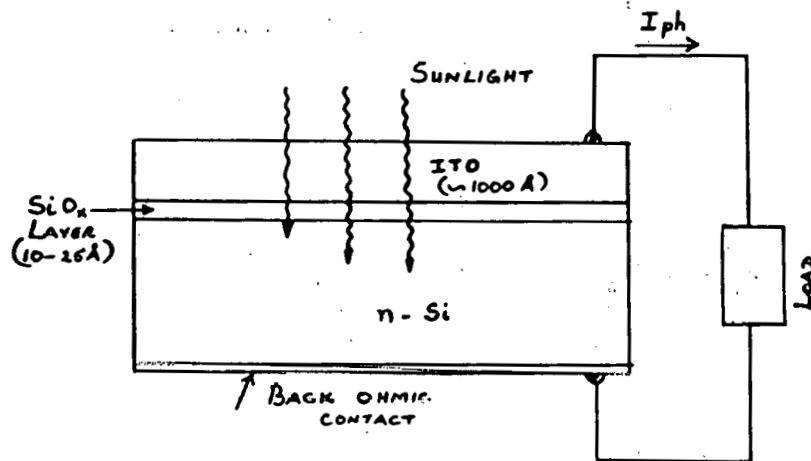


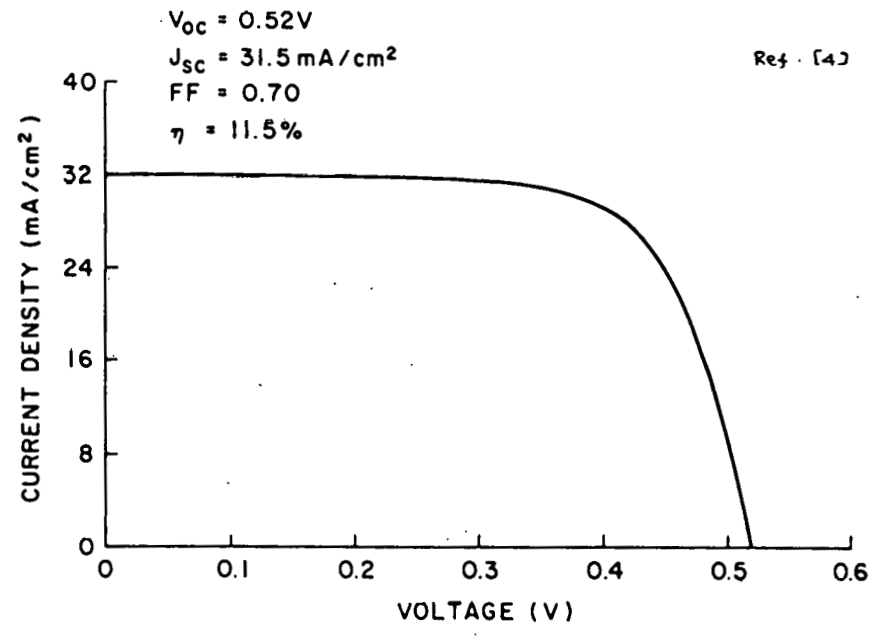
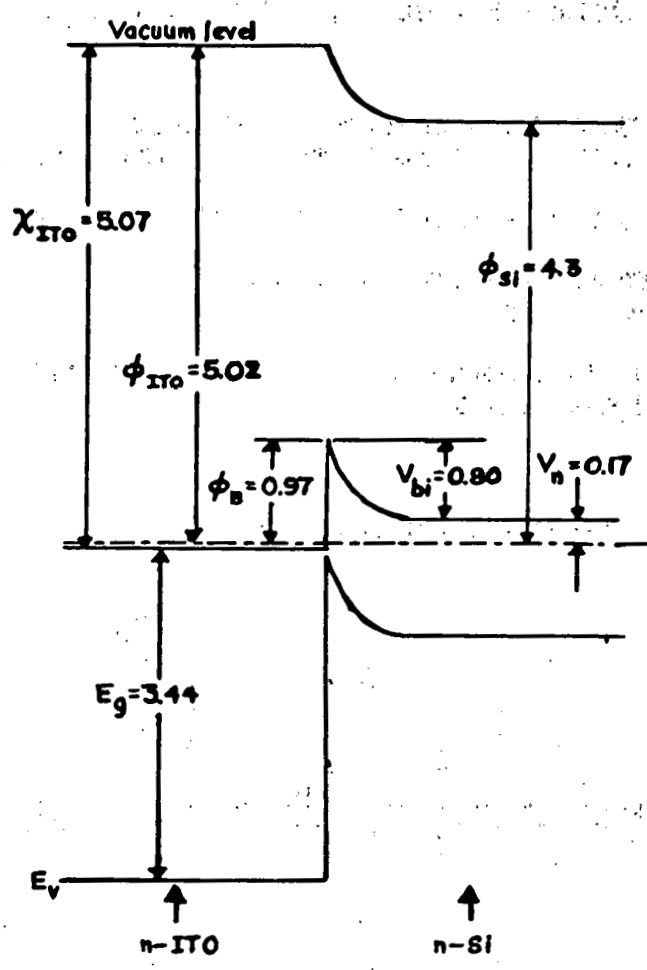
Ref. [4]

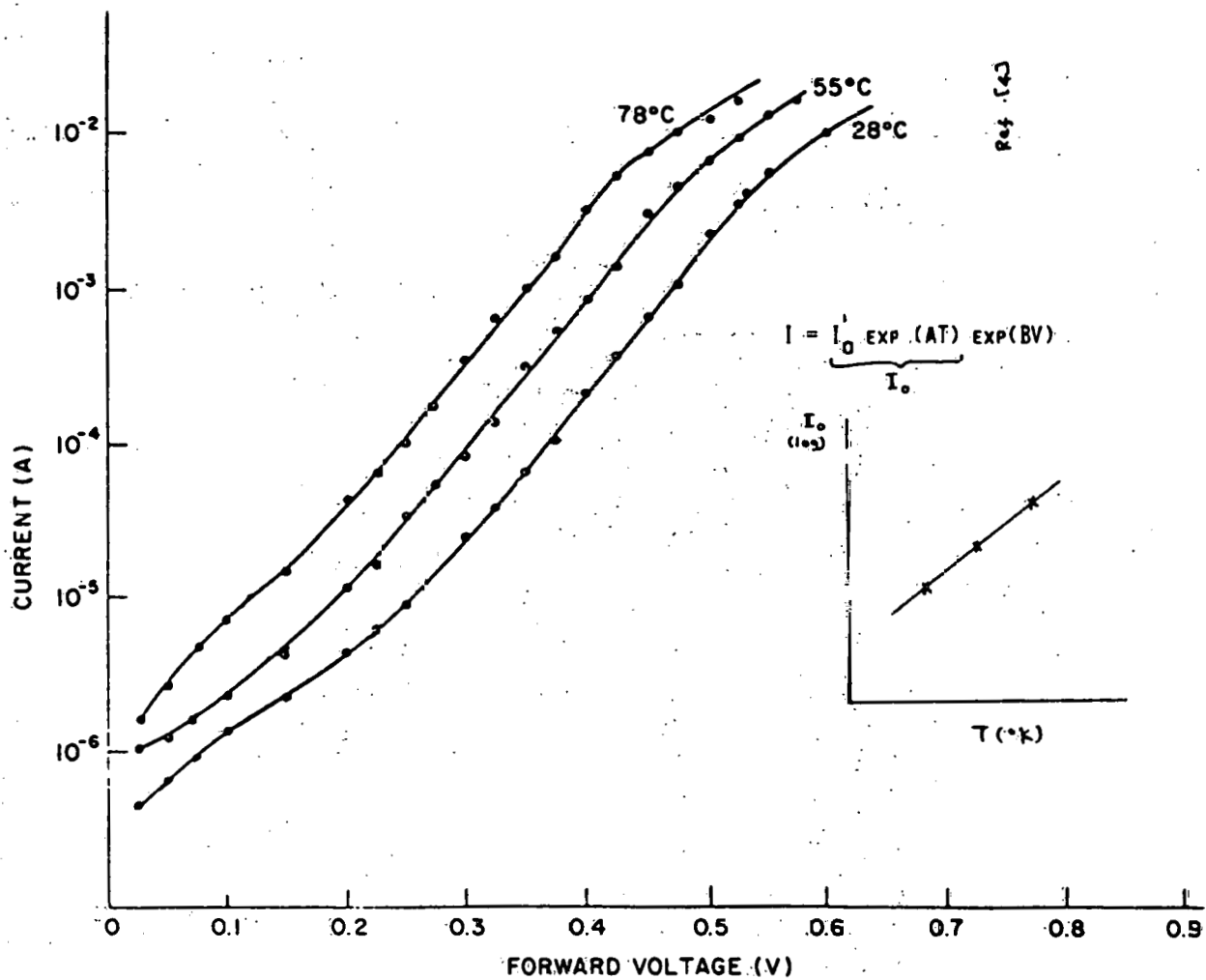
## ITO Optical & Electrical Characteristics

1. ALLOY COMPOSITION CHOSEN FOR BEST OPTICAL TRANSMISSION, LOWEST ELECTRICAL RESISTANCE, AND BEST PHOTOVOLTAIC RESPONSE.
2. ITO BANDGAP IN THE RANGE 3.2 - 3.45 eV FOR VARYING COMPOSITION.
3. ELECTRON MICROGRAPH SHOWS POLYCRYSTALLINE FILM WITH 400-1000 Å GRAINS.
4. SPRAY ITO FORMS BARRIER CONTACT WITH N-TYPE Si AND OHMIC CONTACT WITH P-TYPE Si.

### ITO-SiO<sub>x</sub>-n-Si SIS Solar Cell







# Best Reported Performance of ITO—n-Si & SnO<sub>2</sub>—n-Si Cells

(SPRAY PROCESS)

CELL TYPE.	$J_{SC}$ (MA/CM <sup>2</sup> )	$V_{OC}$ (V)	FF	EFFICIENCY(%)
ITO/N-SI (SINGLE XTAL SI)	30.2	0.626	0.73	13.7
SnO <sub>2</sub> /N-SI (SINGLE XTAL SI)	29.1	0.615	0.615	12.3
ITO/N-SI (WACKER POLY SI)	29.8	0.557	0.67	11.2
SnO <sub>2</sub> /N-SI (WACKER POLY SI)	26.6	0.56	0.68	10.1

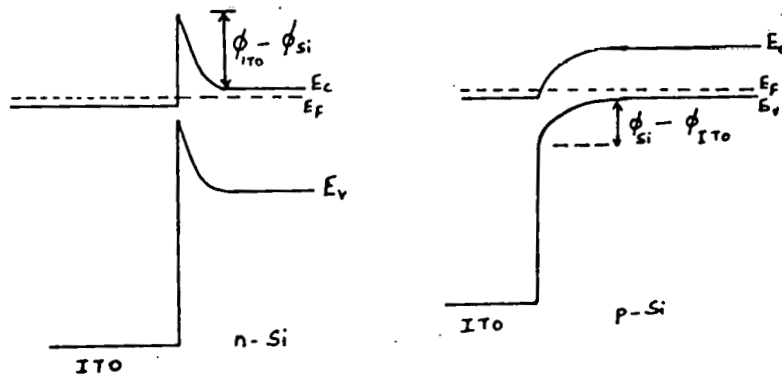
## ITO—Si Heterojunction Anomaly

SPRAY OR ELECTRON-BEAM EVAPORATED ITO -

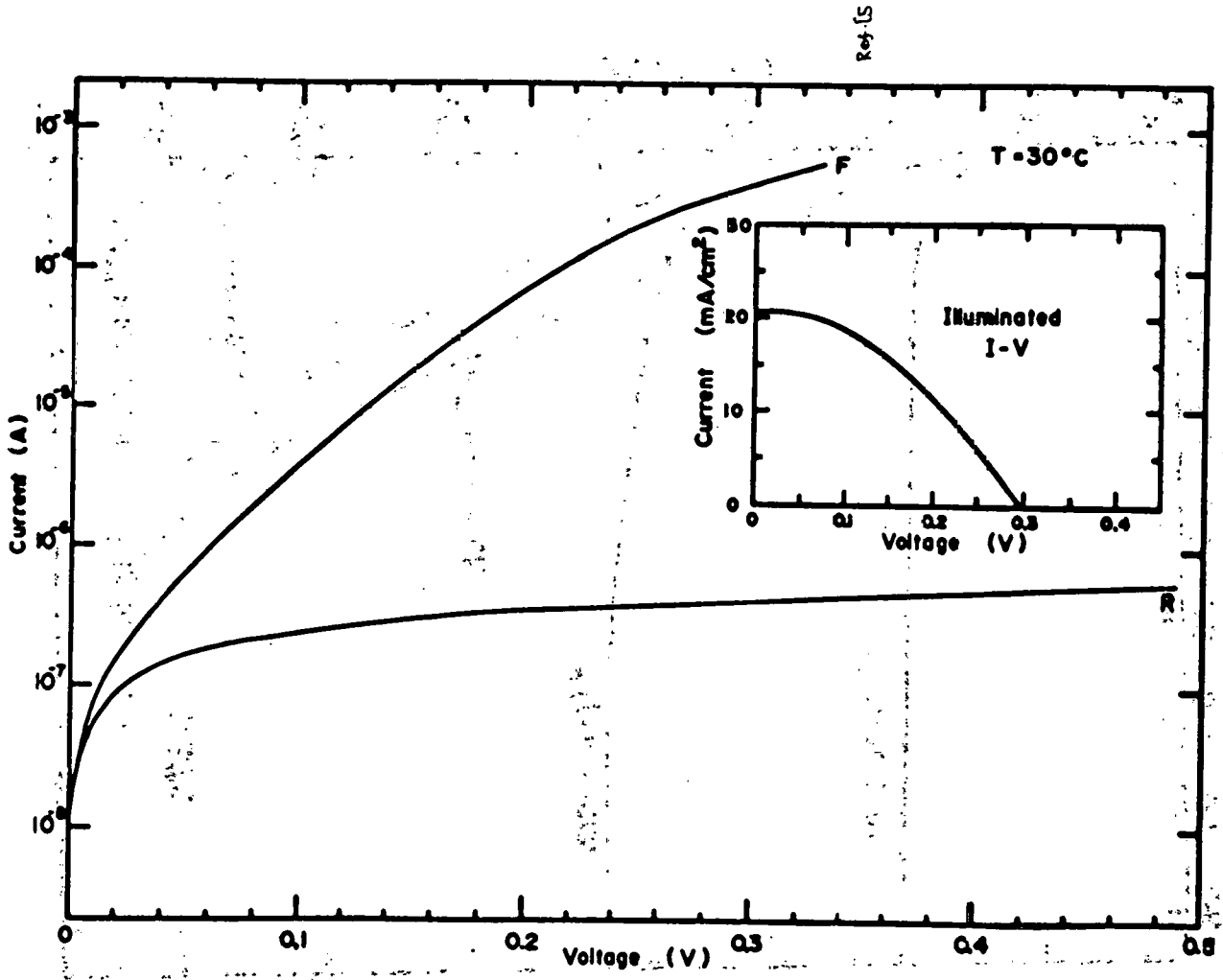
RECTIFYING JUNCTION ON N-SI (SOLAR CELL)  
OHMIC CONTACT (LOW BARRIER) ON P-SI

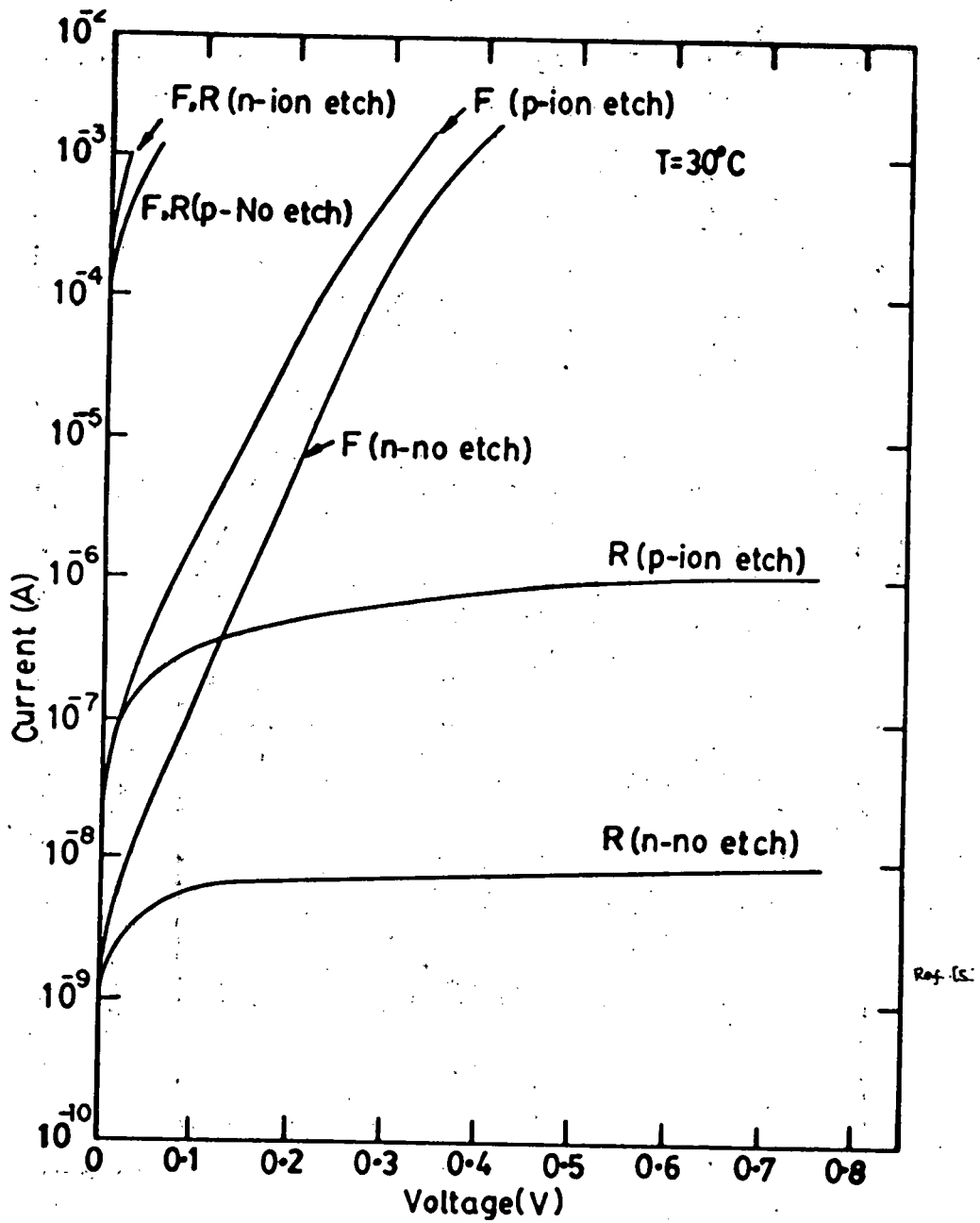
ION-BEAM SPUTTERED ITO -

RECTIFYING JUNCTION ON P-SI (SOLAR CELL)  
OHMIC CONTACT (LOW BARRIER) ON N-SI

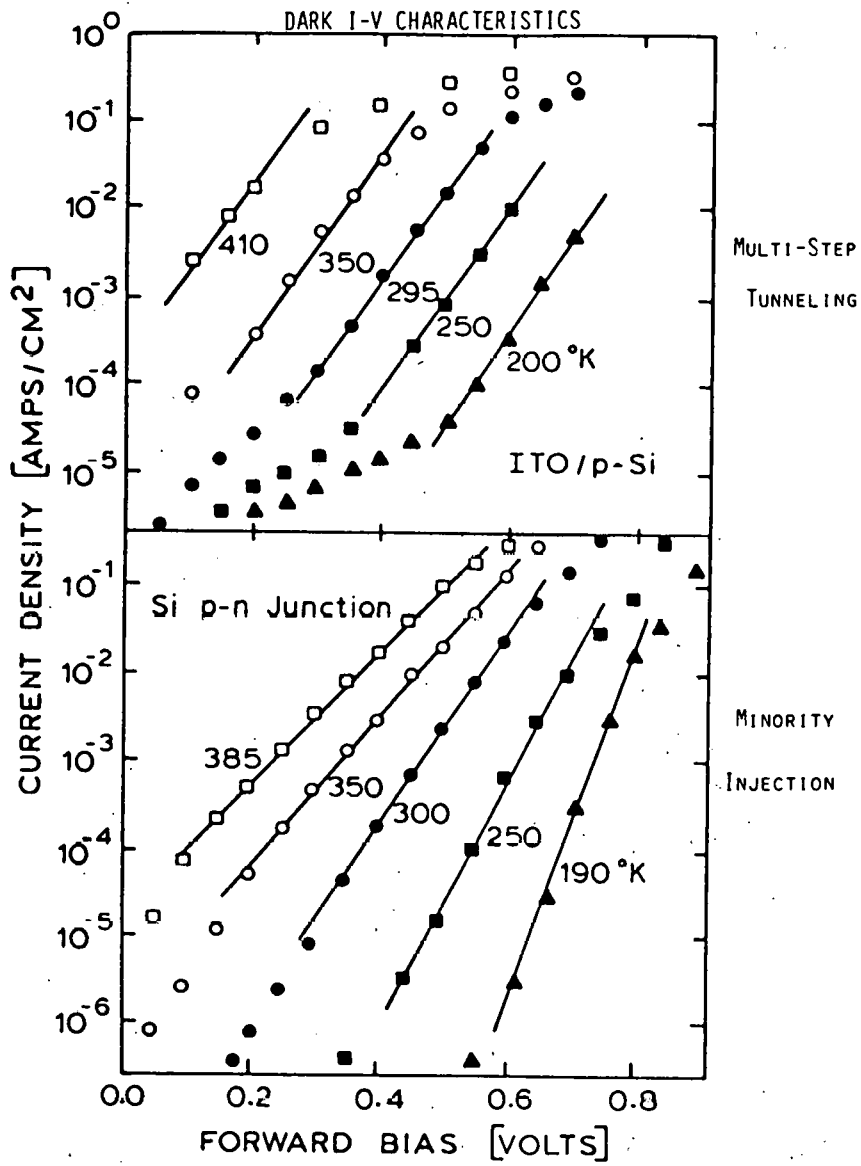


Ref. (5)

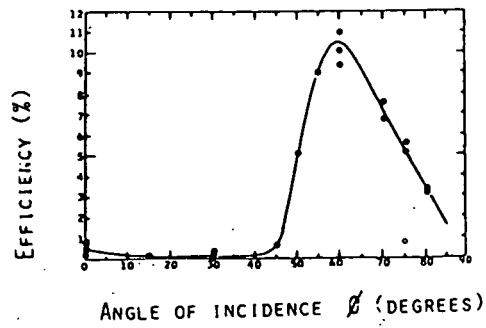
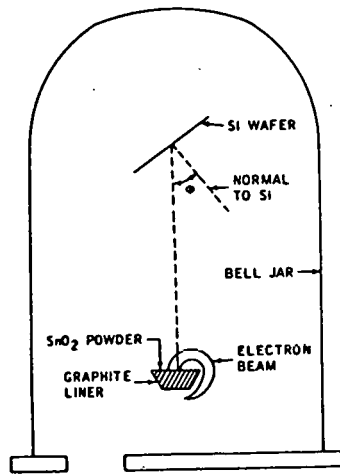








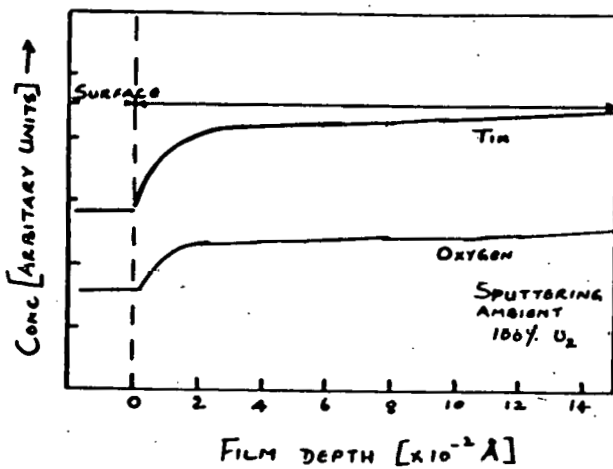
# Angle-of-Incidence Dependence of Electron-Beam-Deposited SnO<sub>2</sub>-n-Si Cells



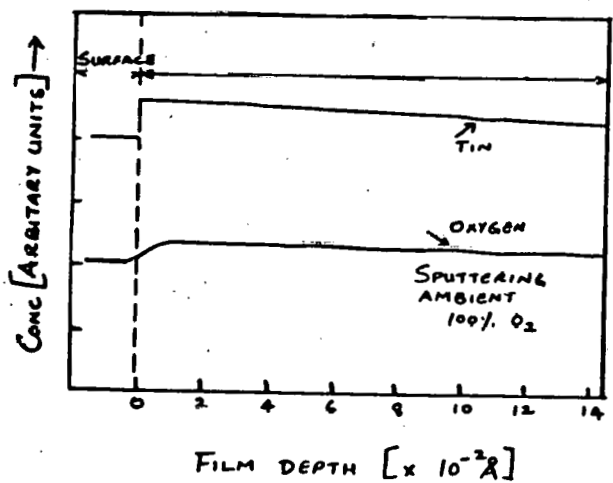
Ref. [c]

# AES Profiles

RF sputtered SnO<sub>2</sub>



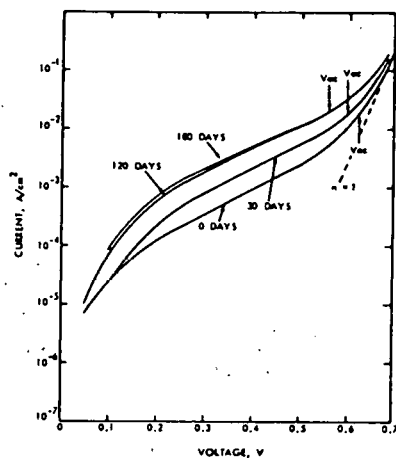
After heating  
in air  
for 200 °C



As sputtered

Ref. [7]

## Light-Induced Degradation of Spray SnO<sub>2</sub>-n-Si Cells

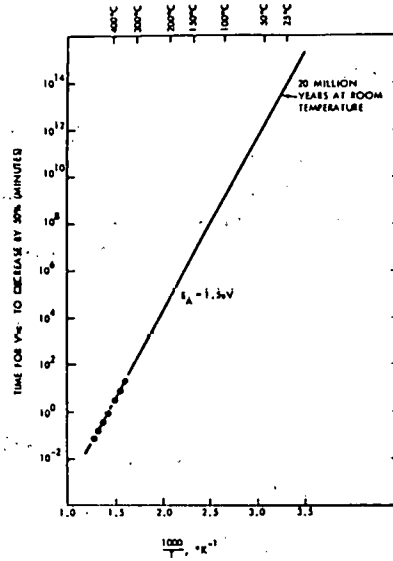


CHANGE IN DARK I-V CHRCS. DUE TO LIGHT

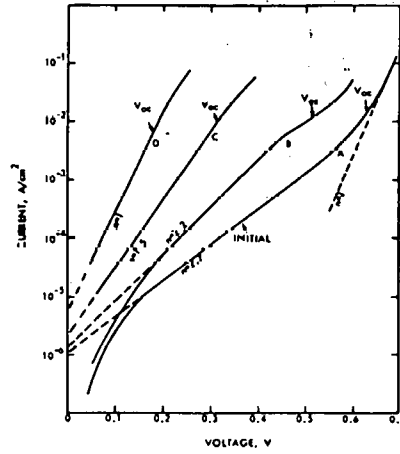
MECHANISM - CHARGE TRAPPING AT Si/SiO<sub>2</sub> INTERFACE WITH  
RESULTANT CHANGE IN BARRIER HEIGHT.  
DUE TO ULTRA-VIOLET COMPONENT.

Ref. [8]

# Thermal Degradation of Spray SnO<sub>2</sub>-n-Si Cells



ACTIVATION ENERGY PLOT



Ref. [8]

DARK I-V DEGRADATION WITH PROGRESSIVE HEATING IN AIR  
AT 350° C

# Surface Barrier Height Control

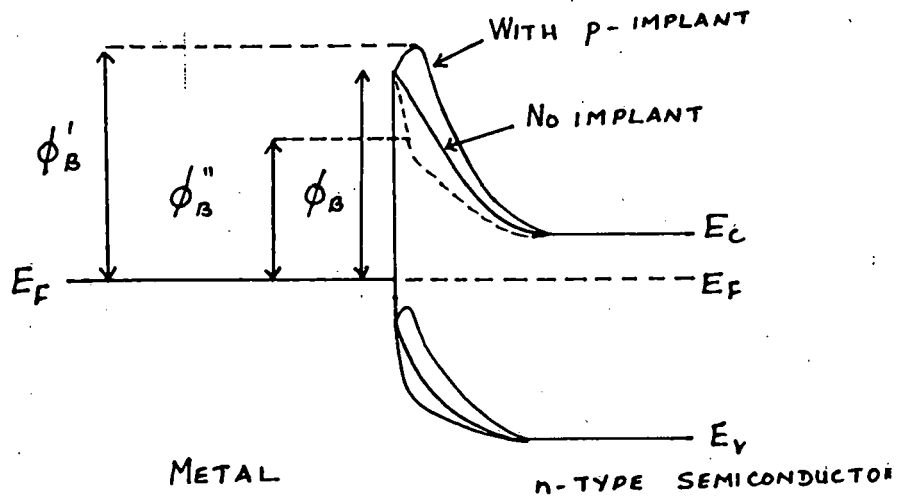
BARRIER HEIGHT ENHANCEMENT BY VERY SHALLOW ION IMPLANT.

$\sim 50 - 150 \text{ \AA}$  PROJECTED RANGE

ION ENERGY 5 - 15 KEV

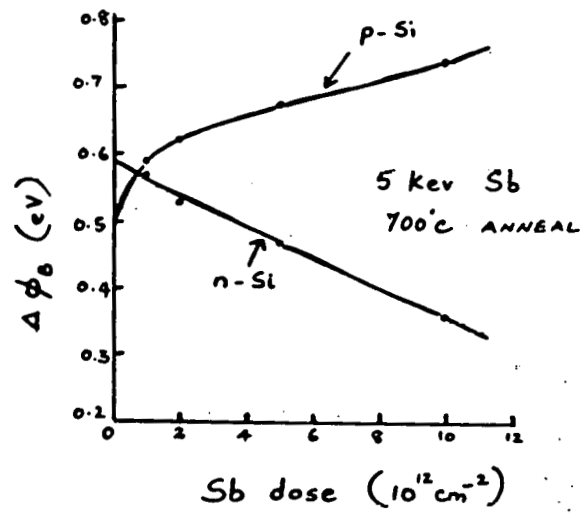
ION DOSE  $10^{12} - 10^{13} \text{ cm}^{-2}$

IMPLANT ION TYPE - OPPOSITE TO SUBSTRATE CONDUCTIVITY TYPE  
(DONOR FOR P-SUBSTRATE, ACCEPTOR FOR N-SUBSTRATE), WITH LOW DIFFUSION CONST.



Ref. [9]

## Barrier Height Change vs Shallow Implant Dose



Ref. [9]

### Problem Areas

1. ROLE OF "DOPANTS"
2. INFLUENCE OF DEPOSITION CONDITIONS ON ELEC. INTERFACE
3. CONTROL OF PARAMETERS
4. CRITERIA FOR COMPARING FILMS PREPARED BY DIFFERENT TECHNIQUES
5. FURTHER AGING AND INTERFACE STABILITY STUDIES
6. AMORPHOUS TRANSPARENT CONDUCTORS ?

## DISCUSSION

WOLF: When you list E, the transmission factor E, is that purely due to absorption or does that still include reflection?

ASHOK: That is due to absorption.

WOLF: Then it must be thickness dependent.

ASHOK: Yes, but we have to have--in order to have a good AR coating, you have to have about 1000 Angstroms. If you make it too thick, then it is going to increase even more.

SOMBERG: Have you have done any work with dual AR using a transparent conductor?

ASHOK: No, I am not aware of any. The two different transparent conductors have been tried for a different reason. One is used to form a good barrier and the other one to reduce surface reflection.

SOMBERG: I am just talking about optimizing the antireflection barriers. The other question is, why do you say you have to have a 1000-Angstrom-thick layer for a good AR, rather than something around 600 to 800 Angstroms?

ASHOK: It was a round figure. I just rounded it off without giving an exact figure.

GALLAGHER: In your enhanced work function graph, you showed work functions going up in the 7 to 8 region. Since the work function and the VOC is almost the same, what measurable VOCs did you get in those devices?

ASHOK: With the last viewgraph?

GALLAGHER: Yes.

ASHOK: I showed the change in the work function.

GALLAGHER: You got up to 0.7 --

ASHOK: It is not the work function. It is the body barrier height.

GALLAGHER: Oh, it's the barrier height, excuse me, I misunderstood.

WONG: I have a question on the fluorinated tin oxide. What kind of a conductor mechanism does fluorinated tin oxide utilize?

ASHOK: Well, it is similar to the other cases.

WONG: The reason I am asking this question is because tin oxide is n-type. The conductor mechanism is by oxygen vacancies, right? The available oxygen vacancies? By adding fluorine atoms -- fluorine is -1 -- you are actually occupying an ion vacancy rather than giving up an ion vacancy.



So actually I am thinking the opposite way -- so that you lose the conductivity that way.

ASHOK: No. It substitutes for an oxygen site.

WONG: Would the fluorine ion go into the oxygen vacancy? Because there is already oxygen vacancy there. So very easily it will go to the oxygen vacancy, and energetically is more favorable, so I would see the opposite mechanism going on. I know there is a more complicated answer but this is what I naively see.

ASHOK: I am not sure of the exact answer for that.

HOGAN: The light-and-temperature-induced changes -- are those independent of the method of the ITO fabrication?

ASHOK: Well, this one is on the straightforward system. I would think they would be comparable.

FIRESTER: Typically, for example, the sputtered ITO is unstable above the temperature in which it is sputtered. The resistivity goes up, depending on what the sputter temperature is.

WOLF: The substrate temperature?

FIRESTER: Yes.

QUESTION: What about light-intensity changes?

ASHOK: That is only to the interfaces. It is not to the bulk, I don't think. It is to the silicon-SnO<sub>2</sub> interface. It changes at the interface.

HOGAN: So that should be independent of the method of deposition?

ASHOK: I would think so, yes.

STEIN: There is another method of deposition that we have used, not for this purpose, but we make a metallo-organic composition that gives an ITO film. When printed and fired at between 550° and 600°C, the light transparency or transmission is higher than you have indicated in some of the films you have described. We have seen greater than 95%. The resistivity is not as low; sheet resistivity is in the order of 1000 ohms per square. You can modify that upward by quite a bit. You can't get much lower than 400 or 500--it's a function of firing temperature. The stability of these films is good to about 500°C, which more or less coincides with what our friend has said. They are sensitive to moisture. I don't know if the same is true in some of the films that you have described. The resistivity tends to increase with higher relative humidity, and it can be dried out and decreased. It seems to be reasonably reversible.

SCHWUTTKE: Let me ask a general question. Where do you think this technology is going to challenge our standard systems? Will it be costly, will it be high-efficiency, or what do you think? Anyone can answer that.

ASHOK: Well, I think they are comparing two different things. If the efficiency can be boosted up, it obviously can be done when the open-circuit voltage problem can be handled separately by means of the surface treatment of silicon. But the material has to be grown with better transmission characteristics. But there is an interim tradeoff as we increase the conductivity. The plasma edge moves closer to the silicon band gap, and the plasma frequency increases as the electron concentration goes up. But if material can be developed with transmission in the range of 90%, in the range of interest, then it can be useful.

BURGER: What likelihood is there that you may turn up with newer or better transparent conductive coatings along the lines that you have been investigating? In other words, how broad could the field be, or is it a limited set of combinations and permutations?

ASHOK: Unfortunately, much of the information available in this whole field is still empirical. I think, in terms of understanding of the materials, it is comparable to amorphous silicon; probably amorphous silicon is better.

BURGER: I have one additional question. You mentioned that there was an optimal doping. How sensitive is that? I mean, is that a very narrow window or is it easy to achieve?

ASHOK: It can be easily achieved. It is not a problem.

SCHRODER: Who of the solar-cell manufacturers is using this technology?

ASHOK: For a production device?

SCHRODER: Yes, or some serious research.

ASHOK: I don't think anyone is using a pilot line, but at Exxon they have used it in their research.

FIRESTER: Photon Power is selling tin-oxide-coated glass, which is the first layer in their glass-tin-oxide CdS.

SCHWUTTKE: These are the 2% or 3% efficiency cells?

FIRESTER: I don't know what the efficiency is.

SCHRODER: Exxon is using it at least in R&D, and that is it. Are other companies that you are aware of?

ASHOK: I am talking about using it in single-crystal silicon. But as a thin film substrate, it is used.

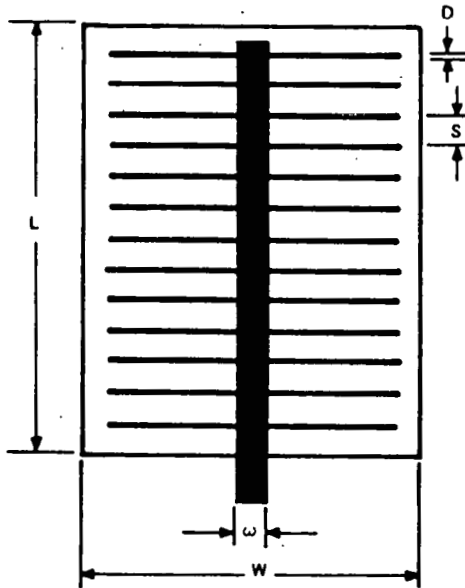
SCHRODER: I am not talking about that.

THIS PAGE  
WAS INTENTIONALLY  
LEFT BLANK

# A METALLIZATION SYSTEM FOR THIN-FILM PHOTOVOLTAIC MODULES

A.H. FIRESTER  
RCA LABORATORIES  
PRINCETON, NEW JERSEY

## Large-Area Cell Losses



$$\begin{aligned}
 \text{LOSS} &= \frac{w}{W} && \text{BUS SHADOW} \\
 &+ \frac{D}{S} && \text{GRID SHADOW} \\
 &+ \frac{1}{3} \cdot \frac{J}{V} R_{\text{CTO}} \left(\frac{S}{2}\right)^2 && \text{CTO } I^2 R \\
 &+ \frac{1}{12} \cdot \frac{J}{V} R_{\text{FG}} \left(\frac{S}{D}\right) w^2 && \text{GRID } I^2 R \\
 &+ \frac{1}{3} \cdot \frac{J}{V} R_{\text{BUS}} \left(\frac{W}{w}\right) L^2 && \text{BUS } I^2 R
 \end{aligned}$$

## BusBar Losses

$$F_B = \frac{w}{W} + \frac{1}{3} \cdot \frac{J}{V} R_B \frac{w}{W} L^2$$

$$(F_B)_{\text{MIN}} = 2L \sqrt{\frac{1}{3} \cdot \frac{J}{V} R_B}$$

$$w_{\text{OPT}} = WL \sqrt{\frac{1}{3} \cdot \frac{J}{V} R_B}$$

## Large-Area Cell Module Loss: Thick-Film Metallization

ALUMINUM: 10 MICROMETER THICK; 2.8  $\mu\Omega$ -CM

$J = 15 \text{ MA/CM}^2$      $V = 800 \text{ MV}$     ( $\eta = 12\%$ )

$R_{CTO} = 10 \text{ } \Omega/\square$      $R_G = R_B = .0028 \text{ } \Omega/\square$

$D = 100 \text{ MICROMETER}$      $G = 1 \text{ MILLIMETER}$

DIMENSIONS	W (CM)	3	3	6	10
	L (CM)	3	10	10	10
	s (CM)	.7	.7	.6	.5
	w (MM)	.38	1.3	2.5	4.2
% LOSSES - GRID SHADOW		1.4	1.4	1.7	2.0
	OHMIC	.3	.3	.9	2.2
	CTO	.8	.8	.6	.4
	BUSBAR	2.5	8.4	8.4	8.4
	GAP	<u>3.3</u>	<u>1.0</u>	<u>1.0</u>	<u>1.0</u>
	TOTAL	8.3	11.9	12.6	14.0

## Large-Area Cell Module Loss: Thin-Film Metallization

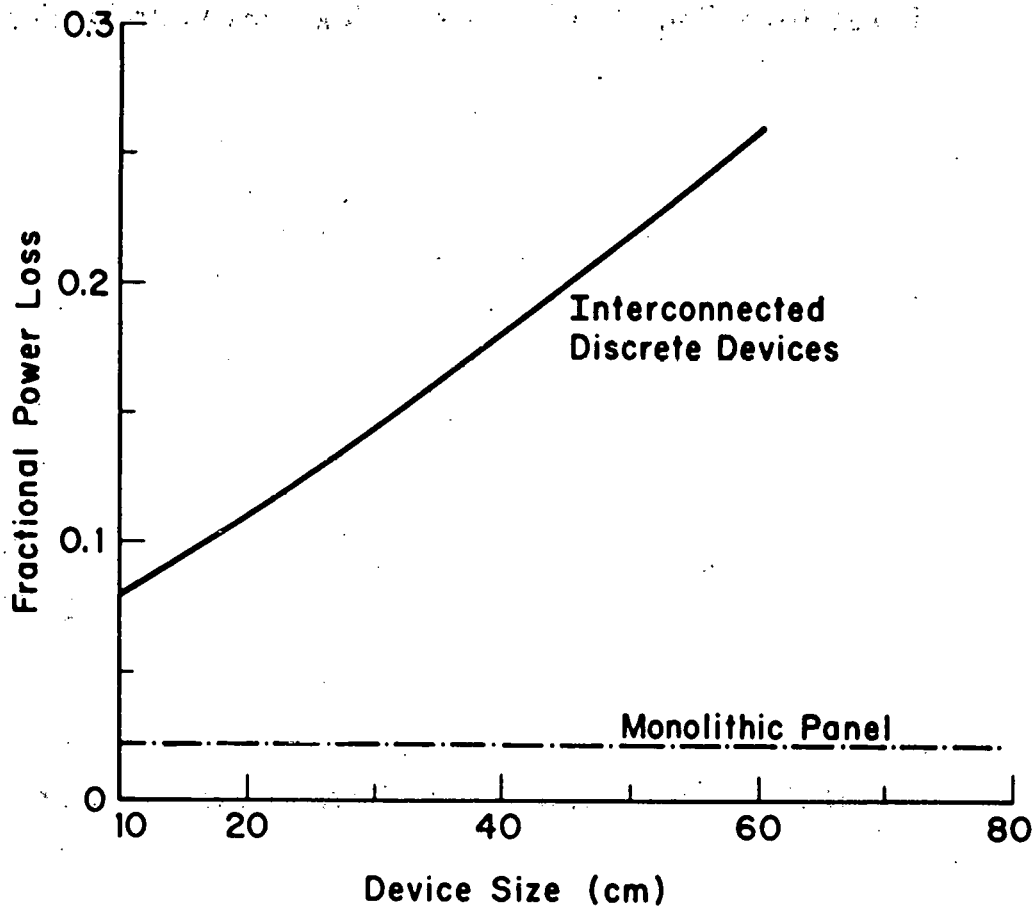
ALUMINUM: 1 MICROMETER THICK; 2.8  $\mu\Omega$ -CM

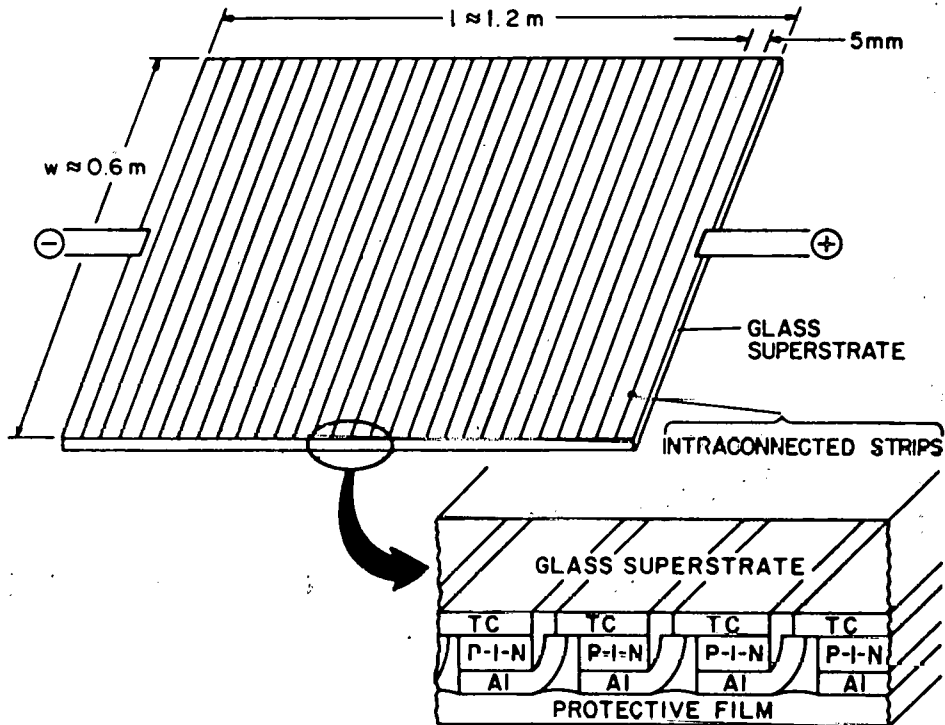
$J = 15 \text{ MA/CM}^2$      $V = 800 \text{ MV}$     ( $\eta = 12\%$ )

$R_{CTO} = 10 \text{ } \Omega/\square$      $R_G = R_B = 0.028 \text{ } \Omega/\square$

$D = 100 \text{ MICROMETER}$      $G = 1 \text{ MILLIMETER}$

DIMENSIONS	W (CM)	2	2	4
	L (CM)	2	5	5
	s (CM)	.7	.7	.4
	w (MM)	.53	1.3	2.6
% LOSSES - GRID SHADOW		1.4	1.4	2.5
	OHMIC	1.2	1.2	2.8
	CTO	.8	.8	.3
	BUSBAR	5.3	13.2	13.2
	GAP	<u>5.0</u>	<u>2.0</u>	<u>2.0</u>
	TOTAL	13.7	18.6	20.8





### Monolithic Panel Loss

$D$  = TOTAL SCRIBE WIDTH     $S$  = SCRIBE SPACING

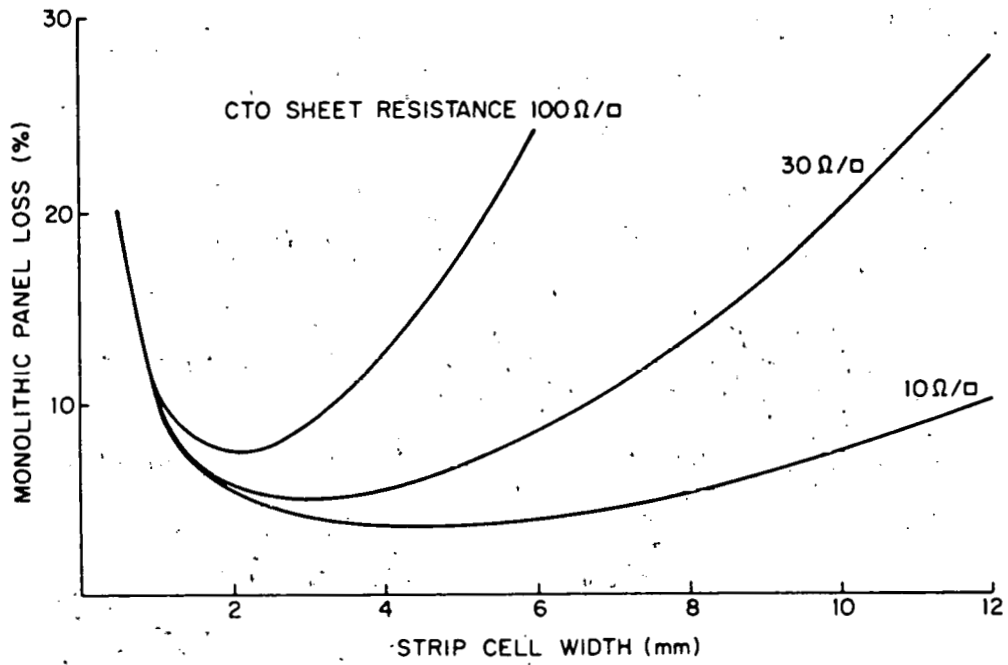
$$F_M = \frac{D}{S}$$

SHADOW LOSS

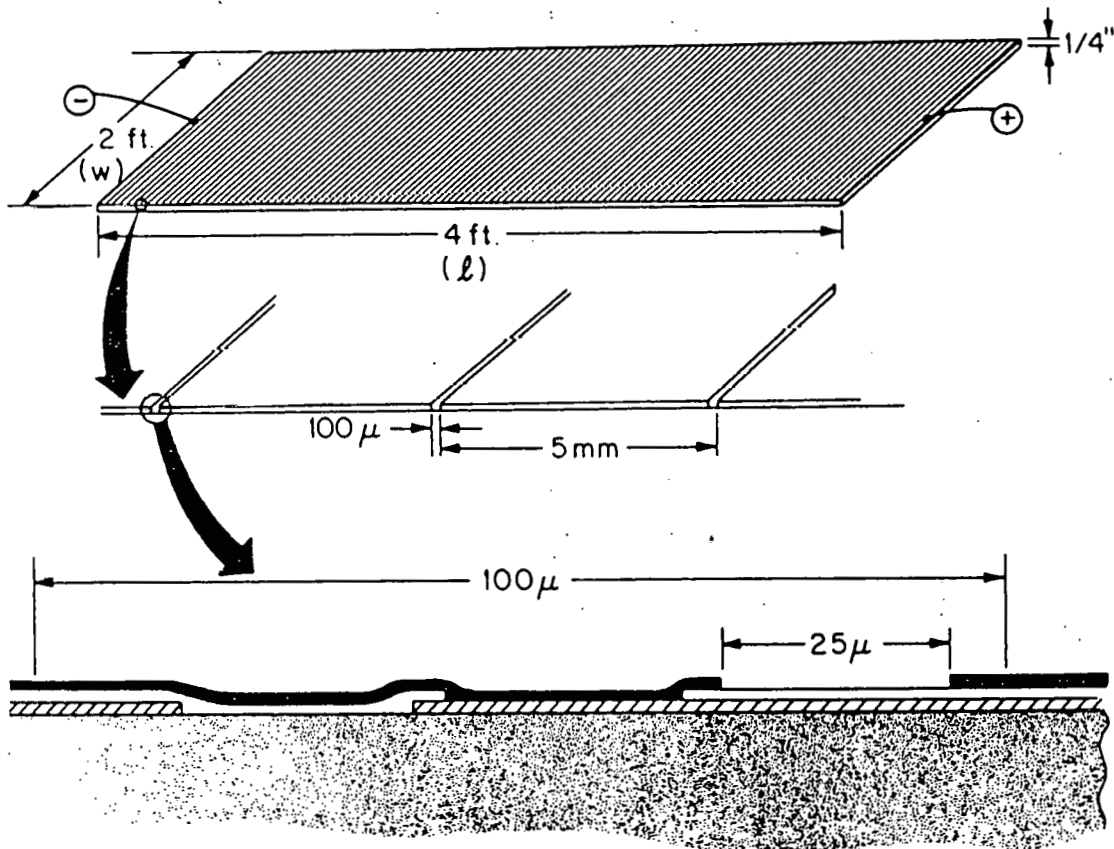
$$+ \frac{1}{3} \frac{J}{V} \frac{R_{CTO}}{T_{CTO}} S^2$$

OHMIC LOSS THRU CTO

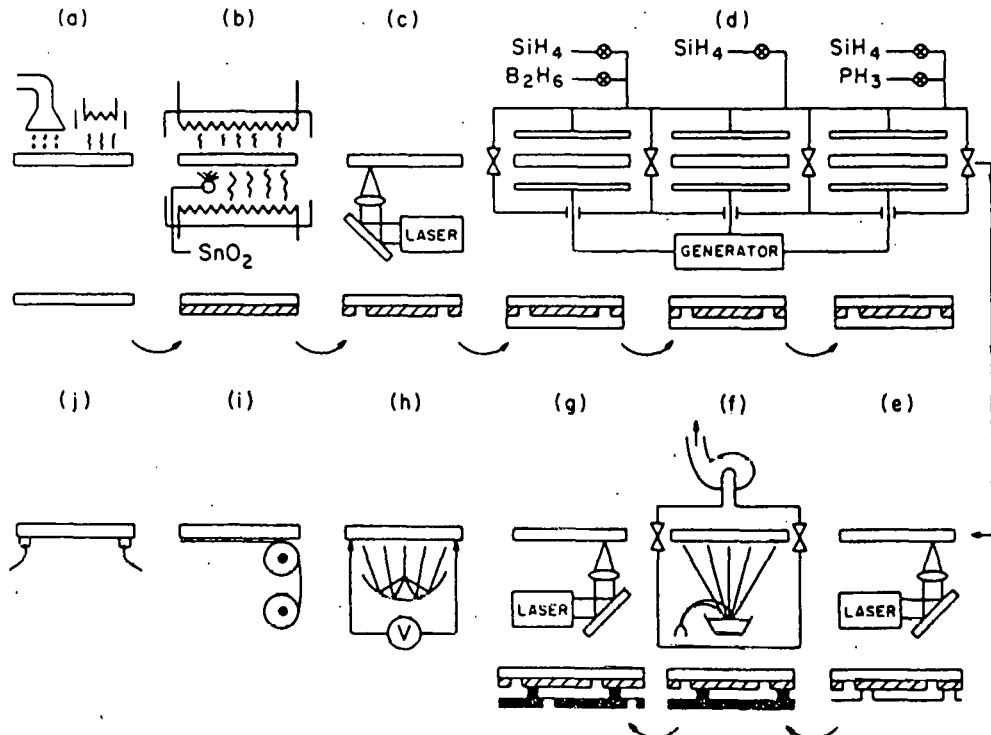
$$(F_M)_{OPT} = \frac{3}{2} \sqrt{\frac{3}{V} \frac{J D^2}{T_{CTO}}}$$



### Monolithic Amorphous Silicon Photovoltaic Panel







## DISCUSSION

QUESTION: You have shown a series-connected 240-cells span here. If one of those cells gets open-circuited, how do you plan to protect them with bypass diodes and how do you plan to connect those bypassed cells on the panel?

FIRESTER: I don't want to go into detail on that. That is the same problem you would have with any large panel, the difference being of course that here you have made it all at once; you can't throw a few cells away or strips away. Opens, by the way, are not a major problem as far as we can tell here. You have an option of doing bypass diodes and everything else, and that is independent of the panel structure. You would have to do that with anything else -- any other cell. Have I answered you?

COMMENT: I am not sure. You still need to need to make some physical connections with those diodes, and you need some metallization for that.

FIRESTER: Yes, you can make physical contact--the integrated circuit industry does it all the time, in thin films. That's not really a problem.

BURGER: Actually, our own view of it is that a structure like this can be looked at as being bullet-proof. I think you could shoot holes through the panel and it would still work, if you really look at what you have, because we have looked at other similar kinds of things from Japan.

FIRESTER: I would like to just balance the two. I am glad to hear that. The only catastrophic thing, though, is an open, and then it would really have to be an open across the entire line -- two feet.

GALLAGHER: Two feet worth of open. Remember that.

FIRESTER: The two-foot dimension is limited if you think about it by the series resistance of the metallization.

QUESTION: What sort of transmission characteristics do you get?

FIRESTER: It is greater than 90%. This gets you into an area where you have to think about one thin-film system versus another in process compatibility. For example, that kind of number can be attained with reactively sputtered indium tin oxide. That kind of number can be attained with chlorinated tin oxide. It is a question of when you do it and whether your material is underneath or on top; wherever you put it is compatible to the process of making it.

SCHWUTTKE: Have you looked at any other systems?

FIRESTER: No.

SCHWUTTKE: Have you made any large-area junction cells?

FIRESTER: I am not sure I understand.

SCHWUTTKE: Where you make, say, a 50 x 50 sheet of silicon, can you make a junction over that area?

FIRESTER: Yes, but then you can't get the current out.

SCHWUTTKE: OK. So does that mean you can't handle those areas?

FIRESTER: No. It doesn't. What you have to do is just play some funny games, forming isolated pockets in your single-crystal, or essentially getting it onto an insulated substrate.

SCHWUTTKE: Is this thin film the whole metallurgy?

FIRESTER: The whole metallurgy here is thin film, and yet if you go to the numbers you find you don't have any problems of current crowding or current densities alone.

BLAKE: This may be a completely absurd question, but I am worried about shadowed cells. In particular, shadows that would be long and thin -- power lines would be one example. Is there a real problem here or not?

FIRESTER: Well, it is a real constraint that you want to orient these panels or any other panels where you have shadowing that could wipe out a whole interconnect in a series array. I think the more serious question that I am concerned about, by the way, is not the site shadowing, but the panel-to-panel shadowing in arrays, and that simply says get the lines running vertically and then there is no problem.

WEAVER: This is the kind of a thing we haven't even talked about, but I have done some looking at rows of things, and there is a diffuse sky component; the bottom of one row is looking at the back of the row in front of it, yet the top of that row is not looking at it. It sees the entire diffused sky and we have found, especially in winter, at the optimum tilt angle, as much as 12% difference in irradiance from the top to the bottom of the module. So I think you had better be very careful about which way you want to run the strips. If you run them vertically -- are you saying you are collecting current this way?

FIRESTER: No.

WEAVER: Or are you collecting horizontally?

FIRESTER: The current is flowing as a sheet from strip to strip and if you shadow it laterally along perpendicular to the strips there is no problem. If you have uneven illumination there is no problem. You can literally take the cell and crack it in half, and it still works. Take these things and scratch the back and it is not going to affect it.

WONG: You have been giving examples of amorphous silicon cell structure and monolithic configuration. Is this type of configuration suitable for high-current-density devices too?

FIRESTER: Yes.

WONG: Like copper indium diselenide?

FIRESTER: Yes. I think a more serious constraint you want to think about is the surface -- of having the metallization systems going down on something that is really not smooth but is polycrystalline. Then you have a coverage problem, or step coverage problem, interdiffusion, but there is nothing that says if you couldn't grow epi on glass or something that we wouldn't do this right off the bat with silicon.

QUESTION: How do you control the separation of the final layer by using the laser scribe, and what is the thickness of that layer, for example? How can we control such a thin layer, and what kind of different layers do we have?

FIRESTER: I didn't want to get into anything specific, or what we are doing with amorphous, on that. That is why I said that I suspect there are going to be at least two good ideas on how to do this process, per guy or gal, in the room. Your observation is correct, though, in that the last scribe, whether it is a scribe or whether it is a printing coupled by a dry-etch operation, cannot go all the way through. It doesn't matter, if you think about it, whether it goes through the cell structure or not. It cannot break up the contact below, whether that is the transparent oxide or whether I have inverted the whole structure.

WOLF: There are some very nice facts here of loss for different sheet resistances of transparent conductive coating, and the optimum spacing resulting from it. Now the transparent coatings on different sheet resistance have different absorption losses. So shouldn't that really have been taken into account?

FIRESTER: Yes. By no means did I mean to suggest that these were true optima; there is the transmission loss. There is also what I have learned through FSA, you want to think about total cost optimization. For example: patterning, whether it is laser scribing or photo lift, is an expensive operation. You may choose to reduce the number of strips, even though it increases the physical loss.

WOLF: You might even want to put fingers over it, again normal to your scribing, to get a larger spacing.

FIRESTER: Well, I would be interested in seeing an optimization that gets me that far.

PROVANCE: Is there any reason that a hybrid approach to thick-film and thin-film could not be used?

FIRESTER: No, there is no reason at all why it couldn't be. I think that Matsuida is doing a screen-printed cad sulphide, which I would classify as a thick-film system that is precisely that kind of an interconnection. I think the point to think about is that it is gridless and of uniform current density.

THIS PAGE  
WAS INTENTIONALLY  
LEFT BLANK

# IRON-COPPER METALLIZATION FOR FLEXIBLE SOLAR CELL ARRAYS

by

HENRY W. LAVENDEL

Senior Staff Scientist

Lockheed Palo Alto Research Laboratory

Palo Alto, California

## RESEARCH GOALS

The aim of the research discussed in this presentation is to explore feasibility of a copper-base metallization for shallow-junction cells applied in flexible solar arrays in space. This type of metallization will reduce usage of precious metals (such as silver), increase ease of bonding (by welding or by soldering) and eliminate heavy high Z interconnects (such as molybdenum). The main points of concern in the investigation are stability against thermally induced diffusion of copper into silicon which causes degradation of shallow cell junctions, and low series resistance of the contact with semiconductor which promotes cell efficiency.

## CURRENT ART SILVER METALLIZATION

A major Flexible Solar Array Technology development program is currently in progress at Lockheed Missiles and Space Company, Sunnyvale, California, with a target design incorporating several hundred thousands of individual large area (5.9 by 5.9 cm) cells (Fig. 1), attached to a Kapton printed circuit substrate by contact welds between silver metallization and copper interconnects as shown in Fig. 2. Both N and P contacts are located on the cell back thanks to a dielectric wraparound for the N tabs (the assembly shown in Fig. 2 has a portion of the printed circuit removed to put in evidence the configuration of the wraparound N contact). Typical structure of the contact weld is shown in Fig. 3 in a cross section made at an angle of  $6^\circ$  to the sample surface in order to increase the thickness resolution by a factor of 10. The bond is a result of solid state diffusion between silver and copper and consists of the two terminal solid solutions (Fig. 4). Metallurgical quality and reliability of the attachment depend on controlling the welding reaction in a manner to avoid generating liquid phases and outgassing from the electroplated silver. An example of structural defects caused by the latter is shown in Fig. 5. Substituting copper metallization for the silver one will eliminate many weld problems since the bond will be made between two pieces of the same metal.

## CANDIDATE COPPER-BASE METALLIZATION

The first order concern in considering copper metallization for solar cells is the tendency of the metal to diffuse into silicon and deteriorate the P/N junction. Consequently, an appropriate

diffusion barrier has to be found. Iron is a potential candidate because: (1) its alloying affinity towards copper is extremely limited below 700°C so that at temperatures prevailing in fabrication and service of the solar arrays copper is essentially insoluble in it (see Fig. 6); (2) it will not contaminate the P/N junction when a silicide contact is formed because the iron/silicon phases (Fig. 7) are formed by unilateral diffusion of silicon into iron. The most serious disadvantage is high resistivity of the iron silicides which poses problems of ohmic losses in an iron silicide contact. The data presented here are addressing only the ability of iron to inhibit diffusion of copper into silicon: dealing with the high ohmic resistivity of the contact is the subject of the next step of the investigation.

#### METALLURGICAL EVALUATION

Experimental solar cell substrates used in the research are single crystal P-silicon wafers with a 0.2  $\mu\text{m}$  deep  $\text{N}^+$  diffused layer ( $\sim 10^{20} \text{ cm}^{-3}$  surface concentration of phosphorus). Initially the contact metallization was applied directly on the front (N) surface by vapor-depositing about 0.1  $\mu\text{m}$  of iron followed by 0.5  $\mu\text{m}$  of copper, and reacting the two layers between themselves and with the silicon at 600°C in vacuum for one hour. The reacted samples were cross sectioned and examined metallographically to determine the nature and extent of interaction. Fig. 8 shows a typical structure which discloses a non-uniform defective interface between the metallization and the silicon. Measurements of series resistance through the generated contact gave values in the order of 200 to 300  $\Omega$ . One probable reason for the high resistance is the defective metallurgical structure. However, the fact that the shallow P/N junction showed a rectifying diode behavior strongly suggests that diffusion of copper into it has been prevented.

Improved uniform bonds were obtained interposing a vapor-deposited layer of amorphous silicon between the iron/copper metallization and the substrate silicon. Fig. 9 characterizes the resulting microstructure in a 6° angle cross section. Fig. 10 is an energy dispersive scan of it. The bond of the metallization to the silicon consists of an 0.5  $\mu\text{m}$  thick Si/Fe/Cu alloy layer. Since the total thickness of combined as-deposited a-silicon and iron layers is of the same order of magnitude, the amorphous silicon acts as a sacrificial reactant in generating the interface while the solar cell material remains unaffected. A heat treatment for additional 2 hours at 500°C leaves this structure unchanged, as seen in Fig. 11. It is, therefore, evident that the ternary alloy generated by iron in the reaction with a-silicon and copper does indeed inhibit diffusion of copper into the cell substrate.

The main experimental difficulty in consistently reproducing this result lies in ensuring a defect-free barrier. Copper tends to shortcircuit the P/N junction by penetrating into the underlying silicon through structural imperfections such as pores or voids in the ternary layer. Fig. 12 shows this effect in a sample with relatively few open diffusion paths. Fig. 13, on the other hand, documents a sample with a heavy defect concentration; the depth of penetration is emphasized in this case by sectioning the sample at an angle of 6° to the surface. Within the single crystal silicon substrate the diffusion proceeds in the [100] direction along (100) planes of the lattice where the distance between atomic layers is the most favorable. The result are distinct geometric regions of a solid solution, or a compound, the composition of which is documented in Fig. 14. Fig. 15 shows the analysis of the Fe/Si/Cu interface layer where it is free of defects and is effective in stopping the copper diffusion.

The investigation summarized above indicates the metallurgical potential of developing a copper-base metallization for solar cells using iron as a diffusion inhibiting agent. Further research will determine whether this concept can also satisfy the requirements of photovoltaic performance.



Figure 1. Front Surface of the Flexible-Array Cell (2X)

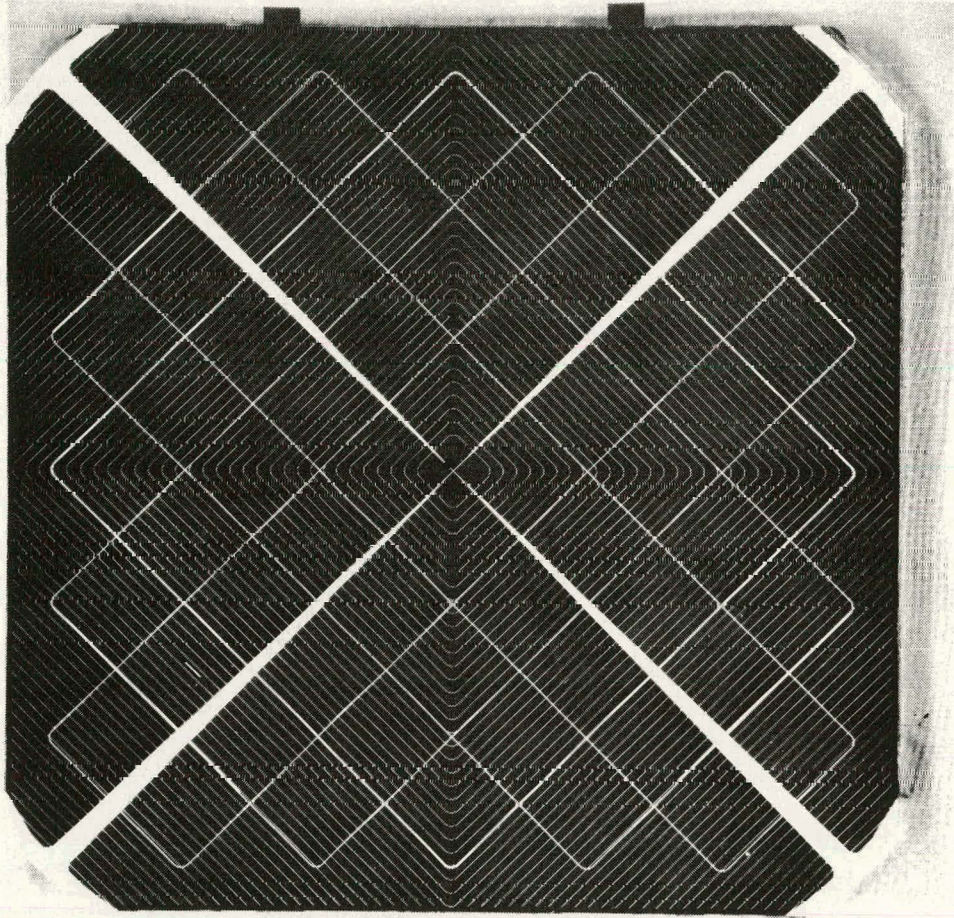




Figure 2. Flexible Blanket Interconnect (0.67X)

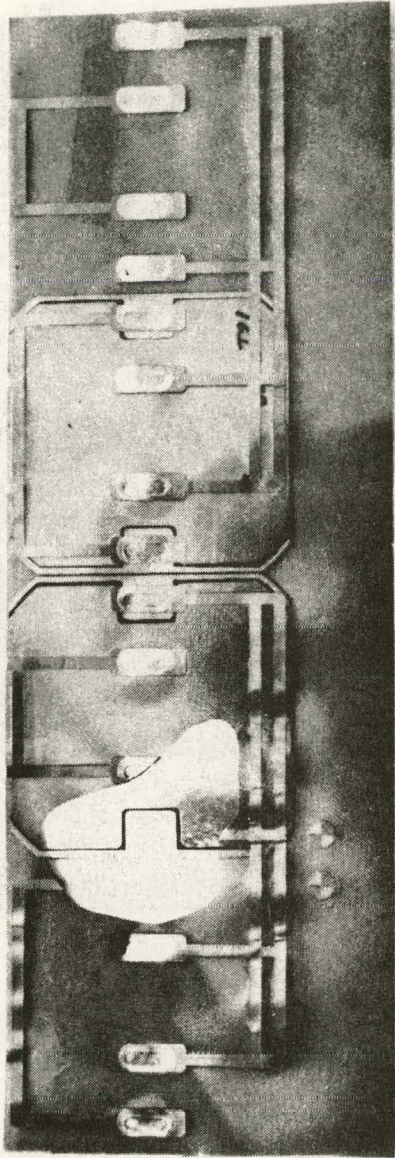




Figure 3. Structure of Ag-Cu Weld (500X)

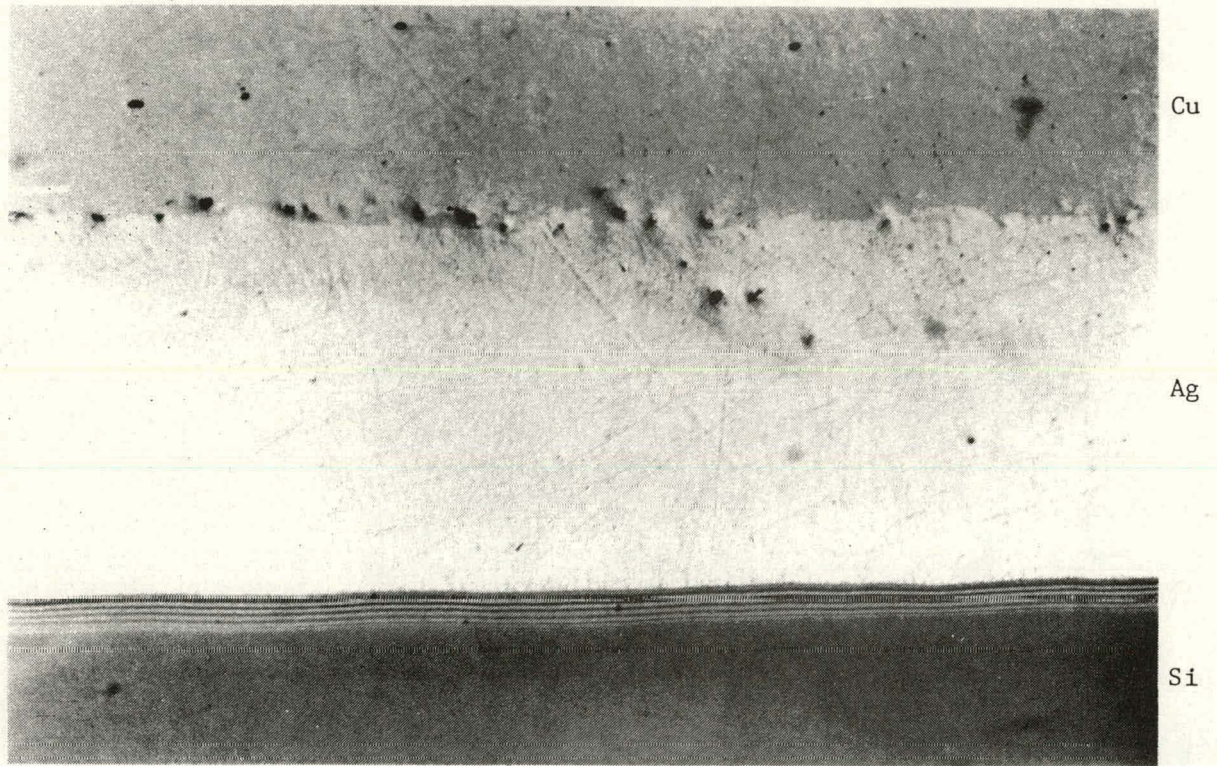


Figure 4. Energy-Dispersive SEM Analysis of Ag-Cu Contact Weld

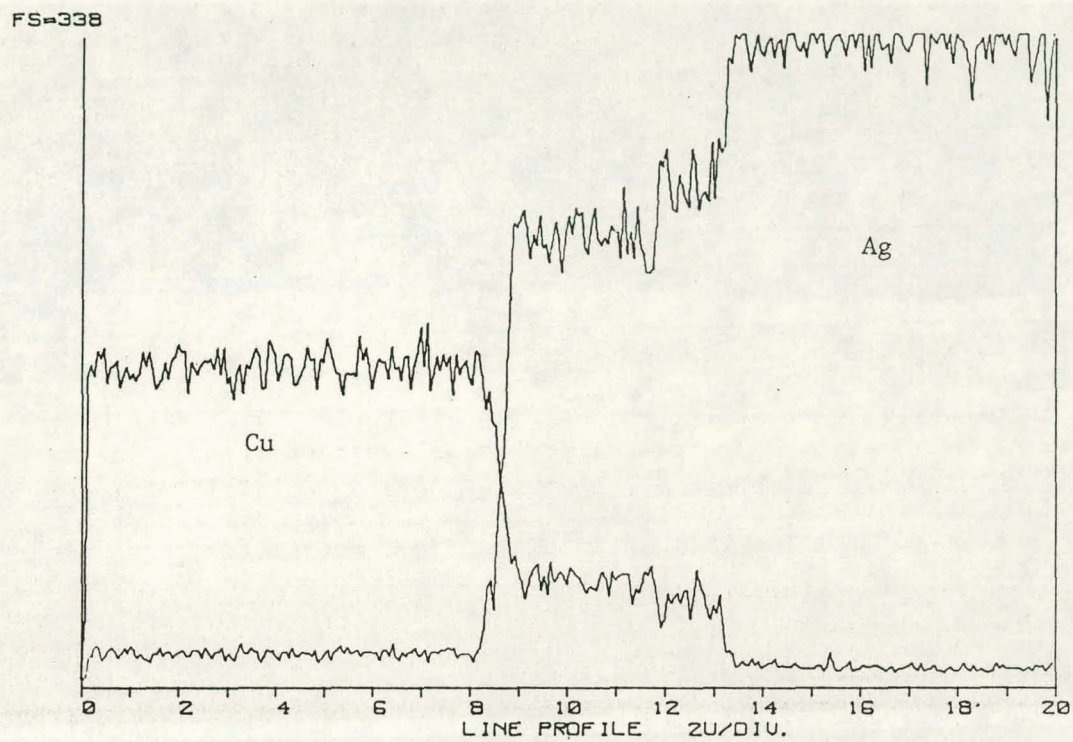




Figure 5. Defects in Ag-Cu Contact Weld (200X)

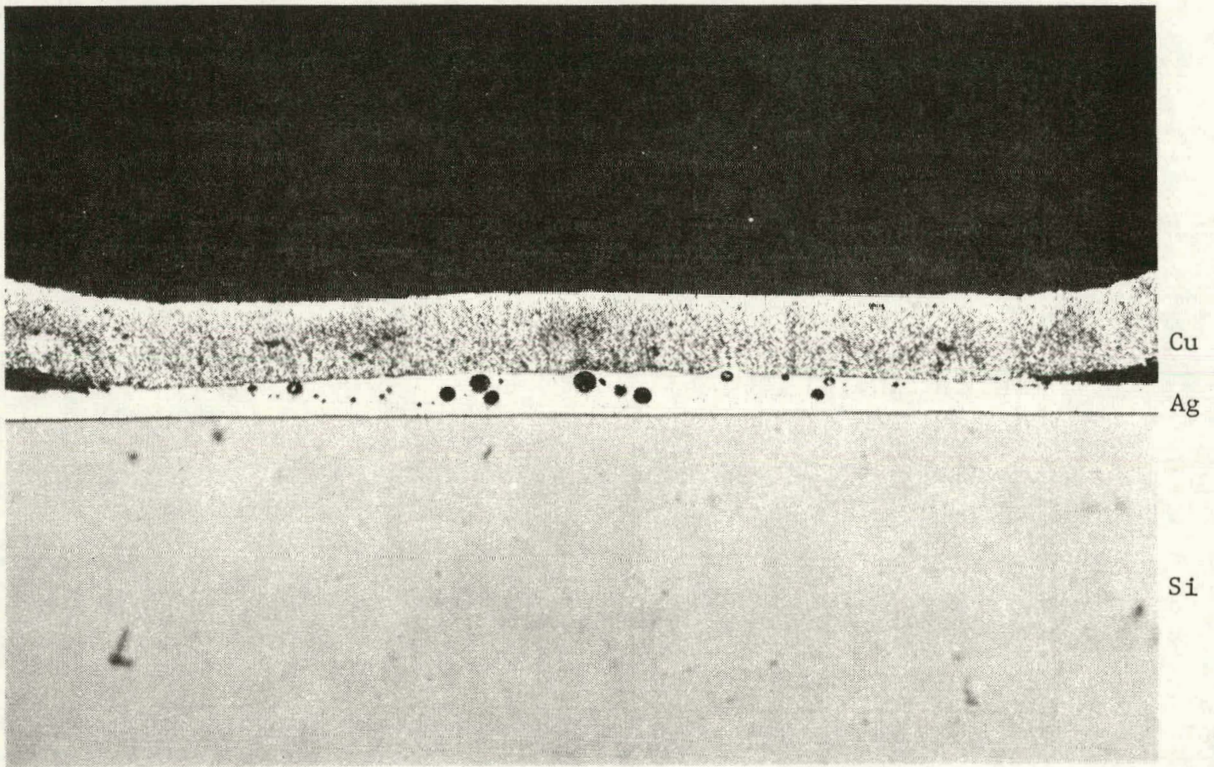


Figure 6. Copper-Iron Phase Diagram

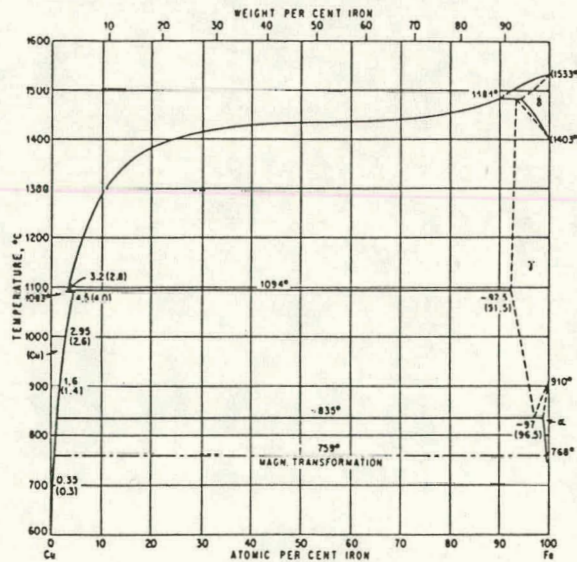




Figure 7. Iron-Silicon Phase Diagram

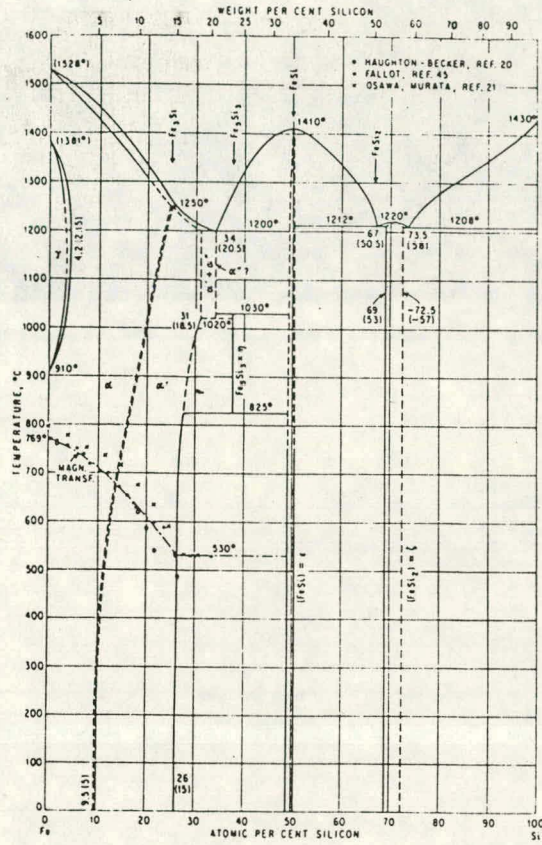
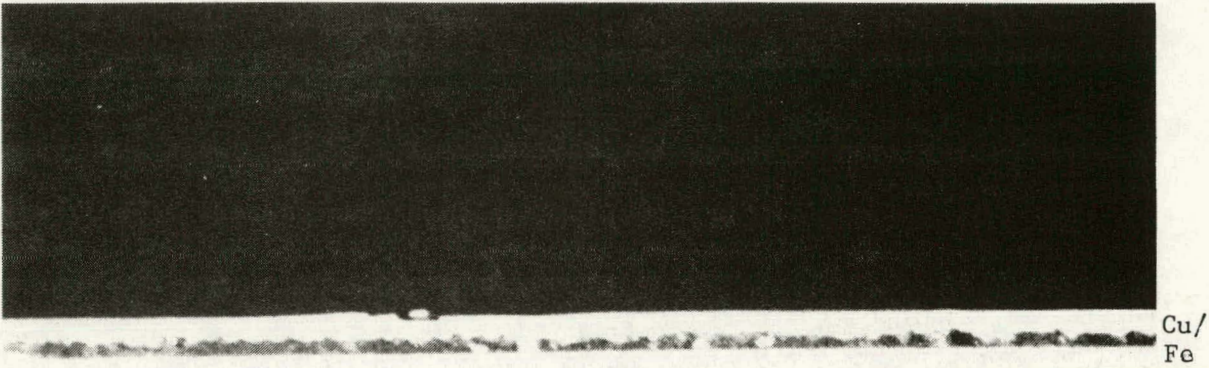


Figure 8. Cu-Fe Bond to Single-Crystal Silicon (200X)



Cu/  
Fe

Si



Figure 9. Cu-Fe-Si to Silicon Bond (1000X)

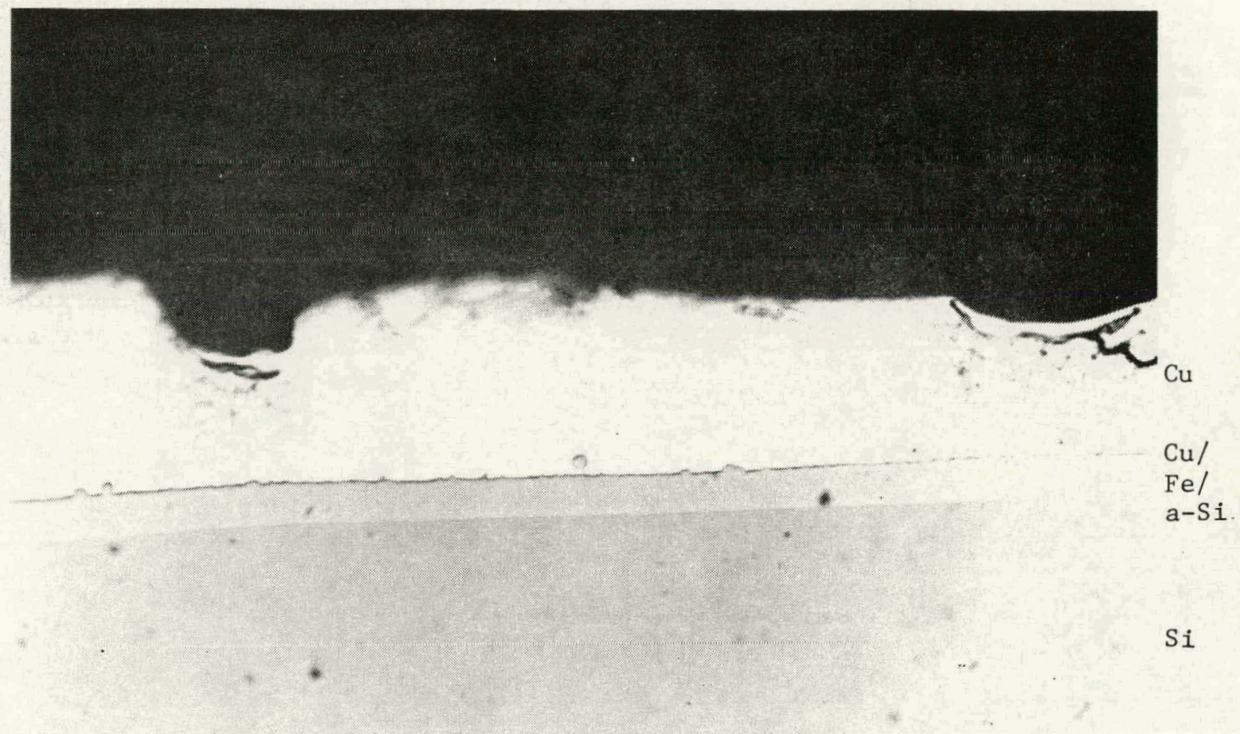
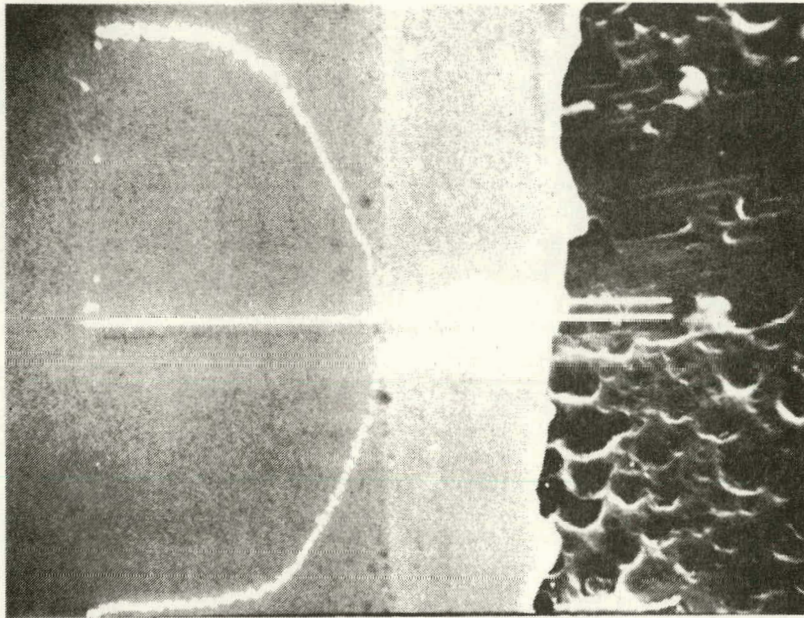
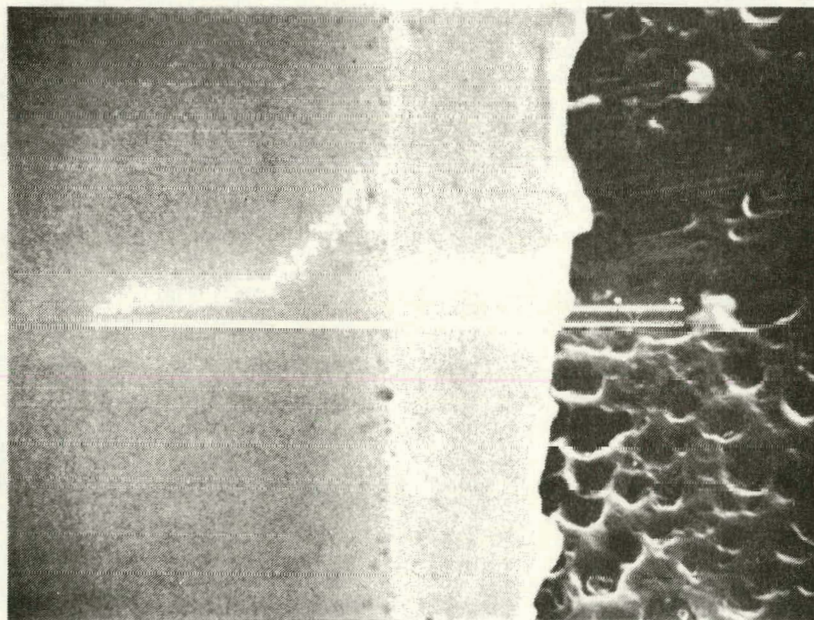




Figure 10. SEM Analysis of Typical Cu-Fe-a-Si Bond (1050X)



A. Silicon (upper scan) and Copper (lower scan)



B. Iron scan

Figure 11. Energy-Dispersive SEM Analysis of Heat-Treated Cu-Fe-a-Si Bond

FE/CU METALLIZATION

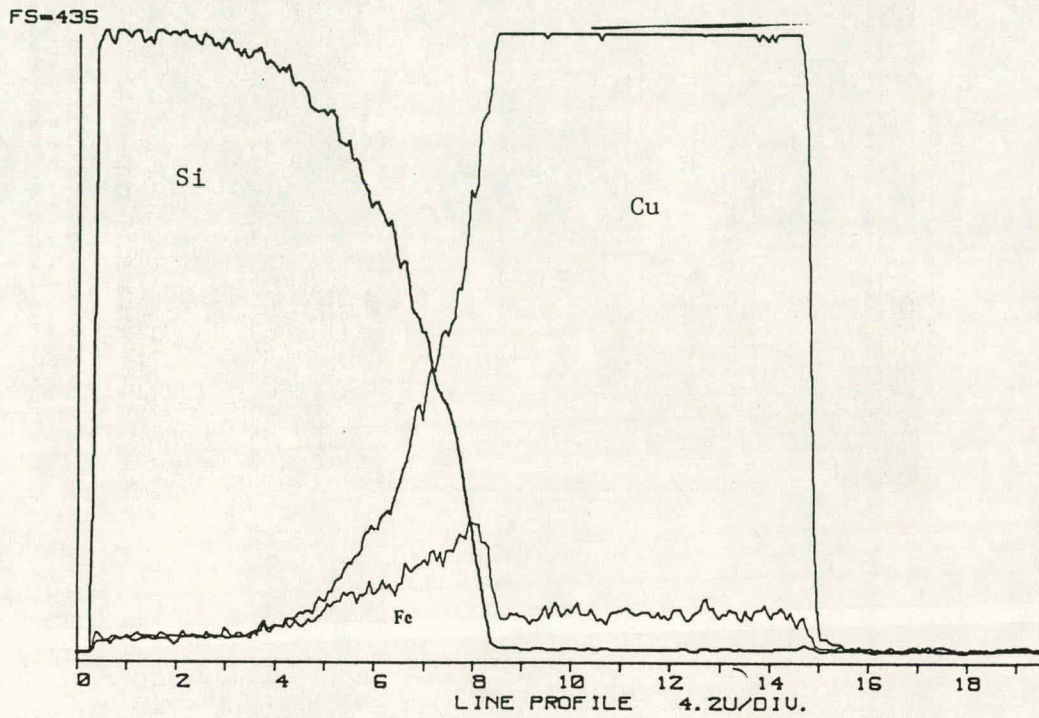




Figure 12. Cross Section of Defective Cu-Fe-a-Si Bond (500X)

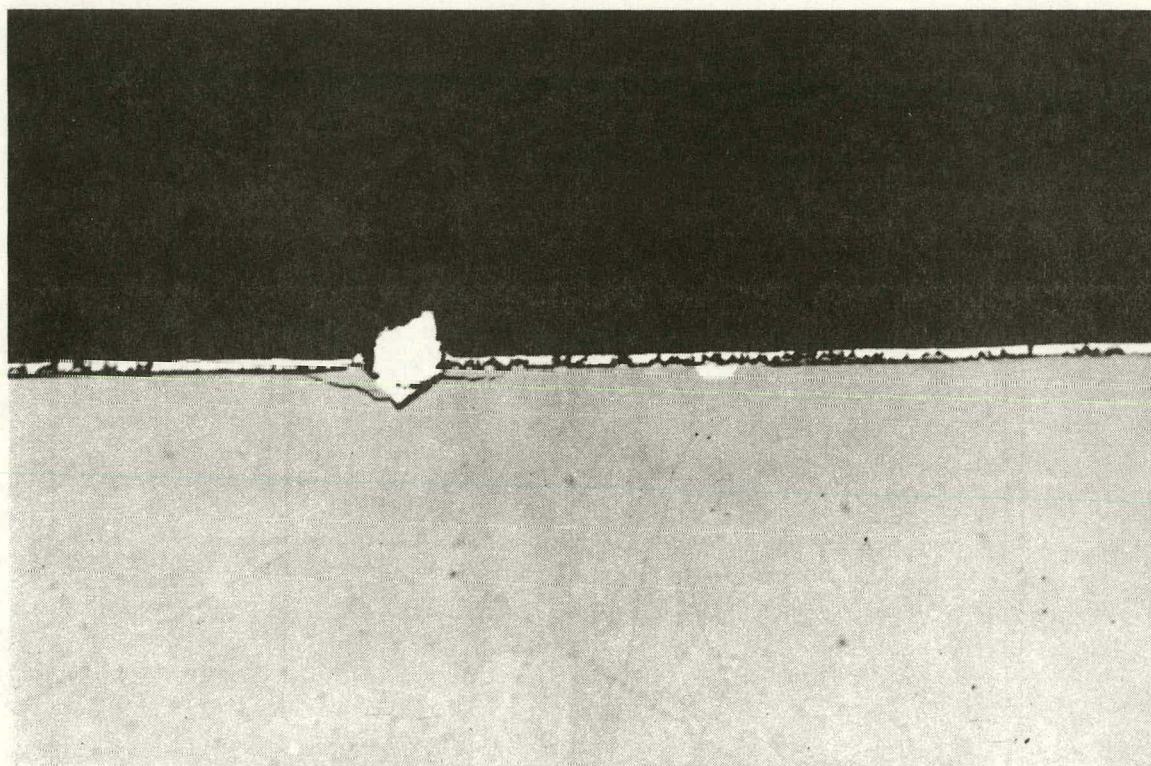




Figure 13. 6-deg-Angle Cross Section of Defective  
Cu-Fe-a-Si Bond (500X)

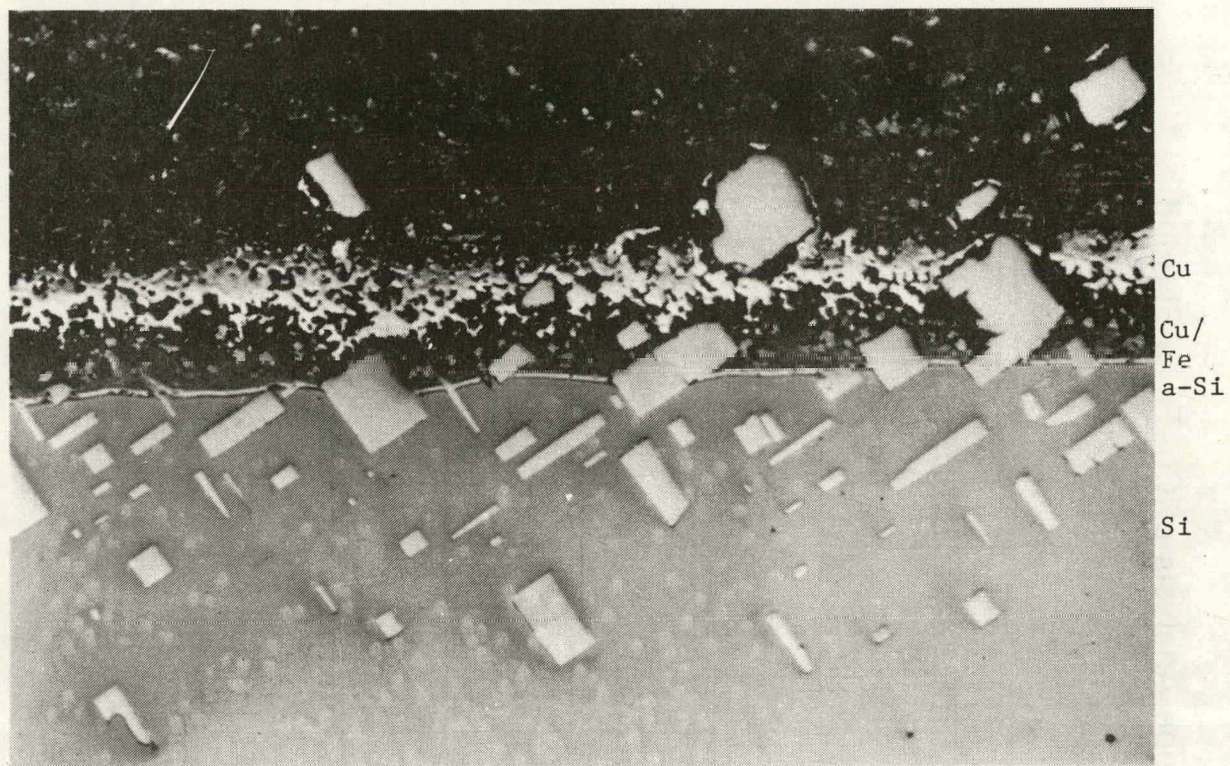
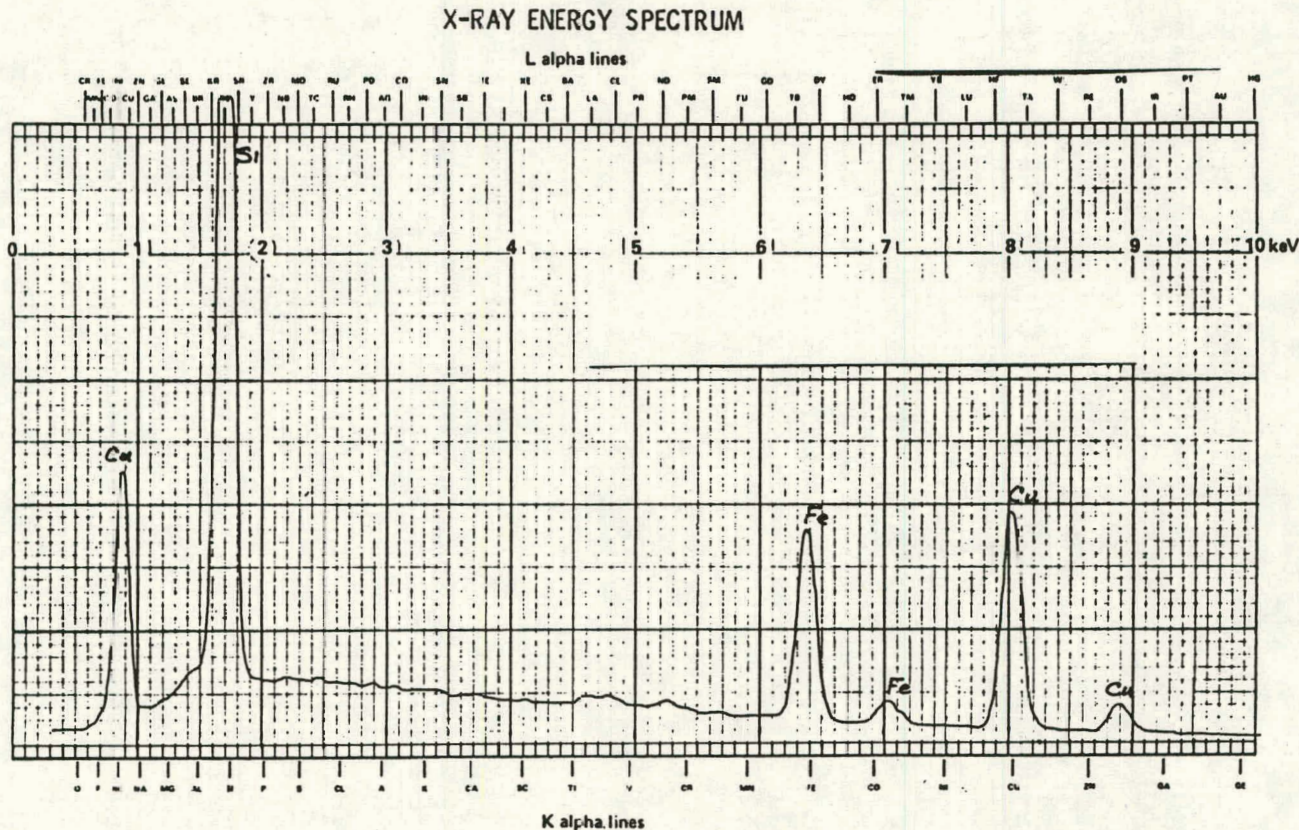




Figure 14. Electron Microprobe Analysis of Cu-Fe-a-Si Bond



390

SAMPLE IDENTIFICATION

NUMBER Run 164 Coating #3

DATE

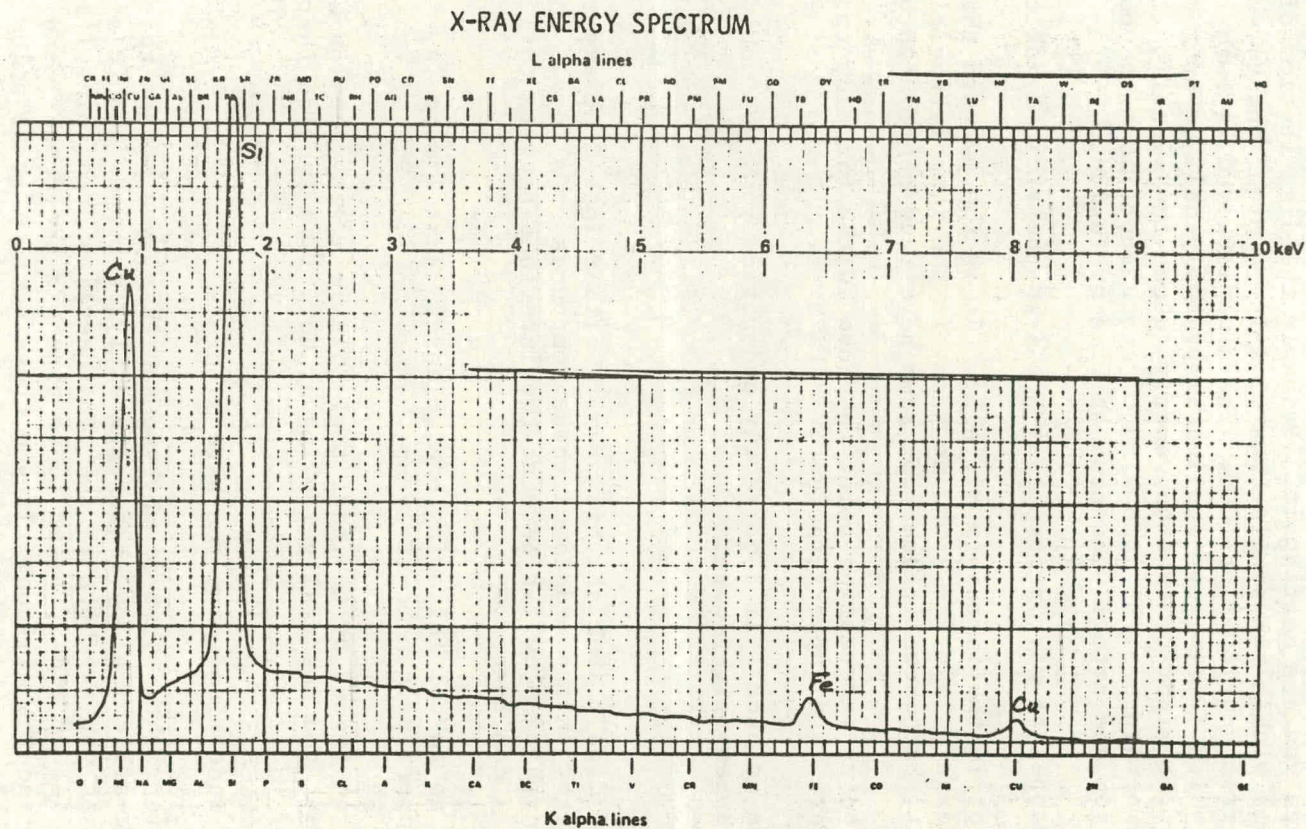
Data 53  
Bank: HL164B

1 Mar KeV 15 Full Scale 2048  
1983 NanA 30 Ct. Time 100 Sec's

\*NOTES ; Au lines may be due to thin conductive coating added.  
Elements not detectable by EMS are C, N, O, B, Li, Be & H.  
Spectral line interference; Mo-S-Pb, Ta-Si, Na-Zn, etc.



Figure 15. Electron Microprobe Analysis  
of Cu-Si Phase in Silicon



SAMPLE IDENTIFICATION

NUMBER Run 164 Partiale  
#3

DATE

Data 53  
Bank: HL 164D

1983

KeV 10 Full Scale 2048  
Chan 30 Ct. Time 100 Sec's

\*NOTES ; Au lines may be due to thin conductive coating added.  
Elements not detectable by EDS are C, N, O, B, Li, Be & H.  
Spectral line interference; Mo-S-Pb, Ta-Si, Na-Zn, etc.



## DISCUSSION

WONG: Those solid solutions or compounds, do you think they are formed during cooling due to precipitation?

LAVENDEL: That is a good question. Well, undoubtedly copper penetrates into silicon when you are heating it. Probably the distribution of the copper atoms within the single-crystal silicon might change when you cool down from your 600° or 500°. The time involved is rather short, by which I mean your cooling is probably half an hour or something. It might be that you mostly quench the situation that arises at high temperature so by some kind of gross approximation you might say that what you see actually happens at time of fusion.

WONG: Did you happen to microprobe other areas in the vicinity of the defect?

LAVENDEL: No, not in the immediate vicinity. It is the pattern that I get from the ternary layer -- I wouldn't say in the immediate vicinity of that defect, but where it does not seem have been penetrated by copper.

WONG: It might be an interesting point to probe in the vicinity to see whether there is a copper gradient.

LAVENDEL: Let me go back. If I correctly understand you, you would like to see what happens right here.

WONG: Yes.

LAVENDEL: No. I didn't look at this area, I either looked at areas like this or smack right in the middle of these compounds or alloys. Whether there is anything peculiar here at the interface between this and the layer here I don't know.

WONG: Would you go to the following one, please? What I mean is, if you probe from the copper perpendicularly up.

LAVENDEL: Don't be fooled by the fact that this is a very shallow section, so actually what you are really looking at here is a section that is done this way.

SCHWUTTKE: Do I understand that you have a bevel?

LAVENDEL: That is right. That is why you see this, you see on this picture, this copper-silicon alloy, both apparently in copper and in silicon, but actually what you see here is the cross section of a thing like that that protrudes up and it seems to be about in the copper, and both in the copper and the silicon. If you cross section it at a low angle like that you will see it on both sides of the internal barrier.

PRYOR: On the samples where you had minimal copper penetration or pinholes, did you succeed in getting a low series resistance?

LAVENDEL: I don't know, I didn't measure it yet. This series of samples is relatively recent, and I really did not have time to get that measurement reliably. I certainly hope to get it within a month or so. If I don't get low series resistance, then we have an additional problem, which means that I will accept the fact that the iron is really effective in stopping the diffusion, but I will have to worry about interposing something between that iron layer and the cell itself at the normal contact.

BLAKE: You use a layer of amorphous silicon as a sacrificial layer; between the silicon and the iron how thick was this, and how was it applied?

LAVENDEL: It was applied by the decomposition of silane. The thickness of that layer was about half a micron.

AMICK: Henry, if you put copper, now, in contact with that top surface and you wait, with time the chemical potential with the copper in the silicon will be governed by the chemical potential of the copper in the copper, will it not? Won't you always have the risk of copper precipitating in the silicon?

LAVENDEL: Yes, you are undoubtedly right. However, our heat treatment of one hour at 600°, and 2 hours at 500° additional to that, did not produce penetration when the barrier was good -- did not produce any measurable penetration of copper into silicon. I would say that if you operate your cells at temperatures of 150°C, 200°C, it will take centuries to get there by diffusion. I don't think that we can ever hope to achieve an ideal, completely impenetratable barrier; the diffusion will always go on. As Marc Nicolet said, you have defects in your structures always, vacancies, grain boundaries. I, as a matter of fact, am amazed that that half a micron of the ternary stops the diffusion to that extent.

AMICK: Do I understand then from the pictures that you consume all the copper that was originally on top?

LAVENDEL: Oh, no, no, no. Let me go back to the pictures, this is pure copper. The whole layer is pure copper. This is the interface. This is silicon, this is chemical potential of pure copper.

WONG: I have another question, if you don't mind. The picture you showed, the silicide at the interface -- the silicide forms cracks perpendicular to the interface; do you think this crack was formed due to the lattice mismatch or due to the thermal cycling?

LAVENDEL: Thermal cycling, I believe.

WONG: OK, it is not formed during formation, in other words?

LAVENDEL: I don't think so. I cannot tell you really that it isn't, I just don't think so, it might be. There might be a contribution of that too.

WONG: Amorphous silicon at the interface, how do you know it is amorphous?



LAVENDEL: By X-ray.

AMICK: Henry, in this picture, is that still free copper on the top surface?

LAVENDEL: Yes, this is free copper, and actually the interface is somewhere here.

STEIN: Could you please describe your welding technique?

LAVENDEL: I'm sorry, it is proprietary. I can only tell you one thing, that it is done by parallel gap welding and it is very, very closely monitored by the system -- by the temperature itself, the cycle itself (the temperature-time cycle). It is very very closely monitored by a set-up that LSMC developed. I, myself, know very little about it. The weld that I have shown you before is a typical result of that operation, so formation of the eutectic there happens very, very seldom and it happens only if their equipment malfunctions.

**SUMMARY AND CLOSING REMARKS**

**Brian D. Gallagher (Jet Propulsion Laboratory), Research Forum Chairman**

THIS PAGE  
WAS INTENTIONALLY  
LEFT BLANK

## SUMMARY AND CLOSING REMARKS

GALLAGHER: Three days ago we started with this viewgraph, and now appears to be a good time to review it in the light of our discussions of the various topics investigated in this Forum.

### Project Constraints

- Economic
  - Module \$0.70/watt
  - Metallization Variable
- Reliability
  - Module 30 years
  - Metallization Compatible
- Efficiency, NOC > 11%

Rather early in the presentations the interrelated requirements of cost, reliability and efficiency seemed to present an almost unattainable goal. As we progressed through discussions from our "snapshot" start we found that we were beginning to deviate from reaction modes and actually were spending more time on evaluating and researching processing mechanisms. We found, as it was so aptly put by Dr. Nicolet: "There is hope."

We found that 14-plus-percent-efficient cells are routinely produced in manufacturing facilities; 16% and 17 % efficient cells are not unheard of. Truly, the efficiency goal is not an impossible one.

Module degradation under field conditions has shown several simultaneous degradation mechanisms with differentiated rates and performance implications. Those attributable to metallization system catalysis have proven not only to have long induction periods under field conditions but also to be metal-specific. This has led to the development of accelerated testing matrices in the laboratory. Environmental test chambers capable of providing elevated temperatures, controlled high humidity, and intense ultraviolet radiation in the presence of accelerating voltages have been used to investigate and quantify these degradation mechanisms. Again: "There is hope."

In the overall area of cost, the relationship between high efficiency and reliability is ever a concern. With high-efficiency cells our cell-fabrication cost allocation can go up (we use more money for the metallization process) and we can still meet our overall cost goals. The major concern in reaching these goals is not the material or the process used, but rather the actual attainable economies of scale in volume production. The yield figures used in SAMICS calculations are

always suspect because they are volume projections. The end result is, we don't really know what the costs actually are until real volume manufacturing cost figures, based on experience, are available. But: "There is hope."

We learned of advanced techniques that have changed processing limitations as we knew them when this Project started. These innovative techniques, combined with the new emerging knowledge about "old" metallization processing mechanisms, have pointed out many fruitful areas for the investment of our research dollars.

In closing this, the first Photovoltaic Metallization Research Forum, I wish to thank you for your attendance and participation, and to extend special thanks to Mary Phillips for her coordination activities and to Dave Tustin for handling our communications.

## APPENDIX A

### CALCULATING SOLAR-CELL POWER LOSSES BY CELCAL

Dale R. Burger  
Jet Propulsion Laboratory  
Pasadena, CA 91109

#### ABSTRACT

Five different power-loss phenomena are associated with the front-surface metallic grid pattern on photovoltaic cells. The CELCAL program calculates each of these losses and their total for any given choice of design input variables. Stepwise variation of inputs by the designer allows grid-pattern optimization for the chosen cell geometry (circular or rectangular); number of horizontal bus bars (1, 2 or 3); and metallization process (defined by choice of input variables).

The program uses a sectional integration approach with constant collector grid-line spacing and non-tapered orthogonal collector grid lines and bus bars. One data card is required for each set of input variables and up to 100 data cards may be run in about 1.5 seconds of main-frame time. The output lists the value of each loss, total losses, and all input data.

#### FORTRAN PROGRAM, CELCAL

A FORTRAN V Program, CELCAL, calculates power losses associated with flat-plate photovoltaic cell front-surface grid metallization. CELCAL was originally written to handle the tedious calculations required by circular cell design. Program capabilities now include rectangular cells and the use of one, two or three bus bars. For simplicity, the calculations are all done for the first quadrant of a cell and multiplied by four except for bus-bar losses, which are done for a whole cell. All of the data necessary to calculate one specific cell design's power loss is input as design variables on a single data card, except for the resistivity of the interconnect, which is fixed at the value for copper. Design traceability is maintained by listing the input variables, the calculated power losses and their total. Five different power losses are considered: front surface sheet resistance, contact resistance, collector grid-line resistance, bus-bar resistance and shadowing. Derivations of these loss factors, and the development of the program, are discussed below.

#### SHEET RESISTANCE

An equation has been derived using sectional integration for sheet resistance losses (Reference 1). The form of this equation that is used is:

$$\Delta P = \frac{J^2 \rho_s S^3 L}{12} \quad (1)$$

where

J = current density, W/cm<sup>2</sup>

$\rho_s$  = sheet resistivity,  $\Omega/\square$

S = collector grid-line spacing (center-to-center), cm

L = collector grid-line length, cm

The acronyms or symbols used in the CELCAL program for the above equation are listed and defined in Table 1 along with all other program variables.

#### CONTACT RESISTANCE

Contact-resistance losses are inversely dependent on the total grid-line length. The equation used (Reference 2) is:

$$\Delta P = \frac{I^2 \sqrt{\rho_c \rho_s}}{\Sigma L} \quad (2)$$

where

I = total cell current, A

$\rho_c$  = contact resistivity,  $\Omega\text{-cm}^2$

$\rho_s$  = sheet resistivity under the grid line,  $\Omega/\square$

L = total collector grid-line length, cm

#### COLLECTOR GRID LINE

An equation has also been derived for collector grid resistance losses (Reference 1). The form of this equation that is used is:

$$\Delta P = \frac{J^2 \rho_m S^2 L^3}{3WH} \quad (3)$$

where

J = current density, W/cm<sup>2</sup>

$\rho_m$  = collector grid metal bulk resistivity,  $\Omega\text{-cm}$

S = collector grid-line spacing, C-C, cm

L = collector grid-line length, cm

W = width of collector grid line, cm

H = height of collector grid line, cm

## BUS BAR

Bus-bar losses can be calculated and summed explicitly for each segment between collector grid lines using the equations and tables developed for parallel bus bars of series interconnects. Since most cells have a large number (>25) of collector grid lines per cell, the equation used is derived from that used for collector grid lines: an effective line length of one third of that of the bus bar is used.

Resistance of the combination of the bus-bar metallization and the attached interconnect is also calculated to allow for thickness and resistivity input variables. A simple program modification would allow for an interconnect width different from that of the bus bar.

## SHADOWING

Shadow losses are directly dependent on the shadow area. This is usually the most significant loss in a properly made cell; therefore, most optimization efforts are toward balancing shadowing losses against other losses.

## PROGRAM LOGIC

The CELCAL program is summarized in a flow chart (Figure 1). The program uses the K index values to branch for rectangular or circular cells and to branch again for shadow-area calculations of circular cells. Circular cells require the calculation of each collector grid line length and the partitioning of each line and summation of the cubes of each segment. Rectangular cells may be handled by multiplying; however, the same SUM variable names are still used for later convenience in calculation.

## PROGRAM LISTING

A listing of the CELCAL program is shown in Figure 2.

## DATA SHEET

A copy of the data sheet is presented in Figure 3.

## PROGRAM OUTPUT

Figure 4 gives the outputs obtained from entering the data from Figure 3.

## REFERENCES

1. Carbajal, B.G., Texas Instruments, Inc., Quarterly Report No. 3, DOE/JPL-954405-76/3, October 1976.
2. Berger, H.H., Solid-State Science and Technology, J. Electrochem. Soc., pp. 507-514, April 1972.



Table 1. CELCAL Variables

<u>VARIABLE</u>	<u>DEFINITION</u>
Loss Variables	
PLSR	Sheet resistance power loss, W
PLCR	Contact resistance power loss, W
PLCG	Collector grid line power loss, W
PLSH	Shadowing power loss, W
PLBB	Bus-bar power loss (includes interconnect), W
TOTL	Total power loss, W
Input Variables	
VPP	Peak power voltage, V
RHOS	Sheet resistivity of cell surface, $\Omega/\square$
RHOM	Grid line & bus bar bulk resistivity, $\Omega\text{-cm}$
RHOC	Contact resistivity, $\Omega\text{-cm}^2$
R	Cell radius or one half of square cell vertical height, cm
S	Collector grid-line spacing C-C, cm
H	Height of bus bar center above center line, cm
WC	Width of collector grid line, cm
WB	Width of bus bar and interconnect, cm
T	Thickness of collector grid line and bus bar, cm
ETA	Cell efficiency, %
SOL	Insolation value, $\text{W}/\text{cm}^2$
P	One half horizontal length of square cell, cm

TBB	Thickness of interconnect, cm
RN	Run number for control purposes
K	Cell shape and bus-bar index code (see below)

<u>No. of Bus Bars</u>	<u>Circular</u>	<u>Rectangular</u>
1	K=1	K=4
2	K=2	K=5
3	K=3	K=6

VARIABLE

DEFINITION

Calculated or Fixed Variables

SUM1	Summation of collector grid-line length
SUM2	Summation of the cube of collector grid line lengths above and below the bus bar
SUM3	Summation of the cube of collector grid line lengths that occur beyond the bus bar in circular cells
RHOB	Interconnect bulk resistivity, usually set at the value for copper: $1.72 \times 10^{-6} \Omega\text{-cm}$
M	Number of collector grid lines in a quadrant
AREA	Area of one quadrant of a cell
DEE	Length of bus bar if not on center line of circular cell
WTH	Diameter or horizontal length of cell
Y	Length of one collector grid line
Y2	Length of one collector grid line above bus bar
SHAD	Shadowed area in one quadrant of a cell
ELL	Total length of all cell bus bars

JAY	Current density
ITOT	Total generated cell current
RES	Resistance of bus bar-interconnect combination
REFF	Effective contact resistance

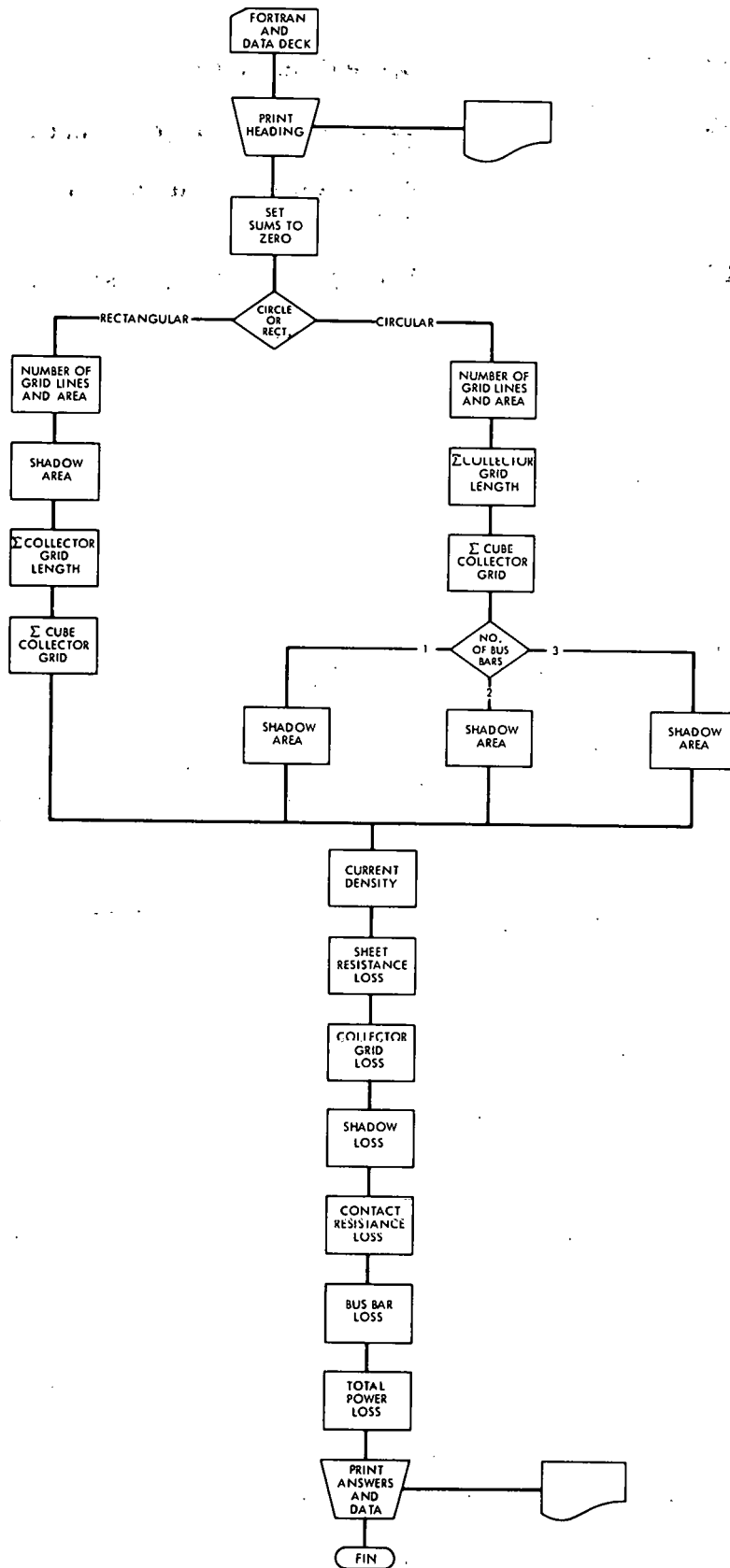


Figure 1. CELCAL Flow Chart

```

1*      C SOLAR CELL GRID LOSS CALCULATION PROGRAM, DRB 21-14-80
2*      REAL PLSR,PLC3,PLSH,PLCR,VPP,RHCS,RHCM,RHCC,R,S,H,WC,WB,T,SUM1,
3*      1SUM2,SUM3,ETA,Y,SOL,Y2,TOTL,SHAD,P,AREA,JAY,ELL,TBB,PIBB,RHCB,
4*      2ITOT,DEE,RES,WTH,REFF
5*      INTEGER M,N,RN,K
6*      C PRINT REPORT HEADINGS
7*      WRITE(6,5)
8*      5 FORMAT('1SH LOSS',1X,'CG LOSS',1X,'SD LOSS',1X,'CR LOSS',1X,
9*      1'BB LOSS',1X,' TOTL ',1X,' VPP',1X,'RHCS',1X,' RHCM ',1X,'RHCC',
10*      21X,' R ',1X,' S ',1X,' H ',2X,' WC ',1X,' WB ',1X,' T ',
11*      31X,'ETA',1X,' SOL',1X,'K',2X,' P ',1X,' TBB ',1X,'RN')
12*      10 READ(5,15,ERR=77,END=55)VPP,RHCS,RHCM,RHCC,R,S,H,WC,WB,T,ETA,SCL,
13*      1K,P,TBR,RN
14*      15 FORMAT(F3.3,F3.0,E6.2,F3.3,F4.3,F3.3,F4.3,F3.4,F3.3,F3.4,F2.2,F3.3
15*      1,I1,F4.3,F3.4,I2)
16*      C SET SUMMATIONS TO ZERO AND INPUT INTERCONNECT RESISTIVITY
17*      SUM1=C
18*      SUM2=C
19*      SUM3=C
20*      RHOP=1.72E-05
21*      C CELL SHAPE/BUS BAR KEY=   CIRCULAR 1,2, CR 3 BUS, K=1,2, CR 3
22*      C                           RECTANGULAR 1,2, CR 3 BUS, K=4,5, CR 6
23*      IF (K-3)2C,2D,6C
24*      C CALCULATIONS FOR CIRCULAR CELLS
25*      C CALCULATE AREA AND NUMBER OF GRID LINES IN QUADRANT
26*      2C M=(R/S)-1
27*      AREA=(3.14157/4.)*(R**2)
28*      C CALCULATE BUS BAR LENGTH AND CELL DIAMETER
29*      DEE=SQRT((R**2)-(H**2))
30*      WTH=2*R
31*      C CALCULATE LENGTH OF EACH COLLECTOR GRID LINE AND SUM
32*      DO 37 N=1,M
33*      25 Y=(SQRT((R**2)-((N*S)**2)))-(K*WB/2.)
34*      SUM1=SUM1+Y
35*      Y2=Y-H+((K-1)*WB/2.)
36*      IF (Y2) 35,3C,3C

```

Figure 2. CELCAL Program Listing

```

37*      30 SUM2=SUM2+(Y2**3)+((K-1)*((H-((K-1)*WB/2.))*((C.5)**(K-2))**3)
38*      GO TO 37
39*      35 SUM3=SUM3+((Y+((K-1)*WB/2.))**3)
40*      37 CONTINUE
41*      C CALCULATE SHADOW AREA AND BUS BAR LENGTH
42*      IF(K-2)40,45,46
43*      40 SHAD=((WB/2.)*R)+(WC*(SUM1+(R/2.)))
44*      ELL=2*R
45*      GO TO 49
46*      45 SHAD=(WB*(SQRT((R**2)-(H**2)))+(WC*(SUM1+(R/2.)))
47*      ELL=4*DEE
48*      GO TO 49
49*      46 SHAD=((WB*(R/2.)+SQRT((R**2)-(H**2)))+(WC*(SUM1+(R/2.)))
50*      ELL=(2*R)+(4*DEE)
51*      GO TO 49
52*      C CALCULATIONS FOR RECTANGULAR CELLS
53*      C CALCULATE AREA AND NUMBER OF GRID LINES IN QUADRANT
54*      60 M=(P/S)-1
55*      AREA=(R*P)
56*      C CALCULATE SHADOW AREA
57*      SHAD=WC*(M*(R-((K-3)*WB/2.))+(R/2.))+WB*((K-3)/2.)*P
58*      SUM1=M*(R-((K-3)*WB/2.))
59*      SUM2=M*((R-H-WB/2.))**3+((K-4)*((H-(K-4)*WB/2.))*((C.5)**(K-5)))
60*      1**3)))
61*      C CALCULATE CELL WIDTH AND BUS BAR LENGTH
62*      WTH=2*P
63*      ELL=(K-3)*WTH
64*      C CALCULATE CURRENT DENSITY
65*      49 JAY=ETA*SOL/VPP
66*      C CALCULATE TOTAL CELL CURRENT
67*      ITOT=(AREA-SHAD)*JAY*4
68*      C CALCULATE EFFECTIVE CONTACT RESISTANCE
69*      REFF=(SQRT(RHOC*RHOS))/SUM1
70*      C CALCULATE SHEET RESISTANCE POWER LOSS
71*      PLSR=((JAY**2)*RHOS*((S-WC)**3)/12.)*(SUM1+(R/2.))*4
72*      C CALCULATE COLLECTOR GRID POWER LOSS

```

Figure 2. CELCAL Program Listing (Cont'd)

```

73*          PLGG=((JAY**2)*RHOM*(1S-WC)**2))/(3.*T*WC)*1*(SUM2+SUM3)*4
74*    C CALCULATE SHADOWING LOSS
75*          PLSH=SHAD*ETA*SOL*4
76*    C CALCULATE CONTACT RESISTANCE LOSS
77*          PLCP=((ITOT/4.)*2)*REFF*4
78*    C CALCULATE BUS BAR LOSS
79*          RES=(WTH*RHOM)/(WB*T)*((RHC*TBB)/(RHC*TJ)+1.)
80*          PLBB=(ITOT**2)*RES*((WTH/ELL)**2)/3.
81*    C CALCULATE TOTAL POWER LOSS FOR CELL
82*          TOTL=(PLSR+PLGG+PLSH+PLCR+PLBB)
83*    C PRINT ANSWERS AND INPUT DATA
84*          WRITE(6,50)PLSR,PLGG,PLSH,PLCR,PLBB,TOTL,VFP,RHCS,RHOM,RHCC,R,S,
85*            1H,WB,T,ETA,SOL,K,P,TBB,RN
86*          50 FORMAT( E8.3,1X,E7.3,1X,E7.3,1X,E7.3,1X,E7.3,1X,E7.3,1X,F4.3,1X,
87*            1F4.0,1X,E7.3,1X,F4.3,1X,F5.3,1X,F4.3,1X,F5.3,1X,F5.4,1X,F4.3,1X,
88*            2F5.4,1X,F3.2,1X,F4.3,1X,1,2X,F5.3,1X,F5.4,1X,12)
89*          GO TO 1C
90*    C PRINT READ ERROR FOR BAD DATA CARDS
91*          77 WRITE(6,78)
92*          78 FORMAT(' READ ERROR')
93*          GO TO 1C
94*          55 STOP
95*          END

```

Figure 2. CELCAL Program Listing (Cont'd)



# GRID CALCULATION DATA SHEET

150 mm MASK  
D. R. BURGER  
8-31-81

1	4	7	13	16	20	23	27	30	33	36	38	41	42	46	49
VPP	RHOS	RHOM	RHOC	R	S	H	WC	WB	T	ETA	SOL	K	P	TBB	RN
450	038	172-06	001	7500	400	4150	178	254	004	13	100	3		0	1
					425										2
					450										3
					475										4
					500										5
					375										6
					350										7
					325										8
					300										9
					400		168								10
							158								11
							188								12
							198								13
							178	229							14
								204							15
								279							16
								304							17
								254	005						18
									006						19
					300		168		004						20
							158								21
							178	279							22
								304							23
								329							24
					275			254							25

A-11

Figure 3. CELCAL Data Input Sheet

SM LOSS	CG LOSS	SD LOSS	CR LOSS	BB LOSS	TOTL	VPP	RHCS	RHCR	RHCC	R	S	H	WC	WB	T	ETA	SCI	K	P	TBB	RN
.601-C1	.213-C1	.224+CC	.105-C1	.252+CC	.570+CC	.450	38.	.172-C5	.CC1	7.500	.400	4.150	.C178	.254	.0004	.13	.100	3	.000	.0000	1
.694-C1	.230-C1	.221+CC	.113-C1	.254+CC	.577+CC	.450	38.	.172-C5	.CC1	7.500	.425	4.150	.C178	.254	.0004	.13	.100	3	.000	.0000	2
.773-C1	.247-C1	.216+CC	.120-C1	.255+CC	.585+CC	.450	38.	.172-C5	.CC1	7.500	.450	4.150	.C178	.254	.0004	.13	.100	3	.000	.0000	3
.840-C1	.272-C1	.211+CC	.127-C1	.256+CC	.593+CC	.450	38.	.172-C5	.CC1	7.500	.475	4.150	.C178	.254	.0004	.13	.100	3	.000	.0000	4
.977-C1	.267-C1	.208+CC	.133-C1	.257+CC	.603+CC	.450	38.	.172-C5	.CC1	7.500	.500	4.150	.C178	.254	.0004	.13	.100	3	.000	.0000	5
.520-C1	.203-C1	.234+CC	.124-C2	.250+CC	.567+CC	.450	38.	.172-C5	.CC1	7.500	.375	4.150	.C178	.254	.0004	.13	.100	3	.000	.0000	6
.455-C1	.191-C1	.241+CC	.127-C2	.247+CC	.563+CC	.450	38.	.172-C5	.CC1	7.500	.350	4.150	.C178	.254	.0004	.13	.100	3	.000	.0000	7
.387-C1	.182-C1	.250+CC	.119-C2	.247+CC	.562+CC	.450	38.	.172-C5	.CC1	7.500	.325	4.150	.C178	.254	.0004	.13	.100	3	.000	.0000	8
.323-C1	.157-C1	.258+CC	.117-C2	.245+CC	.558+CC	.450	38.	.172-C5	.CC1	7.500	.300	4.150	.C178	.254	.0004	.13	.100	3	.000	.0000	9
.605-C1	.227-C1	.221+CC	.106-C1	.254+CC	.568+CC	.450	38.	.172-C5	.CC1	7.500	.400	4.150	.C168	.254	.0004	.13	.100	3	.000	.0000	10
.610-C1	.243-C1	.216+CC	.104-C1	.255+CC	.566+CC	.450	38.	.172-C5	.CC1	7.500	.400	4.150	.C158	.254	.0004	.13	.100	3	.000	.0000	11
.574-C1	.201-C1	.232+CC	.105-C1	.251+CC	.573+CC	.450	38.	.172-C5	.CC1	7.500	.400	4.150	.C188	.254	.0004	.13	.100	3	.000	.0000	12
.591-C1	.190-C1	.237+CC	.104-C1	.250+CC	.575+CC	.450	38.	.172-C5	.CC1	7.500	.400	4.150	.C178	.254	.0004	.13	.100	3	.000	.0000	13
.604-C1	.217-C1	.214+CC	.106-C1	.243+CC	.590+CC	.450	38.	.172-C5	.CC1	7.500	.400	4.150	.C178	.229	.0004	.13	.100	3	.000	.0000	14
.608-C1	.220-C1	.201+CC	.104-C1	.222+CC	.617+CC	.450	38.	.172-C5	.CC1	7.500	.400	4.150	.C178	.204	.0004	.13	.100	3	.000	.0000	15
.577-C1	.210-C1	.237+CC	.105-C1	.227+CC	.557+CC	.450	38.	.172-C5	.CC1	7.500	.400	4.150	.C178	.279	.0004	.13	.100	3	.000	.0000	16
.573-C1	.207-C1	.251+CC	.104-C1	.206+CC	.547+CC	.450	38.	.172-C5	.CC1	7.500	.400	4.150	.C178	.304	.0004	.13	.100	3	.000	.0000	17
.603-C1	.171-C1	.226+CC	.105-C1	.202+CC	.516+CC	.450	38.	.172-C5	.CC1	7.500	.400	4.150	.C178	.254	.0005	.13	.100	3	.000	.0000	18
.601-C1	.142-C1	.226+CC	.105-C1	.168+CC	.479+CC	.450	38.	.172-C5	.CC1	7.500	.400	4.150	.C178	.254	.0005	.13	.100	3	.000	.0000	19
.324-C1	.170-C1	.251+CC	.162-C2	.246+CC	.554+CC	.450	38.	.172-C5	.CC1	7.500	.300	4.150	.C168	.254	.0004	.13	.100	3	.000	.0000	20
.320-C1	.182-C1	.244+CC	.168-C2	.248+CC	.551+CC	.450	38.	.172-C5	.CC1	7.500	.300	4.150	.C158	.254	.0004	.13	.100	3	.000	.0000	21
.323-C1	.157-C1	.270+CC	.153-C2	.220+CC	.545+CC	.450	38.	.172-C5	.CC1	7.500	.300	4.150	.C178	.279	.0004	.13	.100	3	.000	.0000	22
.317-C1	.155-C1	.282+CC	.147-C2	.200+CC	.537+CC	.450	38.	.172-C5	.CC1	7.500	.300	4.150	.C178	.304	.0004	.13	.100	3	.000	.0000	23
.317-C1	.152-C1	.274+CC	.145-C2	.182+CC	.531+CC	.450	38.	.172-C5	.CC1	7.500	.300	4.150	.C178	.329	.0004	.13	.100	3	.000	.0000	24
.270-C1	.145-C1	.271+CC	.145-C2	.242+CC	.561+CC	.450	38.	.172-C5	.CC1	7.500	.275	4.150	.C178	.254	.0004	.13	.100	3	.000	.0000	25

Figure 4. CELCAL Data Output

APPENDIX B  
OPTIMIZATION PROGRAM AND METHODOLOGY FOR DESIGNING  
SOLAR-CELL GRID PATTERNS

R. Daniel, D. Burger, H. Stone  
Jet Propulsion Laboratory  
California Institute of Technology  
4800 Oak Grove Drive  
Pasadena, California 91109

Abstract

One of the most critical areas affecting solar cell efficiency is the design of the current-collecting grid pattern. An interactive APL computer program has been developed to find optimal (minimum power lost) values for design variables such as fine-grid-line width, fine-grid-line spacing and bus-bar width on round and rectangular cells. The program can serve as an easy-to-use design tool for maximizing cell efficiency and for performing sensitivity analyses.

Introduction

Extensive literature is available on analyzing series resistance and other power losses associated with the grid patterns on rectangular solar cells. No reports, however, have focused on optimal (minimum power lost) grid-pattern designs for round cells or for rectangular cells with more than two design variables.

An interactive APL computer program has been developed that uses a nonlinear optimization technique, a modified Newton-Raphson method (Reference 1), to determine the optimal grid pattern parameters. The power-loss equations modeled in the program are similar in approach to those of Moore (Reference 2), Redfield (Reference 3), and Flat and Milnes (Reference 4) in earlier reports. The basic grid design, whose power losses are analyzed by the program, has the bus bar and fine grid lines orthogonal to one another. Three different patterns are available: one and two bus bars on a round cell and one or more bus bars on a rectangular cell (Figure 1). Other cell shapes or patterns require shape-specific power loss analysis.

The user must input reasonable starting values for the variables to be optimized and the step size used in the optimization. Documentation for the program and specific instructions on running the program are being prepared for the Computer Software Management and Information Center (COSMIC).

In addition to generating optimal designs, the program can be used to perform sensitivity studies on selected variables. As a result, the program can serve as an easy-to-use design tool.

## Power Loss Analysis

To model solar-cell power losses accurately, an analysis was made of the resistive losses in the photoconductor sheet, metallic grid and bus bars. Power losses due to the shadowing of the cell by the fine grid and the bus bars and the contact resistance of the fine grid to the sheet were also made.

This program is limited to round cells of one or two bus bars and rectangular cells of one or more bus bars where the bus bars and fine grid lines are orthogonal. The power-loss analysis makes several assumptions:

- (1) The photocurrent is generated uniformly on the surface of the cell.
- (2) Power loss in the photoconductor sheet between grid lines is calculated using sectional integration rather than solving Poisson's equation for the potential as a function of position in the active area. Davis\* compared the methods and showed that the power loss in the sheet varied by less than 10% (the change in design is insignificant) when the ratio of the length of the grid line to the space between lines is greater than 3:1 (the variation decreases as the ratio increases).
- (3) The bus bars and grid lines are rectangular in cross section.
- (4) The bus bar is either of the same metallization and thickness as the fine grid or can be strapped (with a metallic ribbon of specified thickness) over the variable-thickness bus bar.
- (5) The fine-grid-line width and the metallization thickness are set at a fixed ratio as an input parameter. This approach was used because some metallization processes will produce fine lines as some ratio of the metallization thickness, and because the program will converge more rapidly. The program can be altered to handle those variables independently.

Figure 2 identifies the usual power losses encountered in a solar cell. A general form of power loss from a resistive source can be expressed as

$$P = \int I^2 dR \quad (1)$$

Then the power losses due to resistance in the photoconductor sheet ( $P_{SH}$ ), resistance in a fine grid line ( $P_{FG}$ ) and resistance in the bus bar ( $P_B$ ) are found by solving the following equations:

---

\*J.R. Davis, Westinghouse R&D Center, private communication.

$$P_{SH} = 2 \int_{y=0}^{y=s/2} \frac{(J_M l_x y)^2}{l_x} \rho_s dy \quad (2)$$

$$P_{FG} = \int_{x=0}^{x=l} \frac{(J_M s x)^2}{bt} \rho_M dx \quad (3)$$

$$P_B = 2 \int_{y=0}^{y=L_B} \frac{(J_M l_x y)^2}{W_B t} \rho_M dy \quad (4)$$

The remaining resistive power loss is caused by the resistance of the contact  $R_C$  of the fine grid line to the photoconductor sheet. This contact resistance has several formulations available. Two forms available for the program, one of which is to be chosen, are:

$$R_C = \frac{\rho_c}{\text{fine grid area}} \quad (5)$$

$$R_C = \frac{\sqrt{R_s c}}{l_x} \quad (6)$$

The first represents a condition in which the current enters the contact uniformly. The second represent a condition in which the current is crowded at the edge of the contact.

The power loss due to contact resistance is represented as

$$P_C = (J_M l_x s)^2 R_C \quad (7)$$

Last, the power lost to the cell from shadowing on the cell caused by the fine grid lines and the bus bar(s) is:

$$P_S = J_M V_M (\text{fine grid area and bus bar area}). \quad (8)$$

In Equations 2 through 7

- $J_M$  (A/cm<sup>2</sup>) = current density at maximum power
- $V_M$  (volts) = voltage at maximum power
- $R_s$  ( $\Omega$ ) = semiconductor sheet resistance below the contact

$\rho_M$ ( $\Omega\text{-cm}$ )	=	resistivity of metal
$\rho_S$ ( $\Omega/\square$ )	=	resistivity of sheet
$\rho_C$ ( $\Omega\text{-cm}^2$ )	=	contact resistivity
$W_B$ (cm)	=	width of the bus bar
$s$ (cm)	=	space between fine grid lines
$b$ (cm)	=	width of fine grid lines
$t$ (cm)	=	metallization thickness
$l_x$ (cm)	=	length of fine grid line
$L_B$ (cm)	=	length of bus bar

The calculation of losses associated with a rectangular cell is much simpler than for a round cell, because the losses attributed to each fine grid line and sheet loss between them are identical. Therefore, only one calculation is needed; its result is then multiplied by the number of lines to get the total losses. Because the round cell has fine grid lines of varying lengths, the losses associated with each fine grid line also vary. Therefore, an analytical approximation of the total losses from the grid lines and the spaces between was derived. Without this approximation the total effect of the losses would be represented as a summation over each grid line and during the optimization procedure would require the program to run through many loops. The closed-form approximation was derived by converting the summation of each line into an integral; this treats the fine grid lines as a continuum rather than as discrete lines. This integral solution will overestimate the losses, but it can be shown that it varies from the discrete solution by less than 1% when there are as few as 10 grid lines.

The resistive loss in the bus bar assumes that the current is collected at the end of the bus bar and that the current collected is uniformly increasing as the contact (collecting point) is approached.

The program can calculate the contact resistance in two ways, either as an inverse-area relationship, used by Moore (Reference 2) and Redfield (Reference 3) or as an edge effect, discussed by Berger (Reference 5).

### Optimization Methodology

The optimization procedure uses the sum of the previously described power-loss equations as the objective function

$$P_T = P_{SH} + P_C + P_{FB} + P_B + P_S = \text{total power lost} \quad (9)$$

A necessary condition for optimality is that the first partial derivative of this function be equal to zero.

$$\frac{\delta P_T}{\delta \theta_i} = 0 = F_i(X) \quad (10)$$

where the  $\theta_i$  's are the design variables and  $i = 1, 2, \dots, m$ .

In the program, this function is approximated by taking a small finite difference of the function with respect to each of the design variables. These equations are then solved by a modified Newton-Raphson method. The Newton-Raphson procedure is effective for the grid optimization problem because the power-loss curve is concave; the power loss varies continuously with respect to the design variables. The Newton-Raphson procedure begins with first-order Taylor's series expansion of the function about a starting point:

$$F_i(X) \approx F_i(X^k) + \Delta F_i(X^k)(X - X^k) \quad (11)$$

where  $X^k$  is the starting point.

This gives a system of simultaneous linear equations of first-order differences.

These first-order differences are the adjustments to be made to the initial parameter values. The new value for each variable is substituted into the objective function and the process is started over again. Rewriting the previous expression in matrix notation (Reference 6) yields

$$A_k + B_k (X - X^k) = 0 \quad (12)$$

or

$$x = X^k - B_k^{-1} A_k \quad (13)$$

Convergence is decided by a weighted-squares criterion (Reference 7); i.e., the program stops if:

$$\sum_{i=1}^m W_i F_i(X)^2 < 1 \quad (14)$$

$W_i$  is chosen to be  $1 \times 10^6$  [its value depends on the units chosen for  $F_i(x)$ ].

### Program Routines

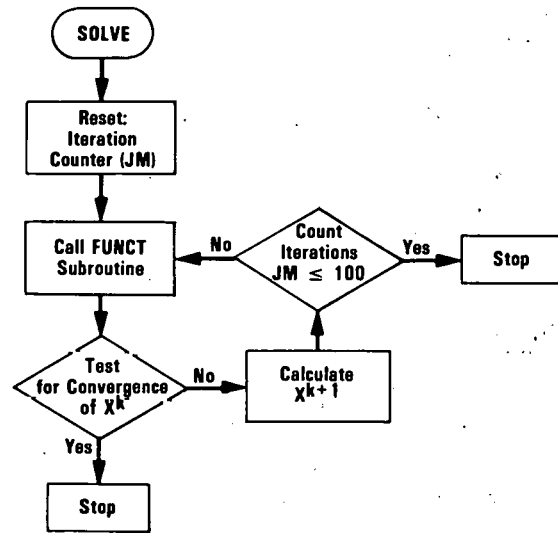
The program is divided into five major subroutines; the FUNCT (Reference 7), SOLVE, Power Losses, Input, and Output. A copy of the FUNCT and SOLVE subroutines for rectangular cells is shown on the next page. The Power Losses subroutine is called SQLOSS for rectangular cells. The Input and Output subroutines are solely for those functions and are appropriately formatted for ease of use.



```

    ∇X←SOLVE XI; Y; I; J; FX
[1]  J←1
[2]  X←XI
[3]  Q:F←FUNCT X
[4]  →(1>+/WCx F*2)/O
[5]  FX←ρO
[6]  I←1
[7]  RX:Y←X
[8]  Y[I]←X[I]+E[I]
[9]  FX←FX, ((FUNCT Y)-F)÷E[I]
[10] →(N≥I←I+1)/RX
[11] FX←φ(N,N)ρFX
[12] X←X-SIZEx FEFX
[13] 'W,A,B,WB: ',(10 5 X,WB)
[14] 'F: ';F
[15] SQLOSS
[16] 'PTOT: ';PTOT
[17] →(JM>J←J+1)/Q

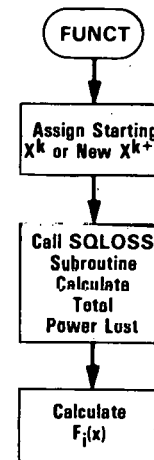
```



```

    ∇F FUNCT X
[1]  ρ CHECK N,X,WC,E,SIZE
[2]  F←3ρO
[3]  WB←X[1]
[4]  A←X[2]
[5]  B←X[3]
[6]  SQLOSS
[7]  PO←PTOT
[8]  WB←WB+E[1]
[9]  SQLOSS
[10] F[1]←(PTOT-PO)÷E[1]
[11] WB←X[1]
[12] A←A+E[2]
[13] SQLOSS
[14] F[2]←(PTOT-PO)÷E[2]
[15] A←X[2]
[16] B←B+E[3]
[17] SQLOSS
[18] F[3]←(PTOT-PO)÷E[3]
[19] B←X[3]

```



The FUNCT subroutine calculates the  $F_i(X)$  values. Lines 3, 4, and 5 are the starting values for the design variables  $W_B$  (bus-bar width),  $A$  (fine-grid-line spacing) and  $b$  (fine-grid-line width). The total power lost (PTOT) is calculated at Line 6. Lines 7 through 19 solve for the partial derivatives of the objective function with respect to each design variable; the  $E_i$ 's are the small finite differences mentioned in the previous section ( $E_i \approx 1 \times 10^{-3}$  to  $1 \times 10^{-4}$ ).

The SOLVE subroutine calculates the new point  $X$  (Line 12) and carries out the convergence test (Line 4). The SIZE variable (Line 12) is the equivalent of a step size for gradient search procedures (Reference 8).

However, here it is not an optimal value. This program uses the SIZE variable to control the size of the adjustment to be made on the old  $X^k$  (usually, 0 SIZE 1). Line 17 counts the number of iterations made by the program. The program will stop if the number of iterations equals JM (JM = 100).

The SQLOSS subroutine is not shown since it contains only power-loss equations. This subroutine (and its analog for round cells) is often used by itself when doing sensitivity analyses and not running the program in the optimization mode. Its contents will be available when the COSMIC documentation is completed.

### Examples

The following examples may not correspond to any real solar cells; they were created to demonstrate the versatility of the program.

In the first two examples a round cell is considered to be 16.9% efficient with a maximum output power (before losses) of 1068 mW at 80 mW/cm<sup>2</sup> insolation. Using the fixed parameters in Table 1, a two-bus-bar pattern (Figure 3) is optimized with the design variables being the width of the bus bars ( $W_B$ ), the fine-grid-line spacing (A), and the fine-grid-line width (B). The fixed parameters not previously defined are: Deg ( ), the angular displacement from the centerline of the cell to the end of a bus bar (centerline and bus bar are parallel); R, cell radius;  $\rho_B$ , the resistivity of the metal used for the strap; and B:T, the ratio of the fine grid line width to the metallization thickness.

Table 1. Round Cell 2-Bus Optimal Design

Input of Fixed Parameters	Resulting Design	Single Metallization	Strapped Bus (50 $\mu$ m)
Deg ( $\alpha$ ) = 24	$W_b$ , cm	0.222	0.102
R = 5 cm	A, cm	0.410	0.248
$J_M = 0.03$ A/cm <sup>2</sup>	B, m	275.0	93.6
$V_M = 0.45$ volts	T, m	11.0	3.7
$\rho_M = 1.6 \times 10^{-6}$ $\Omega$ -cm	Bus vol., cm <sup>3</sup>	$4.48 \times 10^{-3}$	$0.7 \times 10^{-3}$
$\rho_B = 1.7 \times 10^{-6}$ $\Omega$ -cm	Grid vol., cm <sup>3</sup>	$4.68 \times 10^{-3}$	$0.91 \times 10^{-3}$
$\rho_S = 38$ $\Omega/\square$	Resulting Power Loss		
$\rho_C = 0.001$ $\Omega$ -cm <sup>2</sup>	$P_T$ , mW	189.2	112.8
B:T = 25	Loss, %	17.8	10.6

The first example, Table 1, compares a single metallization grid pattern with one whose bus bars have a 50- $\mu$ m-thick strap overlaid on the bus bar. The bus volume and grid volume refers to the metal volume deposited during the metallization. Note the tremendous power savings realized by adding the strap. This represents an increase in output efficiency from 13.9% to 14.9%.

The second example has two parts. The first part displays the optimal design sensitivity to a changing current density  $J_M$  (Table 2). The  $J_M$ 's in Table 2 are actually a change of +25% from the  $J_M$  in Table 1. Therefore, the single-metallization data in Table 1 can be compared with those in Table 2. The change in  $J_M$  can be thought of as a change in efficiency from 12.7% to 21.1%. The second part of this example refers to the possibility that after the design of Table 1 has been created it is discovered that the current density,  $J_M$ , is actually some other value. Thus, if  $J_M$  is varied by +25% of the value in Table 1, the calculated power loss  $P_T$  differs only very slightly from the power loss that would be expected had the optimal design associated with that current density been used. In short, the total power lost is insensitive to the design when varying the current density  $J_M$ .

Table 2. Single-Metallization Design Sensitivity to  $J_M$

$J_M$	0.0225	0.0375
$W_B$	0.197	0.244
A	0.442	0.388
B	260	287.5
T	10.4	11.5
$P'_T$	127.4	260.6
$P_T$	126.2	258.9
% loss	15.9	19.5

The third example refers to a rectangular cell 5.0 x 0.5 cm that has an ideal efficiency (with no losses) of 15% at 100 mW/cm<sup>2</sup> AM1 (37.5 mW maximum). The pattern is a single bus bar of length 0.5 cm. The fixed parameters are found in Table 3. This example tests the sensitivity of the optimal design and power loss to varying the fine-grid-line spacing (A), which is equivalent to varying the number of fine grid lines. The significant result is the total metal used in the pattern (fine grid volume plus bus bar volume). Figure 4 shows the percentage of power lost and the total metal volume versus the number of grid lines. Note that the optimal design has four grid lines. In Figure 5 the power output and the metal volume/output power are plotted against the number of grid lines.

The significant result is that increasing the number of grid lines (from 4 to 10) changes output power very little; at the same time, the metal volume per unit of output power decreases by about 30%. This is the same as a decrease in the cost of the metal used on the cell per watt.

Table 3. Fixed Parameters

---

Width	5.0 cm
length	0.5 cm
No. buses	1
$J_M$	0.03 A/cm <sup>2</sup>
$V_M$	0.5 volts
M	$1.7 \times 10^{-6} \Omega\text{-cm}$
S	60 $\Omega/\square$
C	0.001 $\Omega\text{-cm}^2$
B:T	3.1

---

Experimental Efforts

In the Cell and Module Formation Research Area of the Flat-Plate Solar Array Project at the Jet Propulsion Laboratory a series of experiments is under way, designed to verify the predictive accuracy of the power-loss equations. Experiments are also being done to determine the nature of the most correct equations describing the contact resistance of the grid lines on solar cells.

The program's design solution for a rectangular cell has been compared with a calculation by M. Wolf (Reference 8). In a recent report he calculates the losses in a 2.5 x 0.5-cm cell; his total losses are 4.35%, which compares well with the program's calculation of 4.5%. The small difference in the results is due to the placement and geometry of the bus bar. Similar comparisons for round cells have not been found in the literature.

Summary

It is believed that the program method can be extended to include other design geometries and cell characteristics, such as bulk resistivity, cell thickness and junction depth, and to make rudimentary cost studies.

Although some of the designs may propose parameter values now thought to be beyond technical desirability or feasibility, it is believed that the program is useful in that it suggests new design work that may be worthy of consideration. Technical limitations can be handled by altering the optimization procedure in any of several different ways.

The grid pattern designer will find the program most useful because he can now find optimal design values rapidly when there are two or more design parameters. The losses it predicts are the same as would be calculated using any other method that uses the customarily accepted series resistance loss equations.

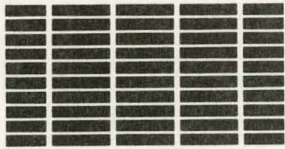
## Acknowledgments

The research described in this paper was carried out at the Jet Propulsion Laboratory, California Institute of Technology, and was sponsored by the U.S. Department of Energy through an agreement with NASA.

## REFERENCES

1. D. Simmons, Nonlinear Programming for Operations Research, pp. 110-113, Prentice-Hall, Inc., 1975.
2. A. Moore, "An Optimized Grid Design for a Sun-Concentrator Solar Cell," RCA Review, 40, p. 144, 1979.
3. D. Redfield, "Optimization of Solar Cell Contacts by System Cost-Per-Watt Minimization," RCA Review, 38, p. 475, 1977.
4. A. Flat and A. Milnes, "Optimization of Multi-Layer Front-Contact Grid Patterns for Solar Cells," Solar Energy, 23, pp. 289-299, 1979.
5. H.H. Berger, "Contact Resistance and Contact Resistivity," J. Electrochem. Soc.: Solid State Science and Technology, pp. 507-514, April 1972.
6. H.A. Taha, Operations Research an Introduction, p. 537, MacMillan Publishing Co., 1976.
7. D. Sonnabend, "APPLY - User's Guide and Reference Guide," JPL Engineering Memorandum 314-223, Jet Propulsion Laboratory, Pasadena, California, October 1980.
8. M. Wolf, "Analysis and Evaluation of Processes and Equipment," DOE/JPL-956034/15, Jet Propulsion Laboratory, Pasadena, California, 1981.

**MULTIPLE-BUS RECTANGULAR CELL**



**ROUND CELLS**

**ONE-BUS CELL**



**TWO-BUS CELL**

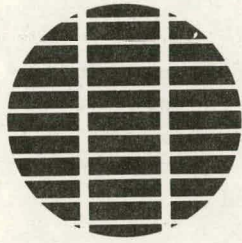


Figure 1. Cell Shapes and Grid Geometries That Can Be Analyzed by the Program

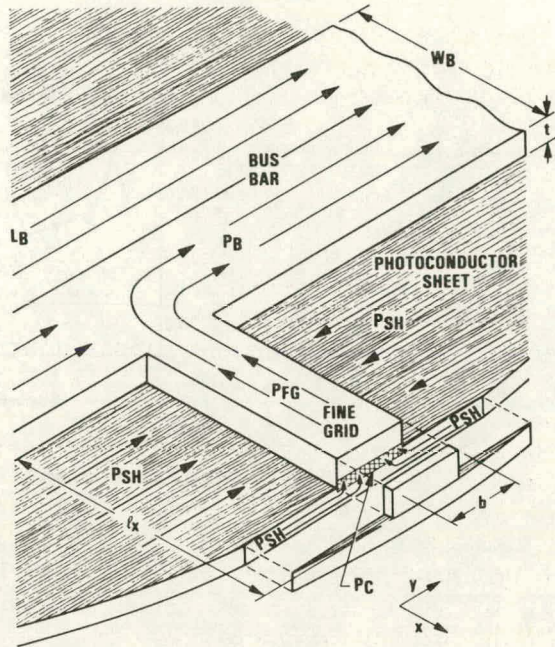


Figure 2. Power Losses in Solar Cell (Intersection of Fine Grid Line & Bus Bar)

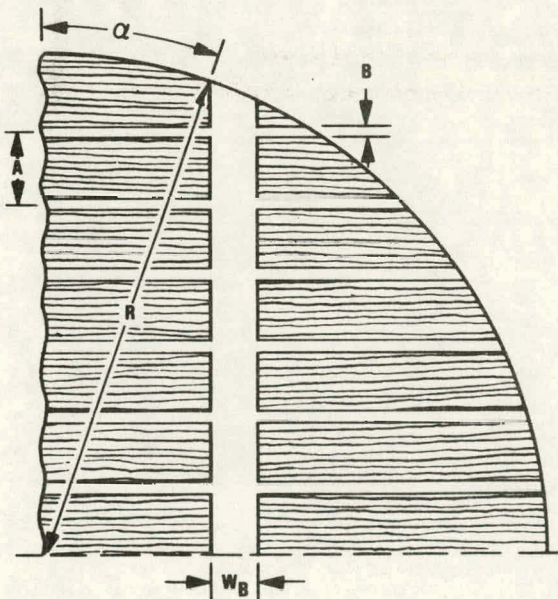


Figure 3. Quadrant of Two-Bus-Bar Round Solar Cell

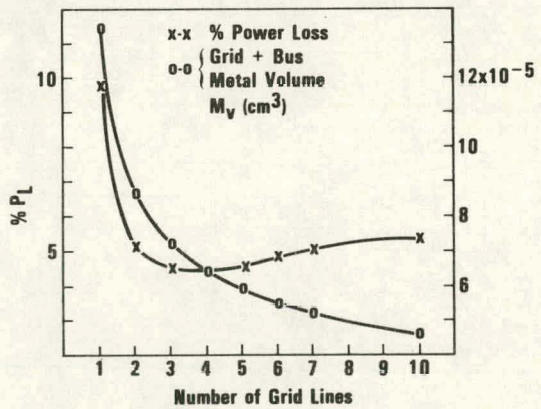


Figure 4. Sensitivity of % Power Loss and Metal Volume in Grid Lines on 0.5 x 5.0-cm Rectangular Cell



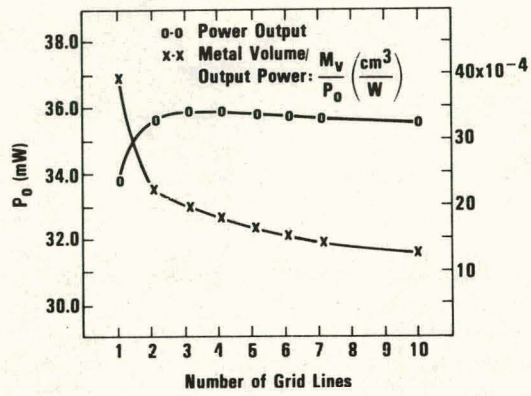


Figure 5. Sensitivity of Power Output and Metal Volume/Output Power to Number of Grid Lines on 0.5 x 5.0-cm Rectangular Cell